Characterisation of Alcelaphine Herpesvirus-1 ORF50

Fiona MacGregor Frame

Thesis submitted for the Degree of Doctor of Philosophy

University of Edinburgh

April 2001

Declaration

I declare that all the work presented in this thesis has been composed and performed by myself. Contributions to the work of this thesis by colleagues are fully acknowledged in the text.

This work has not been, and is not currently being submitted for candidature for any other degree.

Fiona MacGregor Frame

A setback is an opportunity to begin again more intelligently.

Henry Ford

Enjoy failure, you never learn from success.

Anthony Hopkins

CONTENTS

Chapter 2 – MATERIALS AND METHODS

Chapter 3 - RESULTS

Chapter 4 – RESULTS

Chapter 5 – DISCUSSION

List of Figures

Chapter 1

Chapter 3

Chapter 4

Chapter 5

List of Tables

Acknowledgements

I would like to thank the following people who have been invaluable to me throughout the course of this project:

Dr. Robert G. Dalziel for his support, guidance and patience as my supervisor.

Leena and the members of Dr. Dalziel's group for their support and company.

Paddy and Alasdair for their patience with my questioning and their assistance.

Carolyn Fiskerstrand for demonstrating EMSAs to me.

Dr. Hugh Reid and Miss Irene Pow for their provision of cells and virus.

All the staff of the veterinary pathology department for their approachability and assistance.

The PhD students in the department for their invaluable support.

My other friends for their encouragement.

My family who have each played a part in this project – I thank you for your unlimited support in all the forms it has taken.

The Veterinary Faculty for my personal funding.

The Wellcome Trust for the project funding.

Abbreviations

α	alpha
aa	amino acid(s)
AIDS	acquired immunodeficiency syndrome
AlHV-1	alcelaphine herpesvirus-1
AlHV-2	alcelaphine herpesvirus-2
AlHV-3	alcelaphine herpesvirus-3
Amp	ampicillin
Amp^r	ampicillin resistance gene
AP	activator protein
ATCC	American Type Culture Collection
ATP	adenosine triphosphate
ATPase	adenosine triphosphatase
att	attenuated
β	beta
BAC	bacterial artificial chromosome
Bcl-2	B-cell lymphoma/leukaemia-2 oncogene
BHK	baby hamster kidney
BHV-3	bovine herpesvirus-3
BHV-4	bovine herpesvirus-4
BMLF1	BamH1 M left reading frame
BMRF1	BamH1 M right reading frame
bp	basepairs
BRLF1	BamH1 R left reading frame
BT	bovine turbinate
BUdR	bromodeoxyuridine
BZLF1	BamH1 Z left reading frame
bZIP	basic region leucine zipper
CA	cell-associated
CAM	cell adhesion molecule
CD	complex of differentiation
cDNA	complimentary DNA
CF	cell-free
CMV	cytomegalovirus
CPE	cytopathic effect
CpHV-2	caprine herpesvirus-2
CR2	complement receptor
Δ	delta
dATP	2'-deoxyadenosine 5'-triphosphate
DBP	DNA-binding protein
dCTP	2'-deoxycytidine 5'-triphosphate
DE	delayed early
dGTP	2'-deoxyguanosine 5'-triphosphate

dH_2O	deionised water
dIdC	poly-deoxy-inosine-deoxy-cytidylic acid
DL	duplicated left
DMEM	Dulbecco's Modified Eagle's Medium
DMSO	dimethyl sulfoxide
DNA	deoxyribonucleic acid
DNase	deoxyribonuclease
dNTP	deoxy (any 2'-deoxynucleoside [A,C,G or T]) 5'-triphosphate
DR	duplicated right
DTT	dithiothreitol
dTTP	2'-deoxythymidine 5'-triphosphate
E	early
EB1	BZLF1-encoded EBV trans-acting factor
EBERs	EBV-encoded small RNAs
EBNA	Epstein-Barr virus nuclear antigen
EBV	Epstein-Barr virus
EA	early antigen
EDTA	ethylenediaminetetraacetic acid
EGFP	enhanced green fluorescent protein
EHV-2	equine herpesvirus-2
EMSA	electrophoretic mobility shift assay
E2F	factor that interacts with the adenovirus early region 2 (E2) promoter
ϕ	phi
FACS	fluorescent activated cell sorter
FCS	foetal calf serum
γ	gamma
GFP	green fluorescent protein
γHV	gammaherpesvirus
GMEM	Glasgow Modified Eagle's Medium
gp	glycoprotein
h	hour(s)
HCl	hydrogen chloride
HCMV	human cytomegalovirus
H-DNA	high GC content DNA
HEPES	N-[2-Hydroxyethyl] piperazine-N'-[2-ethanesulfonic acid]
HHV-6	human herpesvirus-6
HHV-7	human herpesvirus-7
HHV-8	human herpesvirus-8
HiHV-1	hippotragine herpesvirus-1
His	histidine
HSV-1	herpes simplex-1
HSV-2	herpes simplex-2
HVA	herpesvirus ateles
HVS	herpesvirus saimiri

ICP0	infected-cell polypeptide 0
IE	immediate early
Ig	immunoglobulin
IL-2	interleukin-2
IL-6	interleukin-6
IL-8R	interleukin-8 receptor
IPTG	isopropylthio-β-D-galactoside
IR	internal repeat
IRF	interferon regulatory factor
KAc	potassium acetate
Kan	kanamycin
Kan^r	kanamycin resistance gene
kb	kilobases
K-bZIP	KSHV – basic region leucine zipper
KCl	potassium chloride
kDa	kilodalton
KS	Kaposi's sarcoma
KSHV	Kaposi's sarcoma-associated herpesvirus
L	late
L-DNA	low GC content DNA
LAK	lymphokine activated killer cell
LATs	latency associated transcripts
LB	Luria-Bertani
LGL	large granular lymphocyte
LH	left hand
LMP	latent membrane protein
LP	latent protein
LTR	long terminal repeat
luc	luciferase
M	moles
mAmps	milli-amps
MCD	multicentric Castleman's disease
MCF	malignant catarrhal fever
MCFV-WTD	malignant catarrhal fever virus – white-tailed deer
mCi	millicurie
MCMV	murine cytomegalovirus
MCS	multiple cloning site
µf	micro-Faraday
µg	microgram
$MgCl_2$	magnesium chloride
MHV-68	murine herpesvirus-68
min	minutes
µl	microlitre
ml	millilitre

mM	millimoles
MMLV	Moloney murine leukaemia virus
MOPS	3-(N-Morpholino)propanesulfonic acid
mRNA	messenger RNA
ms	millisecond(s)
Mta	M-transactivator
MW	molecular weight
N	any 2'-deoxynucleoside (A,C,G or T)
NaCl	sodium chloride
NaOH	sodium hydroxide
NBCS	newborn calf serum
N-CAM	neural cell adhesion molecule
Neo	neomycin
Neo^r	neomycin resistance gene
ng	nanogram
NK	natural killer
NLS	nuclear localisation signal
nm	nanometre
Nt	nucleotide
NWA-MCF	non-wildebeest-associated-malignant catarrhal fever
Ω	ohms
O.D.	optical density
^oC	degrees centigrade
Oct-1	cellular octamer binding protein
ORF	open reading frame
ori	origin
oriP	latent origin of replication for EBV
OvHV-2	ovine herpesvirus-2
PAA	phosphonoacetic acid
PAC	Pl-derived artificial chromosome
PAN-RNA	polyadenylated nuclear RNA
PBS	phosphate buffered saline
PCNA	proliferating cell nuclear antigen
PCR	polymerase chain reaction
PEL	primary effusion lymphoma
PMSF	phenylmethylsulfonyl fluoride
pRB	retinoblastoma protein
PRV	pseudorabies virus
R	R-transactivator
RACE	rapid amplification of cDNA ends
RE	response element
RH	right hand
rIL-2	recombinant interleukin-2
RNA	ribonucleic acid

RNase	ribonuclease
rpm	revolutions per minute
RSB	resuspension solution buffer
RT	reverse transcription
Rta	R-transactivator
RLU	relative light units
SA	splice acceptor
SA-MCF	sheep associated malignant catarrhal fever
SAP	shrimp alkaline phosphatase
SC-35	spliceosome component
SD	splice donor
SDS	sodium dodecyl sulphate
SDS-PAGE	sodium dodecyl sulphate-polyacrylamide gel electrophoresis
Sp1	specificity protein 1
SV40	simian virus 40
TAE	Tris-acetate EDTA
TBE	Tris-borate EDTA
TBP	TATA box binding protein
TEMED	N,N,N',N'-tetraethylene diamine
TFIID	transcription factor IID
TK	thymidine kinase
TNE	Tris-HCl/NaCl/EDTA
TPA	12-O-tetradecanoylphorbol-13-acetate
TR	terminal repeat
Tris	tris (hydroxymethyl) aminomethane
tRNA	transfer RNA
TPB	tryptose phosphate broth
ts	temperature sensitive
U	units
UL9	unique long
UV	ultraviolet
V	volts
vir	virulent
vIRF	virus interferon regulatory factor
vMIPII	viral macrophage inflammatory protein II
VP16	virion protein
v/v	volume per volume
VZV	varicella zoster virus
WA-MCF	wildebeest-associated malignant catarrhal fever
WD-MCF	wildebeest-derived malignant catarrhal fever
w/v	weight per volume
X-gal	5-bromo-4-chloro-3-indolyl-β-D-galactoside

YAC	yeast artificial chromosome
Z	Z-transactivator
ZEBRA	*Bam* HI fragment Z Epstein-Barr replication activator
Zta	Z-transactivator

Abstract

Malignant catarrhal fever (MCF) is a lymphoproliferative, degenerative and often fatal disease of members of the *Artiodactyla* family such as cattle and deer. The causal agents of MCF are a group of gammaherpesviruses of which alcelaphine herpesvirus-1 (AlHV-1) is a member. AlHV-1 is the most well characterised of the group and its genome has been sequenced. Continued passage of AlHV-1 in bovine cells results in attenuation of the virus. Comparison of genomes from wild-type and attenuated viruses suggested that open reading frames (ORFs) are affected including ORF50.

The ORF50 gene products of Kaposi's sarcoma-associated herpesvirus (KSHV), herpesvirus saimiri (HVS), murine gammaherpesvirus–68 (MHV-68) and their equivalent, the BRLF1 gene product of Epstein-Barr virus (EBV) are called R-transactivators (Rtas). They have a crucial role in the key mechanism of reactivating the virus from latency as well as acting as transactivator proteins activating a variety of virus and cellular promoters.

The aim of this study was to characterise AlHV-1 ORF50. It was demonstrated that the ORF50 gene product, referred to as AlHV-1/Rta, acted as a transactivator. The ability to transactivate three AlHV-1 promoters was investigated. It was shown that AlHV-1/Rta activates AlHV-1 ORF57 and AlHV-1 ORF6 putative promoters but not the thymidine kinase putative promoter. The ORF57 promoter was examined and the transcriptional start site and splice acceptor and splice donor sites were located. Also, activation of the ORF57 promoter by AlHV-1/Rta was investigated further.

Truncated ORF57 promoters were generated and their ability to be activated by AlHV-1/Rta was investigated. It was found that AlHV-1/Rta required sequences at least 385 bp upstream of the ORF57 transcriptional start site to exert its effect on ORF57 transcription. A potential AlHV-1/Rta-responsive region was identified and this was investigated further using electrophoretic mobility shift assays.

A second approach to characterise AlHV-1 ORF50 was also taken. Various strategies were designed to generate a recombinant AlHV-1 lacking ORF50. The method pursued was to generate a bacterial artificial chromosome containing the entire AlHV-1 genome. These strategies will be discussed.

Chapter 1 – INTRODUCTION

Introduction

> "Because of their diversity, each herpesvirus, whether human or animal, presents a unique challenge..." (Roizman and Baines, 1991).

1.1 Herpesviruses

Most vertebrate organisms investigated so far are hosts for at least one of the 120 known herpesviruses and, in addition, a herpesvirus has been identified in molluscs (Minson *et al.*, (2000). Different herpesviruses cause a variety of symptoms and pathology, ranging from asymptomatic to fatal. For example, herpes simplex virus 1 (HSV-1) which causes cold sores can also, under different circumstances, cause severe encephalitis. Epstein-Barr virus (EBV) ranges from having no clinical manifestation to causing infectious mononucleosis and is also associated with several tumours such as nasopharyngeal carcinoma and Burkitt's lymphoma (Roizman and Baines, 1991).

All herpesviruses have four properties in common: (i) they encode for enzymes involved in nucleic acid synthesis and DNA metabolism, (ii) viral DNA synthesis and capsid assembly occurs in the nucleus, (iii) destruction of the cell occurs when infectious progeny viruses are released and (iv) herpesviruses have the ability to establish a latent infection in the host cell where the virus genome is maintained as a circular molecule (Roizman *et al.*, 1992).

The name given to the herpesvirus family is *Herpesviridae,* and this is further divided into three subfamilies, the *Alphaherpesvirinae, Betaherpesvirinae and Gammaherpesvirinae* (Minson *et al.,* 2000). These subfamilies have distinct biological properties. The subfamilies are further classified into genera depending on

DNA and protein sequence homology and genome sequence arrangement. Herpesviruses are named according to the family or subfamily of the natural host species in which they are found. Where there is more than one virus found in a host serial arabic numbers are used. The viruses also have common names that refer to the common name of the host or occasionally the effect of the virus (Roizman and Baines, 1991) (See Table 1.1).

Table 1.1: Classification of subfamilies of the *Herpesviridae* and their defining biological properties

(HSV – herpes simplex virus, VZV – varicella zoster virus, HCMV – human cytomegalovirus, MCMV - mouse cytomegalovirus, HHV - human herpesvirus, EBV – Epstein-Barr virus, HVS – herpesvirus saimiri, HVA – herpesvirus ateles).

Alphaherpesvirinae -	Variable host range Short reproductive cycle Rapid spread in culture Efficient destruction of infected cells Establish latent infection predominantly in sensory ganglia Genera - *Simplexvirus* (e.g. HSV-1+2) - *Varicellovirus* (e.g. VZV)
Betaherpesvirinae -	Restricted host range Long reproductive cycle Slow spread in culture Frequent formation of cytomegalia Carrier cultures readily established Establish latent infection in lymphoreticular cells, secretory glands, kidneys and other tissues Genera - *Cytomegalovirus* (HCMV) - *Muromegalovirus* (MCMV) - *Roseolovirus* (HHV-6, HHV-7)
Gammaherpesvirinae -	Host range frequently limited to family or order to which the natural host belongs *In vitro* replication occurs in lymphoblastoid cells and also sometimes in epitheloid and fibroblastic cells. Usually specific for T- or B-lymphocytes Latent virus is predominantly found in lymphoid tissue Genera - *Lymphocryptovirus* (e.g. EBV) - *Rhadinovirus* (e.g. HVS, HVA)

All herpesviruses have a similar structure consisting of a core of linear double-stranded DNA, an icosadeltahedral capsid of 100-110 nm in diameter and an amorphous substance encompassing the capsid named the tegument, which is surrounded by a membrane, the envelope, from which glycoproteins project (Figure 1.1). The overall size of a herpesvirus particle ranges from 120-300 nm. Herpesvirus genomes range from 124-235 kb long and their DNA base composition varies from 32-75% G+C (Minson *et al.,* 2000).

Herpesviruses have one of six different genome structures, which differ in the presence and location of repeat sequences (Figure 1.2). Due to varying sizes of these repeat regions, there can be variation in genome size between different preparations of the same virus.

Herpesvirus genomes encode structural proteins and proteins necessary for virus replication. However, they also contain a third group of non-essential genes that are not common to all herpesviruses. Although these genes are usually not essential for replication in tissue culture, they are likely to be important in the pathogenesis of the virus *in vivo*. For example, they may encode proteins involved in modulating the host immune system or regulating host cell growth (Krajcsi and Wold, 1998; Damania *et al.,* 2000; Neipel *et al.,* 1997). Since some of these virus genes show a high degree of sequence and/or functional similarity to some cellular genes, it is believed that they may have been acquired by the virus during co-evolution with its host species (Nicholas, 2000).

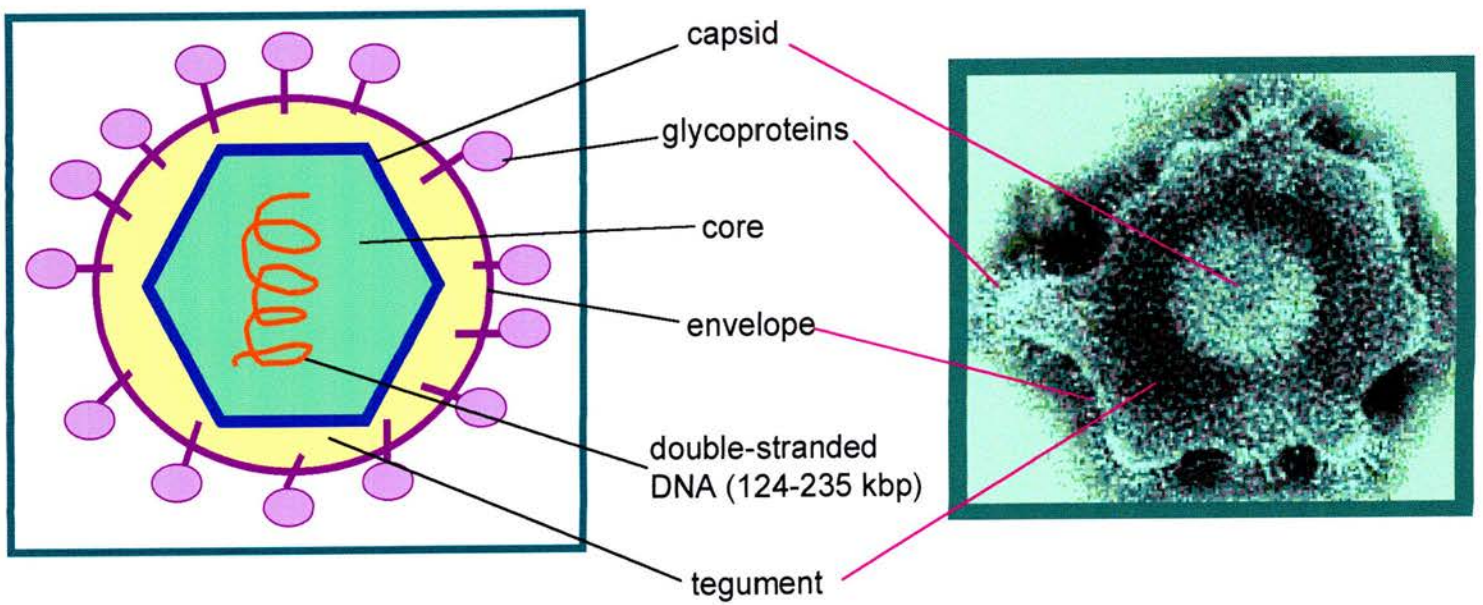

Figure 1.1: Herpesvirus Particles

Diagrammatic representation of a herpesvirus particle and a negatively stained electron micrograph (EM) image of a herpesvirus particle. EM image reproduced with kind permission from Linda M. Stannard, University of Cape Town.

1.1.1 Herpesvirus replication

Once herpesviruses have entered a cell, one of two outcomes follows. The virus may undergo a lytic phase of replication, also described as productive infection, where a cascade of virus gene expression is initiated and infectious virus particles are produced. Alternatively, the virus will enter a latent state in which infectious virus progeny are absent and there is only limited virus gene expression (Lehman and Boehmer, 1999).

1.1.2 Herpesvirus lytic replication

Based on HSV-1 replication, infection begins with attachment of the virus glycoproteins to cell surface receptors followed by fusion of the cell membrane and virus envelope with subsequent release of the naked capsid into the cell. Heparan sulphate proteoglycan on the cell surface is involved in binding of HSV-1 to the host cell, although it is not the sole receptor. HSV-1 itself has 10 envelope glycoproteins which are involved in a complex attachment and penetration process (Kasamatsu and Nakanishi, 1998; Laquerre *et al.,* 1998). In contrast, EBV uses one main glycoprotein for attachment, gp350/220 which attaches to a B-lymphocyte surface protein called CR2 (Gong and Kieff, 1990).

The HSV-1 naked capsid is transported to the nuclear pores in association with microtubules and dynein, where DNA then enters the nucleus (Kasamatsu and Nakanishi, 1998). Virus DNA is transcribed in the nucleus by host RNA polymerase II and the mRNA is translated in the cytoplasm. The temporal pattern of gene expression of herpesviruses is classified according to that of HSV-1. Gene expression

in the lytic phase of virus replication occurs in a sequential manner, which can be classified into three main stages: immediate early (IE), early (E) and late (L) which are also named α, β and γ respectively. Virus transactivator VP16 and the cellular octamer DNA-binding protein, Oct-1, activate the IE genes. The products of IE genes are then involved in activating the E genes which encode proteins required for DNA replication, for example DNA polymerase, single-stranded DNA-binding protein, origin-binding protein and enzymes involved in deoxynucleotide metabolism such as thymidine kinase (TK). These components of the DNA replication machinery are conserved between bacteria, yeast, mammals and viruses. The L genes encode proteins which provide the structural components of the virus (Lehman and Boehmer, 1999).

When virus DNA enters the nucleus, it assumes a circular configuration which is necessary for initiation of viral replication. The origin of replication can be ori_S, of which there are two copies in the 'c' sequences (IR_S, TR_S) of the genome or ori_L of which there is one copy in the U_L region of the genome (see Figure 1.2). There are inverted repeat sequences surrounding the origins to which the UL9 origin-binding protein binds. Virus DNA replication occurs in the nucleus through a rolling circle mechanism (Lehman and Boehmer, 1999). The replicated DNA is in the form of head-to-tail concatemers which are cleaved at specific sites within the '*a*' sequences and packaged into capsids (Deiss *et al.,* 1986; Vlazny *et al.,* 1982).

Virus assembly occurs in the nucleus and the nucleocapsids have been observed budding through the nuclear membrane. The mechanism of egress is not fully

Figure 1.2: Herpesvirus genome structures

Schematic diagram of six *Herpesviridae* genome groups.

An example of a virus having each of these structures is listed.

(I) ictalurid herpesvirus 1 (channel catfish herpesvirus)
(II) saimirine herpesvirus 2 (herpesvirus saimiri)
(III) human herpesvirus 3 (varicella zoster virus)
(IV) human herpesvirus 1 (herpes simplex virus 1)
(V) human herpesvirus 4 (Epstein-Barr virus)
(VI) tupaiid herpesvirus 1 (tree shrew herpesvirus)

 = unique or quasi-unique region.

 = reiterated domains.

 = orientation of repeated sequence.

(I) LTR – left terminal repeat
RTR – right terminal repeat
(II) The terminal repeats are reiterated many times and their number can vary.
(III) IR – internal repeat
TR – terminal repeat
(III) & (IV) U_L – unique long region
U_s – unique short region
These components invert giving the potential for isomers (2 in group (III), 4 in group (IV)).
IR_L – internal repeat long
IR_S – internal repeat short
TR_L – terminal repeat long
TR_S – terminal repeat short
(VI) R1-R4 – repeat regions.

This diagram is a composite adapted from Davison (1991), Roizman *et al.*, (1992) and Minson *et al.*, (2000).

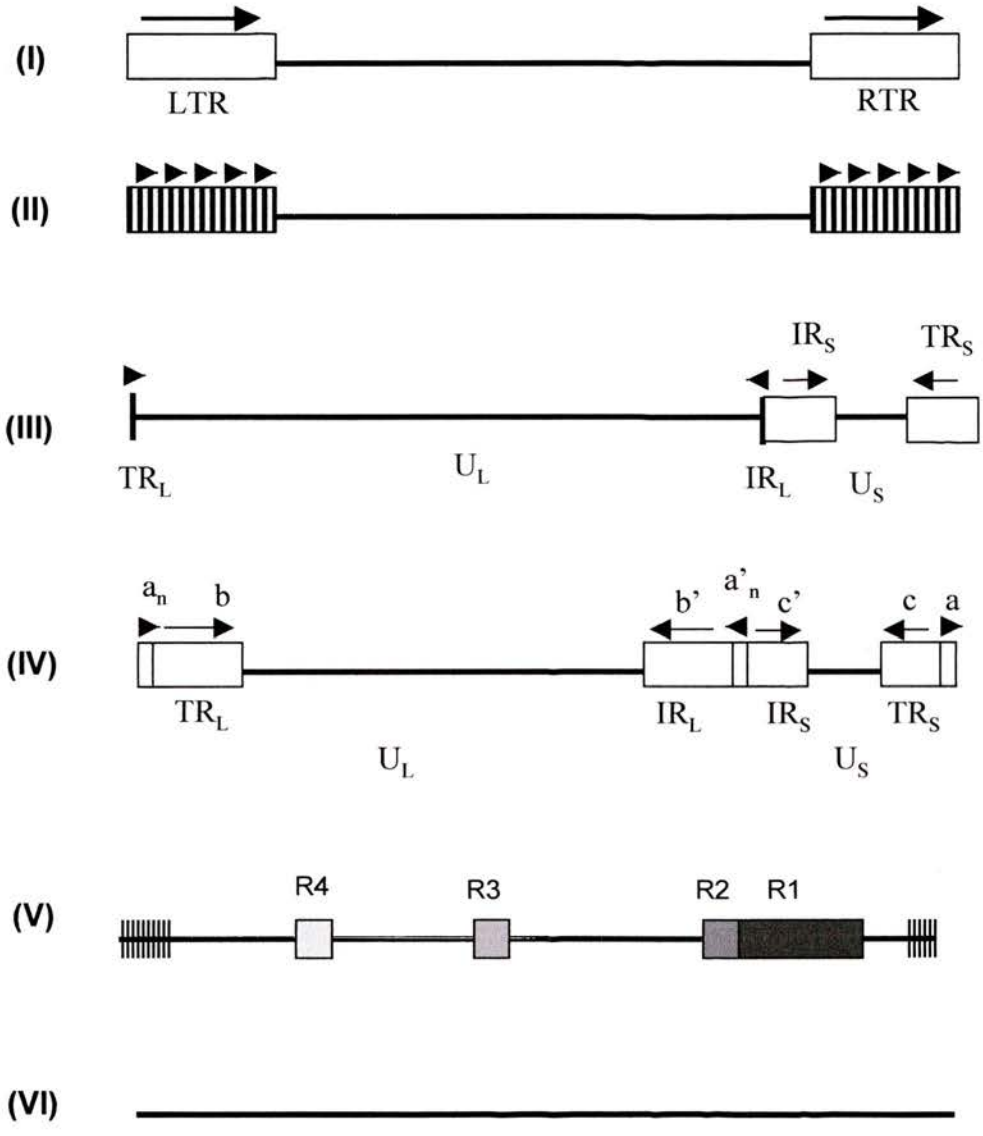
(I)
LTR
RTR
(II)
(III)
IRS
TRS
TRL
UL
IRL
US
(IV)
an
b
b'
a'n
c'
c
a
TRL
IRL
IRS
TRS
UL
US
(V)
R4
R3
R2
R1
(VI)

understood. The nucleocapsids may then be transported to the cell surface and exocytosed. It has also been suggested that de-envelopment and re-envelopment processes occur such that the final envelope of HSV-1 is derived from a post-endoplasmic reticulum compartment rather than the nuclear membrane as the first model predicts (Whiteley *et al.,* 1999).

1.1.3 Herpesvirus latency

> "The evolution of exquisite and diverse mechanisms for the establishment and maintenance of latency and the reduced capacity of herpesviruses to cause severe disease in their natural hosts as compared to heterologous hosts suggests that herpesviruses have evolved a relationship with their hosts that permits them to survive and be perpetuated." (Roizman and Baines, 1991)

Latency is defined as a persistent infection where the virus genome is present without production of infectious virus particles (Stevens, 1989). During latency the virus DNA is in a circular episomal form and limited virus gene expression occurs. The ability to establish a latent infection enables the virus to persist for the lifetime of the host largely because the virus remains undetected by the host immune system. There are various theories as to how and why latency may occur, which have been based mainly on analysis of HSV-1 and EBV.

Skin, mucous membranes and corneal epithelium are the common primary sites of HSV-1 infection. The virus can then infect neurons of the peripheral sensory ganglia. Once it has entered it ascends the nerve axons by retrograde axonal transport to the somas. Here the virus establishes the latent state and virus replication has to be prevented. Latency associated transcripts (LATs) are the only transcripts expressed

by latent HSV-1 (Wheatley *et al.*, 1991; Steiner, 1996; Mellerick and Fraser, 1987). LATs are encoded within the long repeats of the virus genome. However, studies using mutant viruses have indicated that expression of LATs is not essential for establishment or maintenance of latency or indeed for reactivation from latency. Nevertheless, these studies did show that reactivation is greatly enhanced by the LATs (Javier *et al.,* 1988). All mutant viruses that have been studied are able to establish latency albeit with different efficiency, therefore implying that no single virus gene product is absolutely essential for the establishment of latency (Stevens, 1989). Establishment of latency of HSV-1 is associated with inefficient expression of IE genes in neurons, which may arise through different pathways (Preston, 2000). The function of LATs has been described in two alternative models:

1) If present in the nucleus, LATs may inhibit translation of the IE gene ICP0 thereby reducing lytic gene expression resulting in reduced virus replication and establishment of latency.
2) If LATs are in the cytoplasm they may be translated and the resulting products may stimulate replication and therefore encourage reactivation.

When and why either of these two models may occur is not clear and there is no general consensus on LAT function (Millhouse and Wigdahl, 2000).

In contrast with HSV, EBV establishes latency in dividing cells and up to 11 EBV genes are expressed. The maintenance of latency is therefore likely to involve a different mechanism to that of HSV-1. The pattern of latent gene expression in various EBV-associated tumours differs. Latent genes expressed are six Epstein-Barr virus nuclear antigens (EBNAs) -1, -2, -3A, -3B, -3C and -LP, three latent membrane

proteins (LMPs) 1, 2A and 2B and two non-polyadenylated (non-coding) RNAs called EBERs 1 and 2. Three types of latent infection have been described. Latency type I: EBNA-1 expression is observed in endemic and sporadic Burkitt's lymphoma. Latency type II: EBNA-1 and the LMPs are expressed in nasopharyngeal carcinoma, Hodgkin's disease and T-cell lymphomas. Latency type III: Expression of all six EBNAs and the LMPs is detected in immunoblastic lymphomas. All EBV positive tumours express the EBER RNAs (Young *et al.,* 2000).

EBNA-1 is associated with chromatin and is involved in replication of the virus DNA and its maintenance as an episome as well as its replication. It achieves this through interaction with the origin of replication (oriP), which is distinct from that used in the lytic cycle. EBNA-2 has a crucial role in the transformation process and can act as a transcriptional activator of cellular and virus genes (Young *et al.,* 2000). EBNA-3A and EBNA-3C are essential in the process of lymphocyte transformation *in vitro*, whereas EBNA-3B and EBNA-LP are not (Cohen *et al.*, 1989; Tomkinson *et al.*, 1993). LMP-1 is important for cell transformation and cell phenotypic changes. LMP-2 and -3, although not essential for transformation, appear to have roles in signalling pathways (Young *et al.*, 2000; Stevens, 1989).

1.1.4 Gammaherpesviruses

The main distinguishing characteristic of gammaherpesviruses (γHVs) is their ability to achieve latency in lymphocytes. *Gammaherpesvirinae* are split into the γ1 and γ2 genera, known formally as the *Lymphocryptovirus* (B-cell tropic) and *Rhadinovirus* (B- or T-cell tropic) genera (Efstathiou *et al.,* 1990). All γHVs causing significant

veterinary diseases are in the *Rhadinovirus* genus. In ungulates and non-human primates, γHVs have been identified which pose no threat to their natural host, but cause lymphoproliferative diseases in related animals (Murphy *et al.*, 1999).

1.2 Malignant catarrhal fever

Malignant catarrhal fever (MCF) is a lymphoproliferative and degenerative disease which affects members of the *Artiodactyla* family such as cattle and deer. MCF is a worldwide disease affecting domestic and exotic animals, predominantly ruminants, which can be living freely or in captivity (Plowright *et al.,* 1960; Hoffman and Young, 1989; Metzler, 1991; Howard, 1993; Jones *et al.,* 1997; Reid, 2000). The first description of MCF in Africa was in 1923 (Mettam, 1923) and work published in 1930 described the first reports of MCF in cattle in Europe (Goetze and Liesse, 1930).

1.2.1 Symptoms of MCF

MCF has a variety of symptoms and the affected animal can show many or practically none. Some common symptoms are shown in Figure 1.3. The outcome was thought to be almost always fatal. Subsequent work has revealed that symptomless cases may occur, which had previously gone undetected (Reid *et al.,* 1984; Milne and Reid, 1990). There may also be more animals recovering than once thought (O'Toole *et al.,* 1997).

(a)

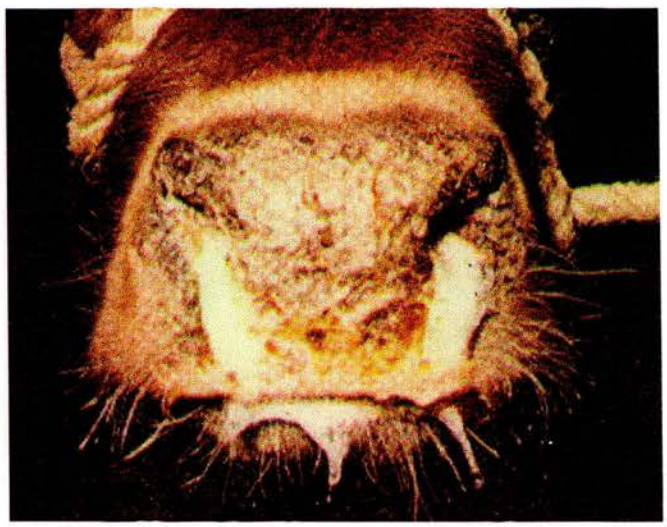

(c)

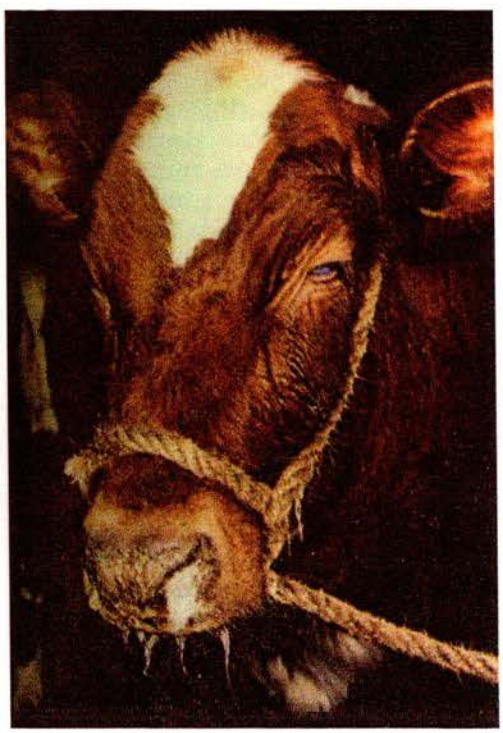

(b)

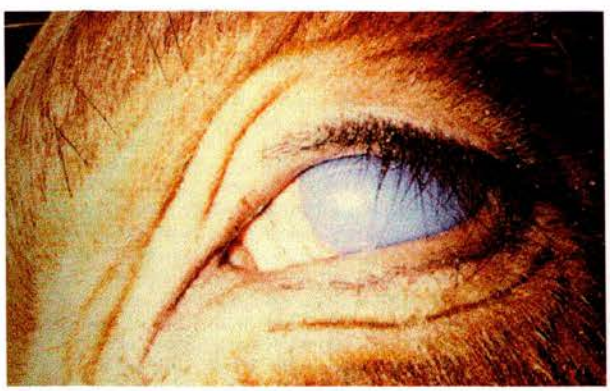

Figure 1.3: Symptoms of malignant catarrhal fever.
a) Dry, cracked and encrusted appearance of muzzle, bilateral mucopurulent nasal discharge and hypersalivation.
b) Corneal opacity.
c) Typical case with encrustation of muzzle, eye lesions, hypersalivation and nasal discharge.
Reproduced with kind permission from Selman *et al* , (1974).

The symptoms of MCF have been categorised into four forms. These are :

(i) the peracute form with generalised disease,

(ii) the intestinal form,

(iii) the head and eye form,

(iv) the catarrhal form.

In the peracute form, which is the most severe, the animal initially exhibits a fever and depression and can die within a few hours of these first visible symptoms showing (Reid *et al.,* 1984). In most cases the animals die within 2-12 days after the onset of fever (Howard, 1993).

1.2.2 Clinical signs

Examples of the many symptoms include high fever, inflammation of conjunctival, oral and nasal mucosa, lymphadenopathy and leukopenia (Metzler, 1991; Jones *et al.,* 1997). Rectal temperature can rise to 41-42°C (Selman *et al.*, 1974; Pierson *et al.,* 1978; Reid *et al.,* 1979). There is also nasal and ocular discharge which starts as clear and watery but progresses to a mucopurulent secretion (Selman *et al.,* 1978; Howard, 1993). The muzzle epidermis may become dry and cracked and bleeding occurs (Selman *et al.,* 1974; Liggitt *et al.*, 1978). Depending on the type of MCF, diarrhoea or constipation can occur (Florzinek, 1990). Necrosis and vasculitis as well as lymphocyte proliferation and tissue infiltration are other features (Metzler, 1991). The disease can involve the respiratory and alimentary tract where lesions or erosions can occur as well as pneumonia and necrotic pharyngitis, laryngitis and tracheitis (Florzinek, 1990). In addition, the lymphoid organs can be affected. A variety of skin

lesions may also be observed (Howard, 1993). Extensive muscle tremors are seen, along with incoordination, a twisted neck, random eye movements, ear-twitching and aggressive behaviour (Florzinek, 1990).

1.2.3 Gross pathological changes

Many body systems are affected by MCF and autopsy exposes numerous gross pathological changes. Necrosis and erosion of the epithelia can occur in the alimentary tract, from the pharynx to all chambers of the stomach. Areas of the intestine also exhibit congestion, fresh blood and mucus. Cellular infiltration into the liver is observed as round foci and the liver is usually swollen (Daubney and Hudson, 1936).

Haemorrhaging occurs in the turbinates and septum in most of the head-and-eye cases. Lesions found on the tongue and in the mouth and throat can be red erosions, ulcers or areas of necrosis (Daubney and Hudson, 1936). Bronchopneumonia along with congestion and edema occurs in the lungs of 40% of the fatal cases.

Dense cellular infiltration is observed in the swollen kidneys as mottled areas and there are wedge-shaped areas of dead tissue. The cortical areas of the adrenal glands have haemorrhaging. Haemorrhage and erosion also occurs in the urinary bladder along with the congested mucosa in this area. Also, vaginitis is observed with necrosis, mucosal erosion and mucopurulent discharge.

Generalised lymph node enlargement is observed in 80% of cases. This is most

prominent in the lymph nodes around the head and neck area and also the bronchial and renal areas. The spleen is usually slightly enlarged. Generalised synovitis is observed in some cases (Selman *et al.,* 1974; Liggitt *et al.*, 1980). The cerebrospinal and synovial fluid collected from an animal which had died from MCF were shown to be cloudy and contained significantly higher amounts of protein and mononuclear cells than normal (Pierson *et al.,* 1978).

1.2.4 Histopathology

MCF lesions are characterised by epithelial degeneration, vasculitis, hyperplasia and necrosis of lymphoid organs and accumulation of lymphoid cells in non-lymphoid tissues through interstitial infiltrations.

Destruction of small lymphocytes occurs in the germinal follicles of the lymph node cortex and the cell debris is ingested by macrophages. Proliferation of lymphocytic and lymphoblastoid cells occurs in distinct regions of the lymph node, namely the interfollicular and paracortical areas.

Vasculitis is mainly observed in medium-sized arteries and is accompanied by infiltration of lymphocytes, lymphoblasts and macrophages into the endothelial layer of the blood vessels. As a result, the endothelial cells multiply excessively and/or are enlarged. Due to the increased number of lymphoid cells and the multiplication of endothelial cells the blood vessels can become blocked (Reid *et al.,* 1979; Liggitt and DeMartini, 1980a). Connective tissue and the smooth muscle surrounding the blood vessels can undergo degeneration.

The connective tissue of the lymph nodes and spleen are also subject to cell infiltration and degeneration. This also occurs in the intestines where smooth muscle degeneration occurs (Denholm and Westbury, 1982; Liggitt and DeMartini, 1980b). The sites in which vascular lesions are most commonly observed are the kidney, brain, meninges, lung, lymph nodes, adrenal glands and the carotid arteries (Liggitt *et al.,* 1978). Infiltration of lymphoid cells into the liver and kidney are characteristic of MCF (Liggitt *et al.*, 1978; Reid *et al.,* 1979).

The main ocular lesion is inflammation of the cornea due to infiltration of lymphoid cells and degradation of the corneal epithelium which leads to corneal opacity (Huck *et al.,* 1961).

In summary, the two key components of MCF pathology are tissue necrosis and T-lymphocyte proliferation. T-lymphocyte proliferation is discussed further in section 1.5 below.

1.2.5 Socio-economic impact

The study of MCF is important because of the devastating economic losses the disease can cause on individual farms. The disease occurs predominantly in African and Indonesian cattle. However, it is also a problem in deer farms (Reid *et al.,* 1984; Dinter and Morein, 1990), and in zoos and wildlife parks (Reid *et al.,* 1987; Bridgen *et al.,* 1989) where conservation and breeding programmes may be drastically affected. The most recent estimate indicated that 33 different species have presented with MCF (Gulland *et al.*, 1989; Blake *et al.,* 1990).

The first report of MCF in deer occurred in 1976 (Anonymous, 1976) and from 1979-1985 it was the most important disease of farmed deer in New Zealand (Orr, 1986). When red deer (*Cervus elaphus*) farming in Europe and New Zealand was initiated outbreaks of MCF occurred which in some cases affected as much as 50% of the herd. This pattern has since changed and now sporadic incidents, affecting only a single animal, are more common. There could be two reasons for this: either the deer are being isolated from the carriers of the virus, or the virus and deer may be co-evolving. Many projects trying to establish the farming of Père David's deer (*Elaphurus davidianus*) were abandoned in their early stages due to the devastating losses which occurred as a result of MCF.

The disease has had increased relevance in South Africa in the last 10-20 years due to increased game farming and game conservation. Some farms have reported a 20% loss of cattle (Barnard and Pypekamp, 1988). This has also become a concern in North America where bison farming is becoming more common and MCF is also proving to be a significant disease of this species (Reid, 2000; Schultheiss *et al.,* 2000). Outbreaks have also occurred in swamp buffalo (*Bubalus bubalis*) (Hoffman *et al.,* 1984; Hill *et al.,* 1993). There have been reported incidences of MCF in pigs in Scandinavia and Europe, the first of these occurring in Germany in 1950 (Løken *et al.,* 1998; Reid, 2000). These cases expanded the host range because although pigs belong to the *Artiodactyla* family they are non-ruminants.

1.2.6 Incidence of MCF

Table 1.2: Examples of outbreaks of MCF.

	Cattle				
Year	Total no.	Deaths	Deaths (%)	Location	Reference
1960	500	100	20	Kenya Masailand	Plowright, 1964
1970	10 000	700	7	Kenya Masailand	Plowright *et al.*, 1975
1973	231	87	38	Colorado	Pierson *et al.*, 1973
1984	20	5	25	Japan	Taneichi *et al.*, 1986
1987	320	49	15	Republic of Ireland	Hamilton, 1990
1988	250	35	14	Republic of Ireland	Hamilton, 1990
1988	500	100	20	Indonesia	Daniels *et al.*, 1988

Obtaining current figures for the number of MCF cases is a problem. In the UK if an animal is suspected of having MCF, the animal is usually sacrificed without diagnosis being confirmed. At the Moredun Institute, Edinburgh, there are ~300 confirmed cases of MCF a year, the majority of which are from the UK. Most of these cases are in cattle although there are also some in deer. Similarly, in Africa there is no system in place for quantifying the number of cases of MCF although there does seem to be an increased incidence.

There are several factors contributing to an increased incidence of MCF in Africa including increased game farming in South Africa and increased wildebeest populations in East Africa - a six-fold rise in the last 30 years. In addition, the land area available for use by the Masai for their cattle is decreasing due to expansion of arable land. This forces them to occupy land which lies in the path of migrating wildebeest, one of the natural carriers of an MCF-causing virus (H. Reid, pers. comm.).

1.2.7 Types of MCF

Until recently, three types of MCF had been identified, the two main ones being the wildebeest-associated or wildebeest-derived forms of MCF (WA-MCF or WD-MCF) and the sheep-associated or non-wildebeest-associated forms (SA-MCF or NWA-MCF) (Metzler, 1991). WA-MCF is found in Africa and in zoos. Transmission occurs from the black and blue wildebeest (*Connochaetes gnu* and *Connochaetes taurinus taurinus*). SA-MCF is found outside Africa and predominantly affects cattle and deer.

The blue wildebeest and sheep are the primary hosts and act as reservoirs of infection but do not succumb to the disease themselves (Plowright *et al.,* 1960; Plowright, 1968; Baxter *et al.,* 1997). Both of these types of MCF can occur as isolated cases or as epizootics, although SA-MCF is more likely to occur as the former (Reid *et al.,* 1984; Bridgen and Reid, 1991). Sheep and wildebeest are the main but not the sole reservoirs as MCF has been found in areas in which neither are present (Mirangi, 1991a).

The third type of MCF is found in North America in feedlot cattle which have no contact with sheep. This type is more difficult to transmit in experimental conditions than the wildebeest-associated form and also has a longer incubation period but with a shorter period exhibiting symptoms. The causative agent of this type of MCF is unknown (Fenner *et al.,* 1993; Pierson *et al.,* 1979).

1.3 Causal agents of MCF

The causal agents of MCF are a group of γHVs. WA-MCF is caused by alcelaphine herpesvirus-1 (AlHV-1) (Plowright *et al.,* 1960; Reid *et al.,* 1984). SA-MCF is caused by ovine herpesvirus-2 (OvHV-2). Although OvHV-2 has not been isolated, a DNA clone from lymphoblastoid cells of diseased cattle, deer and rabbits has been sequenced and shows similarity to other γHVs and particularly AlHV-1 (Bridgen and Reid, 1991).

The data regarding types of MCF and the causal agents have become increasingly convoluted due to the discovery of new MCF-causing viruses. For example, virus recovered from roan antelope was named hippotragine herpesvirus-1 (HiHV-1). This virus produced MCF in rabbits but disease caused by this virus in non-experimental conditions has not been observed (Bridgen and Reid, 1991). A virus has been discovered in hartebeest (*Alcelaphus buselaphus*) and topi (*Damaliscus korrigum*) which has been named alcelaphine herpesvirus-2 (AlHV-2) (Seal *et al.*, 1989; Roizman and Baines, 1991). This virus has not been associated with any naturally-occurring disease. However, it causes MCF in rabbits and cattle following experimental transmission (Bridgen and Reid, 1991). Other authors have used the term AlHV-2 to describe the virus from hartebeest and have classified the virus from topi as AlHV-3. A highly virulent virus has been identified as the causal agent of MCF in white-tailed deer and has been named MCFV-WTD. This is genetically related to AlHV-1 and OvHV-2. The reservoir for this virus is not known (Li *et al.,* 2000a).

Most recently an MCF-causing γHV has been discovered in goats; it has been named caprine herpesvirus-2 (CpHV-2). Goats had been thought to be a source of OvHV-2 and OvHV-2 sequences have been found in a small percentage of goats studied. The sequence of the DNA polymerase gene from CpHV-2 was compared to the homologues in AlHV-1, OvHV-2 and MCFV-WTD and it was found to have 67%, 71% and 73% identity respectively. CpHV-2 has been noted as the causal agent of chronic disease in Sika deer (Li *et al.,* 2001).

The discovery of new viruses and the observation that there are more varied presentations of the disease, such as undetected symptomless cases as previously mentioned, have suggested that the survival rate may be higher than once thought (O'Toole *et al.,* 1997). These discoveries could assist in identifying natural hosts of these viruses and therefore be of practical assistance in, for example, wildlife parks with regard to determining which species can co-habit enclosures. Also these emerging MCF viruses could solve some of the mysteries regarding the possible sources for MCF which is neither sheep- nor wildebeest-associated. They provide an added dimension to the study of MCF, and may prove useful in the future in determining underlying causes and mechanisms of MCF.

1.3.1 Alcelaphine herpesvirus-1 – causal agent of WA-MCF

In 1960 the agent of MCF from wildebeest was described as a virus and showed similarities to other known herpesviruses (Plowright *et al.*, 1960). Further characterisation of its growth and visualisation by electron microscopy was soon carried out to confirm the initial findings (Plowright *et al.,* 1963).

AlHV-1 was originally named bovine herpesvirus-3 (BHV-3) but is now called AlHV-1 because the carrier host, the wildebeest, is in the subfamily *Alcelaphinae* (Blake *et al.,* 1990; Castro *et al.,* 1985; Mushi and Rurangirwa, 1981a). The full classification of AlHV-1 is that it is in the family *Herpesviridae*, subfamily *Gammaherpesvirinae* and genus *Rhadinovirus* (Ensser *et al.,* 1997; Bridgen *et al.,* 1989; Bridgen, 1991).

In nature, AlHV-1 generally infects animals of the same family as the carrier host. AlHV-1 can be passed to domestic cattle, gaur, greater kudu, ibex, white-tailed wildebeest, white-bearded wildebeest, cape hartebeest (Shih *et al.,* 1989), roan antelope (Gulland *et al.,* 1989), white-tailed deer (Castro *et al.,* 1982), nilgai, sika deer, axis deer (Castro *et al.,* 1985) and Père David's deer (Reid *et al.,* 1987), to name a few.

In wildebeest secretions AlHV-1 is both cell-associated (CA) and cell-free (CF) whereas in cattle it is only CA. The virus from cattle, when cultivated in cell culture, causes cells to form syncytia.

1.3.2 Sequencing of AlHV-1

At least 26 herpesviruses, including examples from each subfamily, have been sequenced (Murphy *et al.,* 1999). The sequence of the low passage C500 strain of AlHV-1 was published in 1997 (Ensser *et al.,* 1997) (Figure 1.4). The genome consisted of a region of DNA, 130,608 bp in length, with low GC content (46.17%) DNA (L-DNA), flanked by 20-25 repeats with high GC content (71.83%) DNA (H-

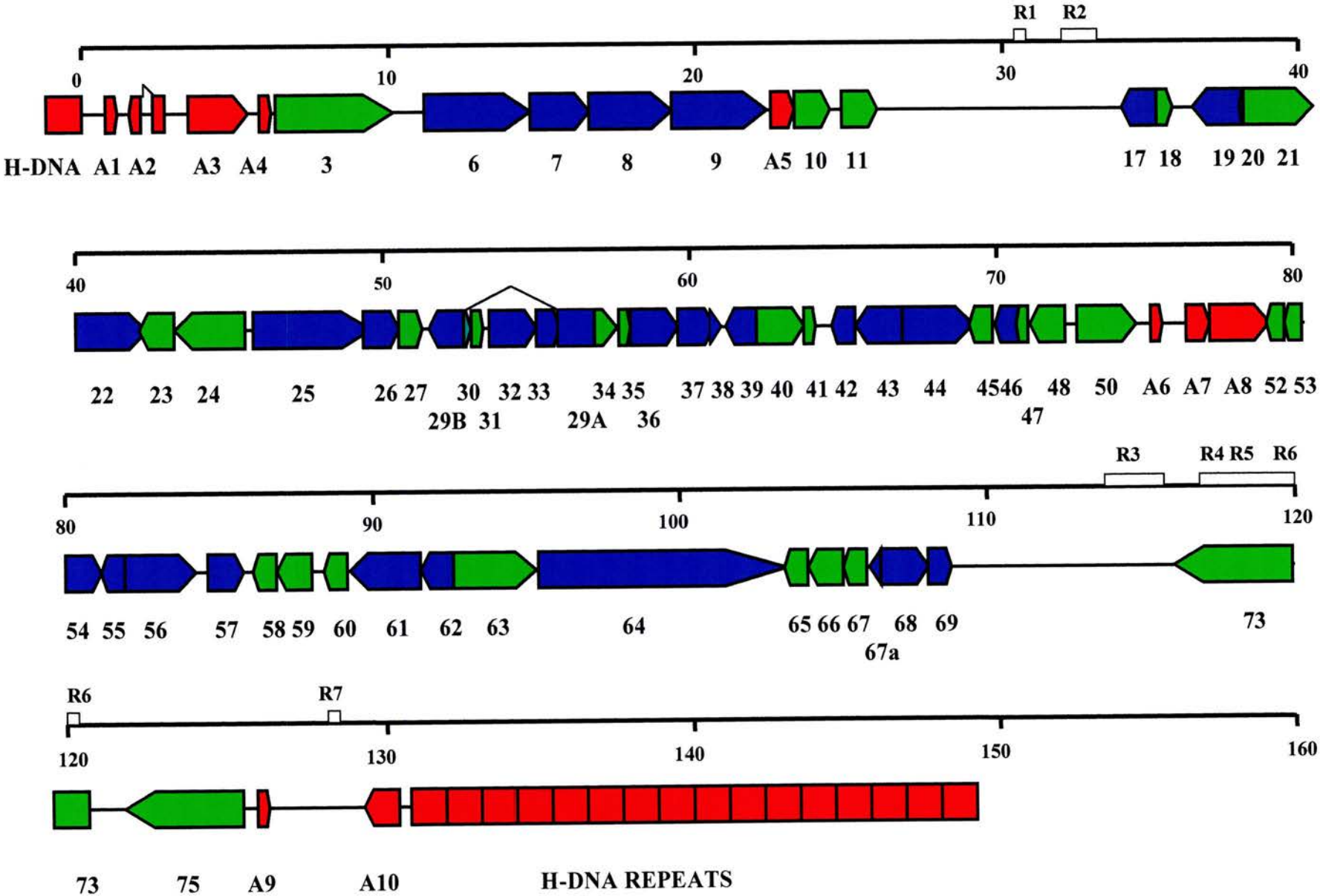
R1
R2
0
10
20
30
40
H-DNA A1 A2 A3 A4 3 6 7 8 9 A5 10 11 17 18 19 20 21
40
50
60
70
80
22 23 24 25 26 27 30 32 33 34 35 37 38 39 40 41 42 43 44 4546 48 50 A6 A7 A8 52 53
29B 31 29A 36 47
R3
R4 R5 R6
80
90
100
110
120
54 55 56 57 58 59 60 61 62 63 64 65 66 67 68 69 73
67a
R6
R7
120
130
140
150
160
73 75 A9 A10 H-DNA REPEATS

Figure 1.4: Organisation of the AlHV-1 genome

Schematic diagram of the C500 AlHV-1 genome adapted from Ensser *et al.* (1997) by Dr. R.G. Dalziel.
The ORFs are numbered and R1-R7 indicate the repetitive regions.
The colours indicate the conservation of ORFs between the α, β and γ subfamilies.

DNA) of 1113-1118 bp. The L-DNA sequence was analysed revealing 70 open reading frames (ORFs), with 61 showing similarity to other herpesvirus genes. These ORFs are arranged in blocks separated by non-conserved ORFs. The blocks are collinear with the genomes of other *Rhadinoviruses*, such as herpesvirus saimiri (HVS), equine herpesvirus-2 (EHV-2) and Kaposi's sarcoma-associated herpesvirus (KSHV [human herpesvirus-8]) (Ensser *et al.,* 1997) (Figure 1.5). In all *Rhadinoviruses* there are some genes, mainly to the far right and far left of the genome close to the repeat regions, which have homology to cellular genes. *Rhadinoviruses* also have several unique genes and in this respect AlHV-1 is no exception (Ensser *et al.,* 1997).

AlHV-1 has similar epidemiological and biological properties to the prototype rhadinovirus, HVS. Both viruses are asymptomatic in their natural hosts, but cause lymphoproliferative disorders in susceptible animals. AlHV-1 is also similar to many other γHVs such as KSHV, murine gammaherpesvirus-68 (MHV-68), bovine herpesvirus-4 (BHV-4), EHV-2, herpesvirus ateles (HVA) and the prototype *Lymphocryptovirus*, EBV.

1.3.3 Attenuation of AlHV-1

Attenuation is defined as the reduced capacity of a pathogen to cause disease. It has been observed that when AlHV-1 is passaged through bovine cell cultures, it changes from being cell-associated and virulent to cell-free and virulent after approximately 10 passages and then becomes cell-free and attenuated after a further 20 passages. Figure 1.6 shows the two forms of cytopathic effect (CPE) caused by virulent and by

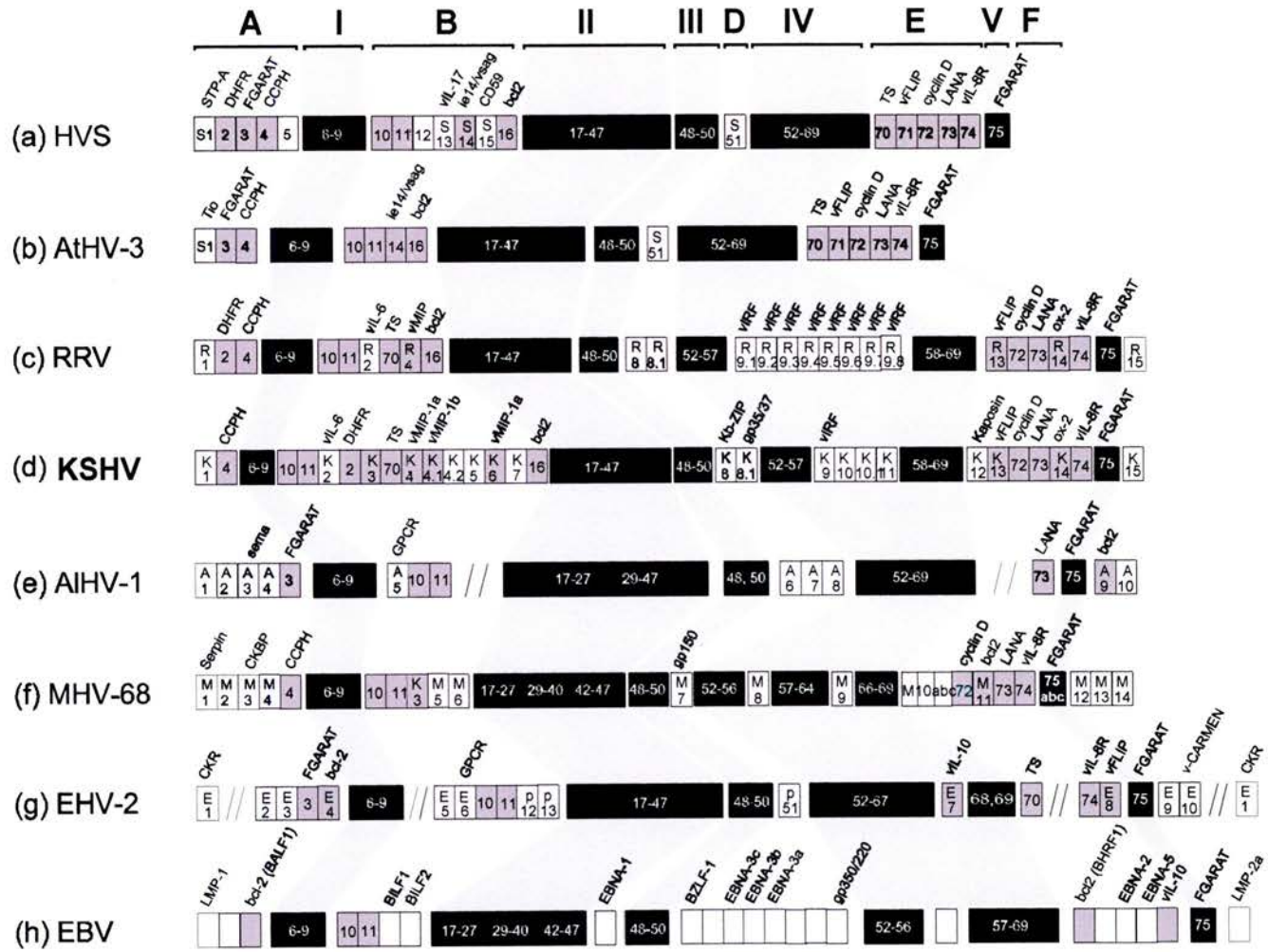
A
I
B
II
III
D
IV
E
V
F
(a) HVS
(b) AtHV-3
(c) RRV
(d) KSHV
(e) AlHV-1
(f) MHV-68
(g) EHV-2
(h) EBV

Figure 1.5: Genome organisation of the fully sequenced gammaherpesviruses

(a) herpesvirus saimiri (HVS), Albrecht *et al.* (1992).
(b) herpesvirus ateles (AtHV-3), Albrecht *et al.* (2000).
(c) rhesus monkey rhadinovirus (RRV), Searles *et al.* (1999).
(d) Kaposi's sarcoma-associated herpesvirus (KSHV), Russo *et al.* (1996).
(e) alcelaphine herpesvirus-1 (AlHV-1), Ensser *et al.* (1997).
(f) murine herpesvirus-68 (MHV-68), Virgin *et al.* (1997).
(g) equine herpesvirus-2 (EHV-2), Telford *et al.* (1995).
(h) Epstein-Barr virus (EBV), Baer *et al.* (1984).

ORFs are shown as rectangles.
ORFs that are conserved among all gammaherpesviruses are shaded black.
ORFs that have counterparts in some but not all gammaherpesviruses are indicated with medium shading.
ORFs that are unique to a particular virus are not shaded and have been assigned corresponding prefixes:
HVS and AtHV-3 - S, RRV - R, KSHV - K, AlHV-1 - A, MHV-68 - M, EHV-2 - E.
I - V indicate the conserved gene blocks and the light shading between genomes highlight these areas.
A-F indicate variable regions.
Diagonal lines indicate non-coding regions.

Diagram adapted from Coulter *et al.* (2001).

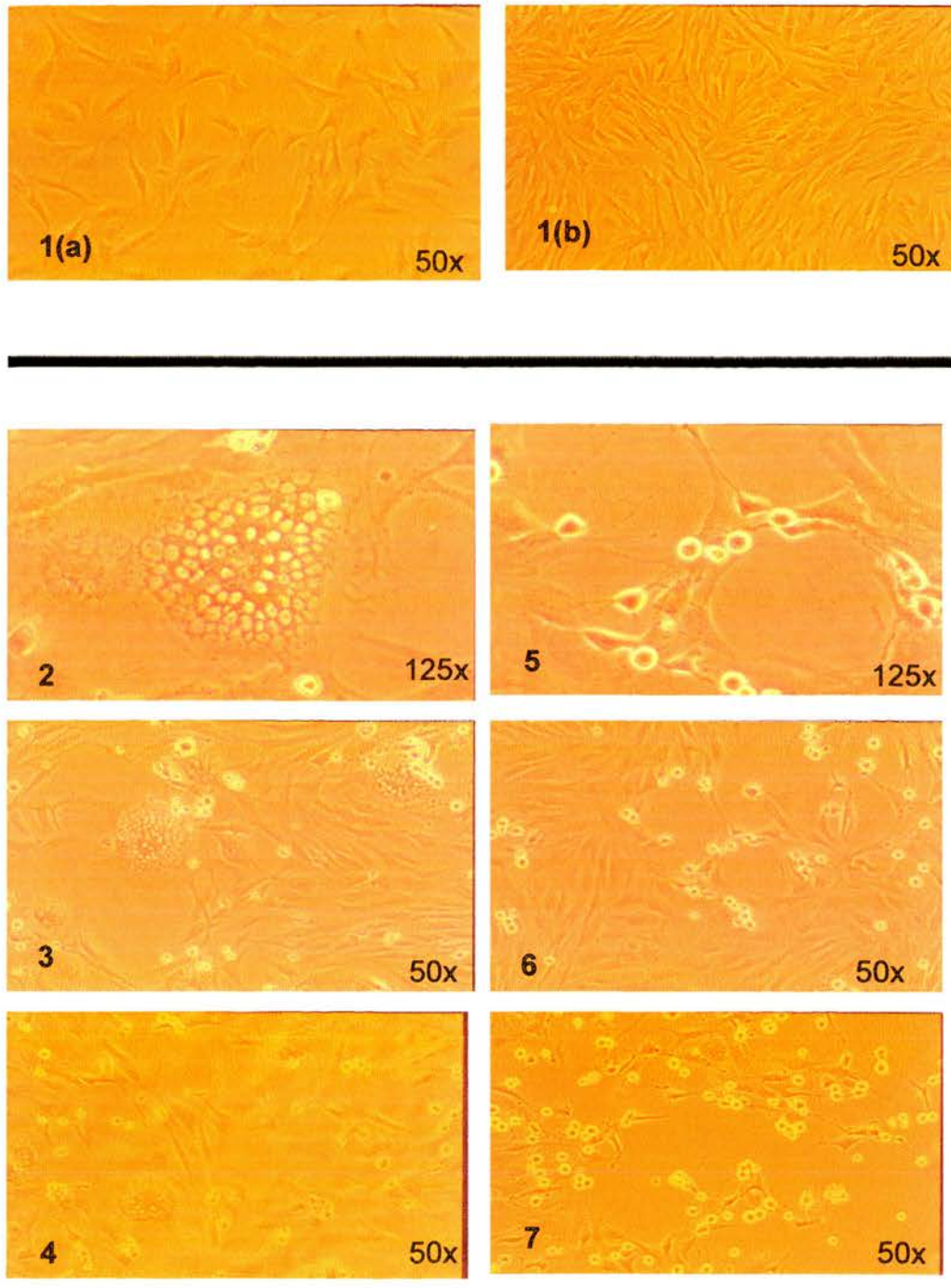

Figure 1.6: Cytopathic Effects of Virulent and Attenuated Virus on Bovine turbinate cells

1(a)- subconfluent BT cells; 1(b) - confluent BT cells;
2-4 - BT cells infected with virulent AlHV-1;
5-7 - BT cells infected with attenuated AlHV-1.

attenuated viruses. Both viruses cause rounding of the cells and thinning of the monolayer but only the virulent form induces formation of syncytia. (These images were taken within this project). In the case of AlHV-1, attenuation is measured as the loss of ability to cause disease symptoms in the laboratory model, the rabbit. Genomes from the virulent and attenuated forms of the virus have been analysed and it was proposed that an alteration had occurred in the genome (Handley *et al.,* 1995).

Since the report by Handley *et al.* (1995), further work has been carried out to determine the nature of the alteration (H. Wright pers. comm.). A few ORFs were proposed to be affected by the genome alteration, including ORF50, which is predicted to encode an R-transactivator (EBV) homologue (Ensser *et al.,* 1997). Northern blot analysis showed ORF50 mRNA to be present in LGLs containing the cell-associated virulent form of the virus and also in bovine turbinate (BT) cells infected with this virus, but not in BT cells infected with the cell-free attenuated form of the virus. Southern blots and PCR have been used to investigate the rearrangement that occurs. (H. Wright, pers. comm.). In the published sequence of AlHV-1, ORF50 is present near the middle of the genome at 70-80 kb. Analysis placed ORF50 sequences adjacent to or flanked by repeat sequences and it was suggested that the ORF50 sequence had been removed from the middle of the genome and inserted close to the terminal repeat sequences. Further investigation has led to the suggestion that more than one rearrangement had occurred (H. Wright, pers. comm.).

1.3.4 Ovine herpesvirus-2 – causal agent of SA-MCF

SA-MCF was first recognised as a cattle disease in Europe (Goetze and Liesse, 1930; Baxter *et al.,* 1997) but has since been observed worldwide in several susceptible species, in particular Bali cattle, Asian swamp buffalo and deer, the latter being more susceptible than cattle to SA-MCF (Hoffman and Young, 1989).

Initially, only circumstantial evidence connected sheep to the disease (Reid *et al.,* 1984). The observation of herpesvirus particles in a sample obtained from a rabbit with experimental SA-MCF suggested that a herpesvirus was the causative agent (Schuller *et al.,* 1990). Also, sheep sera were found to contain antibodies, which were reactive to AlHV-1 although they were not virus neutralising (Rossiter, 1981). In fact, >95% of sheep from many different countries have antibodies that react with antigens of AlHV-1 in immunofluorescence tests (Florzinek, 1990). In addition, cattle with SA-MCF had antibodies that were reactive to AlHV-1 although they too were not virus neutralising (Rossiter, 1983). These studies suggested that SA-MCF and WA-MCF were caused by two very similar, but not identical, agents. This evidence implicated OvHV-2 as the causal agent of SA-MCF (Baxter *et al.,* 1993). Unlike AlHV-1, OvHV-2 has not been isolated though it has been partially characterised (Baxter *et al.,* 1997).

Screening of a genomic library obtained from a lymphoblastoid cell line from an SA-MCF infected cow using probes from AlHV-1 DNA showed that OvHV-2 DNA had high homology to AlHV-1 DNA (Bridgen and Reid, 1991). A PCR test has since

been developed to detect OvHV-2 specifically. The primers do not amplify DNA from AlHV-1 or other related viruses and can be used to diagnose clinical cases. Evidence that sheep are the carriers of the causal agent was strengthened when sheep peripheral blood leukocytes were tested by PCR and shown to contain OvHV-2 DNA (Baxter *et al.,* 1993).

Recent work has been carried out during which almost the entire OvHV-2 genome has been cloned into cosmids. Sequence analysis of these should resolve some of the mystery surrounding OvHV-2 and they also provide the possibility of having an infectious clone of OvHV-2, which could be used in further studies (J. Rosbottom, R.G. Dalziel and J.P. Stewart, pers. comm.).

1.4 Transmission

1.4.1 Transmission of WA-MCF

Wildebeest are infected with AlHV-1 while *in utero* and AlHV-1 has been shown to be present in foetal spleen but not in wildebeest foetal membranes and fluid released during parturition, making it unlikely that these substances are the source of infection for cows as had been thought. Also, scavengers remove these substances from pastures (Rossiter *et al.*, 1983). AlHV-1 has been isolated from nasal and ocular secretions and from nasal turbinate cells harvested from wildebeest calves. The calves display viraemia during the first three months of life, when virus particles are secreted, but overcome it at a time coincident with production of neutralising IgA antibodies (Mushi *et al.,* 1980a; Barnard and Van de Pypekamp, 1988). It is likely that pastures which are grazed by cattle are contaminated by the secretions of young

wildebeest calves. Alternative explanations of transmission, such as droplet inhalation, are unlikely when the wildebeest and cattle are far apart (Rossiter *et al.*, 1983). Nevertheless, some cases have occurred where there is substantial distance between the natural and susceptible hosts, for which there is still no explanation.

The seasonal occurrence of WA-MCF is in accordance with wildebeest calves being the source of infection (Mushi *et al.,* 1980a). An interesting exception to this seasonal pattern is seen in South Africa where the disease has been reported to have occurred through non-direct contact and when wildebeest calves are 8-10 months old, not under 3 months. Climatic conditions and bad diet resulting in stress and subsequent virus reactivation in the calves have been implicated, as have vectors such as flies which may act as intermediates in virus transmission (Barnard and Pypekamp, 1988). At the moment there is no evidence to support this last suggestion and indeed there is some to discount it. Although African face flies (*Musca xanthomelas*) were able to carry AlHV-1-infected material after feeding on wildebeest tears, they would have to regurgitate into the eyes of cattle within 30 minutes for transmission of the virus to occur. Furthermore, the titre of the virus they could carry was so low that transmission was deemed to be highly unlikely (Barnard *et al.,* 1990).

1.4.2 Transmission of SA-MCF

Seasonal occurrence of SA-MCF has been noted in a similar fashion to WA-MCF. A high incidence of the disease is associated with the lambing season (Buxton and Reid, 1980; Baxter *et al.,* 1997). As with WA-MCF, the virus is transmitted from the

natural host, the sheep, to susceptible hosts such as cows and deer but not between the susceptible hosts (Reid, 2000).

In conclusion, there appears to be more than one mode of transmission of MCF. The theory of intermediate vectors has not been totally discounted and a mystery remains on how transmission occurs over large distances.

1.4.3 Experimental transmission

A variety of experiments have been carried out to determine transmissibility of MCF-causing viruses to various species. Unlike natural transmission which usually occurs as a result of close proximity of susceptible species to host species, experimental transmission involves inoculation of blood products or cell suspensions derived from the spleen, lymph nodes, kidney, brain and tonsils of the carrier animal.

In one such experiment inocula consisting of lymph node or peripheral blood leukocyte suspensions from SA-MCF-affected cattle were administered to calves, rabbits and deer. To assess whether the disease had been transmitted, typical signs of MCF such as fever followed a few days later by catarrhal discharge and diarrhoea were used. All the cases in rabbits were confirmed by histology. The results showed that transmission from cattle to calves was possible but not consistent and from cattle to deer was unsuccessful. In one case where transmission to a calf was successful, it was able to be subpassaged to another calf and a rabbit. Transmission from affected deer to unaffected deer and to rabbits was successful. Transmission to calves was still unsuccessful even when subpassaging the virus from these rabbits and infecting with

suspensions as described. Incubation times varied from around 50-90 days in the calves to 5-17 days in the rabbits. Also subpassaged virus from rabbits was used to infect Syrian hamsters which reacted within 24-45 days; virus continued to be passaged in this species. It is not clear why the transmission success varies between cattle and deer to such an extent (Reid *et al.*, 1986).

Perinatal lambs have been tested for presence of OvHV-2. The results showed that perinatal lambs were largely uninfected with OvHV-2 and lambs removed from the flock at 2.5 months of age could be OvHV-2-free. (Li *et al.*, 1998). With a view to determining whether OvHV-2-free sheep could remain so, studies were carried out to investigate experimental transmission of SA-MCF in adult sheep and lambs. They showed that both were susceptible to OvHV-2 infection. Transmission was carried out by intravenously injecting leukocytes or whole blood from OvHV-2-positive sheep or by housing OvHV-2-free sheep with sheep infected with the virus. In fact, the efficiency of transmission of the virus was more successful by horizontal means than by direct inoculation of whole blood. Successful infection was measured by PCR. Furthermore, injection of peripheral blood leukocytes did not result in infection. The authors have conjectured that this may mean the virus infection in the leukocytes is largely unproductive (Li *et al.*, 1999; Li *et al.*, 2000b).

Rabbits have been important as experimental models of both WA-MCF and SA-MCF as when they are infected with the virus or virally-infected material, they show similar symptoms to those seen in the natural disease (Buxton and Reid, 1980). The use of rabbits along with cows and monolayer tissue culture was used for propagation

of AlHV-1 ultimately leading to its isolation (Plowright *et al.*, 1960). Rabbits have since been used in the investigations of the symptoms, transmission and molecular basis of the disease (Buxton and Reid, 1980; Reid *et al.,* 1984).

Alternative animal models for MCF were also investigated. Hamsters are highly susceptible to both WA-MCF and SA-MCF and show typical signs of the disease whereas mice do not show any symptoms. Rats and guinea-pigs are susceptible to WA-MCF but resistant to SA-MCF (Jacoby *et al.,* 1988a and b; Dinter and Morein, 1990; Bridgen *et al.,* 1992).

1.5 Target cells

Much work has been carried out to examine the target cells involved in MCF, particularly SA-MCF. Lymphoblastoid cell lines have been derived from both AlHV-1- and OvHV-2-infected animals, including cattle, deer and rabbits, which have the characteristics of large granular lymphocytes (LGLs). LGLs can be natural killer (NK) cells or cytotoxic T-cells as the latter type can also assume the granular morphology (Abbas *et al.*, 1994). Cultures of this cell type can be obtained from a range of tissues, such as thymus, spleen, lymph node or cornea from MCF-infected animals. The generation of these cell lines is difficult but can be improved by the addition of feeder cells and rIL-2 to the medium. The derived cell line can lose the requirement for these over time (Reid *et al.*, 1989).

LGLs cultured from infected red deer and cattle were shown to be cytotoxic for both primary cell cultures and for established cell lines. Examples of the cells used were

bovine and ovine kidney cells, BT cells and deer testes cells. This activity was not directed only to histocompatible target cells but also to heterologous cells. This led to the suggestion that these cells have NK cell-like activity and are not classical cytotoxic T-cells (Reid *et al.,* 1989).

The LGLs have been described as having similar properties to lymphokine-activated killer (LAK) cells which are NK cells with enhanced cytotoxicity due to cytokine stimulation. Also, following addition of IL-2, the LGLs acquire T-cell markers. The difference between LGLs obtained from a cow with MCF and similar cell populations obtained from a healthy animal is not the ability to kill, but the ability of the cells from a diseased animal to be propagated in culture for long periods of time. It has been extrapolated from this that infection by the virus may therefore enhance the cell's ability to proliferate (Cook and Splitter, 1988).

T-lymphocytes involved in mediating the immune reponse can be classified according to their surface markers. Cytotoxic T-lymphocytes are CD8+ and CD4- whereas helper T-lymphocytes have the opposite marker profile. Monoclonal antibodies and a fluorescent activated cell sorter (FACS) are used to detect and analyse the surface markers on the LGLs. In one study, the LGLs from three cows were classified as cytotoxic lymphocytes on the basis that they were CD8+/CD4- although one other cow did have LGLs with the opposite marker profile and thus were classified as helper lymphocytes. Two cell lines derived from infected deer in this study were found to be CD4-/CD8-. Both sets of LGLs, from the cattle and the deer, were classified as NK cells and all contained virus DNA sequences. Only the

deer cell lines could transmit the disease to both deer and rabbits. The bovine LGLs could not transmit the disease. Thus this study suggests that there are three T-cell subsets, CD4+/CD8-, CD4-/CD8+ and CD4-/CD8-, and only the latter is involved in the pathogenesis of MCF (Burrells and Reid, 1991). However, this conclusion may be misleading because the ability to transmit the disease may be associated with the species of the infected animal and not the marker profile of the LGLs. As has been mentioned (Li *et al.,* 2000b; Reid *et al.,* 1989) transmission by leukocytes does not always occur efficiently or at all.

The pathogenic mechanism of the virus is thought to be indirect as only one cell in 100 000 was positive for virus DNA or virus antigen in a lymph node examination. Immunohistochemical examination utilising monoclonal antibodies for CD43, a pan T-cell marker and proliferating cell nuclear antigen (PCNA) demonstrated extensive T-cell hyperplasia in the spleen and lymph nodes. Analysis of the spleen and lymph nodes in rabbits infected with AlHV-1 showed the T-cell hyperplasia was due to CD8+ T-cell expansion (Nakajima *et al.,* 1992; Schock and Reid, 1996). Since there is very little virus gene expression in MCF lesions, it has been proposed that the virus infection of LGLs disrupts their normal function and leads to polyclonal T-cell expansion (Cook and Splitter, 1988).

Lymphocytes are thought of as the main target cell for MCF infection in rabbits. Virus replication has been observed in the lymphocytes of the spleen followed by other lymphoid organs (Edington and Patel, 1981; Patel and Edington, 1981). However, some infectivity has been detected in macrophages and monocytes

(Rurangirwa and Mushi, 1982). It is possible that these may be carrier cells involved in the spread of virus throughout the body but which do not support productive virus replication themselves. They may also be the underlying cause of immunosuppression of the infected animal because their usual functions such as phagocytosis and antigen presentation may be compromised by the presence of the virus (Mushi and Rurangirwa, 1981b).

Administration of cyclosporin-A, a potent T-lymphocyte suppressor, before infection prevents lymphoproliferation. However, necrosis of tissues still occurs therefore implying that the polyclonal T-lymphocyte proliferation is not directly involved in tissue degradation (Buxton *et al.*, 1984). If the T-cell proliferation in normal disease progression is due to dysregulation of an aspect of the immune system, it is feasible that other aspects of the immune system are also affected so leading to the other symptoms characteristic of MCF.

1.5.1 MCF disease model

A model developed to explain the pathogenesis of MCF, which is both a lymphoproliferative and degenerative disease, is that it is a result of an immune dysfunction caused by virus infection. The traditional roles of the LGLs are to act as NK cells by killing virally infected and transformed cells and suppressing excessive T-lymphocyte responses. If these cells are disrupted by virus infection then in theory unchecked T-cell proliferation and non-specific cell killing would ensue. Indeed, both T-cell hyperplasia and non-specific tissue destruction are seen in MCF (Reid *et al.*, 1984). The normal function of these cells is to kill virally-infected cells, but they

themselves are infected and being 'controlled' by the virus. Dysregulation of the IL-2 cellular messenger has been implicated in having possible involvement in the acute stages of the disease mechanism. The suggestion is that proliferation and necrosis occur in different phases of the disease. The lymphocyte proliferation is due to increased IL-2 production which is as a result of dysregulation of NK cells. The necrosis occurs through a more severe NK cell dysregulation and the destruction of host cells results (Schock and Reid, 1996).

1.6 Treatment and immunisation

There is presently no effective treatment available for MCF. Current advice involves distancing susceptible hosts from reservoir hosts by keeping animals in separate housing or using land not grazed by reservoir hosts. However, this is not always possible for economic or practical reasons. Also the increasing numbers of viruses and potential reservoir hosts may mean that this approach will not always be effective.

Levamisole, a powerful antihelmintic, which works by restoring T-cell function in immunocompromised individuals, was used to successfully treat a gaur with MCF. However, it had no effect on the course of infection in rabbits (Mushi *et al.,* 1980b).

MCF is a serious enough problem in some parts of the world to warrant interest in vaccine development. To date, no suitable vaccine has been developed. One of the first attempts used an avirulent strain of AlHV-1, called WC11, both in a live form and in a formalin-inactivated form, to vaccinate cattle. A formalin-inactivated form

of the virulent C500 form has also been used. Although high levels of virus-neutralising antibodies were produced in every case, this did not confer protection to challenge from virulent virus by exposure to wildebeest herds, implying that humoral mechanisms are not sufficient to confer resistance (Plowright *et al.,* 1975).

This was corroborated by a study investigating MCF in immunosuppressed versus immunostimulated rabbits. There was no change in the course of the disease in the two sets of rabbits, irrespective of the presence of antibodies, implicating the involvement of cell-mediated immunity in protection from virus infection (Rurangirwa and Mushi, 1984).

More successful approaches towards vaccination have involved the use of inactivated virulent cell-free virus as the vaccine. This protected rabbits against challenge by cell-free virulent virus but not cell-associated virus administered in the form of a rabbit lymph node suspension (Edington and Plowright, 1980; Russell, 1980). There has been success against challenge with virus infected rabbit lymphoid cells after immunisation with virus-infected cultured rabbit kidney cells although the immunity diminished after 47 weeks. This is a significant improvement (relative to the lifetime of the rabbit), but potential difficulties are highlighted in previous vaccination experiments that showed some success in rabbits but not in cattle. Moreover, the method used was complex, expensive and therefore impractical (Rossiter, 1982).

There has also been success in immunising cattle with the virulent 707K herpesvirus isolate from MCF-affected cattle in the USA. Two inoculations conferred immunity

in 3 out of 4 cows up to 9.5 months. A disadvantage with this approach was that while one inoculation was not sufficient, repeated inoculations increased the risk of the animal developing the disease (Mirangi, 1991a; Mirangi, 1991b).

Further investigation of the immune response to these viruses as well as more information on the general pathogenesis of MCF is needed to enable an efficient vaccine to be developed.

1.7 Gene expression in gammaherpesviruses

The diversity of cell types and cell function within higher organisms results from the strict regulation of their extensive genetic information. This regulation is achieved by a variety of mechanisms including the organisation of chromosomes into highly condensed, transcriptionally inactive heterochromatin and potentially transcriptionally active euchromatin. Also, methylation of the DNA is associated with transcriptionally inactive regions. In addition, there is control at the sequence level including promoter sequences upstream of the coding sequence and also enhancer sequences that may be position and orientation independent.

In contrast, viruses have a size constraint imposed on their genome. They exploit the cellular regulatory processes to their own advantage. For example, viruses use a wide variety of mechanisms to promote or repress cellular gene expression, in order to create a more favourable cellular environment for replication of its nucleic acid. The main purpose of virus gene expression is to facilitate the production of multiple copies of the virus genome and infectious virions. Despite the constraints on genome

size, virus gene expression is a highly regulated process. The genome sequence is used in a highly efficient manner, with multiple overlapping ORFs and transcriptional control sequences for one gene contained within the sequence of an adjacent gene.

1.8 R-transactivator homologues in gammaherpesviruses

Herpesviruses code for several trans-acting factors, which regulate the gene expression cascade. The sequence of AlHV-1 has shown that AlHV-1 ORF50 has weak homology to other herpesvirus genes such as the BRLF1 gene encoding the Epstein-Barr virus R-transactivator protein (Rta), and the ORF50 genes of HVS, KSHV, MHV-68, BHV-4 and EHV-2 (Ensser *et al.,* 1997). Fortunately, γHV gene nomenclature is largely co-ordinated between different viruses, so in all cases other than EBV this open reading frame is called ORF50. The Rta nomenclature referring to the gene product of BRLF1 has been adopted for the gene products of HVS, KSHV and MHV-68 ORF50.

1.8.1 Epstein-Barr Virus

The Epstein-Barr virus, a human herpesvirus, was discovered in 1964 in tumour samples during a search for the causal agent of endemic (African) Burkitt's lymphoma (Epstein *et al.,* 1964). It is now known that EBV infects the majority of the world's adult population and persists throughout life without causing serious illness. However, if primary infection is delayed, teenagers may suffer from infectious mononucleosis. More significantly, EBV is associated with many human malignant proliferations including lymphomas and oral hairy leucoplakia in

immunocompromised individuals such as AIDS patients, endemic Burkitt's lymphoma in children, where falciparum malaria is hyperendemic, and nasopharyngeal carcinoma in Chinese and Inuit adults. EBV is also a powerful immortalizing agent *in vitro* (Epstein and Crawford, 1998).

1.8.2 EBV transactivators

EBV has several transactivators, namely R, Z, M and EBNA-1 and -2. The gene transcripts for BZLF1 which encodes the Z-transactivator (also known as Z, Zta, ZEBRA or EB1) and BRLF1 which encodes the R-transactivator (also known as R or Rta) are the only IE RNAs (Biggin *et al.,* 1987). The products of BZLF1, BRLF1 and BMLF1 (Zta, Rta and Mta, respectively) are key EBV gene expression regulators (Farrell, 1989). Rta and Mta homologues are present in all γHV family members whereas Zta homologues are absent or are not well conserved (Ragoczy *et al.*, 1998).

Zta and Rta both seem to function in a cell-specific manner, sometimes working in synergy (Holley-Guthrie *et al.,* 1990). Zta is expressed from two promoters, one giving a monocistronic mRNA and one as a bicistronic mRNA along with Rta (Ragoczy *et al.,* 1998).

The EBV R-transactivator was identified in 1988 and shown to activate several virus promoters including one promoter producing a cytoplasmic early antigen which is homologous to the Bcl-2 oncogene (Hardwick *et al.,* 1988). Rta also transactivates the promoter for the BMLF1 gene which encodes the Mta transactivator (Gruffat *et al.,* 1992). Rta-responsive elements have been identified in the promoters of genes

induced by Rta. The transcriptional activation domain is located in the C-terminus of Rta. *In vitro*, Rta has been shown to bind as a homodimer to an Rta responsive element (Manet *et al.,* 1991). In contrast, it can autoregulate itself as well as the EBV DNA polymerase gene through an indirect mechanism (Zalani *et al.,* 1992; Liu *et al.,* 1996). Rta activates the Zta promoter (Ragoczy and Miller, 1999) and has also been shown to activate the human c-myc promoter in transient transfection assays (Gutsch *et al.,* 1994). In turn, Rta itself can be activated by the Sp1 cellular transcription factor mechanism (Zalani *et al.,* 1992). Thus, Rta acts as a transactivator for both cellular and virus genes and can itself be activated by both cellular and virus transcription factors.

Zta is a sequence-specific DNA-binding transcription factor which binds as a dimer (Lieberman and Berk, 1990). It is a member of the c-Jun/c-Fos/GCN4 family of proteins which bind AP-1 consensus sequences (Chang *et al.,* 1990). Zta interacts directly with TFIID, an essential component of the transcriptional complex and stabilises the interaction of TFIID with DNA (Lieberman and Berk, 1991). Zta activates the promoters for ORFs BMLF1 (Mta) and BMRF1, which codes for a subunit of DNA polymerase, and downregulates promoters encoding latent products (Kenney *et al.,* 1989a). It also activates the Mta promoter although this is probably via an indirect mechanism mediated through the Rta transactivator which is a direct target of Zta (Kenney *et al.,* 1989b). Since Rta induces expression of Zta, both transactivators stimulate their own expression (Sinclair *et al.,* 1991; Flemington *et al.,* 1991). Different domains of the Zta protein are required for the different functions (Kenney *et al.,* 1989a).

1.8.3 EBV transactivators in latent to lytic switch

Both Zta and Rta have been implicated in reactivation of the virus from the latent phase to a lytic cycle. Expression of Zta in latently infected B-lymphocytes induced the lytic cycle (Countryman and Miller, 1985; Chevallier-Greco *et al.,* 1986; Takada *et al.,* 1986). Previous studies had shown that Rta alone was unable to disrupt latency in a lymphocyte cell line and it was thought that both Zta and Rta may be required (Cox *et al.,* 1990). However, it has since been shown that Rta can disrupt latency in a B-cell line as well as in epithelial cells (Ragoczy *et al.,* 1998; Zalani *et al.,* 1996). Thus either protein appears to be sufficient for reactivation.

1.8.4 EBV transactivators - interaction with the cell cycle

A common strategy of DNA viruses is to interfere with the regulation of the cell cycle to enable their propagation to continue (Swenson *et al.,* 1999). Rta has been shown to bind *in vivo* to the retinoblastoma protein (pRB), a cell cycle regulator, after lytic cycle intitiation. This binding occurs in conjunction with the release of E2F, a transcription factor, from the RB-E2F complex (Zacny *et al.,* 1998). Zta has been shown to bind *in vivo* to p53, a tumour suppressor protein, thereby inhibiting the transactivation ability of p53. This interaction also prevents Zta from inducing a latent to lytic switch (Zhang *et al.,* 1994). Zta has been shown to induce a growth arrest (Rodriguez *et al.*, 1999), which could be beneficial to the virus as EBV replication occurs most efficiently in growth-arrested cells. Paradoxically, Rta has been shown to induce S-phase in contact-inhibited fibroblasts.

Caution should be taken when investigating these interactions in isolation. Clearly, complex mechanisms are occurring involving the two key EBV transactivators and host cell cycle regulating proteins, either as a strategy by the virus or as a result of reaction by the host cell, and there may be opposing strategies in different cell types.

1.8.5 Herpesvirus saimiri

The natural host of herpesvirus saimiri (HVS, saimirine herpesvirus-2) is the squirrel monkey (*Saimiri sciureus*) which is apparently unaffected by the virus. When passed to susceptible species such as other new world primates, HVS can cause T-cell lymphomas. It can also transform simian and human T-lymphocytes in tissue culture. The HVS genome has been sequenced (Albrecht *et al.,* 1992) and much work has been carried out on determining the genes responsible for the transforming ability of this virus and on its transactivators.

1.8.6 HVS transactivators

There are two stable IE transcripts detected in HVS-infected cells treated with cycloheximide. These are transcribed from genes homologous to the EBV BRLF1 and BMLF1 genes encoding the R and M transactivators respectively. Initial studies using transient transfections and an HVS delayed-early promoter showed that these gene products also behaved as transactivators and were therefore functionally equivalent to Rta and Mta of EBV. Subsequent analysis of their amino acid sequence indicated that they shared common protein domains with the EBV transactivators (Nicholas *et al.,* 1991). This was the first report to identify an Rta homologue.

The HVS Rta homologue is encoded by HVS ORF50. This ORF encodes for two transcripts; ORF50a is a spliced transcript expressed in the early stages of replication, ORF50b is expressed from a promoter located in the second exon of ORF50a and is expressed later in the lytic cycle. Both products can activate the ORF6 promoter, encoding a component of the major DNA binding protein, but the product of ORF50a is five-fold more effective (Whitehouse *et al.,* 1997a). ORF50 responsive elements have been identified in the ORF6 promoter through deletion analysis and gel retardation assays (Whitehouse *et al.,* 1997b). The ORF50 response elements will be discussed further in Chapter 5.

The Mta homologue of HVS, encoded by ORF57, can either activate or repress promoters depending on the absence or presence of an intron within the coding region. The ORF57 gene product activates expression when there is no intron (Whitehouse *et al.,* 1998a). The mechanism underlying this action may involve the redistribution of the spliceosome complex by the ORF57 gene product (Cooper *et al.,* 1999). ORF57 therefore controls gene regulation through a post-transcriptional mechanism (Whitehouse *et al.,* 1998b). The domains of ORF57 required for these various functions have been identified. A hydrophobic domain is involved in transactivation and nuclear localisation and a zinc finger-like domain is required for the transactivation, repression and the spliceosome redistribution functions (Goodwin *et al.,* 2000).

Similar to the situation in EBV, in which Rta activates Mta expression, the ORF50a gene product of HVS activates the ORF57 gene. In turn the ORF57 gene product

downregulates expression of ORF50a therefore creating a negative feedback mechanism. In contrast, the ORF57 gene product enhances the transactivation ability of ORF50b (Whitehouse *et al.,* 1998a and b). The C-terminus of ORF50b is essential for transactivation. This activation domain contains essential hydrophobic residues and is necessary for interaction with the TATA-box binding protein (TBP). These hydrophobic residues are commonly found in activation domains, for example in the herpes simplex VP16 protein and in EBV Rta (Hall *et al.,* 1999).

A very recent study investigating the mechanism of the latent-lytic switch in HVS has reported that the HVS ORF50a protein under the control of the CMV IE promoter, though not its own promoter, can reactivate the virus in the A549 cell line in which HVS is maintained as an episome. The lytic replication cycle is induced resulting in infectious virus particles (Goodwin *et al.,* 2001).

1.8.7 Kaposi's Sarcoma-associated herpesvirus

Kaposi's sarcoma-associated herpesvirus (KSHV) or human herpesvirus-8 (HHV-8) was discovered in 1994 (Chang *et al.,* 1994). KSHV is associated with Kaposi's sarcoma, primary effusion lymphoma (PEL) and multicentric Castleman's disease (MCD) (Schulz, 1998). Since its discovery there has been intense research on KSHV and it too has been sequenced (Russo *et al.*, 1996). The genome has several genes which are homologues of genes encoding cell cycle regulatory proteins and signalling molecules such as IL-6, CC chemokines, interferon response factor, OX-2 (N-CAM transmembrane protein), Bcl-2, cyclin D2 and G-protein coupled receptor homologue IL-8R (Russo *et al.,* 1996; Neipel *et al.,* 1997).

1.8.8 KSHV Transactivators

KSHV has homologues of ORF50 and ORF57 (Russo *et al.,* 1996). Also, K8, which was first thought to be a unique KSHV gene, is a Zta positional homologue (Lin *et al.,* 1999). One IE transcript of KSHV that was identified encoded ORF50 and K8 (Zhu *et al.,* 1999; Seaman *et al.,* 1999). KSHV ORF50 is classified as an IE gene, being expressed 4 h after chemical induction in the presence of cycloheximide. K8 is classified as an early gene, which appeared 8-13 h after stimulation. ORFK8 is not always expressed with ORF50 (Sun *et al.,* 1999). For KSHV the gene product of ORF50 is referred to as KSHV/Rta.

The KSHV Zta homologue is called K-bZIP because like EBV Zta, it belongs to the basic-leucine zipper (bZIP) family of transcription factors. There are several spliced variants of the K-bZIP protein. The C-terminus of full-length K-bZIP is involved in forming homodimers (Lin *et al.,* 1999). In one study K-bZIP could not heterodimerise with other members of the bZIP family, such as c-Jun and c-Fos, and likewise EBV Zta only formed homodimers. K-bZIP is a structural homologue of Zta but it is not yet known whether it is a functional homologue (Gruffat *et al.,* 1999). No Zta homologue has been found in the other γHVs (Zhu *et al.,* 1999).

In transient transfection reporter assays, KSHV/Rta activated the early promoters for polyadenylated nuclear RNA (PAN-RNA [also called nut-1]), TK, DNA binding protein (DBP) and kaposin. Two late promoters for the assembly protein and glycoprotein B genes were not activated by KSHV/Rta (Lukac *et al.,* 1998). KSHV/Rta was also capable of auto-activation as shown both by reporter assays and

by induction of ORF50 from latent viral genomes after transfection of an ORF50 expression plasmid (Deng *et al.,* 2000).

The activation of PAN RNA by KSHV/Rta was investigated further. PAN-RNA is a novel non-coding RNA. It is also the most abundant (80%) of all KSHV poly-A transcripts. An Rta-responsive element in the PAN-RNA promoter was identified and purified. KSHV/Rta was shown to bind very stably to this element (Song *et al.,* 2001).

Recent work has proposed that KSHV/Rta activates two classes of lytic promoters: 1) highly responsive promoters activating other virus regulatory proteins such as K-bZIP and ORF57 and 2) less responsive promoters driving genes such as PAN-RNA and kaposin. Two different response elements have been identified to which KSHV/Rta binds either directly or indirectly through a cellular complex (Lukac *et al.,* 2000). The response elements will be discussed further in Chapter 5.

The ORF57 gene product of KSHV acts through post-transcriptional regulation to enhance accumulation of certain virus transcripts, including ORF50, ORF59 and PAN-RNA. The product of ORF57 seems to enhance the activity of KSHV/Rta such that when ORF50 and ORF57 are co-expressed ORF50-responsive promoter activity is enhanced (Kirshner *et al.,* 2000).

The ORF57 gene product localises to the nucleus in a specific punctate distribution and co-localises with the cellular splicing factor SC-35. ORF57 thus shares

properties with ORF57 of HVS and with ICP27 of HSV-1 (Bello *et al.,* 1999).

1.8.9 KSHV transactivators in latent to lytic switch

The KSHV ORF50 gene product, KSHV/Rta, is a potent activator able to activate E and L genes. In a study to investigate the ability of several virus genes to activate lytic gene expression in a B-cell line derived from a PEL tumour, only KSHV/Rta was able to activate the expression of ORF59 (DNA processivity factor) and K8.1 (glycoprotein), two markers for lytic gene expression. This was specific for KSHV/Rta since ORF57, K3 and K5 gene products did not activate these lytic genes. (Lukac *et al.,* 1998).

A similar study was carried out using different lytic gene expression markers. The expression of KSHV lytic genes induced by KSHV/Rta included PAN RNA, viral IL-6, the K8 gene and the K4 gene encoding viral macrophage inflammatory protein II (vMIPII). In this same study the activation of EBV and KSHV lytic genes by KSHV/Rta or EBV Rta or EBV Zta were tested. Each transactivator only activated genes from its parent virus (Sun *et al.,* 1999; Ragoczy *et al.,* 1998).

The lytic cycle is thought to be important for tumour pathogenesis because Kaposi's sarcoma is an endothelial tumour and usually the patient will have had a latent KSHV infection before having a KS tumour. Therefore, reactivation from the B-cells containing latent virus is thought to be necessary (Lukac *et al.,* 1998). If KSHV/Rta controls the entry into the lytic cycle it may therefore be a key factor in tumour development (Sun *et al.,* 1998) and could become a target for therapy. It has been

proposed that since the cellular signalling molecules, which could conceivably be involved in tumour development, are only expressed by KSHV during its lytic cycle, reactivation may be a prerequisite for KS tumours to develop (Lukac *et al.,* 1999). This is not the case for EBV, which is associated with lymphoid tumours, and may not be the case for the other KSHV-associated neoplasia, MCD and PEL.

KSHV/Rta contains phosphorylation sites for protein kinase C. Activators of protein kinase C also activate the lytic cycle. The C-terminus of KSHV/Rta contains an activation domain. Removal of this domain results in a protein that acts in a dominant negative manner and which is able to form multimers with full-length KSHV/Rta. When this truncated form is expressed in latently infected cells the lytic cycle is no longer induced by usual chemical stimulation. Reactivation and virus replication are both suppressed. These experiments indicate that KSHV/Rta plays an essential role in lytic replication and it is thought to be a molecular switch controlling transition from latency to a lytic cycle (Lukac *et al.,* 1999).

Another study reported the ability of KSHV/Rta to activate virus interferon regulatory factor (vIRF) and virus DNA polymerase promoters in three cell types (Chen *et al.,* 2000). This contradicts a previous study, which stated that KSHV/Rta did not activate the DNA polymerase promoter (Lukac *et al.,* 1999). Chen *et al.* also deleted two putative nuclear localisation signals (NLS) from ORF50, which abolished its transactivation ability. Functional Sp1 binding sites were identified in the vIRF promoter and it was suggested that they might be involved in its transactivation by ORF50 (Chen *et al.,* 2000).

A recent study using the HH-B2 PEL cell line showed that a plasmid expressing ORF50 was able to initiate the lytic cycle as measured by determining lytic virus DNA replication, late gene expression and virus release (Gradoville *et al.,* 2000). The other studies mentioned had not examined whether the lytic cycle goes to completion. This study suggests KSHV/Rta alone has the capacity to initiate the lytic cycle, which then goes to completion.

1.8.10 Murine gammaherpesvirus-68

MHV-68, a natural pathogen of rodents, is used as a small animal model to study the pathogenesis and immunology of γHV infection. This small animal model is preferable to the primate models used for HVS (Virgin *et al.,* 1997; Nash *et al.,* 2001).

1.8.11 MHV-68 transactivators

The MHV-68 genome has been sequenced by two groups (Virgin *et al.,* 1997; Nash *et al.,* 2001) and has revealed the presence of an Rta homologue, encoded by ORF50, which is expressed as an IE gene. MHV-68 also has an Mta homologue (ORF57). The ORF50 promoter has been identified and there are two ORF50 transcripts produced. The ORF50 gene product has been shown to activate the ORF57 promoter (Liu *et al.,* 2000).

In vitro the Rta of MHV-68 is capable of disrupting latency and activating virus replication resulting in a complete lytic cycle and production of infectious virus

particles from the S11E cell line (derived from a mouse B-cell lymphoma), which is latently infected with MHV-68 (Wu *et al.,* 2000).

1.9 Project Background

ORF50 has been implicated as one of the genes affected by the deletion and/or rearrangement of the genome that occurs in AlHV-1 following prolonged passage through tissue culture.

The ORF50 homologues of other herpesviruses have been shown to be of major importance both in the crucial mechanism of reactivation, in inducing the cascade of gene expression and in affecting cell cycle regulation. Many functions are conserved through members of the same family of viruses and this is true of the key roles of ORF50 homologues. There is currently a dearth of information on the functions of specific AlHV-1 genes. The potential importance of the ORF50 gene product in the virus life cycle, reactivation and pathogenesis of MCF makes it an excellent candidate with which to engage in functional molecular studies. In keeping with the nomenclature of the other γHVs, the AlHV-1 ORF50 gene product will be referred to as AlHV-1/Rta throughout.

> "The (MCF) disease process is one of the most devastating in nature and its elucidation at the molecular level will provide fundamental information on immunological control mechanisms and viral pathogenesis." (Reid, 2000)

1.10 Project Aim

The aim of this project is to characterise AlHV-1 ORF50.

Chapter 2 – MATERIALS AND METHODS

2.1 Materials

2.1.1 Chemicals and solutions

Unless otherwise stated, all chemicals were obtained from Sigma (Sigma-Aldrich Company Ltd., Fancy Road, Poole, Dorset, BH12 4OH, England) or ICN Biochemicals (ICN Pharmaceuticals Ltd., 1 Elmwood, Chineham Business Park, Basingstoke, Hampshire, RG24 8WG).

All solutions were made using Milli-Q deionised water (dH_2O) (Millipore).

General solutions

TE buffer:	10 mM Tris-HCl pH 7.9 1 mM EDTA
PBS (phosphate buffered saline) (pH 7.4)	137 mM NaCl 2.7 mM KCl 4.3 mM Na_2HPO_4 1.4 mM KH_2PO_4

Solutions for agarose gel electrophoresis

TAE buffer (pH 8.3)	40 mMTris-acetate 1 mM EDTA
6x Loading buffer	10% (w/v) Ficoll 0.25% (w/v) bromophenol blue 0.25% (w/v) xylene cyanol 0.4% (w/v) orange G 10 mM Tris-HCl pH 7.5 50 mM EDTA

Solutions for small scale preparation of plasmid DNA

Resuspension solution	50 mM glucose 25 mM Tris-HCl pH 8.0 10 mM EDTA
Denaturation solution	0.2 M NaOH 1% (w/v) SDS
Neutralisation solution	3 M KAc 2 M acetic acid

Bacterial growth medium

Luria-Bertani (LB) broth:	10 g/l bactotryptone 5 g/l bacto yeast extract 10 g/l NaCl
LB Agar:	LB broth plus 15 g/l bacto-agar
SOC medium:	LB broth 10 mM glucose 10 mM $MgSO_4$ 20 mM $MgCl_2$

Solutions for preparation of DNA from cell-associated virus

RSB (resuspension solution buffer)	10 mM NaCl 1 mM $MgCl_2$ 10 mM Tris-HCl pH 7.5
TNE	10 mM Tris-HCl pH 8.0 100 mM NaCl 1 mM EDTA

Solution for mammalian cell work

Versene (pH 7.2)	200 μg/ml EDTA 1% phenol red sterile PBS

Solutions for RNA work

20x SSPE (pH 7.4)	3 M NaCl 0.2 M $NaH_2PO_4.H_2O$ 20 mM EDTA
20x SSC (pH 7.0)	3 M NaCl 0.3 M sodium citrate
50x Denhardt's solution	1% (w/v) Ficoll 1% (w/v) polyvinylpyrrolidone 1% (w/v) BSA
10x RNA gel-running buffer (pH 7.0)	0.2 M 3-(N-Morpholino)propanesulfonic acid (MOPS) 80 mM sodium acetate 10 mM EDTA
10x RNA gel-loading buffer	50% (v/v) glycerol 1 mM EDTA pH 8.0 0.25% (w/v) bromophenol blue

RNA marker staining solution	0.2% (w/v) methylene blue 0.4 M acetic acid 0.4 M sodium acetate

Solutions for protein work

12% SDS-PAGE resolving gel	12% (v/v) acrylamide* 0.375 M Tris-HCl pH 8.8 0.1% (w/v) SDS 0.1% (w/v) ammonium persulphate** 0.04% (v/v) TEMED**
5% SDS-PAGE stacking gel	5% (v/v) acrylamide* 0.125 M Tris-HCl pH 6.8 0.1% (w/v) SDS 0.1% (w/v) ammonium persulphate** 0.1% (v/v) TEMED**
SDS-PAGE running buffer	48 mM Tris-HCl 0.5% (w/v) SDS 39 mM glycine
Lysis Buffer	100 mM Tris-HCl pH 6.8 20% (v/v) glycerol 2% (w/v) SDS 0.7 M 2-mercaptoethanol 0.2% (w/v) bromophenol blue

Solutions for electrophoretic mobility shift assays

Buffer C	20 mM HEPES 20% (v/v) glycerol 0.42 M NaCl 0.2 mM EDTA 1.5 mM $MgCl_2$ 0.25 mM DTT (added just prior to use) 0.5 mM PMSF (added just prior to use)
D100	20 mM HEPES 20% (v/v) glycerol 0.1 M KCl 0.2 mM EDTA 0.25 mM DTT (added just prior to use) 0.5 mM PMSF (added just prior to use) 100 mM NaCl

TBE buffer (pH 8.3)	45 mM Tris-borate 1 mM EDTA
4% non-denaturing polyacrylamide gel	4% (v/v) acrylamide* 0.5x TBE 0.1% (w/v) ammonium persulphate** 0.2% (v/v) TEMED**

*Molar ratio of acrylamide:N,N'-methylenebisacrylamide is 29:1 (BioRad).
** Added just prior to pouring gel.

2.1.2 Table 2.1: Cloning vectors

Vector	Source	Size (bp)	Selection	Eukaryotic Promoter
pGEM-T Easy TA cloning vector	Promega	3018	Amp	None
pLXSN Retroviral vector	Clontech	5900	Amp/Neo	MMLV LTR
pEGFP-N1 N-terminal enhanced fluorescent protein vector	Clontech	4700	Kan/Neo	CMV IE
pEGFP-C1 C-terminal enhanced fluorescent protein vector	Clontech	4700	Kan/Neo	CMV IE
pGL3-Basic vector	Promega	4818	Amp	None
pGL3-Promoter vector	Promega	5010	Amp	SV40
pRL-SV40 vector	Promega	3705	Amp	SV40
pcDNA3.1(-)/ *myc*-His A,B.	Invitrogen	5500	Amp/Neo	CMV IE

Abbreviations used in table:
LTR - long terminal repeat, MMLV - Moloney murine leukaemia virus, CMV IE - human cytomegalovirus immediate-early promoter, SV40 - simian virus 40.
E.coli drug selection: Amp - Ampicillin, Kan - Kanamycin.
Mammalian cell selection: Neo - Neomycin.
EGFP - enhanced green fluorescent protein.

2.2 Molecular techniques

2.2.1 Polymerase chain reaction

The polymerase chain reaction (PCR) was carried out in a total volume of 50 µl including 1 µl of 1 U/µl Taq polymerase (Boehringer Mannheim/Roche), 5 µl of 10x reaction buffer (100 mM Tris-HCl, 15 mM $MgCl_2$, 500 mM KCl (pH 8.3)), 10 ng of template, 100 ng of each primer, 10 mM dNTP mix (Sigma), 1.5 mM $MgCl_2$ and dH_2O.

A Hybaid Omnigene PCR machine or Hybaid PCR Sprint thermal cycler was used. The standard PCR programme was 1 cycle of 96°C for 2 min; 40 cycles of 96°C for 1 min, 50°C for 1 min and 72°C for 1 min and finally 1 cycle of 72°C for 7.5 min. The annealing temperature was varied and is stated for individual primer pairs. PCR products (25 µl) were analysed on an agarose gel and in some instances bands were excised from the gel for purification.

All primers were obtained from MWG-Biotech. The annealing temperature for each primer was calculated as follows:

[(Number of Gs + Cs) x 4] + [(Number of As + Ts) x 2)] – 5 = annealing temperature

(Suggs *et al.*, 1981)

If a restriction endonuclease recognition site was present in the oligonucleotide primer, its sequence was not included in this equation. Reactions were optimised by varying annealing temperature, $MgCl_2$ concentration, pH or by adding DMSO or glycerol (Pomp and Medrano, 1991).

2.2.2 Reverse transcriptase-polymerase chain reaction (RT-PCR)

DNase I (Gibco BRL Life Technologies) was used to remove DNA from the RNA preparation. To 1 μg of RNA, 1 μl of 10x DNase I buffer (200 mM Tris-HCl pH 8.4, 20 mM $MgCl_2$, 500 mM KCl) and 1 μl of DNase I (1 U/μl) was added and the mixture made up to 10 μl with RNase-free dH_2O. This was incubated at room temperature for 15 min. The DNase I was inactivated by addition of 1 μl of 25 mM EDTA and incubation at 65°C for 10 min.

Superscript II RNase H^- Reverse Transcriptase (Gibco BRL Life Technologies) was used for the reverse transcription reaction. To 1 μg of RNA, which had been treated with DNase I, 1 μl of oligo d(T) primer (500 μg/ml) was added along with 1 μl of dH_2O to make a final volume of 12 μl. This sample was incubated at 70°C for 10 min. To the mixture, 4 μl of 1st strand buffer (250 mM Tris-HCl (pH 8.3), 375 mM KCl, 15 mM $MgCl_2$), 2 μl of 0.1 M DTT and 1 μl of 10 mM dNTP mix was added. The sample was then incubated at 42°C for 2 min followed by addition of 1 μl (200 U) of Superscript II reverse transcriptase and a further incubation at 50°C for 50 min. The enzyme was inactivated by incubating at 70°C for 15 min. PCR was carried out as in section 2.2.1. One tenth of the reverse transcribed sample was used in a PCR reaction.

2.2.3 Restriction endonuclease digest of DNA

Restriction enzymes were purchased from New England Biolabs. Reactions were carried out in a volume of 20 μl – 50 μl with 1 U of enzyme per 1 μg of DNA. The buffers used were those supplied by the manufacturer. Reactions were incubated at

37°C for at least 2 h. Digested DNA (20 µl) was analysed on an agarose gel.

2.2.4 Agarose gel electrophoresis of DNA

Samples were loaded onto a horizontal 1% agarose (Bioline) gel made using 1x TAE buffer and containing 1 µg/ml ethidium bromide. The gel was submerged in 1x TAE buffer and samples electrophoresed at a constant voltage (13 cm x 15 cm gels at 100 V or 6 cm x 7 cm gels at 80 V). Loading buffer (6x) was added to PCR products or products of analytical restriction endonuclease digests. The DNA markers used were *Eco*RI and *Hin*dIII fragments of bacteriophage lambda DNA (sizes in bp: 21226, 5148, 4973, 4268, 3530, 2027, 1904, 1584, 1375, 947, 831, 564, 125) (Promega) and a 100 bp DNA Ladder (sizes in bp: 1500, 1000, 900, 800, 700, 600, 500, 400, 300, 200, 100) (Promega). DNA was visualised using a UV transilluminator (UVP inc.) at a wavelength of 302 nm.

2.2.5 Gel extraction of DNA from agarose gels

DNA fragments were extracted from agarose gels using the QIAquick gel extraction kit (QIAGEN). The gel slice containing the band of interest was excised and placed in a micro-centrifuge tube. The addition of proprietary Buffer QG and incubation at 50°C for 10 min with occasional vortexing resulted in solubilisation of the gel. The sample was added to a QIAquick column containing a silica membrane to which the DNA bound. Salts were washed through the column by addition of proprietary Buffer PE, which contains ethanol. The DNA was eluted in 10 mM Tris-HCl pH 8.5.

2.2.6 Dephosphorylation of DNA

The 5' phosphates of linear vector fragments were removed prior to ligation by direct addition of 5 U of shrimp alkaline phosphatase (SAP) (USB Life Science Research Products) to the restriction digest mix. The mixture was incubated at 37°C for 1 h. SAP was heat inactivated by incubating the reaction mix at 65°C for 15 min.

2.2.7 Filling in recessed ends of DNA

DNA fragments with 3'-recessed ends were filled in for use in blunt-end ligations using Klenow polymerase (DNA polymerase I large fragment) in reaction buffer (50 mM Tris-HCl pH 8.0, 10 mM $MgCl_2$, 50 mM NaCl) (Gibco BRL Life Technologies) with 33 μM dNTPs (Sigma). This mixture was incubated at 37°C for 20 min.

2.2.8 Ligation of DNA

Ligations involving the pGEM-T Easy vector contained T4 DNA ligase (3 U) and 1 μl of the 10x T4 DNA ligase buffer (300 mM Tris-HCl pH 7.8, 100 mM $MgCl_2$, 100 mM DTT, 10 mM ATP) and were incubated at 4°C overnight. Ligations involving other vectors contained T4 DNA ligase (3 U) and 1 μl of 10x T4 DNA ligase buffer (660 mM Tris-HCl pH 7.5, 50 mM $MgCl_2$, 10 mM dithioerythritol, 10 mM ATP) (Boehringer Mannheim/Roche) and were incubated at 16°C overnight. For blunt-ended ligations, T4 DNA ligase (3 U) and 2 μl of 5x T4 DNA ligase buffer (250 mM Tris-HCl pH 7.6, 50 mM $MgCl_2$, 5 mM DTT, 5 mM ATP, 25% (w/v) polyethylene glycol-8000) (Gibco BRL Life Technologies) were used. The inclusion of polyethylene glycol-8000 in the buffer improves the efficiency of blunt-end ligations. All ligations were carried out in a volume of 10 μl with the exception of those

involving pBeloBAC11, which were carried out in a 20 µl volume using the Gibco BRL Life Technologies T4 DNA ligase and buffer.

2.2.9 Quantification of plasmid DNA

Plasmid DNA was quantified using a CECIL spectrophotometer. To 98 µl of water, 2 µl of plasmid DNA was added and optical density (OD) measured at 260 nm and 280 nm. The figure obtained at 260 nm was multiplied by 50 to account for the dilution of the DNA and by 50 again to obtain the concentration per ml. This is based on the fact that 1 OD unit is equivalent to approximately 50 µg/ml of double-stranded DNA. The ratio of OD values at 260 nm to 280 nm indicated the purity of the DNA. A ratio of 1.8-2.0 indicates that the DNA is pure (Sambrook *et al.*, 1989).

2.2.10 Sequencing of plasmid DNA

Sequencing of all constructs was carried out by Mr. Ian Bennet by automated sequencing using a LI-COR DNA sequencer model 4000L (MWG-Biotech). The primers used were: RVprimer3 (5'-CTA GCA AAA TAG GCT GTC CC) designed for sequence analysis clockwise across the multiple cloning site (MCS) of pGL3 reporter vectors; GLprimer2 (5'-CTT TAT GTT TTT GGC GTC TTC CA) designed for sequence analysis counter-clockwise across the MCS of pGL3 reporter vectors; pUC/M13 forward sequencing primer (5'-GTT TTC CCA GTC ACG AC) and pUC/M13 reverse sequencing primer (5'-CAG GAA ACA GCT ATG AC). pUC/M13 primers are for sequencing inserts cloned into the M13 vector and pUC plasmids.

2.3 Bacterial Work

2.3.1 *Escherichia coli* strains

JM109 competent cells (Promega) were used for transformation of plasmid DNA by heat-shock. ElectroMAX DH10B Cells (Gibco BRL Life Technologies) were used for transformation of the bacterial artificial chromosome pBeloBAC11 vector by electroporation. The genotypes for these two strains are shown in Table 2.2.

Table 2.2: Genotypes of bacteria used for transformations

Strain	Genotype
JM109	*end*A1, *rec*A1, *gyr*A96, *thi*, *hsd*R17 (r^-k^-, mk^+), *rel*A1, *sup*E44, Δ(*lac-pro*AB), [F', *tra*D36, *pro*AB $lac^qZ\Delta M15$]
DH10B	F^-, *mcr*A, Δ(*mrr-hsd*RMS-*mcr*BC), ϕ80d*lac*ZΔM15, Δ*lac*X74, *end*A1, *rec*A1, *deo*R, Δ(*ara*, *leu*)7697, *ara*D139, *gal*U, *gal*K, *nup*G, *rps* L, λ^-

2.3.2 Bacterial growth medium

All bacteria were grown in sterilised Luria-Bertani (LB) medium (Sambrook *et al.*, 1989) with addition of appropriate antibiotics. Agar plates were made with 15 g/l bacteriological agar (ICN Biochemicals) in LB medium.

2.3.3 Transformation of competent *E.coli* cells with plasmid DNA

To 4 µl of ligation mix, 50 µl of JM109 cells (Promega) were added and placed on ice for 20 min. The cells were then heat-shocked for 45 seconds at 42°C and quenched on ice for 2 min. SOC medium (800 µl) was added to the cells and the mixture was incubated at 37°C for 1.5 h with shaking (250 rpm). The cells were then centrifuged in a micro-centrifuge at 3500 xg for 2 min, resuspended in 200 µl of

SOC medium and spread on agar plates containing appropriate antibiotics. All plasmids contained genes encoding either ampicillin or kanamycin resistance. Ampicillin and kanamycin were used at final concentrations of 100 μg/ml and 50 μg/ml, respectively. The plates were inspected after ~18 h at 37°C.

For transformations involving the pGEM-T Easy vector, IPTG (isopropylthio-β-D-galactoside) and X-gal (5-bromo-4-chloro-3-indolyl-β-D-galactoside), both from Bio-Gene Ltd., were spread on to agar plates containing ampicillin before use. X-gal (50 mg/ml stock dissolved in dimethylformamide (AnalaR)) was used at 20 μl per plate and IPTG (0.1 M stock, filter-sterilised) was used at 100 μl per plate.

The pGEM-T Easy vector contains the α-peptide coding region of the enzyme β-galactosidase, which allows identification of recombinant clones by blue/white selection. In the presence of IPTG (a *lac* analogue that permits expression of β-galactosidase) and X-gal (a substrate for β-galactosidase), blue colonies are produced. Insertion of a PCR product into the vector disrupts the β-galactosidase gene, resulting in white colonies.

2.3.4 Small scale preparation of plasmid DNA

After transformation, colonies were picked and grown in 5 ml of liquid LB medium with appropriate antibiotic selection. Preparation of plasmid DNA was carried out using a QIAprep Spin Miniprep kit (QIAGEN). The bacterial cells were harvested by centrifugation at 600 xg for 5 min. The bacterial pellet was resuspended in Buffer P1 (50 mM Tris-HCl pH 8.0, 10 mM EDTA, 100 μg/ml RNase A) and then

incubated in Buffer P2 (200 mM NaOH, 1% SDS) to lyse the bacterial cells. Buffer N3 (3 M KAc pH 5.5) was added to precipitate the genomic DNA, proteins, cell debris and SDS. The supernatant containing the plasmid DNA was separated from the precipitate by centrifugation in a micro-centrifuge, and then passed through a column containing an anion-exchange resin. Addition of proprietary Buffer PB followed by ethanol-containing proprietary Buffer PE to the column removed RNA, proteins and low molecular weight impurities. Plasmid DNA was then eluted in 50 µl of Buffer EB (10 mM Tris-HCl pH 8.5).

2.3.5 Large scale preparation of plasmid DNA

Large preparations of plasmid DNA were made using QIAGEN Plasmid Midi and Maxi kits (QIAGEN). The principle of these kits is the same as the QIAprep Spin Miniprep kit described above, except that the column is first equilibrated with Buffer QBT (750 mM NaCl, 50 mM MOPS pH 7.0, 15% isopropanol, 0.15% Triton X-100) before addition of the supernatant containing the plasmid. Impurities were then removed by 3 washes with Buffer QC (1 M NaCl, 50 mM MOPS pH 7.0, 15% isopropanol). The plasmid DNA was eluted in Buffer QF (1.25 M NaCl, 50 mM Tris-HCl pH 8.5, 15% isopropanol) and precipitated with isopropanol. The pellet was then washed once with 70% ethanol to remove excess isopropanol, air-dried and resuspended in TE buffer.

2.3.6 Transformation of competent *E.coli* cells with BAC DNA (electroporation)

This method was used for the pBeloBAC11 vector. The ligation (section 2.2.8) was carried out in 20 µl, which was made up to 200 µl with TE buffer. Phenol/chloroform

and chloroform extractions were carried out (Sambrook *et al.*, 1989). The sample was then desalted using a microcon-30 column (Amicon) to give a final volume of 10 µl. From the sample, 4 µl was added to 40 µl of electrocompetent DH10B cells. These cells have a higher transformation efficiency for use with larger plasmids. The mixture was transferred to a chilled 2 mm electroporation cuvette (Flowgen) and electroporated (2500 V, 25 µF, 156 Ω, 0.004 ms pulse). SOC medium (1 ml) was immediately added and the sample was incubated in a shaker (250 rpm) for 1 h at 37°C. From this, 100 µl of the mixture was spread on an LB agar plate containing 15 µg/ml chloramphenicol, as a gene encoding chloramphenicol resistance is present in the pBeloBAC11 vector.

2.3.7 Small scale preparation of BAC DNA

Single bacterial colonies were grown overnight at 37°C with shaking in 20 ml of LB medium containing 15 µg/ml chloramphenicol. The cultures were then centrifuged at 6000 xg for 10 min. The pellet was resuspended in 200 µl resuspension solution containing 70 µg/ml lysozyme, added just before use, and transferred to a 1.5 ml micro-centrifuge tube. The tube was incubated for 5 min at room temperature. To lyse the bacteria, 400 µl of denaturation solution was added and the sample was placed on ice for 5 min after mixing by inversion. Ice-cold neutralisation solution (300 µl) was added and after inversion the sample was again placed on ice for 5 min. The sample was centrifuged for 5 min in a micro-centrifuge at 9500 xg. The supernatant was transferred to a new micro-centrifuge tube containing 500 µl of isopropanol and this mixture was placed on ice for 15 min. The sample was centrifuged for 5 min in a micro-centrifuge at 9500 xg. The supernatant was removed

and the pellet was air-dried then resuspended in 200 µl TE to which 100 µl of 7.5 M sodium acetate was added. The sample was placed on ice for 15 min then centrifuged for 5 min at 9500 xg. The supernatant was transferred to a new tube to which 600 µl of ethanol was added and the mixture was incubated at –70°C overnight. The sample was centrifuged at 9500 xg for 10 min and the pellet was air-dried and resuspended in 50 µl TE buffer.

2.3.8 Large scale preparation of BAC DNA

A QIAGEN Plasmid Maxi kit was used, the principle of which has been described in sections 2.3.4 and 2.3.5. The "Protocol for Very Low-Copy Plasmid Purification" was used. This has several modifications to the standard maxi-prep protocol, namely that the culture volume is increased to 2.5 litres, as compared with 100 ml for high-copy plasmids, and the volume of the three buffers used to resuspend the pellet, lyse the cells and precipitate the genomic DNA, proteins and cell debris, is increased from 10 ml to 125 ml. In addition, five columns are used instead of one.

2.4 Mammalian cell and virus work

2.4.1 Mammalian cells

Bovine turbinate (BT) cells were grown in Iscove's medium (Gibco BRL Life Technologies) containing 10% foetal calf serum (FCS) (Globepharm), 70 µg/ml penicillin (Merck BDH), 10 µg/ml streptomycin, 2 mM L-glutamine (Merck BDH) and 250 µg/ml Amphotericin B (an anti-fungal agent) (Merck BDH). BT cells were used up to passage 12, after which time their growth rate was substantially reduced. BT cells were provided by Miss Irene Pow, Moredun Research Institute, Edinburgh.

Baby hamster kidney (BHK) cells and thymidine kinase deficient (TK^-) BHK cells were grown in Glasgow Modified Eagle's Medium (GMEM) containing 10% tryptose phosphate broth (TPB) (Gibco BRL Life Technologies), 10% newborn calf serum (NBCS) (Harlan SeraLab), 70 μg/ml penicillin, 10 μg/ml streptomycin and 2 mM L-glutamine. BHK-21 cells are a continuous fibroblastoid cell line from a Syrian golden hamster (Stoker and Macpherson, 1961). The TK^- BHK cells used were the tk^- ts13 BHK-21 cell line (ATCC CRL-1632) (Talavera and Basilico, 1977), a temperature sensitive (ts) derivative of BHK-21, which was provided by Dr. H. Marsden, MRC Virology Unit, Glasgow.

HeLa (human cervical epithelial cell line) cells were grown in Dulbecco's modified Eagle's medium (DMEM) containing 10% FCS, 70 μg/ml penicillin, 10 μg/ml streptomycin and 2 mM L-glutamine.

To harvest BT, BHK and HeLa adherent cell lines, the medium was removed and the monolayers were washed in 5 ml of 0.02% versene (BT cells) or sterile PBS (BHK cells and HeLa cells). The monolayers were then incubated with 5 ml of 0.25% trypsin/EDTA solution (Gibco BRL Life Technologies) until they detached from the flasks. The cells were resuspended in media by pipetting and seeded into new flasks. BT cells were seeded at 1 x 10^6-3 x 10^6 and BHK cells and HeLa cells were seeded at 2 x 10^6-6 x 10^6 per 175 cm^2 (T175) flask.

2.4.2 Long-term storage of mammalian cells

After trypsinisation of exponentially growing cells, cells were counted using a haemocytometer. Cells were centrifuged at 4500 xg for 10 min and the pellet was resuspended in freezing mix (90% FCS, 10% DMSO) at 1 x 10^6 cells/ml. Aliquots (1 ml) were stored in cryovials, frozen at –70°C overnight in cotton wool and then stored in liquid nitrogen.

2.4.3 Preparation of virus stocks

The C500 strain of AlHV-1 was obtained from Dr. Hugh Reid and Miss Irene Pow, Moredun Research Institute, Edinburgh. This virus was isolated from a blue wildebeest and passaged several times through rabbits. To a T175 flask of BT cells at 80% confluence, 0.3 ml of very low passage virus stock (AlHV-1 C500 20/5/96) was added. Virus-infected BT cells were grown in medium containing 2% FCS. Cells were incubated until signs of CPE were observed (~7 days), at which time they were harvested and pelleted by centrifugation at 4500 xg for 10 min. The pellet was resuspended in 2 ml of medium and 1.8 ml of this was used to infect ten T175 flasks of BT cells. The cells were incubated for 8 days and then harvested and pelleted by centrifugation at 4500 xg for 10 min. The pellets were resuspended in 90% FCS and 10% DMSO, pooled and aliquoted into cryovials (0.5 ml), which were stored in liquid nitrogen.

2.4.4 Preparation of virus DNA from cell-associated virus

Cell-associated virus (AlHV-1 C500 strain) was used to infect five T175 flasks of BT cells, which were harvested when 80% CPE was visible. Since the infected cells

were loosely attached to the flask they were harvested by addition of sterile glass beads to the flask with rocking. The cells were pelleted by centrifugation at 5000 xg for 10 min, washed in PBS, resuspended in a total of 5 ml RSB with 0.5% (v/v) Triton X-100 and Dounce homogenised. To remove cell debris, the cells were centrifuged at 4500 xg for 10 min. Virus particles were separated from cellular DNA by centrifugation through a 25% sucrose cushion in RSB at 114,000 xg for 30 min at room temperature. The pellet containing virus particles was resuspended in TNE and digested with 100 μg/ml proteinase K in the presence of 1% SDS in a final volume of 5 ml. This was incubated overnight at 55°C. An equal volume (5 ml) of phenol/chloroform/isoamyl alcohol (25:24:1) was used to carry out four 10 min extractions followed by two 10 min extractions with chloroform/isoamyl alcohol (24:1). The sample was then made up to 15 ml volume with TE buffer and centrifuged in Centriplus 10°S concentrators (microcon columns) (Amicon) at room temperature for 25 min at 5000 xg. This step was repeated until the volume equalled 1 ml.

2.4.5 Transfection of mammalian cells by electroporation

Cells were harvested as described in section 2.4.1, resuspended in medium lacking FCS or NBCS and 800 μl aliquots of this cell suspension were added to 1.5 ml micro-centrifuge tubes containing DNA in a 50 μl volume. BT cells were used at 5 x 10^5 to 1 x 10^6 cells per sample and BHK cells and HeLa cells were used at 2 x 10^6 cells per sample. The DNA-cell mixture was placed in a 4 mm electroporation cuvette (Flowgen) and electroporated at a capacitance of 1050 μF and a voltage of 300 V in an EquiBio EasyjecT Plus electroporator. After electroporation, cells were

plated immediately onto 60 mm dishes containing 3 ml of medium with FCS or NBCS and assayed after incubation at 37°C for 48 h.

2.4.6 Superinfection of transfected cells

In some experiments, cells were infected with virus 24 h after transfection with promoter constructs, and assayed 24 h subsequently.

2.4.7 Transfection of mammalian cells by SuperFect

SuperFect (QIAGEN) is an activated-dendrimer transfection reagent. Dendrimers are branched spherical molecules with a defined size and shape. Activated dendrimers result from removal of amines from dendrimers, which gives them a flexible structure. They assemble DNA into compact structures in a similar manner to histones with eukaryotic DNA. The complexes have a positive charge, which enables them to bind to negatively-charged molecules on the cell surface, and they are then taken up by non-specific endocytosis.

Plasmid DNA was made up to 150 µl with medium containing no serum or antibiotics, and 15 µl of SuperFect transfection reagent was then added. The mixture was vortexed and incubated at room temperature for 5-10 min. During this incubation the pre-seeded cells, at ~70% confluence, were washed with PBS. Cell culture medium (1 ml) containing serum and antibiotics was added to the tube containing the transfection mix. This was added to the plated cells, which were then incubated for 2 h at 37°C. The medium was removed, cells were washed with PBS and fresh medium was added. The cells were assayed 48 h later.

2.4.8 Luciferase assays

The Luciferase Assay System (Promega) was used to assay transfected cells that had no internal transfection control. The cells were washed in sterile PBS and 250 µl of 1x Reporter Lysis Buffer (25 mM Tris-phosphate, pH 7.8, 2 mM DTT, 2 mM 1,2-diaminocyclohexane-N,N,N',N'-tetra-acetic acid, 10% glycerol, 1% Triton X-100) (Promega) was added to each plate and incubated at room temperature for 15 min. Lysates were harvested and transferred to a 1.5 ml micro-centrifuge tube and centrifuged for 2 min at 3500 xg. The luciferase activity was assayed immediately using a Luminoskan RT luminometer and the proprietary luciferase assay reagent.

2.4.9 Dual-luciferase reporter assays

The Dual-Luciferase Reporter Assay System (Promega) was used when the pRL-SV40 *Renilla* expression plasmid was used as an internal control in each sample along with the firefly luciferase reporter vectors that were being tested. Cells were washed with sterile PBS and incubated for 15 min in 400 µl of proprietary 1x Passive Lysis Buffer. Lysates were harvested and transferred to a 1.5 ml micro-centrifuge tube and centrifuged for 2 min at 3500 xg. The samples were assayed using proprietary firefly Luciferase Assay Reagent II. Proprietary Stop & Glo Reagent was then added which quenches the firefly luciferase signal and provides the substrate for the *Renilla* luciferase. The luciferase activities were assayed using a Luminoskan RT luminometer.

2.4.10 Methods to screen for potential virus recombinants

To screen for recombinant virus after using the strategy described in section 4.3.5,

cells exhibiting CPE were analysed using two methods, DNA hybridisation and PCR.

Cells were harvested, transferred to a 1.5 ml micro-centrifuge tube and centrifuged at 12000 xg for 1 min. The cells were resuspended in 200 µl of PBS then freeze-thawed three times and briefly sonicated in a water-bath sonicator to complete cell lysis. The cell extract (50 µl) was spotted on to a nitrocellulose membrane, which was then placed successively on three filter papers soaked for 3 min each in 0.5M NaOH, Tris-HCl pH 7.5 and 2 x SSC, respectively. The membrane was baked for 2 h at 80°C. It was then incubated for 4 h at 65°C in 6x SSC and 5x Denhardt's solution and hybridised with radioactive probe (see section 2.5.6) for 12-18 h at 65°C. The membrane was washed twice for 15 min each in 2x SSC, 0.1% SDS at 65°C and twice for 15 min each in 0.2x SSC at 65°C. The membrane was air-dried and exposed to Biomax MS Kodak scientific imaging film.

To screen virus recombinants using PCR, cells were resuspended in 400 µl PBS and freeze-thawed and sonicated as above. The cells were disrupted by heating at 95°C for 5 min then placed on ice. The PCR was set up (see section 2.2.1) using 3 µl of the disrupted cell extract.

2.4.11 Microscopy and photography

Cells were routinely examined by light and fluorescence microscopy and photographed. To calculate the magnification of cells, the following equation was used:

Eyepiece lens magnification	x	Objective lens magnification	x	Camera lens magnification	x	Camera reducing factor

e.g. (12.5) x (10) x (1.25) x (0.32) = 50

i.e. the cell magnification is 50x.

2.5 RNA Work

2.5.1 Extraction of total RNA from mammalian cells

Total RNA was extracted from cells using the RNAzol B reagent (Biogenesis). Medium was removed from cell monolayers and they were washed with sterile PBS. To lyse the cells, 0.2 ml of RNAzol B per 1 x 10^6 cells was added directly into the culture flask and the mixture passed through a pipette several times before transferring to a micro-centrifuge tube. To 2 ml of cell homogenate, 0.2 ml of chloroform was added. The samples were then vigorously shaken and incubated on ice for 5 min. The suspension was centrifuged at 12000 xg for 15 min. The upper aqueous phase was transferred to a micro-centrifuge tube, mixed with an equal volume of isopropanol and incubated for 15 min at 4°C. Samples were again centrifuged for 15 min at 12000 xg. The RNA precipitate was washed with 0.8 ml of 75% (v/v) ethanol, centrifuged at 7500 xg for 8 min and resuspended in 200 µl of 1 mM EDTA pH 7.0.

2.5.2 Treatment of cells to obtain RNA from AlHV-1-infected cells

RNA representing the three temporal classes of gene expression in AlHV-1 was obtained. To obtain RNA from expression of IE genes, Iscove's medium containing 2% FCS with cycloheximide (100 µg/ml) was added to BT cell monolayers 30 min

prior to addition of virus and maintained throughout the infection. The cells were harvested 8 h after addition of virus. To obtain RNA from expression of E genes, Iscove's medium containing 2% FCS with phosphonoacetic acid (PAA) (0.1 mg/ml) was added at the time of virus addition and maintained throughout infection. Cells were harvested 24 h later. Addition of PAA, a herpesvirus DNA polymerase inhibitor, prevents DNA synthesis. To obtain RNA from expression of L genes, virus was added with no supplement and harvested 24 h later. In all cases, virus was added in 5 ml of medium and left for 1 h before the volume was increased to 30 ml. In preparation for this experiment, 15 T175 flasks of BT cells were infected with AlHV-1 and a further 15 T175 flasks of subconfluent BT cells were prepared. To each flask of subconfluent BT cells, the cells from one virus-infected flask exhibiting 50-70% CPE were added. RNA was harvested as described in 2.5.1.

2.5.3 Electrophoresis of RNA

This was carried out by the method in Sambrook *et al.* 1989. RNA samples were electrophoresed in a 1.2% agarose gel containing 2.2 M formaldehyde and ethidium bromide (1 μg/μl) made with 1x RNA gel-running buffer. The RNA samples were made up to 5.5 μl with dH_2O. To this was added 1 μl 10x RNA gel-running buffer, 3.5 μl formaldehyde and 10 μl formamide. The 0.24-9.5 kb RNA ladder (Gibco BRL Life Technologies) or the RNA Molecular Weight Marker I (Roche) was prepared in the same manner. All samples were denatured at 65°C for 15 min, cooled on ice and mixed with 2 μl 10x RNA gel-loading buffer. The horizontal gel was submerged in 1x RNA gel-running buffer and electrophoresed overnight at 35 V with recirculation of the buffer.

2.5.4 Northern hybridisation

The gel was washed in 50 mM NaOH, 150 mM NaCl for 30 min and then in 0.1 M Tris-HCl pH 7.5, 150 mM NaCl for a further 30 min. The gel was rinsed with Milli-Q water and soaked in 20x SSC for 45 min. Two pieces of 3MM paper were cut to the size of the gel tank and placed over the platform so that both ends were submerged in the wells of the tank, which were filled with 20x SSC. The gel was placed on the paper. Hybond-N nylon transfer membrane (Amersham), cut to the size of the gel, was soaked in 20x SSC and placed on top of the gel. Two sheets of 3MM paper, cut to the size of the gel, were soaked in 20x SSC and placed on top of the membrane followed by a stack of blotting paper and a 500 g weight. Transfer of RNA from the gel to the membrane took place overnight.

The RNA was cross-linked to the membrane by placing it in a 'Stratalinker' (Stratagene) for 45 seconds, which exposes the membrane to UV with a wavelength of 254 nm.

The marker track was cut from the rest of the membrane after cross-linking and air-dried. It was then incubated in 1 M acetic acid for 10 min at room temperature and then in RNA Marker staining solution for 10 min. Finally, it was washed in sterile distilled water until the blue background disappeared.

2.5.5 Probe labelling

To label a double-stranded DNA probe, 25 ng of DNA in 11 µl dH_2O was boiled for 10 min and quenched on ice. To this, 5 µl of [α-^{32}P] dCTP (10 mCi/ml) (Amersham)

followed by 4 µl of High Prime, containing random oligonucleotide primers, 0.125 mM each of dATP, dGTP and dTTP, Klenow enzyme (4 U) and reaction buffer (Boehringer Mannheim/Roche) were added. This was incubated at 37°C for 30 min. To stop the reaction, 5 µl of 2 M NaOH was added. This was followed by the addition of 100 µl of TE buffer. Labelled DNA was separated from unincorporated radiolabelled nucleotides by gel filtration on NICK columns (Amersham Pharmacia Biotech).

2.5.6 Probing the membrane

The membrane was incubated for 1 h at 45°C in 50 ml of pre-hybridisation buffer. The pre-hybridisation buffer was 5x SSPE buffer, 5x Denhardt's solution, 50% (v/v) formamide, 0.5% (w/v) SDS and 100 µg/ml denatured salmon sperm DNA. The pre-hybridisation buffer was replaced with hybridisation buffer (pre-hybridisation buffer plus 10% (w/v) dextran sulphate and 200 µg/ml instead of 100 µg/ml denatured salmon sperm DNA). The labelled probe was then added and incubated with the membrane overnight at 45°C.

Following hybridisation, the membrane was washed twice in 2x SSC, 1% SDS for 15 min at room temperature and twice in 0.5x SSC, 1% SDS for 15 min at 65°C. The membrane was then washed with TE, excess liquid was removed using 3MM paper, and the membrane was wrapped in clingfilm and placed in a phosphorimager cassette. This was analysed using a phosphorimager (Molecular Dynamics).

2.5.7 Slot blots

Slot blots were carried out using a filtration manifold consisting of a Lucite block containing numerous slots and a suction platform. A piece of nitrocellulose membrane cut to the size of the block was moistened in water briefly then soaked in 20x SSC for 1 h at room temperature. Two pieces of 3MM paper, cut to size, were moistened with 20x SSC. The nitrocellulose membrane and 3MM paper were placed between the block and platform, which were clamped together and connected to a vacuum unit. All slots were filled with 10x SSC, which was suctioned through the membrane and then the slots were refilled with 10x SSC. The RNA samples (0.1 μg and 10 μg) were made up to 10 μl in dH_2O, and 20 μl formamide, 7 μl formaldehyde and 2 μl 20x SSC were added. The samples were heated to 68°C for 15 min then placed on ice. Two volumes of 20x SSC were added to the samples. The 10x SSC in the slots was suctioned through the membrane. The samples were suctioned on to the membrane followed by two rinses with 10x SSC. Suction was continued for 5 min, the membrane was air-dried at room temperature and baked for 2 h at 80°C. The membrane was then probed with labelled DNA as described in section 2.5.6.

2.5.8 5'-rapid amplification of cDNA ends

The 5'-Full Rapid Amplification of cDNA Ends (5'-RACE) Core Set from TaKaRa Biomedicals was used. The principles of 5'-RACE can be found in Frohman *et al.* (1988) and Maruyama *et al.* (1995). The method and result are presented in Figures 3.18 (a) and (b). Reverse transcription was carried out with 5 μg of total RNA using a 5'-end phosphorylated RT primer specific to the ORF57 mRNA, 5'-ATA AAC ACA CGC CGC TTG GC (corresponding to Nt 84761-84742 in the AlHV-1

genome). The DNA-RNA hybrid was treated with RNase H to remove the RNA, leaving the single-stranded cDNA. T4 RNA ligase was used to enable the cDNA to form concatemers. PCR was carried out to amplify the DNA straddling the upstream non-translated region. The primary PCR primers used were S1, 5'-GAG AGT GTG GAC GAT TGC AT (Nt 84673-84692) and A1, 5'-CTC CAG GTG AAA GGA GTC AT (Nt 84672-84653). The secondary PCR primers used were S2, 5'-GCA AAC CAA ACA ATC GCC CTA (Nt 84701-84721) and A2, 5'-GAA TCC TCT GCA GAG ATG TCT (Nt 84650-84630). The PCR product was inserted into the pGEM-T Easy vector and sequenced.

2.6 Protein work

2.6.1 Protein sample preparation

Transfected cell monolayers were washed in PBS and lysis buffer was added. The plates were heated at 80°C for 30 min. The cells and lysis buffer were mixed by pipetting, placed in micro-centrifuge tubes and boiled for 3 min before loading onto an SDS-PAGE gel. The Low Molecular Weight Calibration Markers from Pharmacia Biotech were used to estimate sizes of proteins.

2.6.2 SDS-polyacrylamide gels for protein separation

Electrophoresis was carried out using a 12% resolving gel and a 5% stacking gel. The resolving gel was poured first and a layer of n-butanol was added to smooth the surface and to prevent air reaching the gel, therefore accelerating polymerisation. Once the resolving gel was polymerised the n-butanol was removed and the stacking gel was poured on. The gel was run vertically at 100 V for 1-1/2 h in SDS-PAGE running buffer (Sambrook *et al.,* 1989).

2.6.3 Protein gel staining

The protein gels were fixed and stained using brilliant blue G–colloidal concentrate (Sigma). The gels were fixed for 1 h in a solution containing 7% (v/v) glacial acetic acid and 40% (v/v) methanol. The staining solution was prepared by adding 1 part of methanol to 4 parts of 1x Brilliant Blue G-Colloidal Concentrate working solution and mixed by vortexing. The gel was placed in the staining suspension for 2 h and then destained for 60 seconds in 10% (v/v) glacial acetic acid/25% (v/v)methanol. Finally the gel was rinsed and then soaked in 25% (v/v) methanol for up to 24 h.

2.6.4 Western blots

Proteins separated by SDS-PAGE were transferred onto nitrocellulose membranes using a semi-dry electroblotter. The nitrocellulose membrane, gel and 6 pieces of 3MM paper were soaked in transfer buffer (25 mM Tris-HCl/20% (v/v) methanol). Three pieces of 3MM paper were placed on the blotter, followed by the nitrocellulose membrane, the gel and three more pieces of 3MM paper. Transfer was carried out at 120 mA for 2 h. The protein marker tracks were removed from the rest of the membrane and stained in amido black (working solution: 0.2% (w/v) amido black, 10% (v/v) glacial acetic acid, 90% (v/v) methanol) for 5 min and then destained in 50% (v/v) methanol/5% (v/v) acetic acid. The remainder of the nitrocellulose membrane was blocked in 5% (w/v) non-fat milk powder/0.2% (v/v) Tween 20/PBS for 1 h at room temperature. Primary rabbit antibodies were diluted 1/500 in 1% (w/v) non-fat milk powder/0.1% (v/v) Tween 20/PBS, added to the blot and incubated overnight at 4°C. The membrane was washed 5 times in 0.1% (v/v) Tween 20/PBS and then incubated at room temperature for 1 h in the presence of an

alkaline phosphatase secondary antibody (DAKO pig anti-rabbit) diluted 1/1000 in 1% (w/v) non-fat milk powder/0.1% (v/v) Tween 20/PBS. Five washing steps were carried out as before. The membrane was developed by washing very quickly in 0.1 M Tris-HCl pH 9.5, and then incubated in an alkaline phosphate substrate (Sigma fast 5-bromo-4-chloro-3-indolyl phosphate/nitro blue tetrazolium) to allow bands to develop.

2.7 Electrophoretic mobility shift assays

2.7.1 Preparation of whole cell extracts

To prepare whole cell extracts, 8 x 10^7 transfected BHK cells were washed with PBS, harvested then centrifuged. The pellet was then subjected to three cycles of freeze/thawing at -70°C. An equal volume of Buffer C was added to the pellets, which were then Dounce homogenised 10 times in a micro-centrifuge tube. Debris was removed by centrifugation at 9500 xg for 5 min. The supernatant was frozen in 100 µl aliquots at -70°C.

2.7.2 Preparation of labelled double-stranded oligonucleotides

To make a 500 ng/µl stock of double-stranded oligonucleotides, equal amounts (~50 µl) of each single-stranded oligonucleotide (1 µg/µl) were mixed and boiled for 10 min, and allowed to cool slowly to room temperature. The stock was diluted 1:5 with buffer D100 to make a working solution. Radioactive labelling of double stranded oligonucleotides was carried out by adding 100 ng of double stranded oligonucleotides, 1 µl of Klenow fill-in buffer, 1 µl of Klenow enzyme (see section 2.2.7), 1 µl of 10 mM dATP, dTTP, dGTP, 1 µl of [α^{32}P] dCTP (10 mCi/ml)

(Amersham) and 5 µl of water. The mixture was incubated for 15 min at room temperature. The concentration of the oligonucleotide was made up to 0.75 µg/µl with tRNA in a total volume of 30 µl. Unincorporated [α-^{32}P] dCTP was removed using Chromaspin-10 columns that are based on gel filtration chromatography (Clontech). The columns were placed, with a 2 ml collection tube, inside a 15 ml centrifugation tube and centrifuged for 5 min at 700 xg to remove the equilibration buffer. The collection tube was replaced and the labelled double-stranded oligonucleotide sample was placed in the column, which was again spun for 5 min at 700 xg. The collection tube contained the purified labelled probe.

2.7.3 EMSA reactions and acrylamide gel electrophoresis

Reactions were carried out with a final concentration of 100 mM NaCl. Samples contained labelled probe (1 ng), cell extract (1-3 µl), dIdC (0.5, 1, 2.5, 5 or 10 µg), loading buffer (1 µl) and buffer D100 to make a final volume of 5 µl. All components were added to the sides of a 0.5 ml micro-centrifuge tube, which was centrifuged to initiate all reactions simultaneously. Samples were incubated at room temperature for 10 min and analysed on a 14 cm x 16 cm non-denaturing 4% polyacrylamide gel. While samples were incubating, the gel was pre-run at 100 V. Wells were rinsed out using 1x TBE buffer before and after the gel was pre-run. Samples were loaded at 100 V and gels were electrophoresed, in a vertical gel tank in 1x TBE buffer, for 75 min at 250 V. After electrophoresis gels were dried on to 3MM paper at 80°C for 2 h and analysed by exposing to Biomax MS Kodak scientific imaging film in a cassette at -70°C or by using a phosphorimager (Molecular Dynamics).

Chapter 3 – RESULTS

Characterisation of AlHV-1 ORF50

3.1 Introduction

As discussed in the introduction, R-transactivators of γHVs have a role in reactivation of the virus from latency and also act as transactivators. Continued passage of the cell-associated C500 virulent strain of AlHV-1 in BT cells results in the virus becoming cell-free and attenuated (Handley *et al.,* 1995). Concomitant with this attenuation is alteration of the genome affecting ORF50, the homologue of the Rta-encoding genes. The aim of this section of work was to characterise the ORF50 gene product, AlHV-1/Rta.

3.2 Expression of ORF50

3.2.1 Amplification and subcloning of AlHV-1 ORF50

To initiate characterisation of AlHV-1 ORF50, the coding sequence was amplified by PCR with primers 5' - AAG AAT TC**A TG**A GTG CCA ACA ACC (Nt 72825-72840) and 5' - TTG GAT CCA CTC **CCA** AAT ATG G (Nt 74904-74918), which are illustrated in Figure 3.5 as A and B, respectively. These primers were based on the sequence of the AlHV-1 genome published by Ensser *et al.* 1997 and incorporated *Eco*RI and *Bam*HI restriction sites respectively (underlined) for convenient cloning of the PCR product. The start and stop codons are shown in bold. AlHV-1 DNA (see section 2.4.4) was used as a template for PCR. The programme used was: 1 cycle of 2 min at 96°C; 2 cycles of 1 min at 96°C, 1 min at 40°C and 2 min at 72°C; 2 cycles of 1 min at 96°C, 1 min at 45°C and 2 min at 72°C; 36 cycles of 1 min at 96°C, 1 min at 50°C and 2 min at 72°C and finally 1 cycle of 7.5 min at 72°C. The PCR product was inserted into the pGEM-T Easy TA cloning vector, deriving pGEM-T Easy-ORF50 (Figure 3.1(a)).

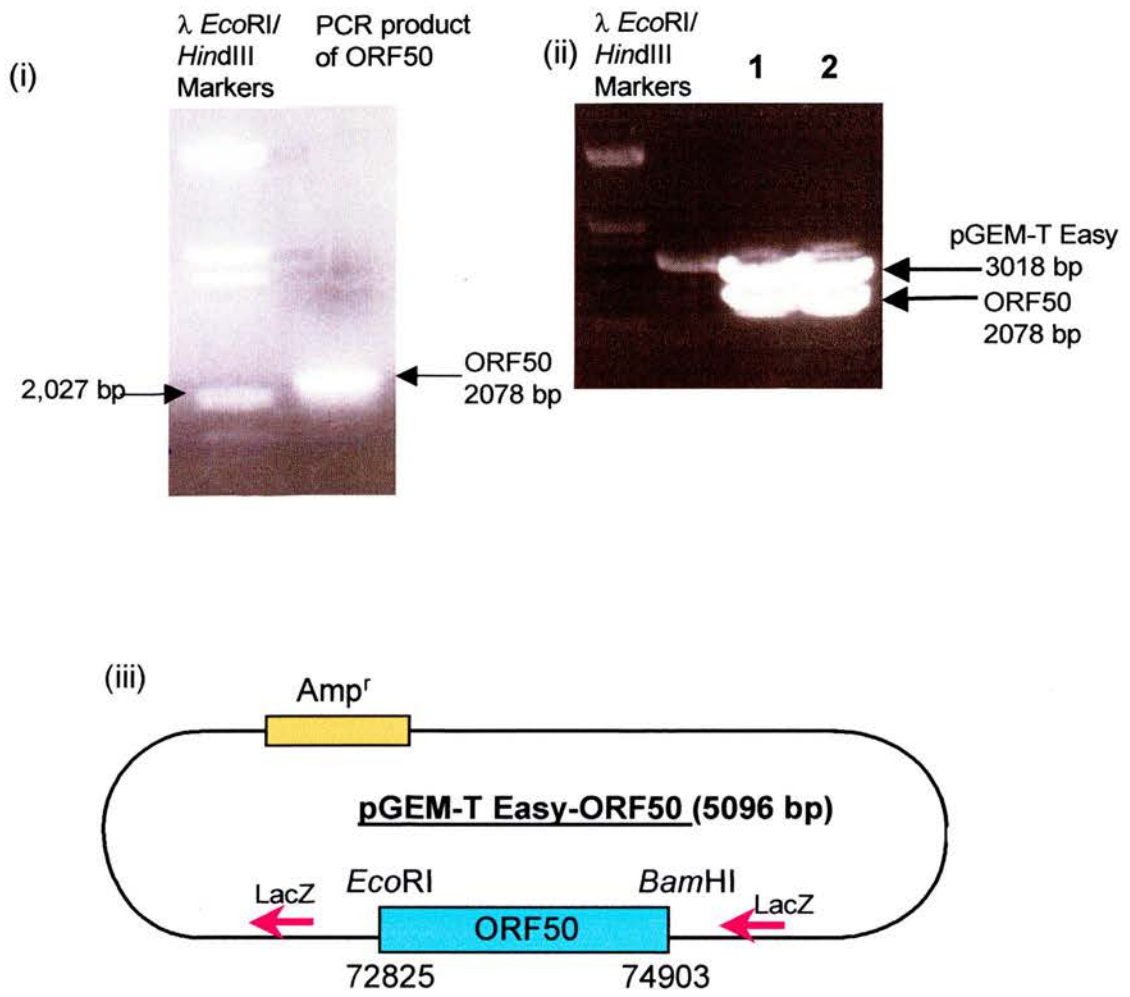

Figure 3.1 (a): Amplification and subcloning of AlHV-1 ORF50

(i) PCR amplification of the AlHV-1 ORF50 sequence.
(ii) Two *Eco*RI and *Bam*HI digests (lanes 1 and 2) of pGEM-T Easy-ORF50 releasing the ORF50 sequence.
(iii) Diagram of pGEM-T Easy-ORF50. Insertion of the ORF50 sequence disrupts the LacZ gene (arrows)

Amp^r – ampicillin resistance gene

3.2.2 Construction and analysis of pLXSN-ORF50 expression construct

To generate a construct that allowed expression of ORF50 in mammalian cells, the 2078 bp ORF50 sequence was excised from pGEM-T Easy via the *Eco*RI and *Bam*HI sites and subcloned into these sites in the pLXSN expression vector (Clontech) to derive pLXSN-ORF50 (Figure 3.1(b)). In the pLXSN vector, gene expression is driven from the MMLV LTR.

A Northern blot was carried out to test for transcription from this expression construct. pLXSN-ORF50 (2 μg) or pLXSN (2 μg) was transfected by electroporation into HeLa cells and total cellular RNA extracted 48 h later (see section 2.5.1). The samples (30 μg) were loaded onto a formaldehyde gel, electrophoresed and transferred onto a membrane. The membrane was hybridised with a probe derived from the ORF50 sequence excised from the pGEM-T Easy-ORF50 vector (see section 2.5.3-2.5.6). A band of 8 kb was detected on the Northern blot, which differed from the expected size of 2 kb (Figure 3.2). The most likely explanation for this is that the RNA was contaminated with pLXSN-ORF50 plasmid DNA, which is 7978 bp.

Western blots were also carried out using crude extract from HeLa cells transfected with pLXSN-ORF50 (see section 2.6.1-2.6.4). The antibody used to detect AlHV-1/Rta was raised in rabbits to a truncated protein expressed from a construct containing nucleotides 73059-74903 of AlHV-1 ORF50 (obtained from Sandi Swa, Moredun Research Institute, Edinburgh). Initial results showed a band indicating the presence of AlHV-1/Rta at the expected size of ~68 kDa (Figure 3.3), but the

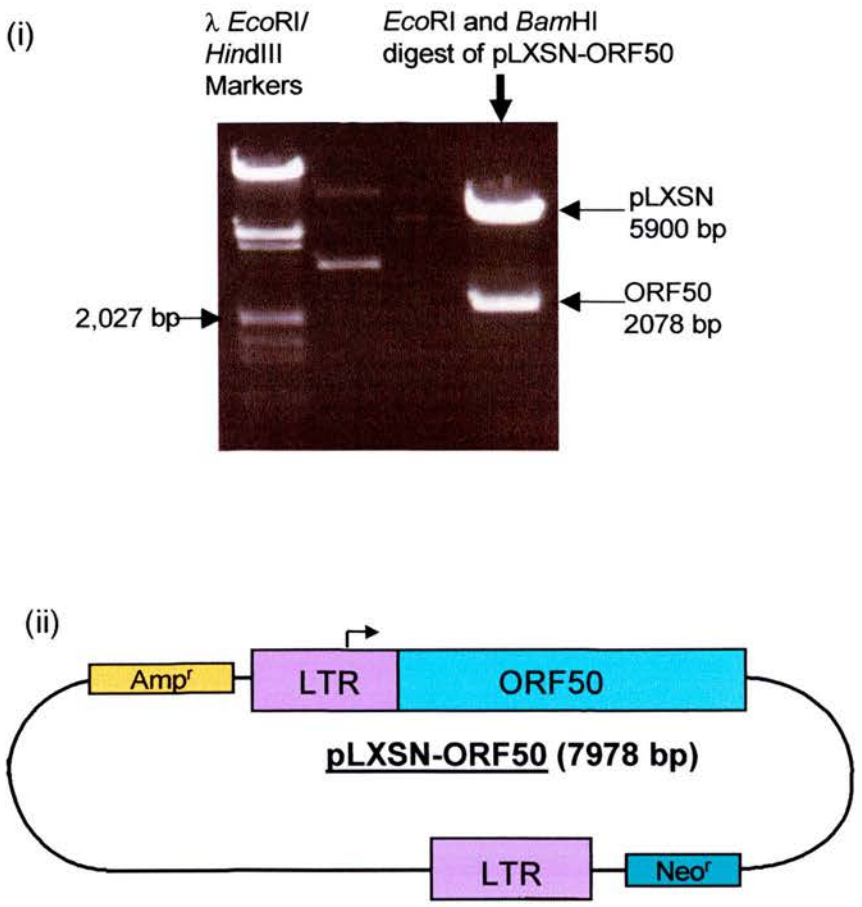

Figure 3.1(b) Construction of pLXSN-ORF50

(i) *Eco*RI and *Bam*HI digest of pLXSN-ORF50 releasing the ORF50 sequence insert.
(ii) Diagram of pLXSN-ORF50.

Amp^r – ampicillin resistance gene.
Neo^r – neomycin resistance gene.

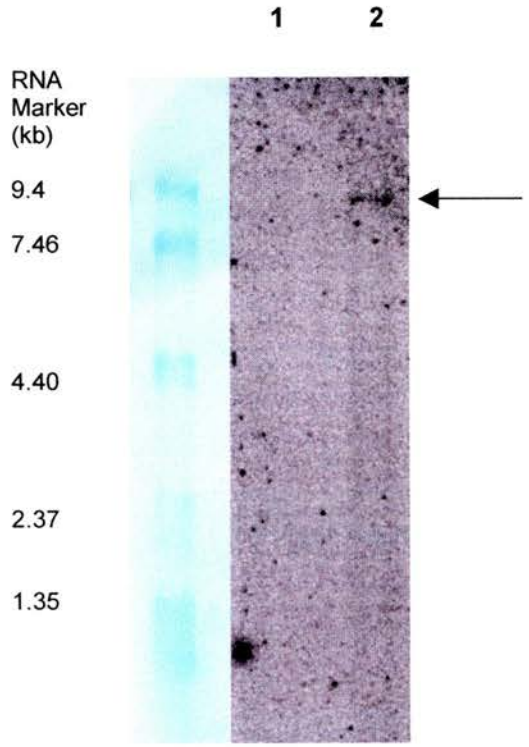

Figure 3.2: Transcription from pLXSN-ORF50

Lane 1 – RNA from cells transfected with 2 μg of pLXSN plasmid.
Lane 2 – RNA from cells transfected with 2 μg of pLXSN-ORF50 plasmid.

Each lane contains 30 μg of total cellular RNA.
The membrane was probed with ORF50 sequence (arrow indicates band).

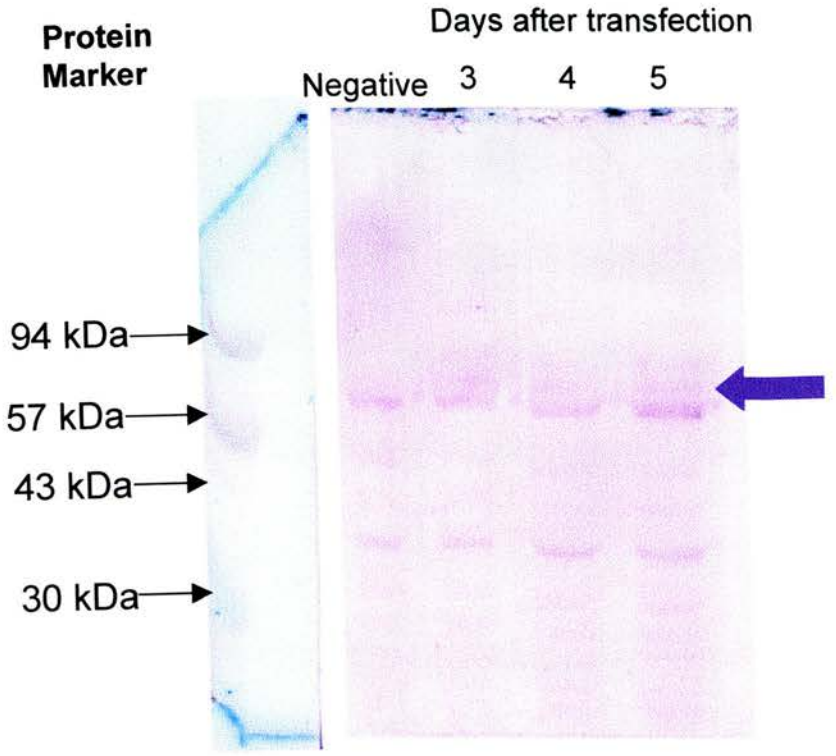

Figure 3.3: Protein Expression of pLXSN-ORF50

Western blot of crude protein extract from cells transfected with pLXSN-ORF50. The negative lane contains crude extract from cells transfected with pLXSN. The blue arrow indicates a band that is present in the samples containing pLXSN-ORF50 and absent in the sample containing pLXSN.

background was high. It is possible that the protein was below the level of detection or that the antibody titre was too low.

3.2.3 Northern analysis of ORF50 gene expression in AlHV-1 infected cells

The transcriptional expression pattern of ORF50 in AlHV-1 infected cells was investigated. The following questions were addressed: (1) when is the transcript expressed in the virus life cycle? (2) are there multiple transcripts? (3) is the transcript(s) spliced? The transcriptional expression pattern of ORFA6 was also investigated since it is adjacent to ORF50 in the AlHV-1 genome. ORFA6 is a positional homologue of the gene encoding EBV Zta although the two proteins have limited sequence homology (Ensser *et al.,* 1997).

Total RNA containing transcripts from each temporal class of expression (IE, E or L) was harvested from virus-infected BT cells (see section 2.5.1 and 2.5.2) and examined by Northern blot analysis; 30μg of total RNA was used (see section 2.5.3-2.5.6). The ORF50 sequence excised from the pGEM-T Easy-ORF50 plasmid was used as a probe. An ORF50 transcript was not detected in any of the samples. The quality of RNA had been verified by agarose gel electrophoresis and ethidium bromide staining, which showed that the RNA was intact. Thus, the level and stability of the transcript were deemed to be the two most likely problems to explain the lack of detection. As is observed in Figure 3.17, β-actin transcripts were detected when 30 μg of total RNA was used, but were not detected when 5 μg of total RNA was used. It is highly likely that the ORF50 transcript is much less abundant than the β-actin transcript and therefore was below the level of detection.

Two approaches were taken to address this problem:

(1) Slot blots (Figure 3.4).

Total RNA (0.1μg and 10μg) from virus-infected BT cells was spotted onto a nitrocellulose membrane using a slot blot apparatus. As positive controls, the pGEM-T Easy-ORF50 and pGEM-T Easy-ORFA6 plasmid DNAs (0.1 and 10 μg) were used. The membrane was probed with either the ORF50 sequence or the ORFA6 sequence excised from the appropriate pGEM-T Easy plasmid. The results indicated that ORF50 and ORFA6 are transcribed as IE genes but not as E genes (Figure 3.4). The results are unusual because it may be expected that IE transcripts would also be transcribed with the E transcripts. In addition, despite the fact that the RNA appeared to be intact by agarose gel electrophoresis and ethidium bromide staining, hybridisation with a β-actin probe was not successful. Thus, no absolute conclusions can be made from this experiment.

(2) PolyA+ mRNA purification.

mRNA accounts for a very small proportion (1-2%) of total RNA. Thus, polyA$^+$ mRNA was purified from total cellular RNA for Northern blot analysis in order to increase the total amount of mRNA loaded on the gel. This approach was unsuccessful and no ORF50 transcripts were detected by this method.

3.2.4 RT-PCR analysis of ORF50 gene expression

Due to the lack of sensitivity of the Northern Blots that were carried out, RT-PCR analysis was used to examine ORF50 transcripts.

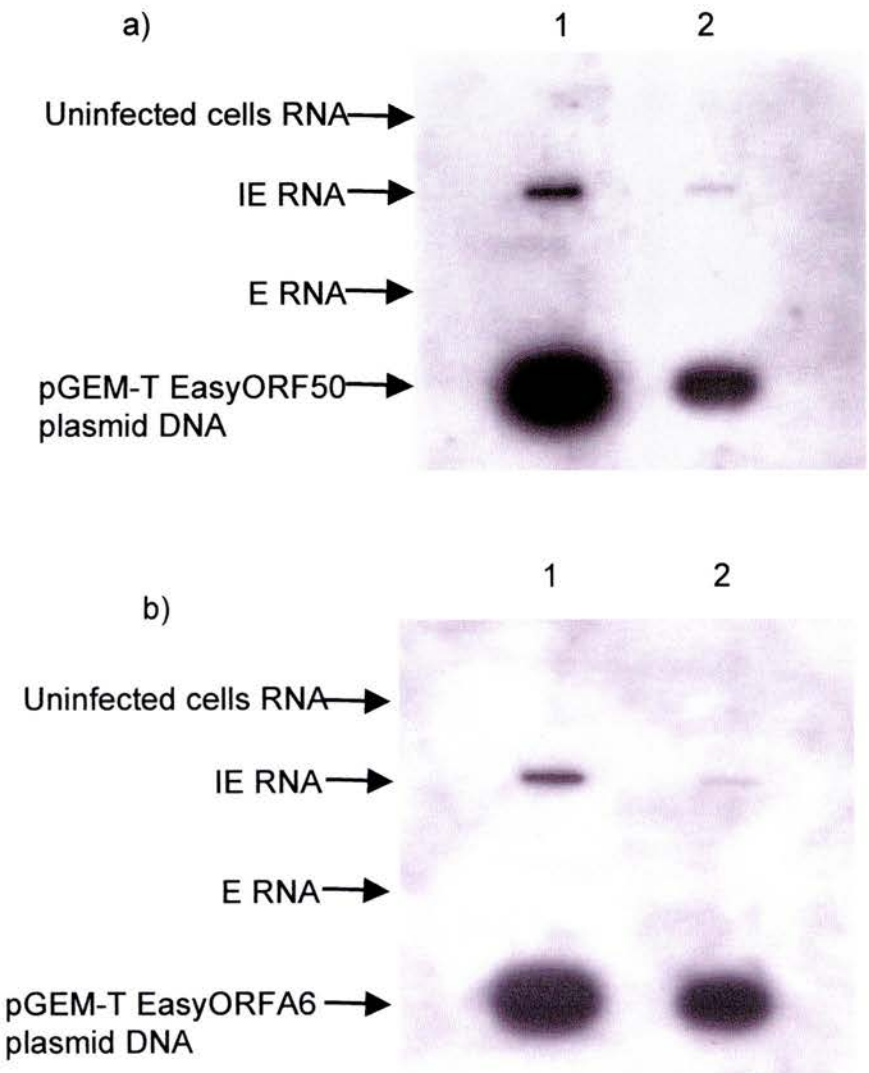

Figure 3.4: ORF50 and ORFA6 expression in AlHV-1

IE and E total RNA was harvested from AlHV-1-infected BT cells and analysed using slot blots. Total RNA from uninfected cells was used as a negative control. Plasmid DNAs containing either ORF50 or ORFA6 sequence were used as positive controls.

Positions 1 and 2 contain 10 μg and 0.1 μg, respectively, of either total RNA or plasmid DNA.

a) Slot blots probed with ORF50 sequence.

b) Slot blots probed with ORFA6 sequence.

PCR primers were designed to test if and when ORF50 and ORFA6 were expressed, if the splice site predicted by Ensser *et al.* 1997 within ORF50 was used and if ORFA6 was co-transcribed with ORF50 (Figure 3.5). The primers used for ORF50 were the same as those used to initially amplify the ORF50 sequence (A and B). Other primers were 5' - AAG AAT TCC ATT TTA CAG AGG AGA C (Nt 73109-73125) (E) and 5' - AAG AAT TCG AAC TGC TTG ATA GAG ACA G (Nt 74709-74728) (F). The sequences of the primers used for ORFA6 (C and D) are given in section 3.7.1.

As templates for RT-PCR analysis, RNA from each class of temporal transcript of virulent (Vir) and attenuated (Att) AlHV-1 was used (section 2.5.2). In Figure 6(a) and (b) they are referred to as Vir IE, Vir E, Vir L and Att IE, Att E and Att L. The RNA from attenuated virus was harvested by L. Devi. RNA was also harvested from mock-infected BT cells referred to as BT. RNA harvested from BHK cells transfected with an ORF50 or ORFA6 expression plasmid, referred to as BHK-ORF50 and BHK-ORFA6 in Figure 3.6(a) and (b), and mock-transfected BHK cell RNA, referred to as BHK, were also analysed.

The RNA samples were treated with DNAse and reverse transcribed using an oligo d(T) primer (see section 2.2.2). Reverse transcribed RNA (RT+) samples were used as templates in the PCR and RNA that had not been reverse transcribed (RT-) was used as a negative control. Water was also used as an additional negative control, and pGEM-T Easy-ORF50 and pGEM-T Easy-ORFA6 plasmids were used as positive controls. Primers were used to amplify adenosine triphosphatase (ATPase) or β-actin

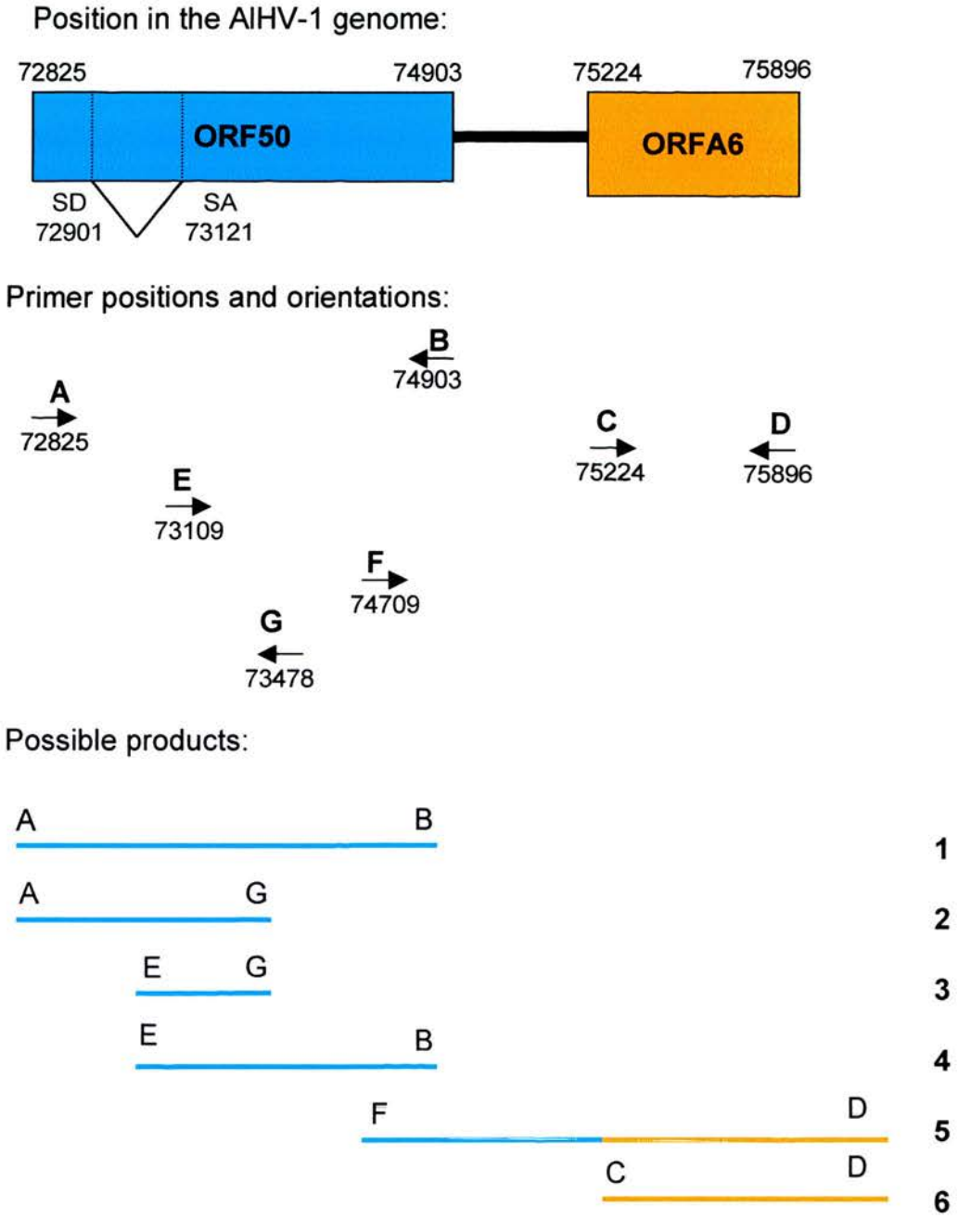

Figure 3.5: RT-PCR primers.

Diagram showing ORF50 and ORFA6 and their nucleotide positions in the AlHV-1 genome taken from Ensser *et al.* (1997). The PCR primers used in the RT-PCR analysis are indicated, as are the putative PCR products.

PCR products 1 and 2, if obtained, would indicate transcription of ORF50.
PCR products 3 and 4, if obtained, would indicate whether ORF50 is spliced.
PCR product 5, if obtained, would indicate if ORF50 and ORFA6 are co-transcribed.
PCR product 6, if obtained, would indicate transcription of ORFA6.

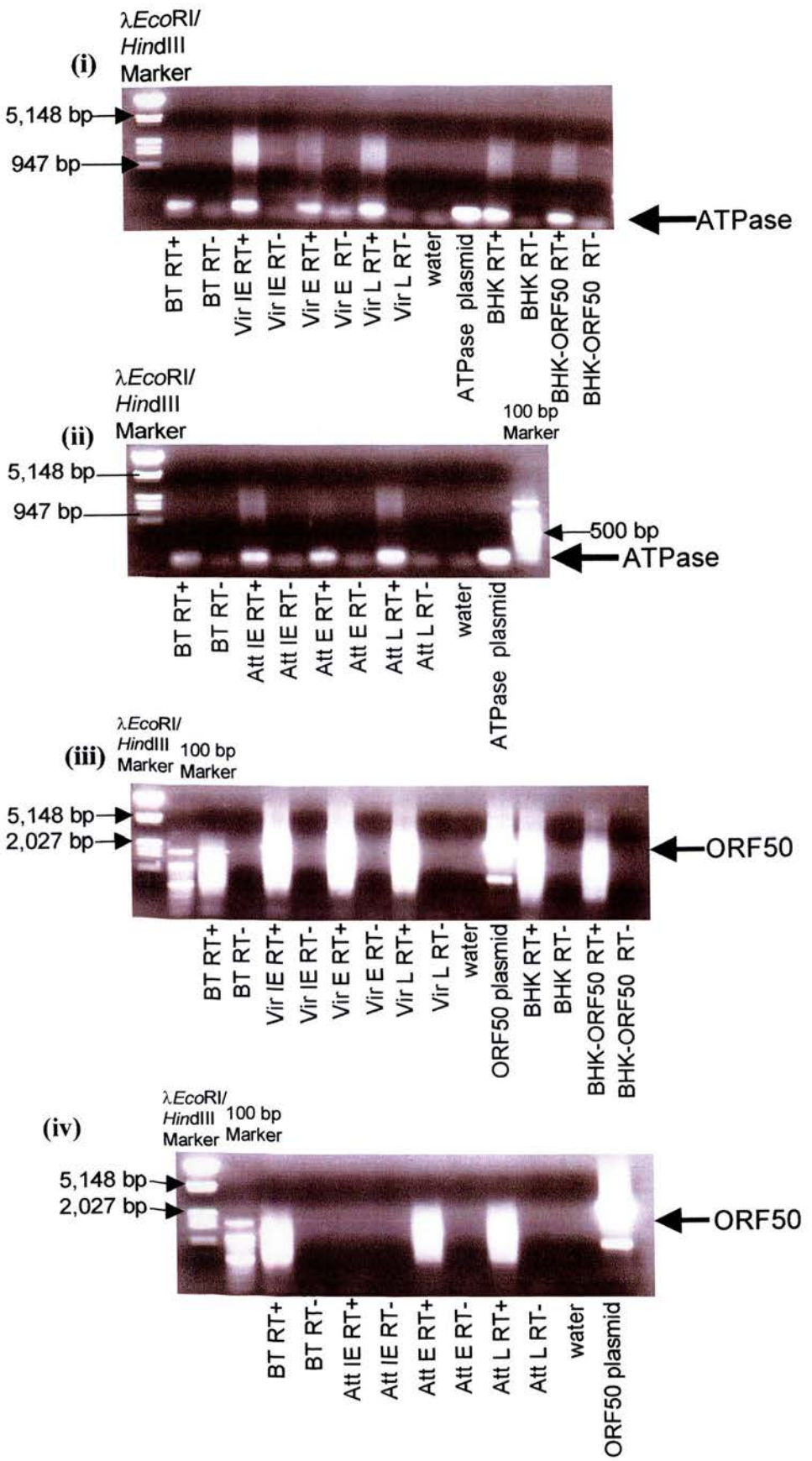
(i)
λEcoRI/ HindIII Marker
5,148 bp
947 bp
ATPase
BT RT+
BT RT-
Vir IE RT+
Vir IE RT-
Vir E RT+
Vir E RT-
Vir L RT+
Vir L RT-
water
ATPase plasmid
BHK RT+
BHK RT-
BHK-ORF50 RT+
BHK-ORF50 RT-
(ii)
λEcoRI/ HindIII Marker
100 bp Marker
5,148 bp
947 bp
500 bp
ATPase
BT RT+
BT RT-
Att IE RT+
Att IE RT-
Att E RT+
Att E RT-
Att L RT+
Att L RT-
water
ATPase plasmid
(iii)
λEcoRI/ HindIII Marker
100 bp Marker
5,148 bp
2,027 bp
ORF50
BT RT+
BT RT-
Vir IE RT+
Vir IE RT-
Vir E RT+
Vir E RT-
Vir L RT+
Vir L RT-
water
ORF50 plasmid
BHK RT+
BHK RT-
BHK-ORF50 RT+
BHK-ORF50 RT-
(iv)
λEcoRI/ HindIII Marker
100 bp Marker
5,148 bp
2,027 bp
ORF50
BT RT+
BT RT-
Att IE RT+
Att IE RT-
Att E RT+
Att E RT-
Att L RT+
Att L RT-
water
ORF50 plasmid

Figure 3.6 (a): RT-PCR

RT-PCR analysis was performed using primers to amplify ATPase and ORF50. RNA samples were obtained from BT cells infected with virulent or attenuated virus at IE,E or L stages of infection (Vir IE, Vir E, Vir L, Att IE, Att E and Att L), or from BHK cells transfected with an ORF50 expression plasmid (BHK-ORF50). Reverse transcribed samples of mock-infected BT cells (BT) and mock-transfected BHK cells (BHK) were used as controls as well as RNA from all of the above samples, which were not reverse transcribed. All reverse transcribed samples are labelled RT+ and all non-reverse transcribed samples are labelled RT-. As positive controls ATPase and ORF50 plasmid DNA were included as templates for the PCR reaction.

(i) and (ii) show RT-PCR analysis with ATPase primers.
(iii) and (iv) show RT-PCR analysis with ORF50 primers.

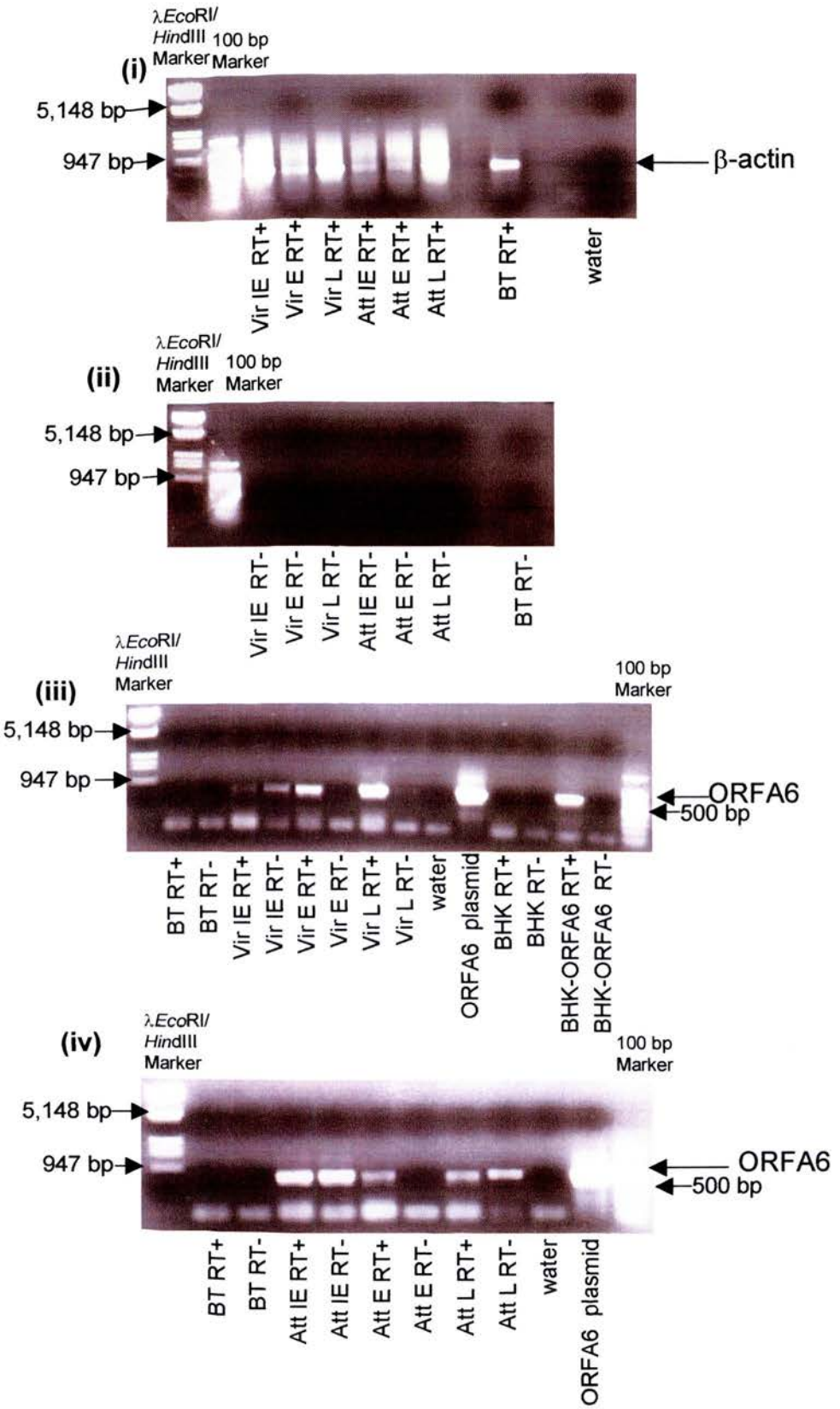
(i)
λEcoRI/ HindIII Marker
100 bp Marker
5,148 bp
947 bp
β-actin
Vir IE RT+
Vir E RT+
Vir L RT+
Att IE RT+
Att E RT+
Att L RT+
BT RT+
water
(ii)
λEcoRI/ HindIII Marker
100 bp Marker
5,148 bp
947 bp
Vir IE RT-
Vir E RT-
Vir L RT-
Att IE RT-
Att E RT-
Att L RT-
BT RT-
(iii)
λEcoRI/ HindIII Marker
100 bp Marker
5,148 bp
947 bp
ORFA6
500 bp
BT RT+
BT RT-
Vir IE RT+
Vir IE RT-
Vir E RT+
Vir E RT-
Vir L RT+
Vir L RT-
water
ORFA6 plasmid
BHK RT+
BHK RT-
BHK-ORFA6 RT+
BHK-ORFA6 RT-
(iv)
λEcoRI/ HindIII Marker
100 bp Marker
5,148 bp
947 bp
ORFA6
500 bp
BT RT+
BT RT-
Att IE RT+
Att IE RT-
Att E RT+
Att E RT-
Att L RT+
Att L RT-
water
ORFA6 plasmid

Figure 3.6 (b): RT-PCR

RT-PCR analysis was performed using primers to amplify β-actin and ORFA6. RNA samples were obtained from BT cells infected with virulent or attenuated virus at IE,E or L stages of infection (Vir IE, Vir E, Vir L, Att IE, Att E and Att L), or from BHK cells transfected with an ORFA6 expression plasmid (BHK-ORFA6). Reverse transcribed samples of mock-infected BT cells (BT) and mock-transfected BHK cells (BHK) were used as controls as well as RNA from all of the above samples, which were not reverse transcribed. All reverse transcribed samples are labelled RT+ and all non-reverse transcribed samples are labelled RT-. As a positive control ORFA6 plasmid DNA was included as a template for the PCR reaction.

(i) and (ii) show RT-PCR analysis with β-actin primers.
(iii) and (iv) show RT-PCR analysis with ORFA6 primers.

transcripts to confirm the presence and quality of intact RNA in the samples. The ATPase primers used were 5'-CAA GAC CAG GAG GAA TTC CG-3' and 5'-GGG CAG TAG GAA AGG AAA GC-3'. The β-actin primers used were 5'-CGT AGA TGG GCA CAG TG and 5'-CTC CGG CAT GTG CAA AG.

Figure 3.6(a) (i) and (ii) show the results of RT-PCR analysis with ATPase primers. The ATPase plasmid gave a 200 bp band as did all RT+ samples. All the RT- samples and the water control did not show a product. This indicated that the RNA was intact and that the reverse transcriptase reactions had worked.

Figure 3.6(a) (iii) and (iv) show the results of RT-PCR analysis with ORF50 primers (A and B). A product of 2078 bp should have been amplified. In agreement with this, the centre of the smeared band obtained when using the ORF50 expression plasmid as a template, was of this size, suggesting that the primers and conditions used were working. No product was seen in the negative controls, the RT- samples or the water control. A band of the correct size, also smeared, was observed in all of the Vir RT+ samples. The mock-infected BT cells and mock-transfected BHK cells also contained a smeared band, however the centre of the band did not correspond to those in the Vir RT+ samples or the positive control suggesting it was an alternative product. It was also noticed that the smeared bands obtained in the Att RT+ samples did not correspond to the positive control band suggesting that they too were alternative products. ORF50 expression therefore appears to be expressed at all times in the virulent virus life cycle but not at all in the attenuated virus life cycle. However, it was reasoned that there might have been some non-specific priming taking place

hence the products being observed as a smear rather than a defined product. Primers to amplify a smaller region of ORF50 were designed and more stringent conditions were used. The primers used for this were the 5' primer used for the full-length ORF50 sequence (A) and 5'- AAG GAT CCC CAT TTG TCA GTG TGC (Nt 73478-73463) (G) to amplify 653 bp of the ORF50 sequence. In the time available successful RT-PCR amplification of ORF50 was not achieved.

Figure 3.6(b) (i) and (ii) show the results of RT-PCR analysis with β-actin primers. Again this showed that all RT+ samples gave a positive band of 500 bp indicating that the RT reactions had worked and the RNA was intact. All of the RT- samples and water gave no band therefore no contamination had occurred.

Figure 3.6(b) (iii) and (iv) show the results of RT-PCR analysis with ORFA6 primers (C and D). All Vir and Att RT+ samples were positive. The mock-transfected BHK cells and mock-infected BT cells gave no product as expected. The only products that gave cause for concern were those obtained with templates Att IE RT-, Att L RT- and Vir IE RT-, which were used as negative controls. Overall, it could be suggested that ORFA6 is expressed at all times during virus replication of virulent and attenuated virus. However, in order to be conclusive these experiments would have to be repeated to ensure that all controls worked satisfactorily. Considering that a master mix was used for each group of reactions, it is clear that it was not contaminated since not all negative samples have a product. Also the RT- preparations cannot have been contaminated with virus DNA since not all of the RT- samples yielded a product.

In the time available the transcription pattern of ORF50 and ORFA6 within the virus life cycle was not elucidated.

3.3 Investigating the function of the AlHV-1/Rta

Transient transfection reporter assays were used to determine if AlHV-1/Rta could act as a transactivator. The principle of this technique is that vectors containing promoter sequences linked to a reporter gene are co-transfected with a plasmid expressing the predicted transactivator. If the product of the expression vector activates the specified promoter, this can be detected by measuring the activity of the reporter gene. The promoters of three candidate AlHV-1 ORFs were chosen to test the transactivation potential of AlHV-1/Rta.

The action of AlHV-1/Rta on promoters from the three different temporal classes of transcripts was examined. No detailed transcript mapping of AlHV-1 had been carried out previously, and so by comparison with other γHVs, ORF57 was chosen as a representative IE gene, TK as an E gene and ORF6 as a delayed early (DE)/L gene. In other γHVs, ORF57 encodes a transcriptional regulator, ORF6 codes for the single-stranded DNA-binding protein and TK codes for thymidine kinase. Constructs containing putative promoters for each of these ORFs were generated.

3.3.1 Construction of reporter constructs with putative AlHV-1 promoter sequences

To ensure that the putative promoter sequences from the AlHV-1 genes were represented in the constructs, approximately 800-900 bp of sequence upstream of the

predicted start codon and ~50 bp downstream of this was amplified from AlHV-1 virus DNA. (Figure 3.7(a)). These figures were estimated by assessing other HV promoters. For example, in HVS the ORF6 and ORF57 promoters required up to 259 bp and 764 bp, respectively, upstream of the transcription initiation site for activation by HVS/Rta (Whitehouse *et al.*, 1997b; Whitehouse *et al.*, 1998a).

The AlHV-1 **ORF57** promoter was amplified by PCR using primers 5' - AAG AGC TCT GGT AGA GGA AGG TC (Nt 83700-83714) and 5'- AAG CTA GCT CTT ACC CTC CAT GG (Nt 84519-84505) with *Sac*I and *Nhe*I sites incorporated, respectively (underlined).

The AlHV-1 **TK** promoter was amplified by PCR using primers 5'- AAG GTA CCG TGG TGA GAT AGT CG (Nt 37540-37559) and 5' - AAC TCG AGC TTT GGG CAC ATC G (Nt 38408-38395) with *Kpn*I and *Xho*I sites incorporated, respectively (underlined).

The AlHV-1 **ORF6** promoter was amplified by PCR using primers 5' - AAG GTA CCG CCA GTA AAT GGA CC (Nt 10435-10449) and 5' - AAG CTA GCA GAT GAA GCC GCA GG (Nt 11341-11327) with *Kpn*I and *Nhe*I sites incorporated, respectively (underlined).

The PCR programme used for amplification of the ORF6 promoter sequence was: 1 cycle of 2 min at 96°C; 40 cycles of 1 min at 96°C, 1 min at 60°C and 1 min at 72°C and finally one cycle of 7.5 min at 72°C. The same programme was used to amplify

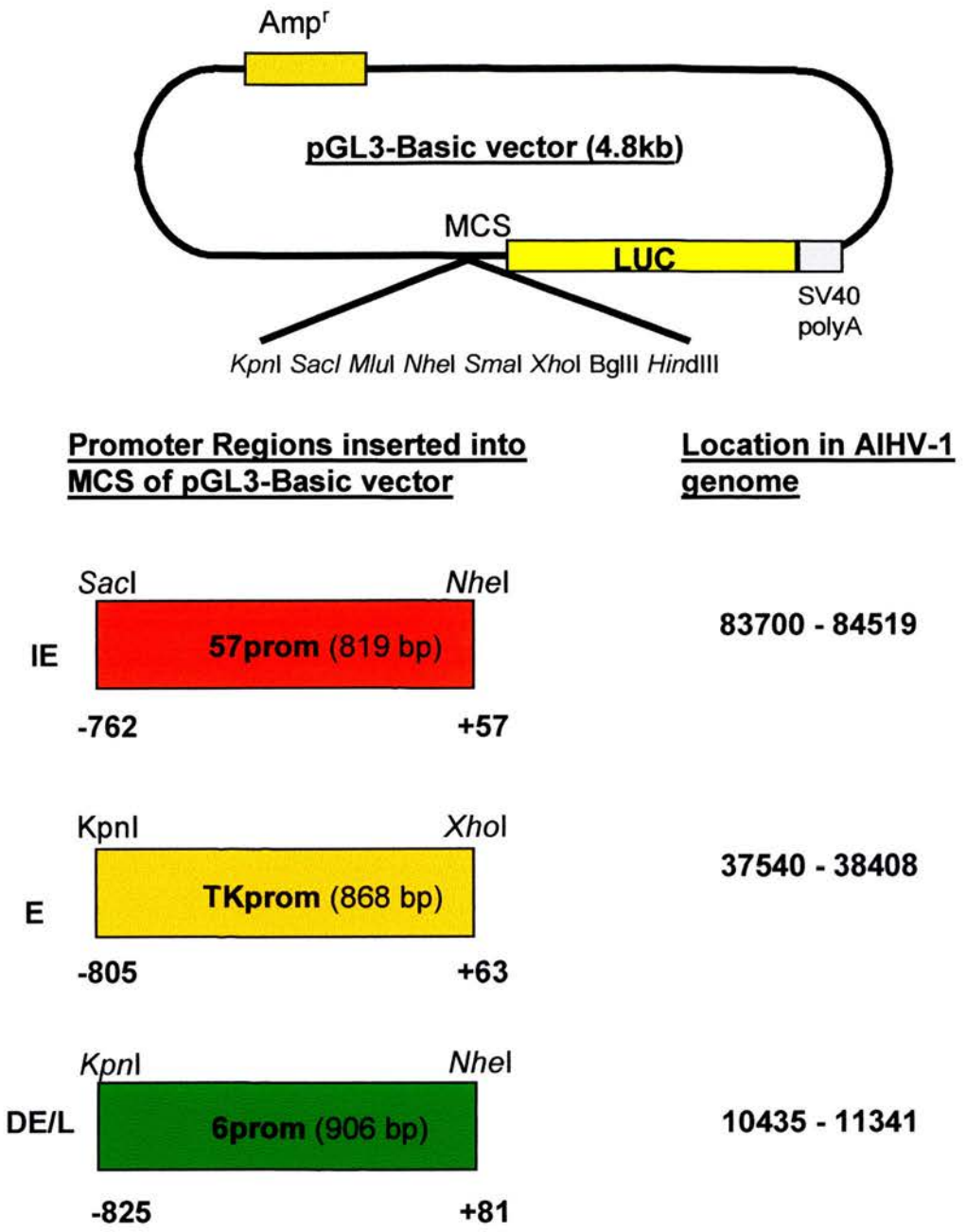

Figure 3.7 (a) Diagrammatic representation of AlHV-1 putative promoter constructs

57prom, TK prom and 6prom are AlHV-1 putative promoter sequences inserted upstream of the firefly luciferase gene in the pGL3-Basic vector. The pGL3-Basic vector is represented indicating the position and contents of the multiple cloning site relative to the luciferase gene.

The restriction enzymes used in the subcloning procedure, the location of the sequences in the AlHV-1 genome, taken from Ensser *et al.* (1997), and their positions relative to their predicted translational start sites within the virus are all shown. Also shown are the predicted temporal classes of the ORFs.

the ORF57 and TK promoters, except that an annealing temperature of 50°C was used. All PCR products were inserted into the pGEM-T Easy vector.

pGL3-Basic is a luciferase reporter vector encoding the firefly luciferase gene but has no promoter or enhancer sequences, allowing testing of potential promoter sequences. To make promoter reporter constructs, each of the amplified and subcloned putative promoter sequences was inserted upstream of the firefly luciferase coding region in the pGL3-Basic vector, thus deriving 57prom, TKprom, and 6prom (Figure 3.7(a) and (b)).

Sections 3.3.2 to 3.3.10 below describe preliminary experiments used to establish a transient transfection reporter assay system with an appropriate cell line, a background control and an internal control for transfection efficiencies of individual samples. Initially BT cells were used but were found to have poor transfection efficiencies. BHK cells were subsequently concluded to be the most appropriate cell line owing to higher transfection efficiencies. Initially the pLXSN-ORF50 expression vector was used but an expression construct with ORF50 being driven by the CMV promoter was then generated to improve expression. Thereafter, in subsequent sections, this system is used for assessing the transactivating abilities of AlHV-1/Rta. The actual luciferase values obtained are termed 'raw' values and they are measured in relative light units (RLU). All 'raw' luciferase values are presented in appendices 1-13.

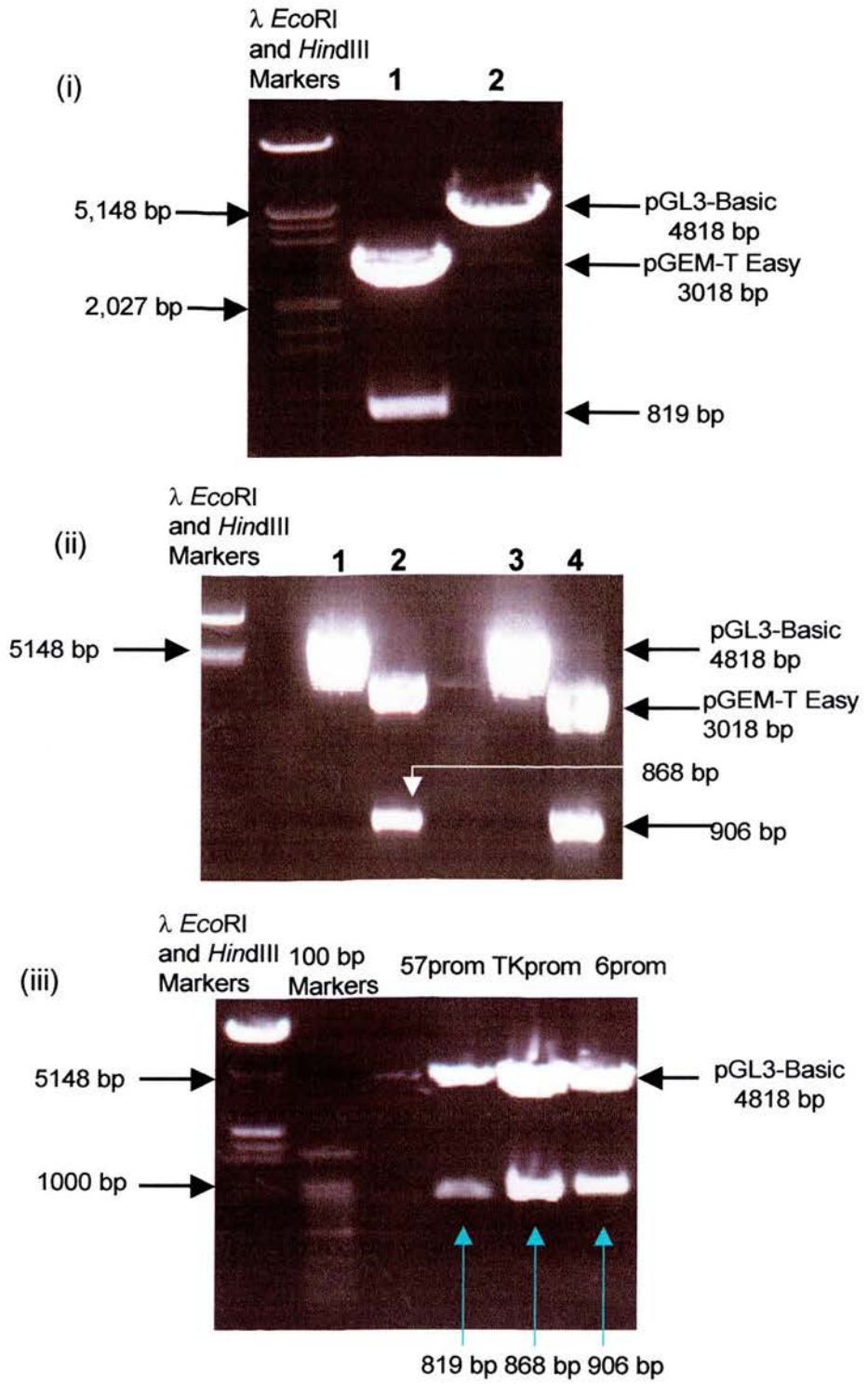

Figure 3.7 (b) Construction of putative AlHV-1 promoters

(i) *Sac* I and *Nhe* I digests of pGEM-T Easy containing the ORF57 promoter sequence (lane 1) and pGL3-Basic (lane 2).
(ii) *Kpn*I and *Xho*I digests of pGL3-Basic (lane 1) and pGEM-T Easy containing the ORFTK promoter sequence (lane 2) and *Kpn*I and *Nhe*I digests of pGL3-Basic (lane 3) and pGEM-T Easy containing the ORF6 promoter (lane 4).
(iii) Digests of 57prom, TKprom and 6prom with *Sac*I and *Nhe*I, *Kpn*I and *Xho*I, and *Kpn*I and *Nhe*I, respectively.

3.3.2 Activity of 57prom, TKprom and 6prom following virus superinfection

To determine if the promoter constructs were functional, their activity during productive virus infection was tested. BT cells were transfected by electroporation with 2 μg of 57prom, TKprom, 6prom or pGL3-Basic and then superinfected with AlHV-1 (C500 virulent isolate) 24 h later. BT cells were used, as they are the cell line used to propagate the virus. The amount of virus used per sample was equivalent to 5 x 10^5 cells exhibiting 70% CPE. Luciferase activity was determined 24 h after superinfection (see section 2.4.8). The pGL3-Basic vector was used as a background control since it contains no promoter sequences. Cells were also transfected with promoter constructs but were not infected with AlHV-1.

To assess whether activation of the promoter had occurred, the luciferase values obtained from the samples infected with virus were divided by the values obtained from uninfected samples to give the fold induction of promoter activity:

$$\frac{\text{Luciferase value obtained from cells transfected with promoter constructs and superinfected with virus}}{\text{Luciferase value obtained from cells transfected with promoter constructs alone}} = \text{Fold Induction}$$

Both the TK promoter and the ORF6 promoter were up-regulated in the presence of virus (Figure 3.8(a) and Appendix 1), 12-fold and 18-fold, respectively. The ORF57 promoter showed no significant activity under the conditions used. Since ORF57 is most likely to be an IE gene, from studies of its functional homologues in other γHVs, a possible explanation could be that at 24 h post-infection there is no longer any transcription of IE genes. However, it should be noted that the results represent a

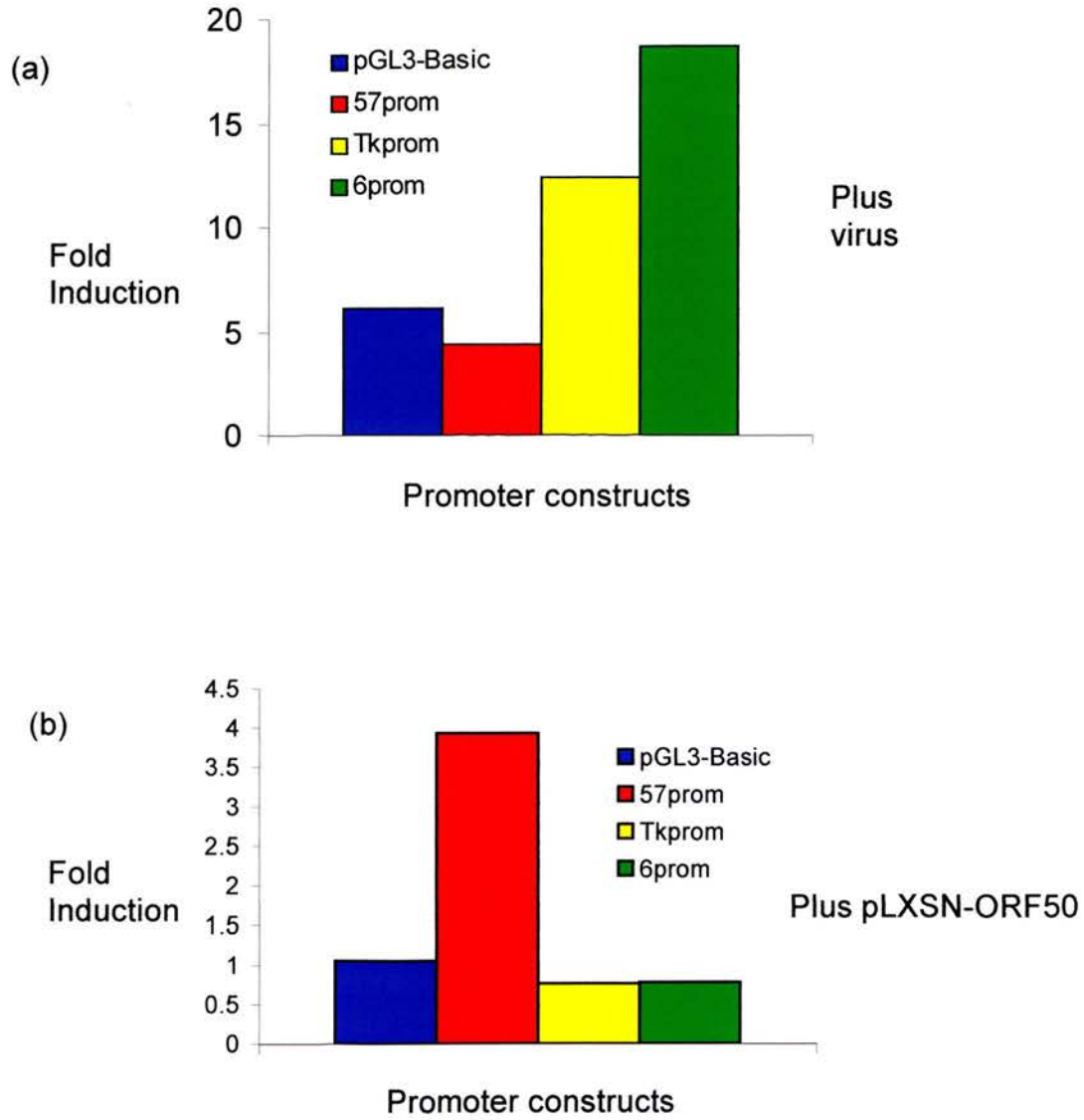

Figure 3.8: Activation of AIHV-1 putative promoters

(a) BT cells were transfected with promoter constructs and 24 h later infected with the C500 isolate of AIHV-1 or left uninfected. The samples were assayed 24 h following infection. Results show the fold induction of activity of samples with virus over those without virus.

(b) BT cells were transfected with promoter constructs with or without co-transfection of pLXSN-ORF50. Results show the fold induction of activity of samples with pLXSN-ORF50 over the activity of those without pLXSN-ORF50.

The results shown are from one experiment.

single experiment and repeat experiments using virus superinfection were not successful, possibly owing to slow growth of the virus.

3.3.3 Activation of putative AlHV-1 promoters by pLXSN-ORF50 in BT cells

Transient transfections and reporter assays were employed to assess if any of the AlHV-1 promoters could be activated by AlHV-1/Rta. BT cells were co-transfected with the ORF50 expression vector, pLXSN-ORF50 (2 μg) and 2 μg of pGL3-Basic, 57prom, TKprom or 6prom. The promoter constructs were also transfected alone to allow fold induction values to be calculated (Figure 3.8(b)).

The luciferase value of each sample was measured to obtain the relative level of promoter activity. The fold induction of activation of the promoters was calculated by dividing the activity obtained from samples transfected with pLXSN-ORF50 by the activity obtained in samples without pLXSN-ORF50:

$$\frac{\text{Luciferase value obtained from cells transfected with a promoter construct and pLXSN-ORF50}}{\text{Luciferase value obtained from cells transfected with a promoter construct alone}} = \text{Fold Induction}$$

The ORF57 promoter appeared to be activated by the AlHV-1/Rta. The activation of the ORF57 promoter was ~4-fold compared to the fold induction of pGL3-Basic which was ~1-fold. In contrast, the other promoters were not activated by AlHV-1/Rta (Figure 3.8 (b) and Appendix 1). However, the 'raw' values obtained in this experiment were unsatisfactorily low and were all below 1.4 RLU (0.037-1.366). Such low values were not thought to be sufficiently accurate.

To address this issue two strategies were pursued:

a) The transfection efficiency of BT cells was examined.

b) A new ORF50 expression construct was made with the intention of improving transcription and therefore the overall yield of AlHV-1/Rta protein.

3.3.4 Optimisation of the transfection efficiency of BT cells

The method of transfection used in the laboratory at the time was electroporation. To optimise this method for BT cells the method of Baum *et al.*, (1994) was used whereby a single parameter, the voltage, is changed. The voltage used was varied across a range from 220-300 V. BT cells were transfected with 2 μg of pCMVluc and the luciferase activity measured 48 h after transfection (Figure 3.9 and Appendix 2). Dr. P. Harrison constructed pCMVluc by inserting the CMV IE promoter, excised from the pEGFP-N1 vector, upstream of the firefly luciferase coding region in pGL3-Basic. The efficiency of transfection did not vary greatly between 220-280 V with 'raw' luciferase values ranging from 163-243 RLU. However, at 300 V the luciferase activity was 428 RLU implying that transfection efficiency was almost twice as great at this voltage. In previous experiments, 280 V had been used as the standard condition. Following this optimisation experiment, 300 V was used subsequently. The values obtained when using pCMVluc are significantly higher than when using the AlHV-1 promoter constructs because of the strength of the CMV IE promoter.

3.3.5 Construction of an ORF50 expression construct - pCMVORF50

In order to improve the expression of ORF50, the 2078 bp ORF50 sequence was excised from the pGEM-T Easy vector using *Eco*RI and *Spe*I restriction enzymes and

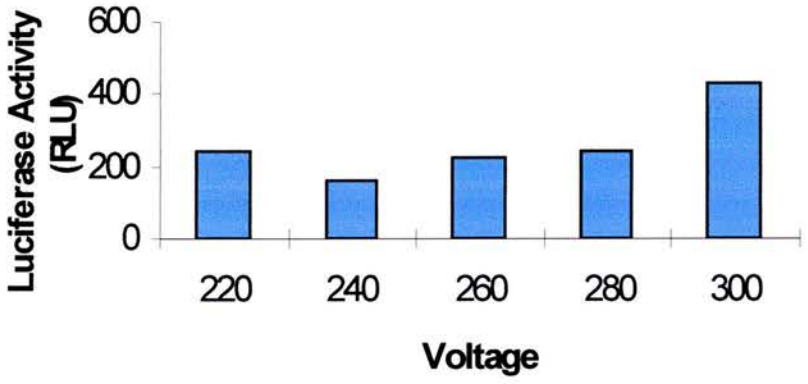

Figure 3.9: Optimisation of electroporation conditions in BT cells.

BT cells were transfected with 2 μg of pCMVluc plasmid and luciferase activity was measured 48 h later.

subcloned into the *Eco*RI and *Xba*I sites of the pEGFP-N1 vector downstream of a CMV IE promoter. The EGFP sequence of this vector was replaced with the ORF50 sequence deriving pCMVORF50 (Figure 3.10).

3.3.6 Activation of putative AlHV-1 promoters by pCMVORF50 in BT cells

The luciferase assay values obtained when using pCMVORF50 in BT cells were still unsatisfactorily low and so were not thought to be sufficiently accurate.

3.3.7 Use of an alternative cell line - BHK cells

At this point it was decided that an alternative cell line that would give high transfection efficiencies was required. Since BHK cells were known to have high transfection efficiencies and since AlHV-1 had been shown to infect hamsters (Jacoby *et al.,* 1988a and b), BHK cells were considered. To determine their suitability, the ability of AlHV-1 to infect BHK cells was tested. It was shown that BHK cells could support AlHV-1 replication, as determined by propagation of the virus through serial monolayer cultures (Figure 3.11). BHK cells were therefore considered suitable for use in the transient transfection assays.

3.3.8 Optimisation of the transfection efficiency of BHK cells

Transfection of BHK cells was optimised in a similar manner to that for BT cells using a range of conditions including double pulse as well as single pulse (Baum *et al.*, 1994) (Figure 3.12 and Appendix 3). Each sample was transfected with pCMVluc (2 µg), a constitutively active luciferase promoter construct, and luciferase values were measured 48 h after transfection. The double pulse 'raw' values ranged

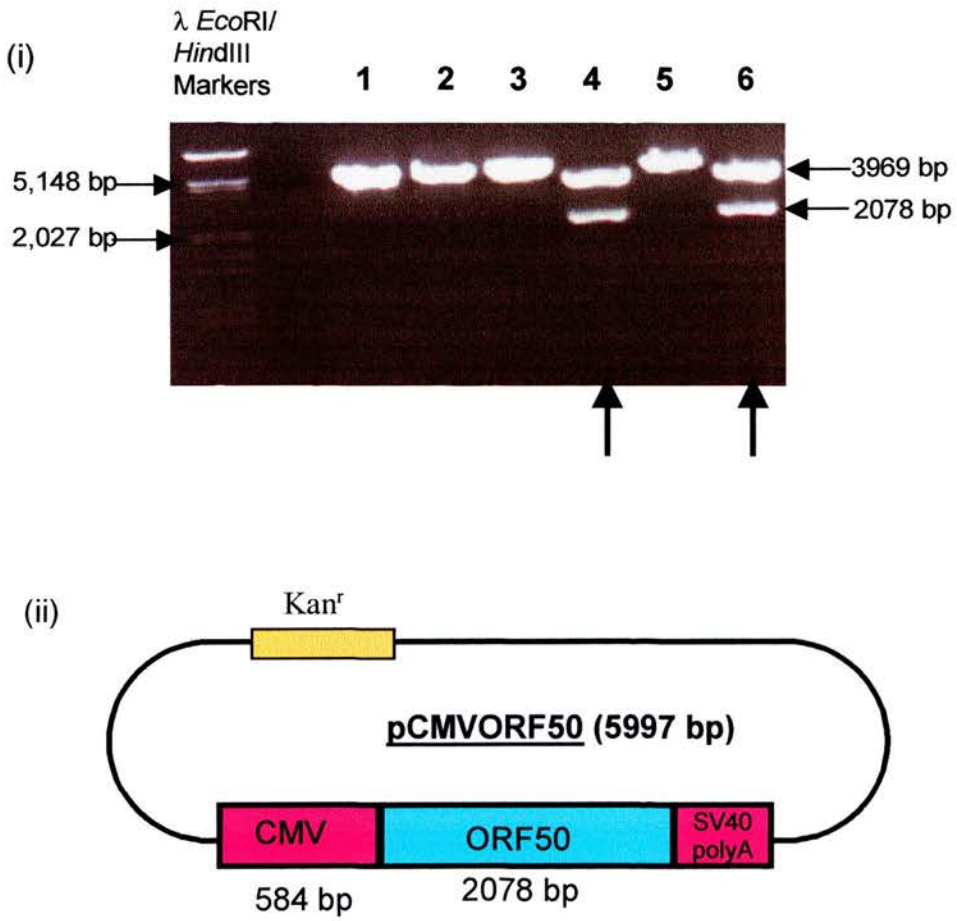

Figure 3.10: Construction of pCMVORF50

(i) Restriction enzyme digests of pCMVORF50. Arrows indicate clones containing the ORF50 sequence (lanes 4 and 6).

(ii) Diagram of pCMVORF50.

Kan^r – kanamycin resistance gene.

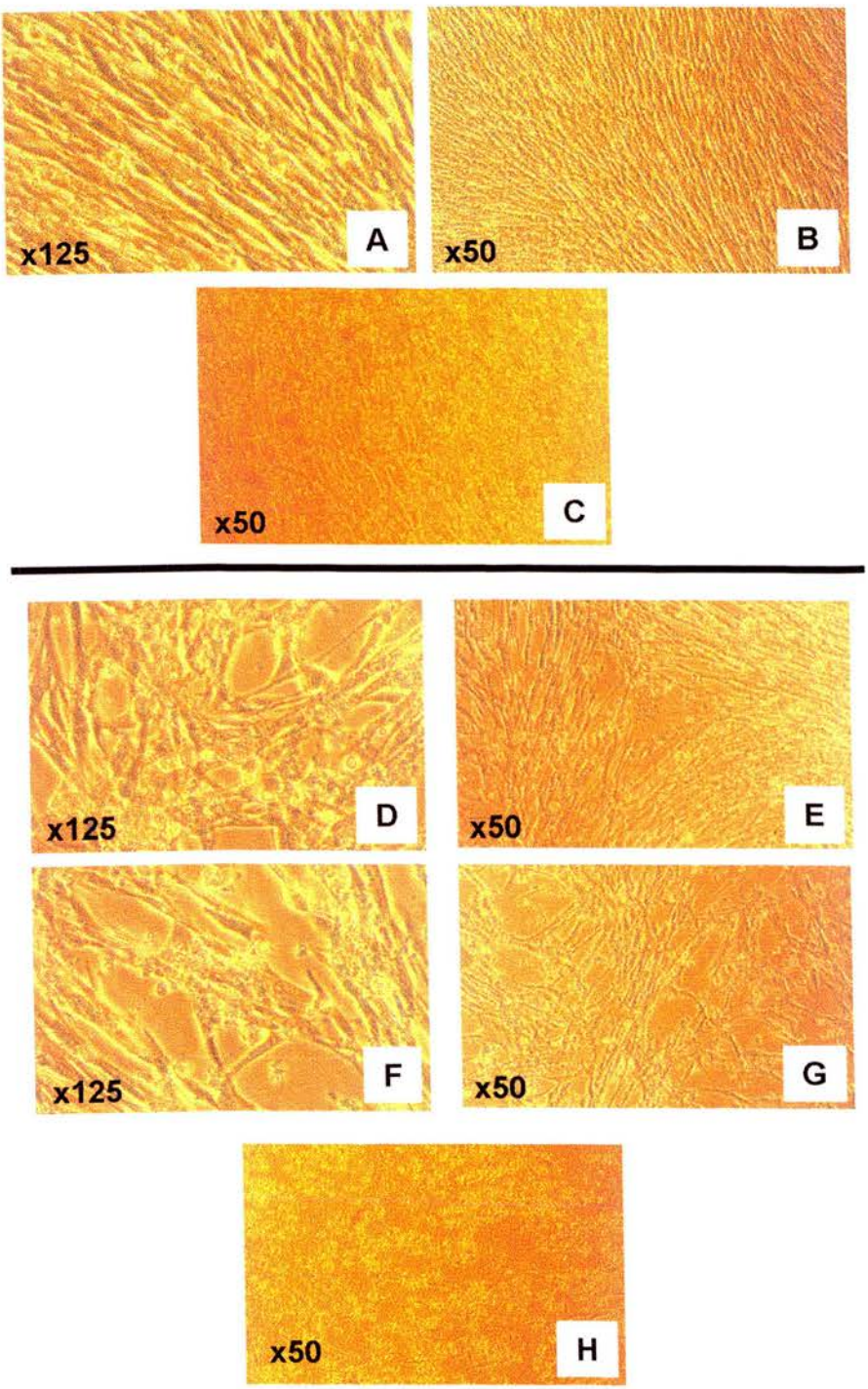

Figure 3.11: BHK cells infected with AlHV-1
A-C - Uninfected BHK cells. D-H - infected BHK cells. CPE is observed as thinning of the monolayer and rounding of cells. A, D and F are higher magnifications of B, E, and G,respectively. E, G, and H show the progressive infection over several days.

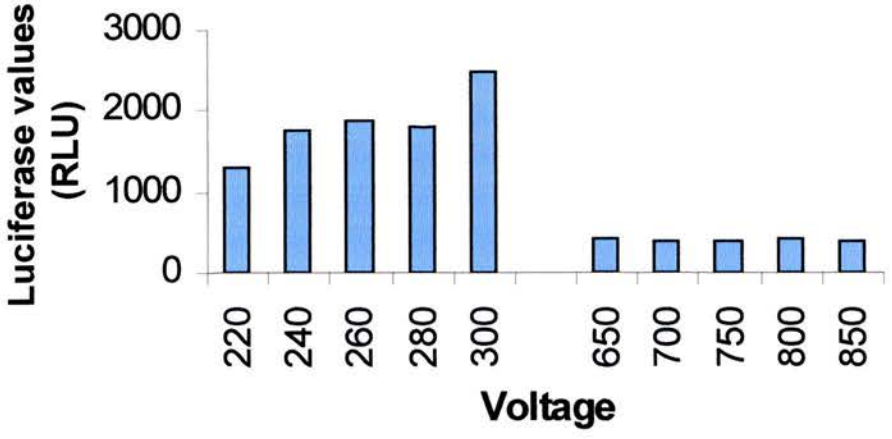

Figure 3.12: Optimisation of electroporation of BHK cells.

BHK cells were transfected with 2 μg of pCMVluc at different voltages and assayed for luciferase activity after 48 h.

Cells were subject to electroporation with either a single or a double pulse:

Single		220-300 V	1050 μF
Double:	1st pulse	100 V	25 μF
	2nd pulse	650-800 V	1500 μF

The results shown represent a single experiment.

from 366-415 RLU, and single pulse values from 1297-2468 RLU. The highest value was obtained using a single pulse of 300 V and this was therefore chosen as the optimal voltage to use with BHK cells. When comparing the single pulse values obtained with BHK cells to those obtained with BT cells there is a 5-10 fold improvement in transfection efficiency when using BHK cells. Table 3.1 shows the 'raw' values and the calculations to support this.

Table 3.1: Comparison of the transfection efficiencies of BT cells and BHK cells.

Voltage	Luciferase values using single pulse electroporation (RLU)		BHK cell value / BT cell value
	BT cells	BHK cells	Fold difference
220	240	1297	5.4
240	162	1733	10.7
260	223	1877	8.4
280	242	1777	7.3
300	428	2468	5.8

3.3.9 Activation of putative AlHV-1 promoters by pCMVORF50 in BHK cells

Assays were carried out by transfecting 2 μg of the promoter reporter constructs alone or with 2 μg pCMVORF50 into BHK cells. The fold induction of activation of the promoters was calculated by dividing the activity obtained from samples transfected with pCMV-ORF50 by that obtained in samples without pCMV-ORF50 (Figure 3.13 and Appendix 4). This experiment was carried out on three separate occasions using single samples and the same trend was obtained each time. The results of these experiments are shown as three separate graphs.

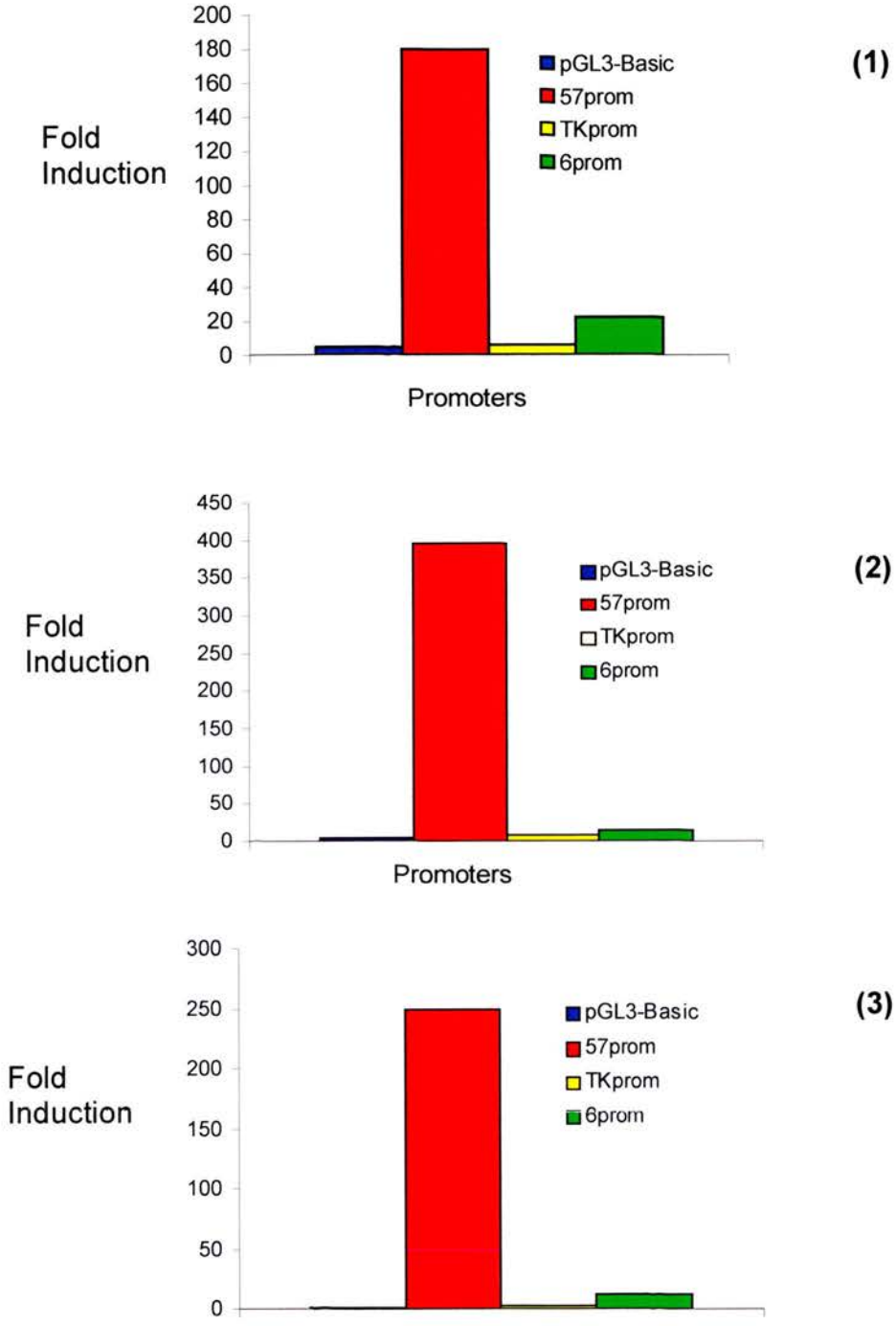

Figure 3.13 : Activation of AlHV-1 promoters by pCMVORF50 in BHK cells
BHK cells were transfected with 2 μg of pGL3-Basic, 57prom, TKprom or 6prom with or without 2 μg pCMVORF50. Results show the fold induction of activity of each promoter in the presence and absence of pCMVORF50. The results from three separate experiments are shown.

The AlHV-1/Rta appeared to strongly induce 57prom between 179-fold to 395-fold. The activation of 6prom was induced to a much lesser degree, and ranged from 13-fold to 22-fold. The activity of TKprom was not considerably higher than that of pGL3-Basic, which lacks promoter sequences, and therefore it was concluded that the putative TK promoter region is not activated by AlHV-1/Rta.

3.3.10 Inclusion of more controls

The experiments outlined above identified an appropriate and efficient cell line for use in these studies and revealed that 57prom and 6prom were activated by the AlHV-1/Rta. However, the system did not include an internal control to account for variations in transfection efficiency between samples. Thus, an internal control was included which made use of the Dual-luciferase Reporter System (Promega). In each transfection mixture, the pRL-SV40 vector (0.2 μg) was added in addition to the promoter construct or promoter construct and expression construct. The pRLSV40 vector contains a gene encoding *Renilla* luciferase under the control of the simian virus 40 (SV40) promoter. 57 prom, TK prom and 6prom, constructed using the pGL3-Basic vector, contain the firefly luciferase gene. These two luciferase enzymes use different substrates and so it is possible to discriminate between their bioluminescence reactions. The activity of the firefly luciferase reporter constructs can thus be normalised against the values obtained in the same sample for *Renilla* luciferase. The fold-induction of the samples with and without pCMVORF50 may then be calculated from the following formula:

$$\frac{\text{(Firefly value/}\textit{Renilla}\text{ value) in the presence of pCMVORF50}}{\text{(Firefly value/}\textit{Renilla}\text{ value) in the absence of pCMVORF50}} = \text{Fold Induction}$$

3.3.11 Activation of putative AlHV-1 promoters by pCMVORF50 in BHK cells using the Dual-luciferase Reporter System

In the experiments described in Figure 3.14, 3.15, 3.16, 3.19(b) and (c) and 3.21(b), BHK cells were transiently transfected with one of the promoter constructs or the empty vector, pGL3-Basic, in the presence of the pRLSV40 control plasmid, with or without pCMVORF50. The average fold induction of activity of pGL3-Basic in the presence of pCMVORF50 for all of these experiments was 3.69+/-2.28 (standard deviation) (Appendix 14). The pGL3-Basic fold induction value was used as the background value in each of the experiments shown.

Figure 3.14 shows the results of three independent experiments using single samples. Figure 3.15 shows the mean of results from an additional experiment performed in triplicate. Standard deviations were calculated and are shown on the graph as error bars (Figure 3.15). All 'raw' luciferase data for these experiments can be found in Appendices 5 and 6.

The results presented in Figures 3.14 and 3.15, which made use of the pRLSV40 internal control, reproduced the findings obtained in Figure 3.13, in that the ORF57 promoter is greatly induced, the ORF6 promoter is moderately induced, and the TK promoter is not induced in the presence of pCMVORF50.

The trends are the same in all sets of experiments although the fold induction values varied. Thus, in Figure 3.14 AlHV-1/Rta activated 57prom from 49-67 fold and 6prom from 12-19 fold. In Figure 3.15 AlHV-1/Rta activated 57prom from 15-36 fold and 6prom from 4-8 fold. One explanation for the range of fold induction values

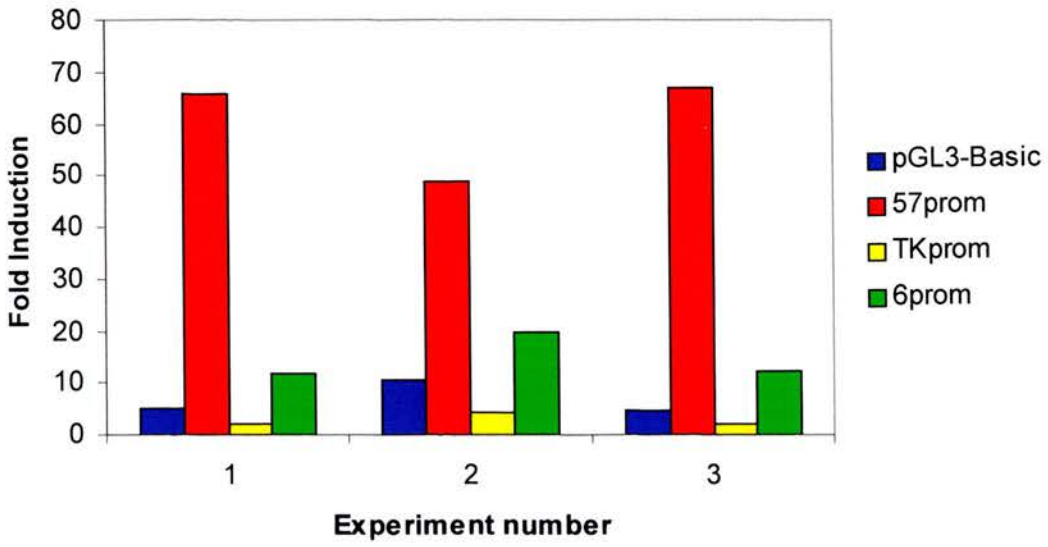

Figure 3.14: Activation of AlHV-1 promoters by pCMVORF50 in BHK cells with a pRLSV40 internal control.

BHK cells were transfected with 2 μg of pGL3-Basic, 57prom, TKprom or 6prom and 0.2 μg of pRLSV40, with or without 2 μg of pCMVORF50. The activity of each promoter was normalised using the *Renilla* luciferase value. The fold induction of activity of each promoter was calculated using the values obtained in the presence and absence of pCMVORF50. The results from three separate experiments are shown.

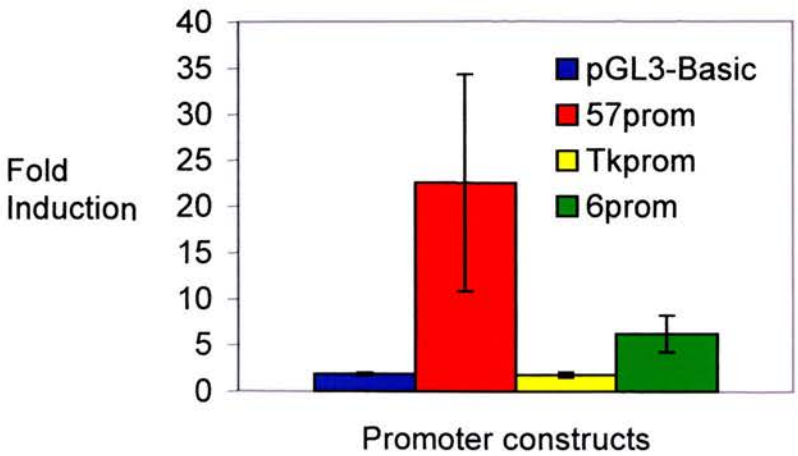

Figure 3.15: Activation of AlHV-1 promoters by pCMVORF50 in BHK cells with a pRLSV4O internal control, in triplicate.

BHK cells were transfected with 2 μg of pGL3-Basic, 57prom, TKprom or 6prom and 0.2 μg of pRLSV40, with or without 2 μg of pCMVORF50. The experiment was performed in triplicate. Results show the average fold induction of each promoter in the presence or absence of pCMVORF50. Error bars indicate the standard deviation. Before calculating fold induction the activities were normalised to the *Renilla* value.

could be variation between samples, as each transfection mix was prepared independently and each sample was electroporated individually.

Moreover, it became clear when using the Dual-luciferase Reporter System (section 2.4.9) that the 'raw' luciferase values obtained with a new kit were higher than the values obtained after repeated use, despite the fact that components were stored as recommended.

From these experiments, using a cell line that gives high transfection efficiency and includes an internal control that accounts for variations between individual sample transfection efficiency, the conclusion is that AlHV-1/Rta can act as a transactivator. AlHV-1/Rta can strongly activate the AlHV-1 ORF57 promoter and to a lesser extent the AlHV-1 ORF6 promoter but does not activate the TK promoter.

3.3.12 Co-transfection of pCMVORF50 with luciferase reporter plasmids containing CMV, SV40 and HSV TK promoters

To establish whether AlHV-1/Rta could act as a promiscuous transactivator, pCMVORF50 was used in transient transfection assays with various non-AlHV-1 virus promoters. The CMV IE promoter, the SV40 promoter and the HSV-1 TK promoter as well as pGL3-Basic were all used with or without pCMVORF50. The experiment was carried out on triplicate. The constructs used were pCMVluc (CMV IE promoter driving expression of the firefly luciferase gene; described in section 3.3.4), pRL-SV40 (SV40 promoter driving *Renilla* luciferase; Promega) and pTKluc (HSV-1 TK promoter driving firefly luciferase; constructed by Louise King by inserting the HSV TK promoter from pRLTK into pGL3-Basic).

The results (Figure 3.16 and Appendix 7) showed that AlHV-1/Rta had no effect on the CMV IE, HSV-1 TK or SV40 promoters. All activities measured were less than that of pGL3-Basic, an empty vector with no promoter sequences. It was therefore concluded that AlHV-1/Rta did not act as a promiscuous transactivator.

3.4 Analysis of the AlHV-1 ORF57 promoter

3.4.1 Transcription of 57prom

As the most significant effect of AlHV-1/Rta was on the ORF57 promoter, this promoter was analysed further. The ORF57 promoter sequence used in the luciferase reporter assays mentioned above was putative. Before it was investigated further, transcription from the construct was analysed to determine where its transcriptional start site was located in relation to the translational start site predicted by Ensser *et al.* (1997).

pCMVORF50 (2 μg) and 57prom (2 μg) were transfected into BHK cells and total cellular RNA was extracted after 48 h (see section 2.5.1). Aliquots of 5 μg or 30 μg of total RNA from transfected or untransfected BHK cells were loaded onto a formaldehyde agarose gel and subjected to Northern blot analysis (section 2.5.3-2.5.4) (Figure 3.17). Digestion with restriction endonucleases within the ORF57 promoter sequence generated two fragments of 353 bp and 466 bp corresponding to the left-hand and right-hand sections of the promoter sequence, respectively (Figure 3.17(c)). These fragments were gel-purified and used to probe the membrane (section 2.5.5-2.5.6).

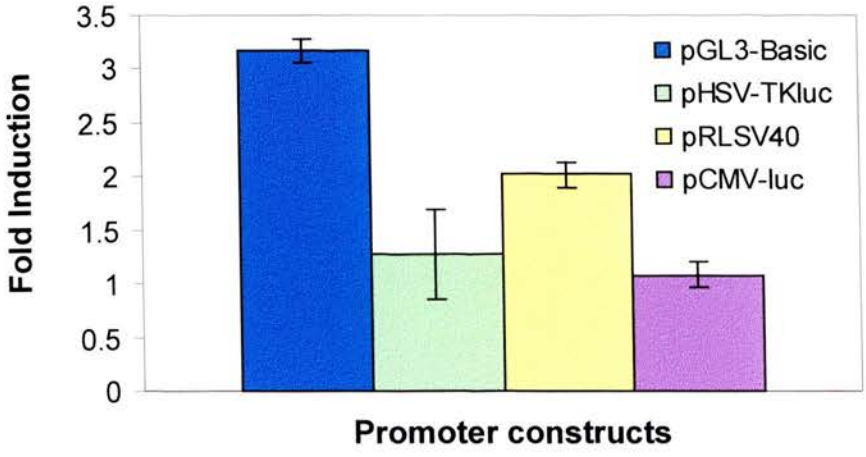

Figure 3.16: Effect of pCMVORF50 on non-AlHV-1 virus promoters

BHK cells were transfected with 2 μg of pGL3-Basic, pHSV-Tkluc, pRLSV40 or pCMVluc with or without 2 μg of pCMVORF50.

The results show the average fold induction of activity of each promoter in the presence or absence of pCMVORF50. The experiment was performed in triplicate and error bars show the standard deviation.

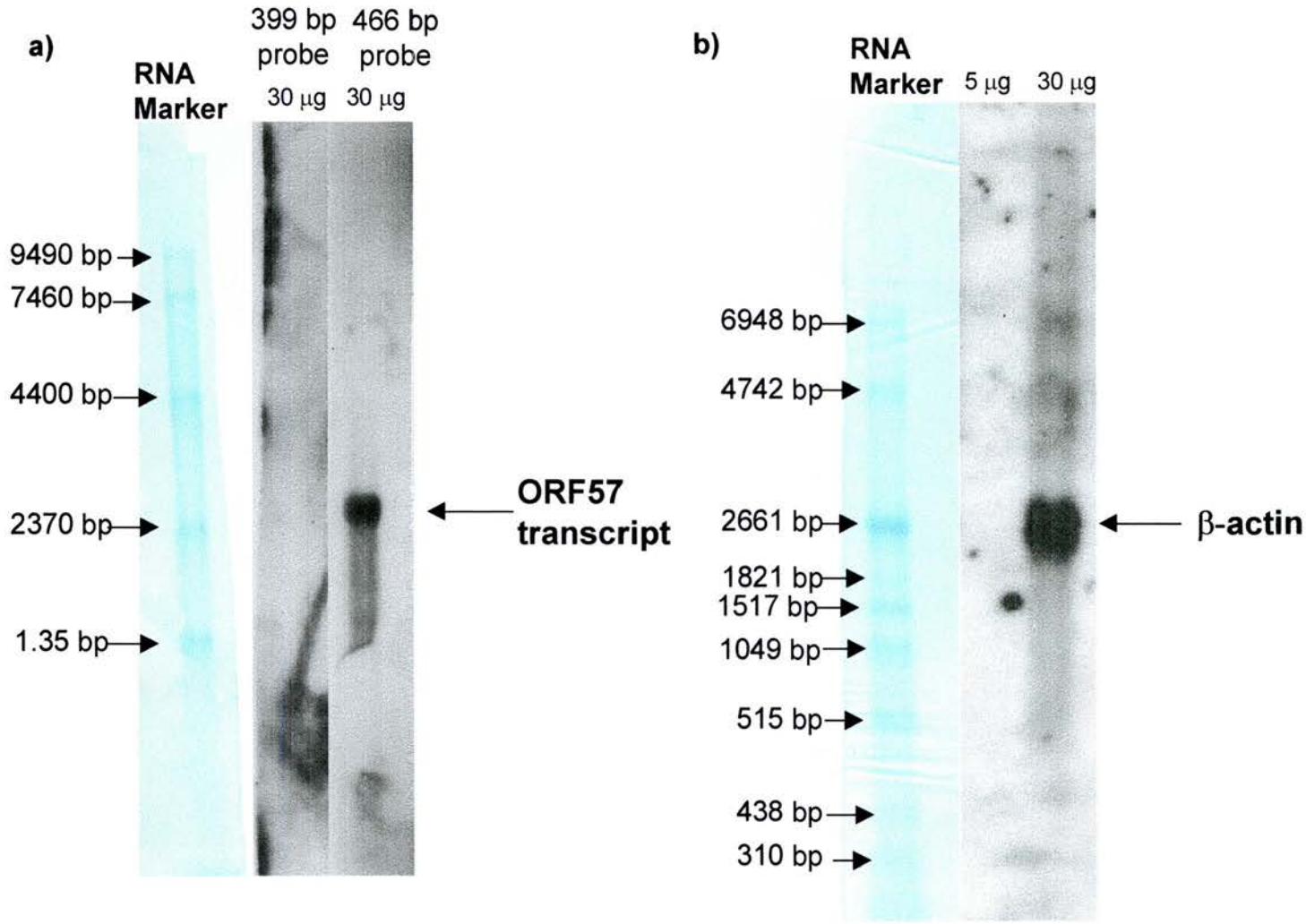
a)
RNA Marker
399 bp probe
466 bp probe
30 μg
30 μg
9490 bp
7460 bp
4400 bp
2370 bp
1.35 bp
ORF57 transcript
b)
RNA Marker
5 μg
30 μg
6948 bp
4742 bp
2661 bp
1821 bp
1517 bp
1049 bp
515 bp
438 bp
310 bp
β-actin

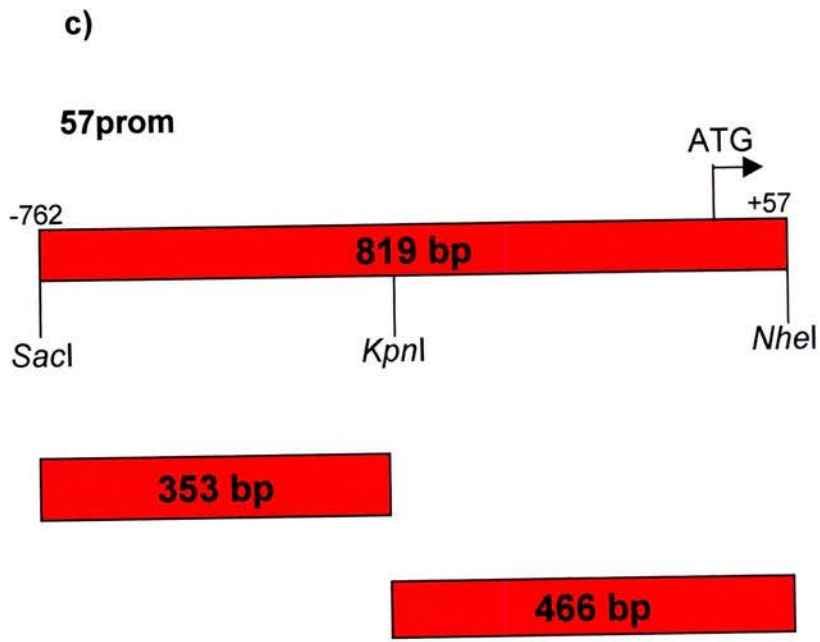

Figure 3.17: Transcription of 57prom

a) Northern blot of RNA extracted from BHK cells co-transfected with 57prom and pCMVORF50. Duplicate RNA samples were electrophoresed on a formaldehyde agarose gel and blotted onto a nylon membrane. One sample was probed with the 353 bp left hand section of the ORF57 promoter sequence and the other probed with the 466 bp right hand section of the ORF57 promoter.

b) 5μg and 30 μg of total RNA used in a) hybridised with a β-actin probe.

c) Diagram indicating the positions of the two probes used relative to the ORF57 promoter. The ATG indicated represents the translational start codon predicted by Ensser *et al.* (1997).

As can be seen in Figure 3.17(a), a band was observed when using the 466 bp (RH) probe but no band was visible using the 353 bp (LH) probe. Aliquots of the same RNA samples were electrophoresed on a second gel and the blot was incubated with a β-actin probe as a positive control (Figure 3.17(b)). β-actin transcripts were detected, showing that the RNA was intact. The *Kpn*1 site used to dissect the promoter was 409 bp upstream of the translational start codon. Since the transcript was only detected by the 466 bp (RH) probe this indicated that the ORF57 transcriptional start site must be located no more than 409 bp 5' of the translational start codon, otherwise it would have been detected by both probes.

3.4.2 Locating the ORF57 transcriptional start site and splice sites

To further analyse transcription from the ORF57 promoter, this time in the context of the virus, the 5'-RACE method was chosen. A diagrammatic representation of the 5'-RACE method is shown in Figure 3.18(a). Total cellular RNA extracted from virus-infected BT cells treated with cycloheximide (section 2.5.1 and 2.5.2) was used for 5'-RACE. The data presented (Figure 3.18(b)) shows that the transcriptional start site of ORF57 is located at position 84438 in the AlHV-1 genome. Ensser *et al.* (1997) predicted the translational initiation codon of ORF57 to be at position 84462 and the TATA box to be at position 84408. The transcriptional start site identified in this study is therefore 24 bp upstream of the predicted translational start site and 30 bp downstream of the predicted TATA box. The cDNA obtained by 5'-RACE also showed splice donor (SD) and splice acceptor (SA) sites at positions 84513 and 84605 respectively.

a)

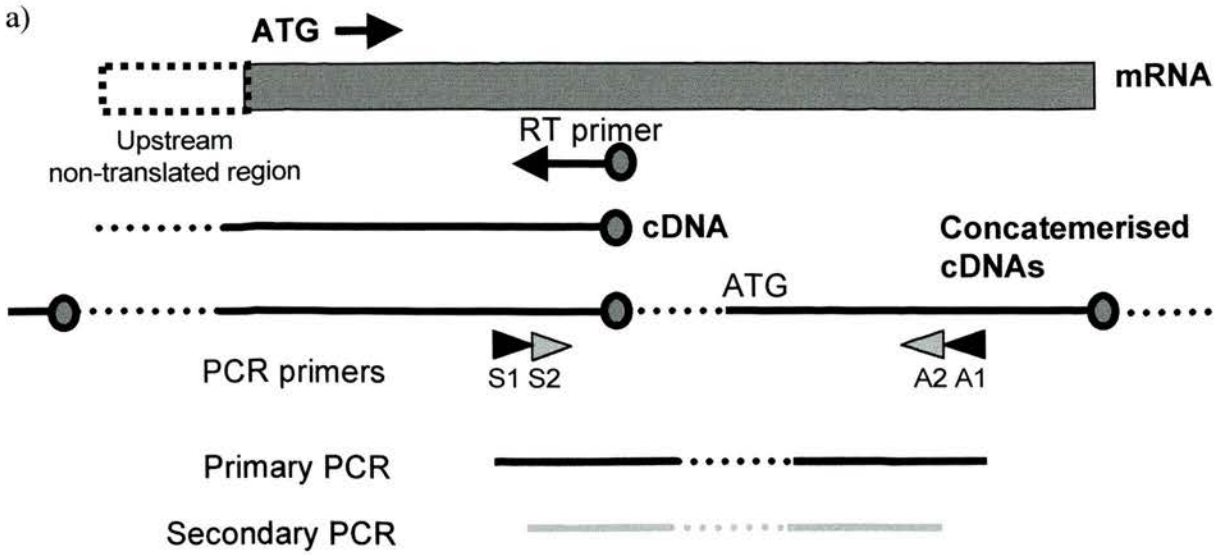

b)

```
                                    TATA box
84388  TTTAGGAAACTATCACTGCCATAAATTAGTTTGAATAACTTCATTTTTCA 84437
       ||||||||||||||||||||||||||||||||||||||||||||||||||
       ..................................................

                                start codon
84438  TCACTTCTCCTGCATCTCAAAAACATGGCTCAGCAGGCAATTGTGACTAT 84487
       ||||||||||||||||||||||||||||||||||||||||||||||||||
       TCACTTCTCCTGCATCTCAAAAACATGGCTCAGCAGGCAATTGTGACTAT

                                    SD
84488  GAGTGCTTTAAGACGCACCATGGAGGGTAAGATATTTCTTTCTTTTTTTT 84537
       |||||||||||||||||||||||||
       GAGTGCTTTAAGACGCACCATGGAGG.........................
                                .
                                .
                                .
                          SA                        A2 primer
84588  CTTTCATGTTGTGTTAGTTTCAGACTCAGGAGATGTCAGTATAGACATCT 84637
                       ||||||||||||||||||||||||||||||||||
       ................TTTCAGACTCAGGAGATGTCAGTATAGACATCT

84638  CTGCAGAGGATTC 84650     AlHV-1 genome sequence
       |||||||||||||
       CTGCAGAGGATTC          5'-RACE product sequence
```

Figure 3.18 - Results of 5'-RACE of AlHV-1 ORF57.

(a) Diagrammatic representation of the 5'-RACE method. The diagram shows the mRNA transcript of ORF57 and position of the complimentary phosphorylated RT primer relative to it. The reverse transcription reaction results in cDNAs with a phosphate group at one end allowing concatemerisation. The concatemerised cDNAs are used as a template for a PCR reaction with primers S1 and A1 to generate the primary PCR product. This product was used in turn as a template for the second round of PCR using primers S2 and A2, The secondary PCR product was subcloned into the pGEM-T Easy vector to permit sequencing with the pUC/M13 primer. The PCR products span the upstream non-translated region.

(b) A sequence comparison of the secondary PCR product (lower line), and the AlHV-1 genome (Genbank accession number AF005370) (upper line) is shown. The location of the A2 primer is shown. The transcriptional start site has been determined to be 24 bp upstream of the predicted translational start site and 30 bp downstream of the predicted TATA box. Also clearly seen are the splice donor (SD) and splice acceptor (SA) sites of ORF57.

3.4.3 Further analysis of the ORF57 promoter

Several of the Rta-responsive genes in other γHVs have specific sequences in their promoters that act as Rta response elements (REs) (Gruffat and Sergeant, 1994; Whitehouse *et al.*, 1997b; Song *et al.*, 2001; Lukac *et al.*, 2001). Investigations were undertaken to locate possible AlHV-1/Rta REs in the ORF57 promoter. It was thought that identification of REs could lead to the discovery of other potential AlHV1/Rta-responsive genes.

3.4.4 Construction of truncated ORF57 promoters

Deletion constructs of the ORF57 promoter, shown in Figure 3.19(a) and (b), were made using appropriate restriction enzymes or PCR. All constructs were named according to their size in bp.

Construct 57p(768) comprises a fragment amplified using the sense primer 5' - AAG AGC TCT GGG CAG CTA GAG AG (Nt 83751-83765) containing a *Sac*I site (underlined) and the same antisense primer used to amplify the initial ORF57 promoter sequence (5' – AAG CTA GCT CTT ACC CTC CAT GG (Nt 84519-84505) containing an *Nhe*I site (underlined)). The PCR programme was the same as that used for the ORF6 promoter (section 3.3.1). The fragment was inserted into pGL3-Basic using *Sac*I and *Nhe*I restriction sites to generate 57p(768).

Construct 57p(686) was generated by digestion of 57prom with *Hin*dIII/*Nhe*I. The fragment was inserted into pGL3-Basic digested with *Sac*I/*Nhe*I to generate 57p(686). The *Sac*I and *Hin*dIII sites were filled in (section 2.2.7) to allow a blunt-

end ligation at the 5' end of the fragment (section 2.2.8).

Construct 57p(579) comprises a fragment amplified using the sense primer, 5'-AAG AGC TCT CAG AAG CAG CTT CC (Nt 83940-84519) containing a *Sac*I site (underlined) and the same antisense primer and PCR programme used to generate 57p(768). The fragment was inserted into pGL3-Basic using *Sac*I and *Nhe*I restriction sites to generate 57p(579).

Construct 57p(466) was generated by digestion of 57prom with *Kpn*I/*Nhe*I. The fragment was inserted into pGL3-Basic using *Kpn*I and *Nhe*I restriction sites.

Construct 57p(180) was generated by digestion of 57prom with *Sau*3AI. The fragment was inserted into the *Sac*I and *Nhe*I restriction sites of pGL3-Basic by blunt-end ligation to generate 57p(180). All sites were filled in to allow blunt-end ligation at both the 5' and 3' end of the fragment.

Construct 57p(194) was generated by digestion of 57prom with *Sau*3AI/*Nhe*I. The fragment was inserted into pGL3-Basic using *Sac*I and *Nhe*I restriction sites to generate 57p(194). The *Sau*3AI and *Sac*I sites were filled in to allow blunt-end ligation at the 5' end of the fragment.

Construct 57p(133) was generated by digestion of 57prom with *Sac*I/*Hin*dIII. The fragment was inserted into the *Sac*I and *Nhe*I restriction sites of pGL3-basic to generate 57p(133). The *Hin*dIII and *Nhe*I sites were filled in to allow blunt-end

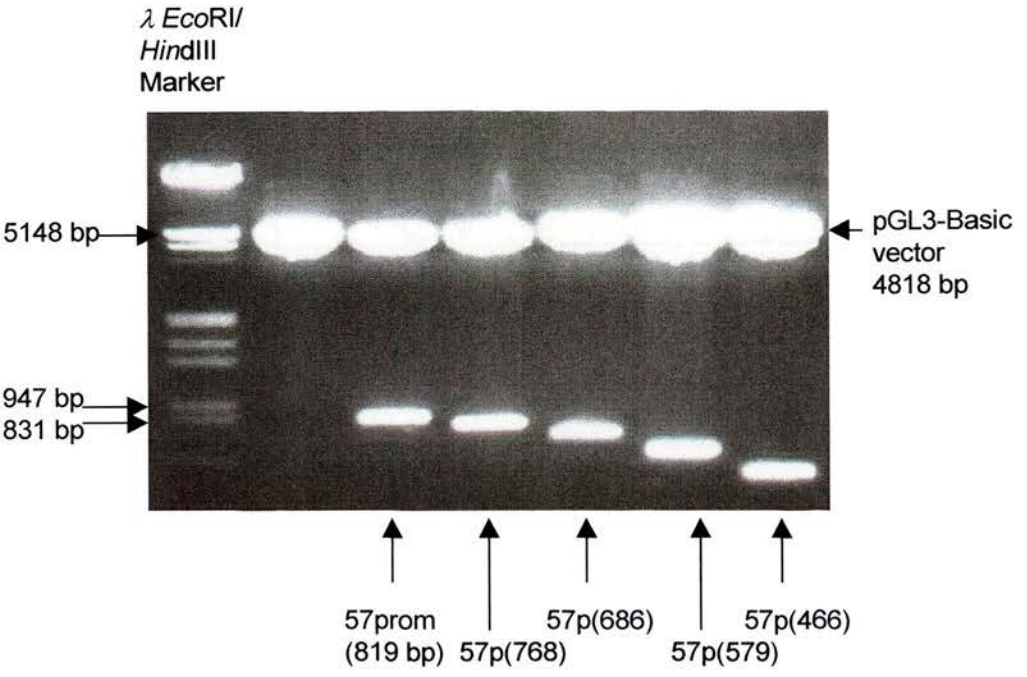

Figure 3.19 (a) Restriction Digests of ORF57 promoter truncations

Restriction digests of the ORF57 promoter constructs, generated using pGL3-Basic, to confirm the sizes of the inserts.
57prom, 57p(768), 57p(686) and 57p(579) were digested with *Sac*I and *Nhe*I. 57p(466) was digested with *Kpn*I and *Nhe*I.

ligation at the 3' end of the fragment.

3.4.5 Activity of truncated ORF57 promoters

Figure 3.19(b) shows the 57prom promoter and the position of the deletion constructs relative to it. BHK cells were transfected with pGL3-Basic or an ORF57 promoter construct both with and without pCMVORF50. The ability of AlHV-1/Rta to transactivate each promoter is indicated by a plus or minus symbol in Figure 3.19(b). As before, pGL3-Basic was used as the background control and any fold induction value above that obtained with this plasmid was regarded as activation. The 'raw' luciferase and fold induction values for the effect of AlHV-1/Rta on these constructs are given in Appendix 8. Constructs were tested as they were made and the data is therefore represented as four separate graphs in Figure 3.19(c) and in a summarised form in Figure 3.19(b).

Constructs 57p(768), 57p(686) and 57p(579) were all activated by AlHV-1/Rta whereas constructs 57p(466), 57p(133), 57p(180) and 57p(194) were not. The results suggest that the sequence present in 57p(579) but absent in 57p(466), 409-522 bp upstream of the translational start codon, is important for activation since 57p(579) is activated by AlHV-1/Rta and 57p(466) is not activated by AlHV-1/Rta.

To confirm this finding, 57p(466), the largest construct that was not activated by AlHV-1/Rta, was remade and tested, and named 57p(466)B. This experiment is seen in Figure 3.19(c) (iv) and the 'raw' luciferase values are in Appendix 8. The construct 57p(466)B was not activated by AlHV-1/Rta thereby confirming the

Figure 3.19 (b): Diagrammatic representation of the ORF57 promoter constructs.

The lengths of each putative promoter sequence, their position relative to the 57prom promoter sequence and their 5' location relative to the translational start codon are indicated. Each promoter was used in co-transfection experiments with pCMVORF50, the results of which are shown on the right hand side of the figure.

This diagram is a summary of several experiments that are shown in graphical format in Figure 3.19(c).

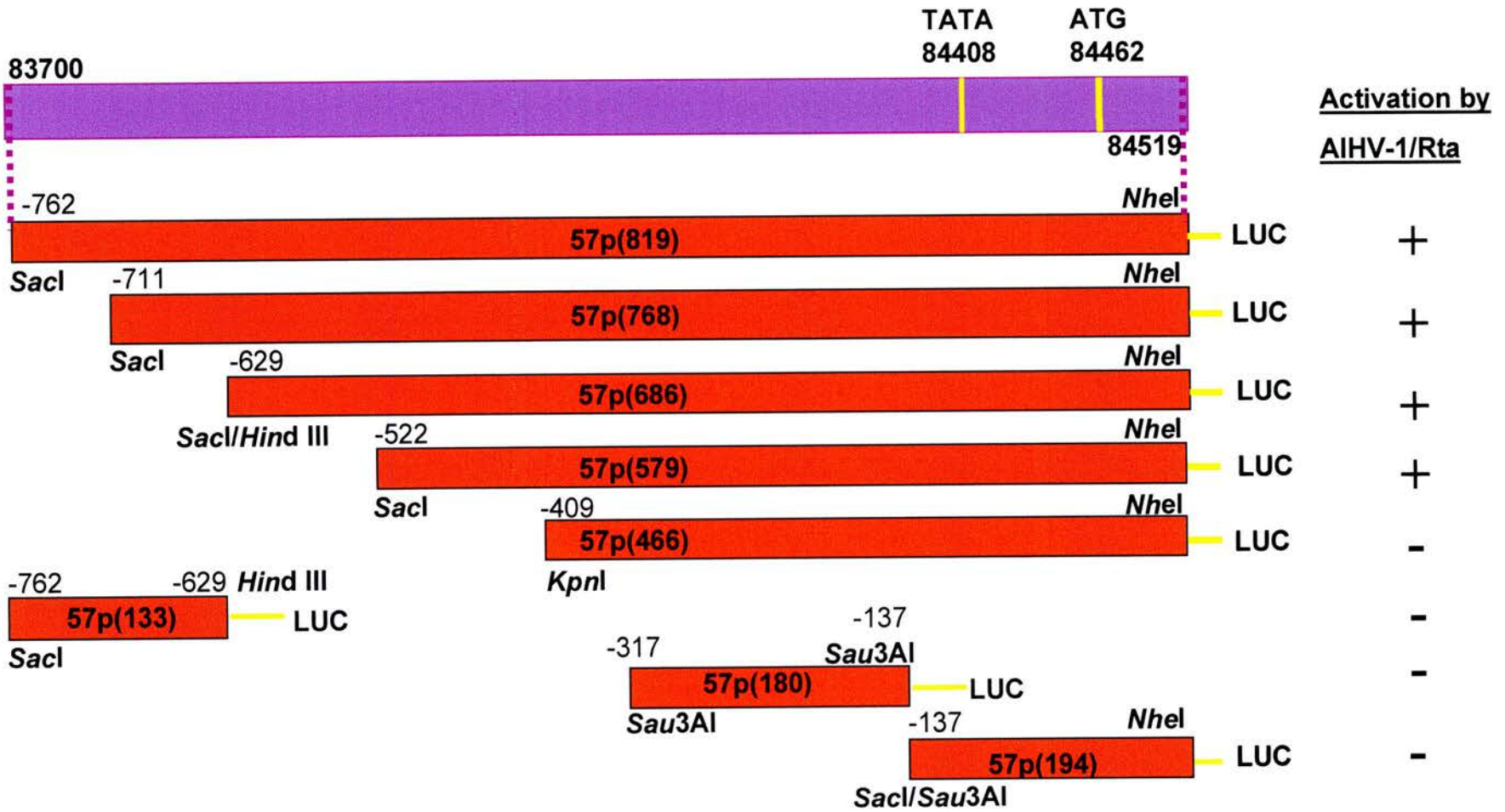
TATA
84408
ATG
84462
83700
84519
Activation by
AlHV-1/Rta
-762
NheI
57p(819)
LUC
+
SacI
-711
NheI
57p(768)
LUC
+
SacI
-629
NheI
57p(686)
LUC
+
SacI/Hind III
-522
NheI
57p(579)
LUC
+
SacI
-409
NheI
57p(466)
LUC
-
KpnI
-762
-629
Hind III
57p(133)
LUC
-
SacI
-137
-317
Sau3AI
57p(180)
LUC
-
Sau3AI
-137
NheI
57p(194)
LUC
-
SacI/Sau3AI

(i)

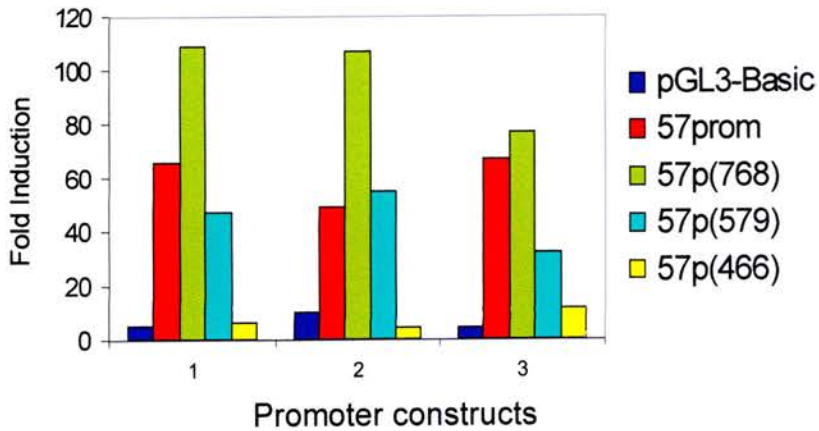
120
100
80
60
40
20
0
Fold Induction
1
2
3
Promoter constructs
pGL3-Basic
57prom
57p(768)
57p(579)
57p(466)

(ii)

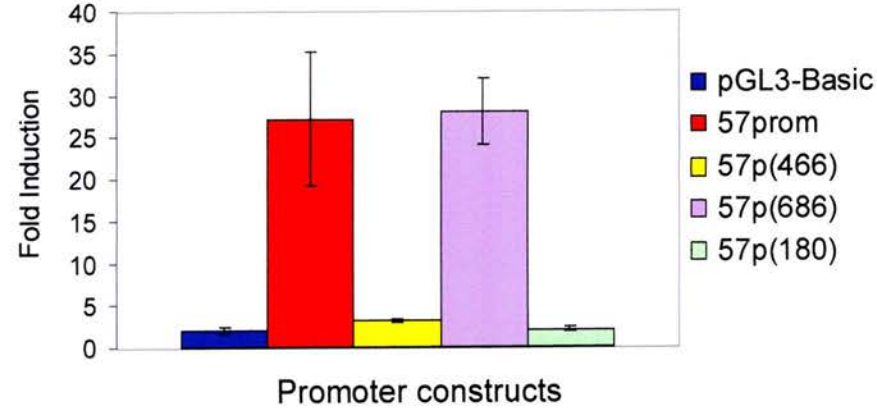
40
35
30
25
20
15
10
5
0
Fold Induction
Promoter constructs
pGL3-Basic
57prom
57p(466)
57p(686)
57p(180)

(iii)

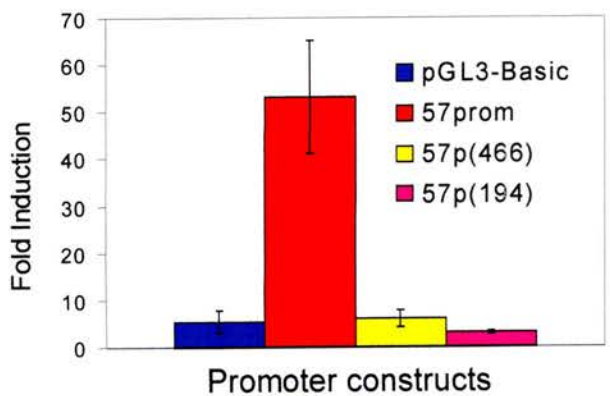
70
60
50
40
30
20
10
0
Fold Induction
Promoter constructs
pGL3-Basic
57prom
57p(466)
57p(194)

(iv)

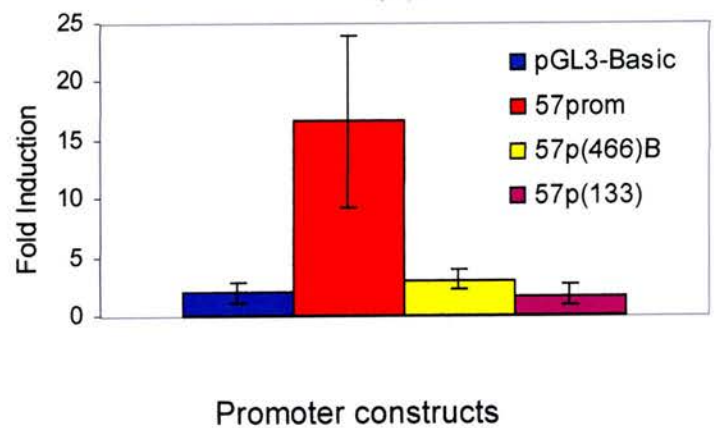
25
20
15
10
5
0
Fold Induction
Promoter constructs
pGL3-Basic
57prom
57p(466)B
57p(133)

Figure 3.19 (c): Experimental Data on the Effect of pCMVORF50 in transient transfections with ORF57 Promoter constructs.

All of the 57prom truncated constructs were made at different times and were tested as they were made therefore the diagram shown in Figure 3.19(c) summarises several experiments, which are presented here.

57prom was used in all experiments because it was previously shown to be activated by AlHV-1/Rta (Figures 3.14 and 3.15), and so acted as a positive control. 57p(466) was not activated by AlHV-1/Rta and was used as a negative control in all experiments.

(i) Results of three separate experiments testing constructs 57p(768), 57p(579) and 57p(466).

(ii) Results of one experiment, carried out in triplicate, testing constructs 57p(686), 57p(180) and 57p(466).

(iii) Results of one experiment, carried out in triplicate, testing constructs 57p(194) and 57p(466).

(iv) Results of one experiment, carried out in triplicate, testing constructs 57p(466)B and 57p(133).

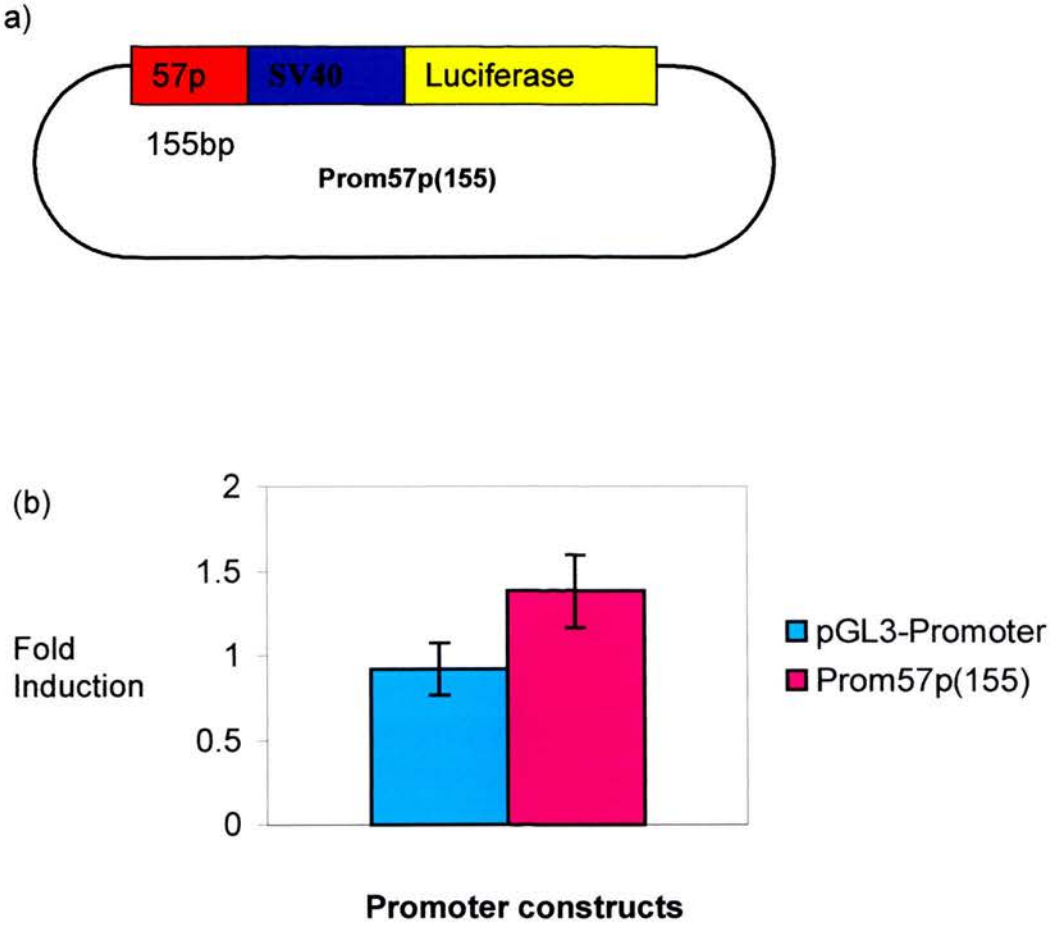

Figure 3.20 Construction and analysis of Prom57p(155)

(a) Diagram of Prom57p(155). The 155 bp of sequence from the ORF57 promoter is inserted upstream of a luciferase reporter gene driven by an SV40 promoter.

(b) BHK cells were transfected with 2 μg of Prom57p(155) or pGL3-Promoter with or without 2 μg of pCMVORF50 and in the presence of 0.2 μg of pRLSV40 control plasmid.

The average fold induction of activity of samples in the presence and absence of pCMVORF50 is presented. Error bars show standard deviation.

original observations.

3.4.6 Analysis of the sequence between 57p(579) and 57p(466) for AlHV-1/Rta specific activity.

Since the 113 bp sequence (409-522 bp 5' of the ATG) present in 57p(579) and absent from 57p(466) was thought to be important for activation by AlHV-1/Rta it was analysed further. There was a possibility that an AlHV-1/Rta-responsive element was contained within this sequence or within close proximity. Indeed, a sequence corresponding to the HVS Rta RE (Whitehouse *et al.*, 1997b) was present in this sequence. This will be discussed further in Chapter 5. A 155 bp sequence consisting of the 113 bp plus 42 bp downstream was amplified by PCR using the following primers; 5' - AAG CTA GCG AGA ACT GCT GCA GT (Nt 84081-84095), which contains an *Nhe*I site (underlined) and the 5' primer used to generate 57p(579) (see section 3.4.4). This fragment was inserted into the pGEM-T Easy vector, then subcloned via *Sac*II and *Nhe*I sites into the pGL3-Promoter vector, thus deriving Prom57p(155). The pGL3-Promoter vector contains an SV40 promoter driving a firefly luciferase gene and allows testing of sequences, which have potential enhancer properties (Figure 3.20(a)). Prom57p(155) and the pGL3-Promoter vector were used in transient transfection assays with or without pCMVORF50. The pGL3-Promoter vector was used as a background control.

Results showed that Prom57p(155) was not activated with the addition of pCMVORF50 and so it was concluded that the 155 bp sequence did not have AlHV-1/Rta-responsive activity in this system (Figure 3.20(b) and Appendix 9).

3.4.7 Activity of an additional truncated ORF57 promoter

Since the sequence present in 57p(579) and absent in 57p(466) did not appear to function in isolation as an AlHV-1/Rta-responsive enhancer (section 3.4.6), the ORF57 promoter was investigated further. Upon examination of the raw data (Table 3.2 and Appendix 8) it was noticed that 57p(180) appeared to have some minimal promoter activity in the absence of pCMVORF50. For example, without AlHV-1/Rta the values obtained for 57prom, 57p(466) and 57p(686) were 1-2 RLU whereas the value with 57p(180) was ~14 RLU. It was therefore possible that the 180 bp with potential minimal promoter activity was important, in addition to the 155 bp tested in section 3.4.6, to facilitate AlHV-1/Rta-responsive transactivation.

Table 3.2 Luciferase values for 57p(180)
This table shows the average luciferase values obtained when BHK cells were transfected with the constructs shown in the absence of pCMVORF50.

Constructs	Average luciferase activity with no additions
57prom	1.49
57p(466)	2.53
57p(686)	1.99
57p(180)	14.49

An ORF57 promoter construct was made (Figure 3.21(a)) to investigate if sequences important for AlHV-1/Rta-responsiveness were present within the 180 bp region. Even though the region had no increased activity with AlHV-1/Rta when studied alone, it was considered that it may interact with sequences upstream. This 180 bp region in the middle of the 57p(579) construct was removed by digestion with *Sau*3AI and the flanking sequences religated to form 57p(399). This construct was tested and was shown to be activated by the AlHV-1/Rta at a level approximately

a)

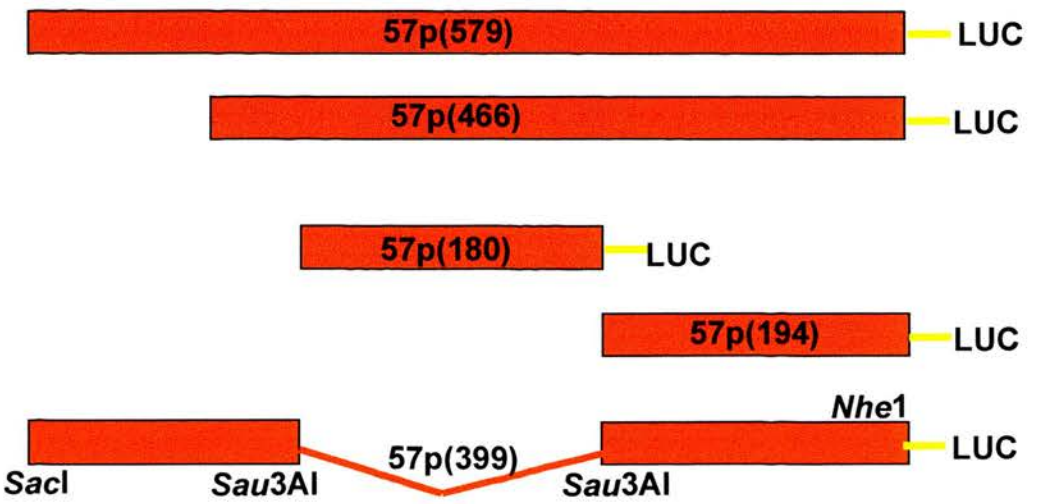

(ii)

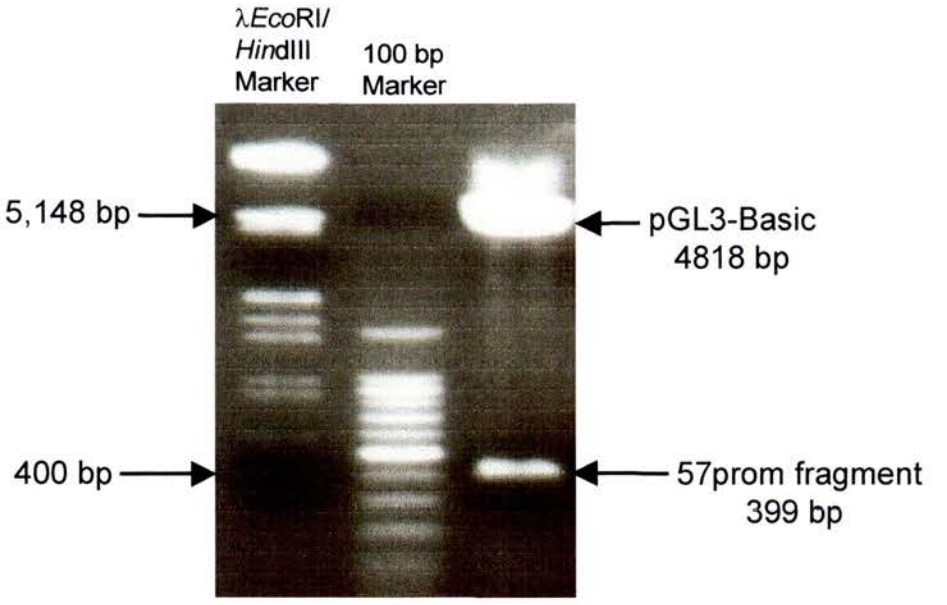

Figure 3.21 (a) Construction of 57p(399)

(i) Diagrammatic representation of the construction of 57p(399) via removal of the central 180 bp from 57p(579).

(ii) *Sac*I and *Nhe*I restriction digest of 57p(399).

half that of the 57p(579) construct (Figure 3.21(b) and Appendix 10). This indicated that although the deleted region was not essential for activation by AlHV-1/Rta, it did exert a positive influence on AlHV-1/Rta transactivation potential. There are two ways this region may be involved in activation: 1) it may contain a specific sequence used for the activation of the promoter; 2) the distance between the two regions on either side of the 180 bp may be important.

Another factor that may have contributed to the activity of 57p(399) is a second sequence within the ORF57 promoter corresponding to the HVS Rta RE (Whitehouse et al., 1997b). As well as one being within the 133 bp 409-522 bp upstream from the start codon, there is another sequence located in the 194 bp sequence at the 3' end of the promoter. Thus, 57p(194), 57p(466) and Prom57p(155), each containing one potential RE, are not activated by AlHV-1/Rta, whereas 57p(399) contains both potential REs and is activated by AlHV-1/Rta. This is discussed further in Chapter 5.

Other deletion constructs of 57prom could be constructed to narrow down the regions of importance for AlHV-1/Rta-responsiveness. Owing to time constraints these constructs were not generated.

3.5 Electrophoretic mobility shift assays

3.5.1 EMSA design and oligonucleotides

Since the 113 bp region between 57p(579) and 57p(466) was deduced to be important for the AlHV-1/Rta-responsiveness of the ORF57 promoter, it was

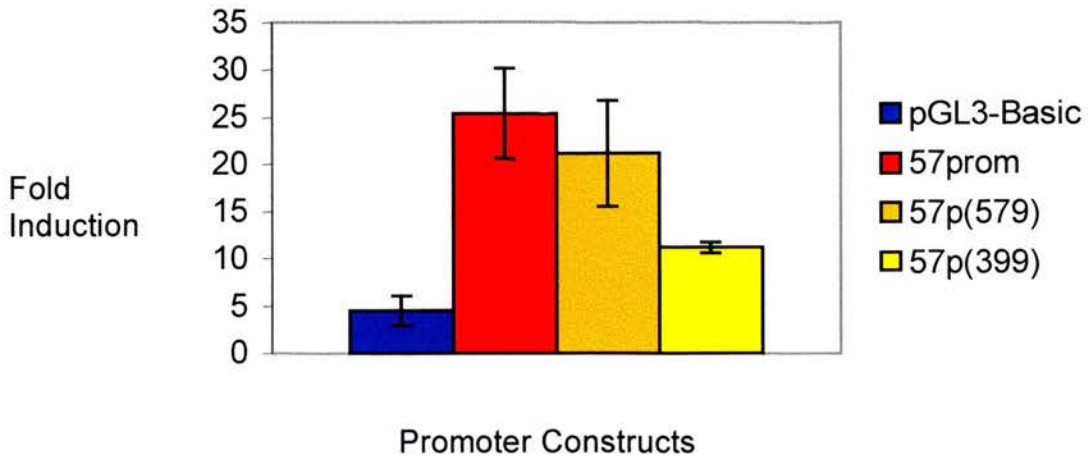

Figure 3.21 (b) : Effect of pCMVORF50 on 57p(399)

BHK cells were transfected with 2 μg of 57prom, 57p(579) or 57p(399) with or without 2 μg of pCMVORF50. All samples were also transfected with 0.2 μg of pRLSV40 as an internal transfection control. Cells were harvested 48 h post-transfection and assayed for luciferase activity. The average fold induction of activity of each promoter was calculated using the values obtained in the presence and absence of pCMVORF50. The experiment was carried out in triplicate. Error bars indicate standard deviation.

investigated further. It is possible that the AlHV-1/Rta binds to this region directly or indirectly. Electrophoretic mobility shift assays (EMSAs) were used to determine if this was the case.

The region to be investigated was expanded to 140 bp because of the possibility that an important sequence could be straddling the region between 57p(579) and 57p(466). Oligonucleotides were designed to cover the potential AlHV-1/Rta-responsive region. For use in EMSAs, four double-stranded oligonucleotides of 35 bp were designed to span the region and three double-stranded oligonucleotides of 35 bp were designed, which overlapped them (Figure 3.22, Table 3.3). All of the double-stranded oligonucleotides had single-stranded overhangs, which were filled in during labelling. The complimentary regions are in bold in Table 3.3.

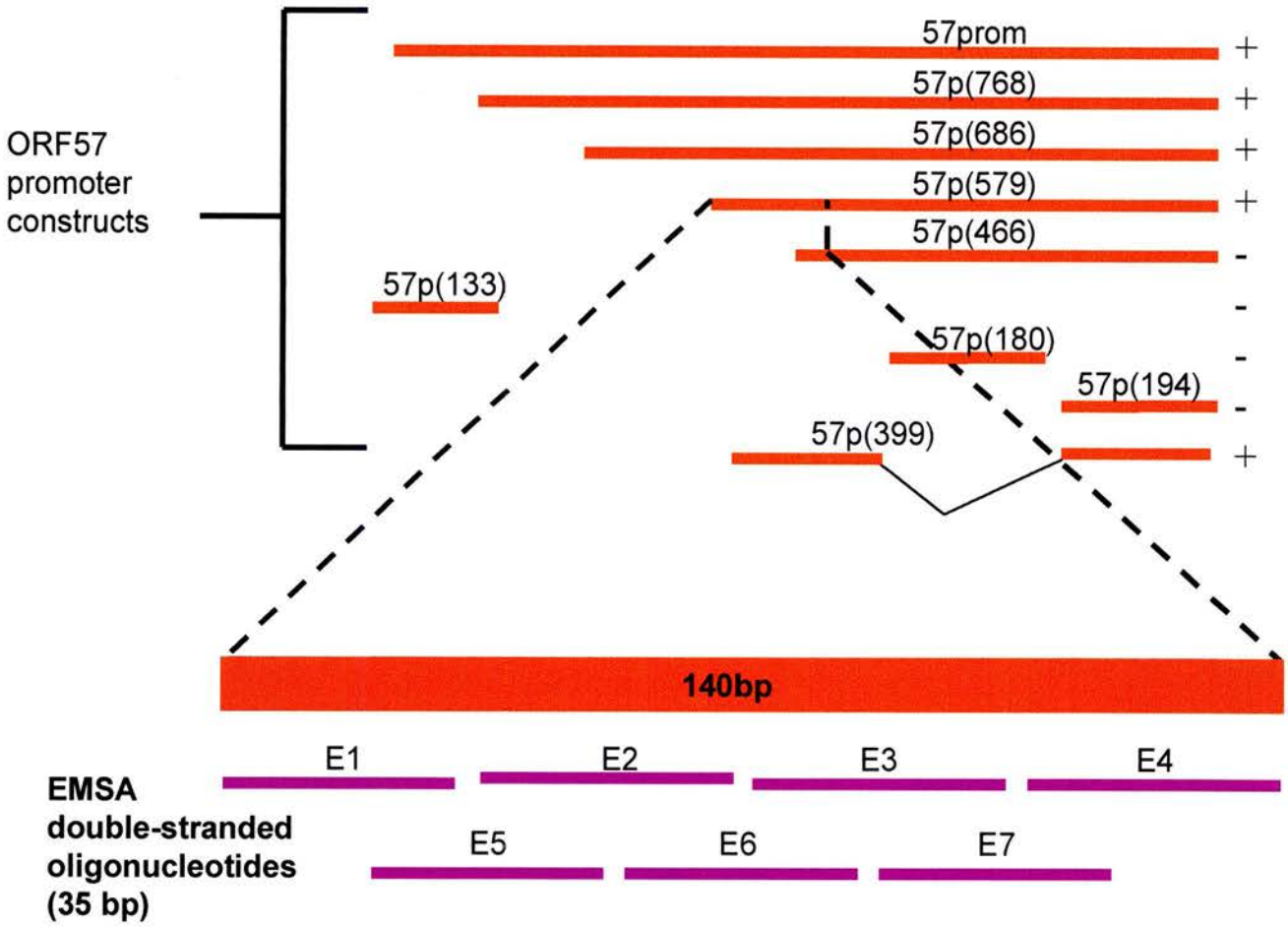

Figure 3.22: Location of EMSA double-stranded oligonucleotides

Schematic diagram of the region examined by EMSAs, showing the location of the seven double-stranded oligonucleotides labelled E1-E7. All ORF57 promoter constructs generated are included in the diagram for reference.

Table 3.3: Oligonucleotides used for EMSAs.

Each single-stranded oligonucleotide indicated in the table forms half of a complementary pair (e.g. e1a and e1b) used to make double-stranded oligonucleotides (e.g. E1) for use in EMSAs as indicated in Figure 3.22. NS - non-specific.

Single-Stranded Oligonucleotide	Sequence (5' → 3')	Complementary Pair
e1a	GTA **TAA ACA TAC GCA GAA GCA GCT TCC TGT CAA GC**	E1
e1b	GAT **GCT TGA CAG GAA GCT GCT TCT GAG TAT GTT TA**	
e2a	ATG **AGG CAG TTA TCC CCT CCA TCG AGC GCC TCT TG**	E2
e2b	GTC **CAA GAG GCG GTG GAT GGA GGG GAT AAC TGC CT**	
e3a	GAC **ACC AGC TTA AAC TGG TTC TTA CTT TCA AAA GT**	E3
e3b	CAG **ACT TTT GAA AGT AAG AAA CAG TTT AAG CTG GT**	
e4a	CTG **GCC CAA GTG TTT TGG TAC CAT CAG GTC TTA CA**	E4
e4b	GCA **TGT AAG ACC TGA TGG TAC CAA AAC ACT TGG GC**	
e5a	GCA **GCT TCC TGT CAA GCA TGA GGC AGT TAT CCC CT**	E5
e5b	TGG **AGG GGA TAA CTG CCT CAT GCT TGA CAG GAA GC**	
e6a	GCA **TCG AGC GCC TCT TGG ACA CCA GCT TAA ACT GT**	E6
e6b	GAA **ACA GTT TAA GCT GGT GTC CAA GAG GCG CTC GA**	
e7a	GTC **TTA CTT TCA AAA GTC TGG CCC AAG TGT TTT GG**	E7
e7b	GTA **CCA AAA CAC TTG GGC CAG ACT TTT GAA AGT AA**	
ns1a	TCG **AAT CCC TTT AAA TTT GCG AGC**	NS
ns1b	TCG **AGC TCG CAA ATT TAA AGG GAT**	

3.5.2 EMSA results

Figures 3.23-3.29 show the results of the EMSAs. Whole cell extract was made (section 2.7.1) from BHK cells that had been electroporated with pCMVORF50 and from BHK cells that had been electroporated with p-EGFP-N1, the vector used to construct pCMVORF50.

Experiments were designed to determine if there was a specific interaction between AlHV-1/Rta and any of the double-stranded oligonucleotides. Whole cell extract was mixed with a labelled double-stranded oligonucleotide (E1 – E7) (section 2.7.2) and the mixture, after incubation at room temperature for 10 min, was electrophoresed on

an acrylamide gel (section 2.7.3). To optimise conditions, varying concentrations of whole cell extract and dIdC were used.

The presence of a band indicates that the labelled double-stranded oligonucleotide is bound to a protein(s) in the cell extract. To determine if this binding was specific, excess unlabelled specific and non-specific double-stranded oligonucleotides were added as competitors at three concentrations (10 ng, 50 ng and 100 ng). Specific binding is defined as a band that can only be competed out by the specific competitor oligonucleotide and not by the non-specific competitor oligonucleotide. Figures 3.23-3.29 show the results for each double-stranded oligonucleotide analysed. Due to time limitations only a few of the oligonucleotides (E1, E3, E4 and E5) were repeated with optimised conditions. When repeated, extract minus pCMVORF50 and extract plus pCMVORF50 were electrophoresed on the same gel to allow comparison between them.

In summary, the results suggest that proteins in the cell extract bound specifically to oligonucleotides E1, E2, E6 and E7 but not E3, E4 and E5. The pattern of bands observed in the extracts minus pCMVORF50 and extracts plus pCMVORF50 was similar in most cases, suggesting that cellular proteins bound to the double-stranded oligonucleotides. None of these bands could be attributed to specific binding between AlHV-1/Rta and the oligonucleotides. In other cases, for example in Figure 3.29 with E7, the pattern of bands in the two extracts differed, suggesting that AlHV-1/Rta may be involved in binding that oligonucleotide, either directly or indirectly.

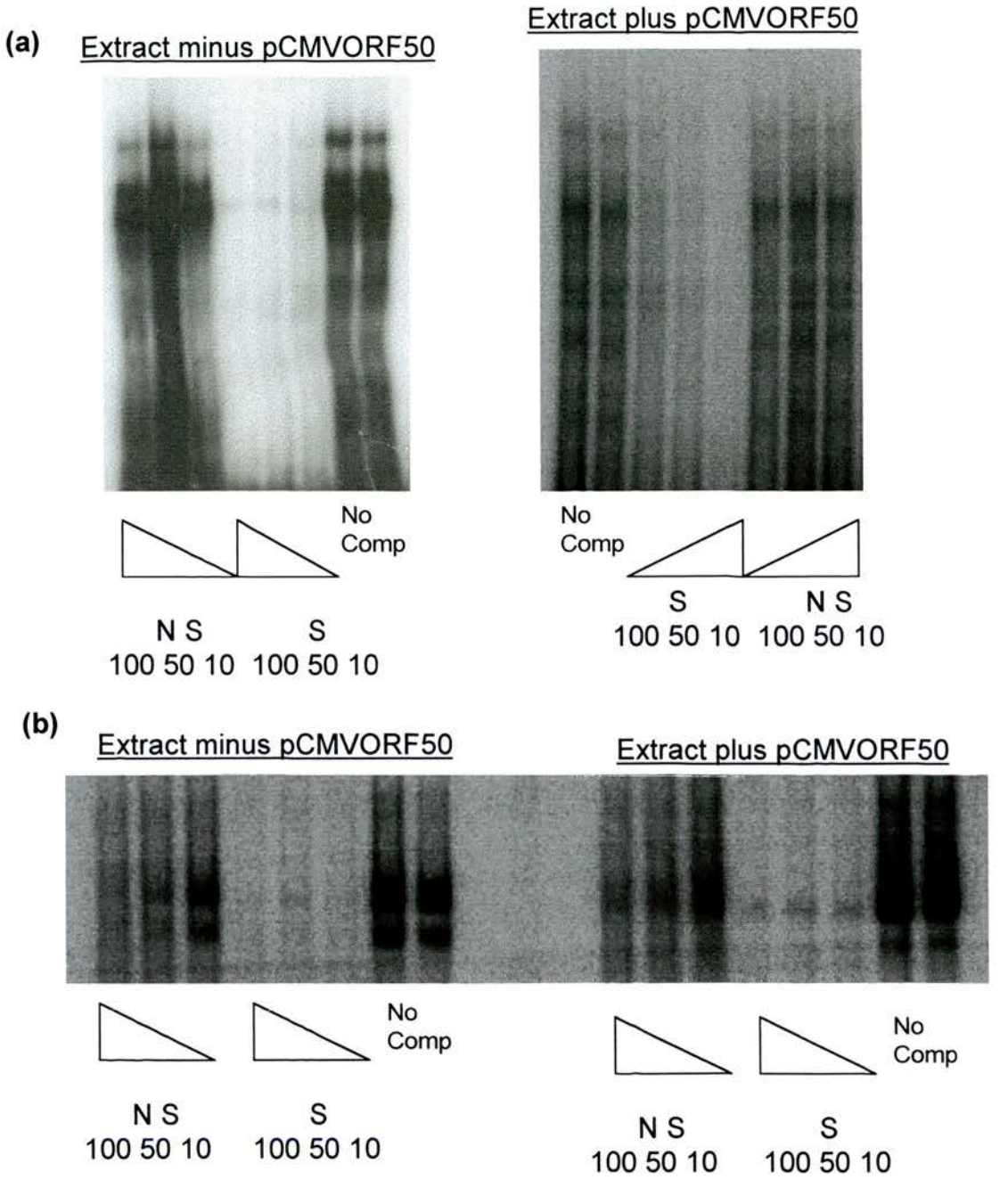

Figure 3.23: EMSAs using E1
Labelled oligonucleotide E1 was incubated with whole cell extract prepared from BHK cells transfected with pCMVORF50 or a control plasmid.
10-, 50- and 100-fold excess competitor was added to the appropriate reactions as indicated (NS - non-specific, S - specific).

In (a) the samples were analysed on two different gels. The samples in (b) were analysed on the same gel to allow comparison between samples with and without pCMVORF50.

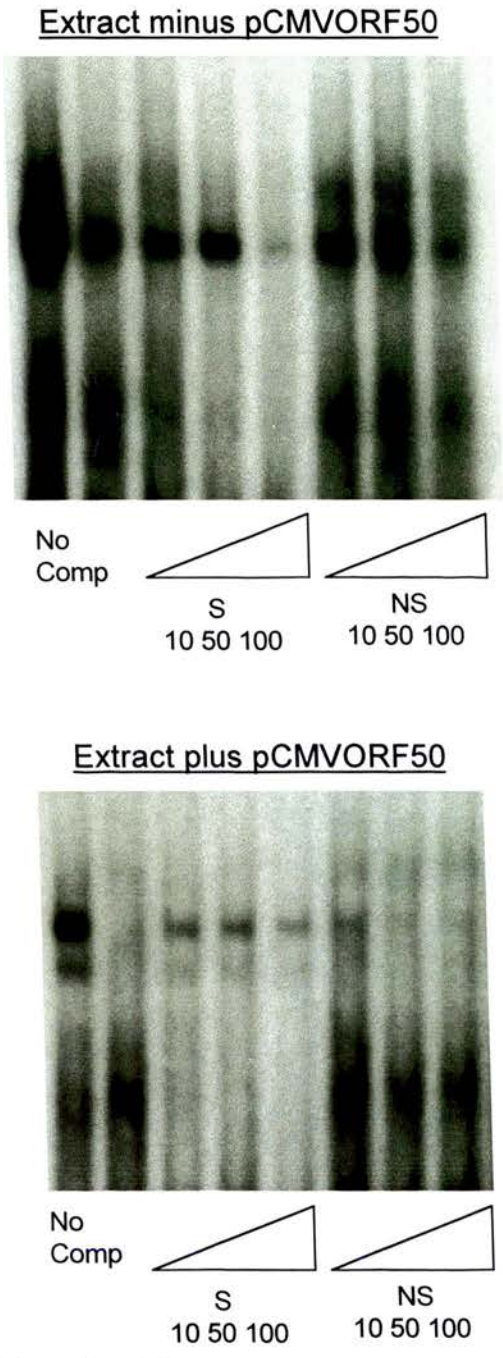

Figure 3.24: EMSAs using E2
Labelled oligonucleotide E2 was incubated with whole cell extract prepared from BHK cells transfected with pCMVORF50 or a control plasmid.
10-, 50- and 100-fold excess competitor was added to the appropriate reactions as indicated (NS - non-specific, S - specific).

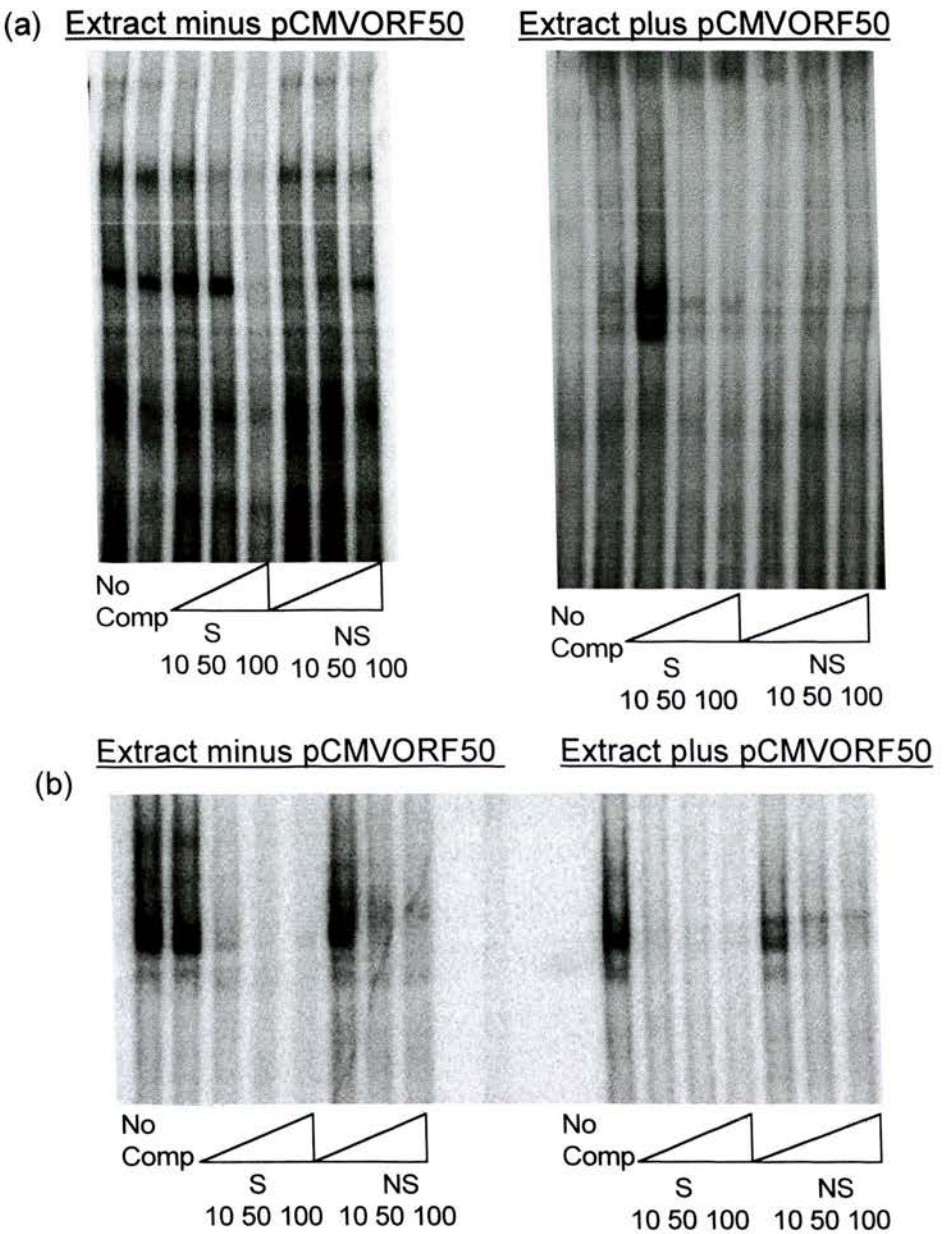

Figure 3.25 : EMSAs using E3

Labelled oligonucleotide E3 was incubated with whole cell extract prepared from BHK cells transfected with pCMVORF50 or a control plasmid.
10-, 50- and 100-fold excess competitor was added to the appropriate reactions as indicated. (NS - non-specific, S – specific)

In (a) the samples are run on two different gels. The samples in (b) are on the same gel to allow comparison between samples with or without pCMVORF50.

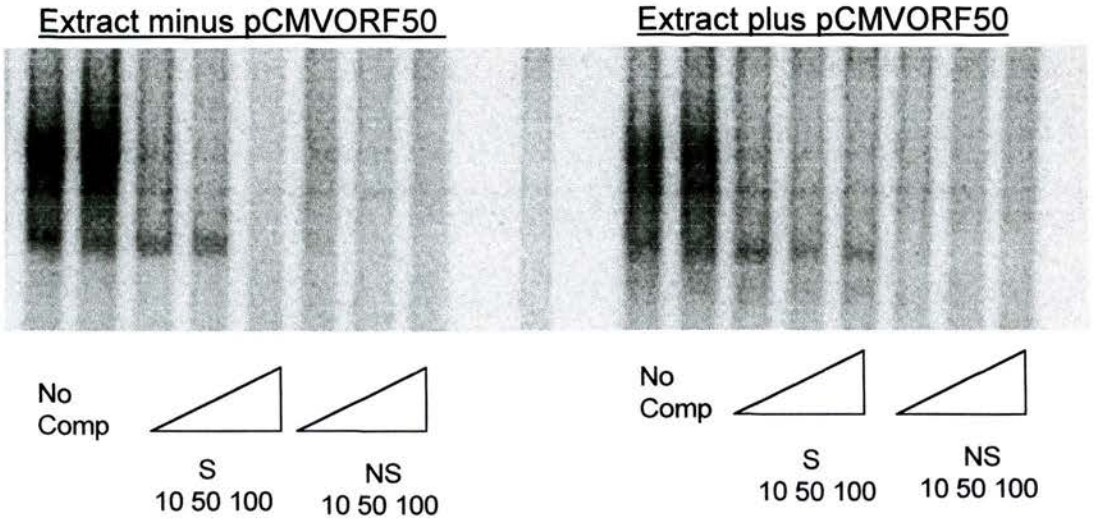

Figure 3.26: EMSAs using E4

Labelled oligonucleotide E4 was incubated with whole cell extract prepared from BHK cells transfected with pCMVORF50 or a control plasmid.
10-, 50- and 100-fold excess competitor was added to the appropriate reactions as indicated (NS - non-specific, S – specific).
The samples shown are on the same gel.

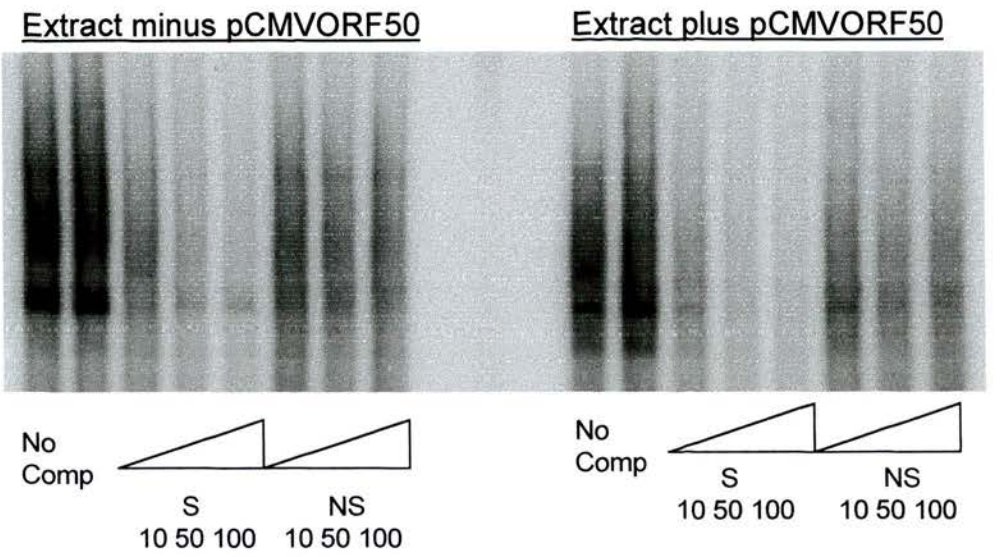

Figure 3.27: EMSAs using E5

Labelled oligonucleotide E5 was incubated with whole cell extract prepared from BHK cells transfected with pCMVORF50 or a control plasmid.
10-, 50- and 100-fold excess competitor was added to the appropriate reactions as indicated (NS - non-specific, S - specific).
The samples shown are on the same gel.

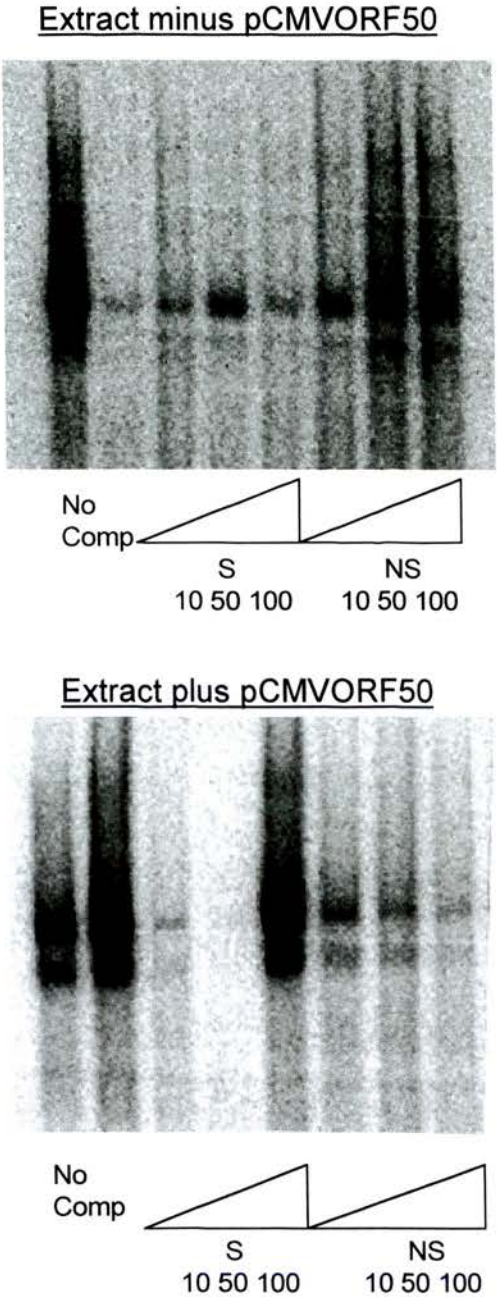

Figure 3.28: EMSAs using E6

Labelled oligonucleotide E6 was incubated with whole cell extract prepared from BHK cells transfected with pCMVORF50 or a control plasmid.
10-, 50- and 100-fold excess competitor was added to the appropriate reactions as indicated (NS - non-specific, S – specific).
The samples shown are on different gels.

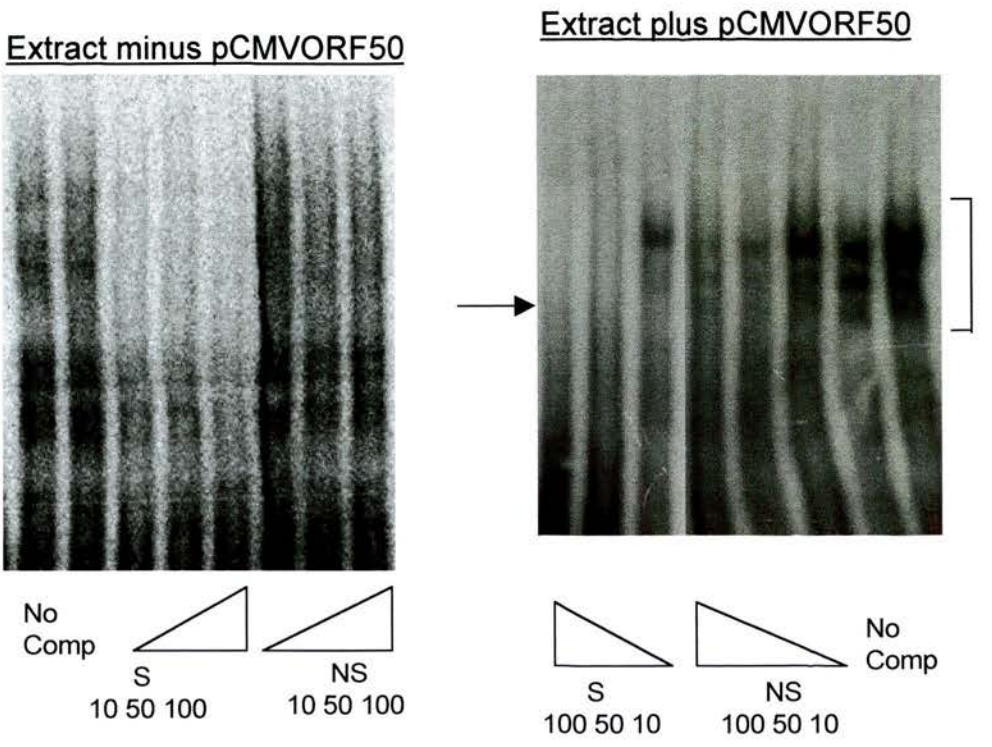

Figure 3.29: EMSAs using E7

Labelled oligonucleotide E7 was incubated with whole cell extract prepared from BHK cells transfected with pCMVORF50 or a control plasmid.
10-, 50- and 100-fold excess competitor was added to the appropriate reactions as indicated (NS- non-specific, S - specific).
A square bracket indicates a region on the gel, which has a different pattern from that obtained with cell extract minus pCMVORF50. This region may therefore contain a band representing AlHV-1/Rta binding. The lowest of the three bracketed bands is competed out by specific competitor.

The samples shown are on different gels.

To deduce if the cellular proteins that could bind to oligonucleotide E7 also bound to common consensus sequences, cellular extracts were incubated with labelled E7 oligonucleotide in the presence or absence of excess unlabelled competitor oligonucleotides containing consensus E-box or Oct-1 motifs. The oligonucleotides containing these sequences were available in the laboratory. Many eukaryotic promoter and enhancer regions contain sequences related to the octamer sequence (ATGCAAAT) to which proteins bind (Sturm *et al.*, 1987). E-boxes (CANNTG) are also a common motif to which proteins bind (Gilmour *et al.*, 1991). The unlabelled competitor probes used were, NS, E7, E-box and Oct-1 (see Figure 3.30 and Table 3.4).

Table 3.4: Oct-1 and E-box oligonucleotides

Each single-stranded oligonucleotide indicated in the table is half of a complementary pair used to make double-stranded oligonucleotides for use in EMSAs. Note that since these oligonucleotides were only used as competitors and were therefore not labelled, there was no requirement for them to have single-stranded overhangs. The Oct-1 double-stranded oligonucleotide does not have overhangs whereas the E-box double-stranded oligonucleotide does. Complimentary sequences are highlighted in bold.

Single-stranded oligonucleotide	Sequence 5'→3'	Complementary Pair
Oct-1a	**TCC CCT AAA TGT AAA ACA AAC CTG CC**	Oct-1
Oct-1b	**GGC AGG TTT GTT TTA CAT TTA GGG GA**	
E-box1a	TCG A**GG AGA GTG TCA CGT GGC TCT CC**	E-Box
E-box1b	TCG A**GG AGA GCC ACG TGA CAC TCT CC**	

In this experiment, all samples had 250 ng of non-specific double-stranded oligonucleotide added to reduce the amount of background. Figure 3.30 shows that the only unlabelled oligonucleotide able to compete with the band was the specific double-stranded oligonucleotide E7. The negative extract and positive extract gave

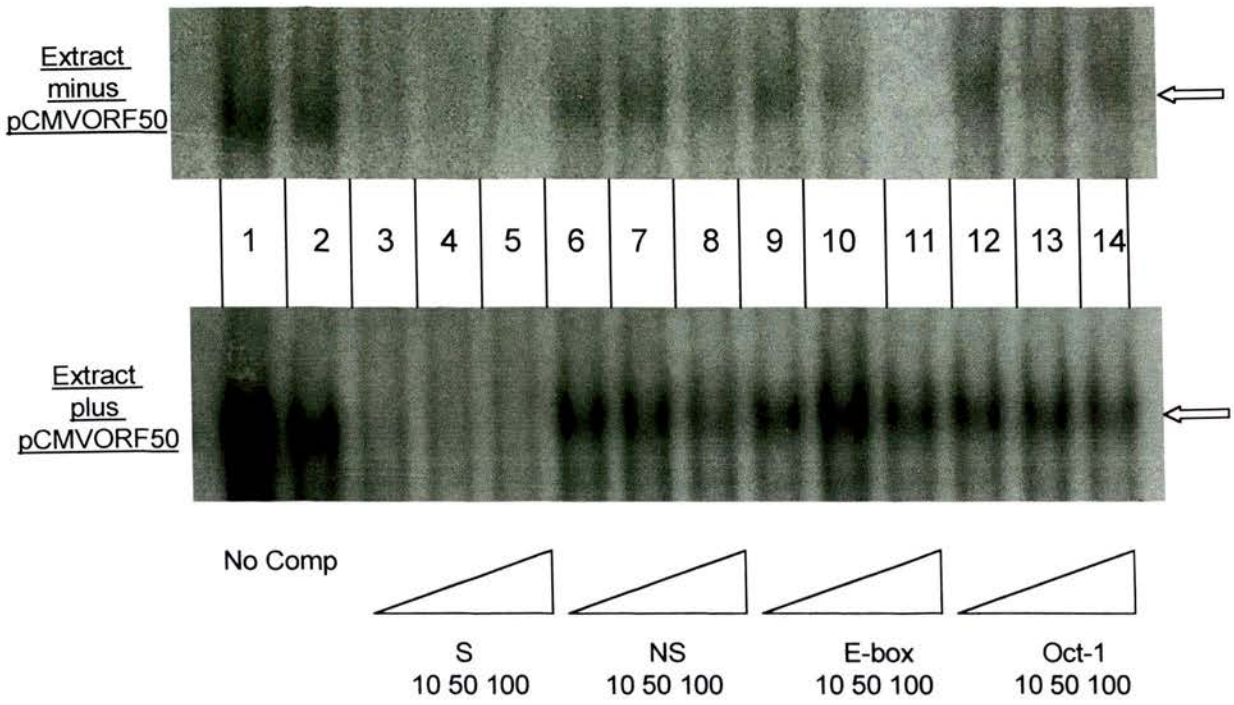

Figure 3.30: EMSAs using E7 with several competitors

Labelled oligonucleotide E7 was incubated with whole cell extract prepared from BHK cells transfected with pCMVORF50 or a control plasmid.

All samples had 250 ng of NS primer in them to reduce background.

10-, 50- and 100-fold excess competitor was added to the appropriate reactions as indicated (S – specific, NS - non-specific, E-box and Oct-1).

Block arrows indicate a single band which is only competed out with the specific competitor.

the same result suggesting that the band represented a cellular protein rather than AlHV-1/Rta. The fact that the E-box and Oct-1 oligonucleotides did not compete suggests that the cellular protein does not bind to the E-box or Oct-1 consensus motifs.

The original aim of the EMSAs was to investigate whether AlHV-1/Rta bound to the region which was suspected to be AlHV-1/Rta-responsive. It is possible that this does happen, but the results obtained indicate that the use of whole cell extract is not satisfactory as there appear to be several cellular proteins that bind to the oligonucleotides tested. Suggestions of how to progress the EMSA analysis with respect to AlHV-1/Rta binding are discussed in Chapter 5.

3.6 Analysis of functional domains of AlHV-1/Rta

Since AlHV-1/Rta was discovered to be a transactivator, studies were initiated to investigate different domains of the protein. Published studies of EBV Rta showed that it contains DNA-binding and transactivation domains (Manet *et al.*, 1991). Analysis of the EBV Rta transactivation domain revealed hydrophobic residues conserved with VP16 of HSV-1 and the Rta of HVS. Substitution of the hydrophobic residues in EBV Rta resulted in loss of transactivation ability (Hardwick *et al.*, 1992). The AlHV-1/Rta amino acid (aa) sequence was analysed using a hydrophilicity plot (Figure 3.31). A point on the plot was chosen to divide the protein into two approximately equal sizes. This point was located between two discernible sequence structures. As can be observed in Figure 3.31, the N-terminal sequence is a mixture of many hydrophilic and hydrophobic sequences, whereas the C-terminal

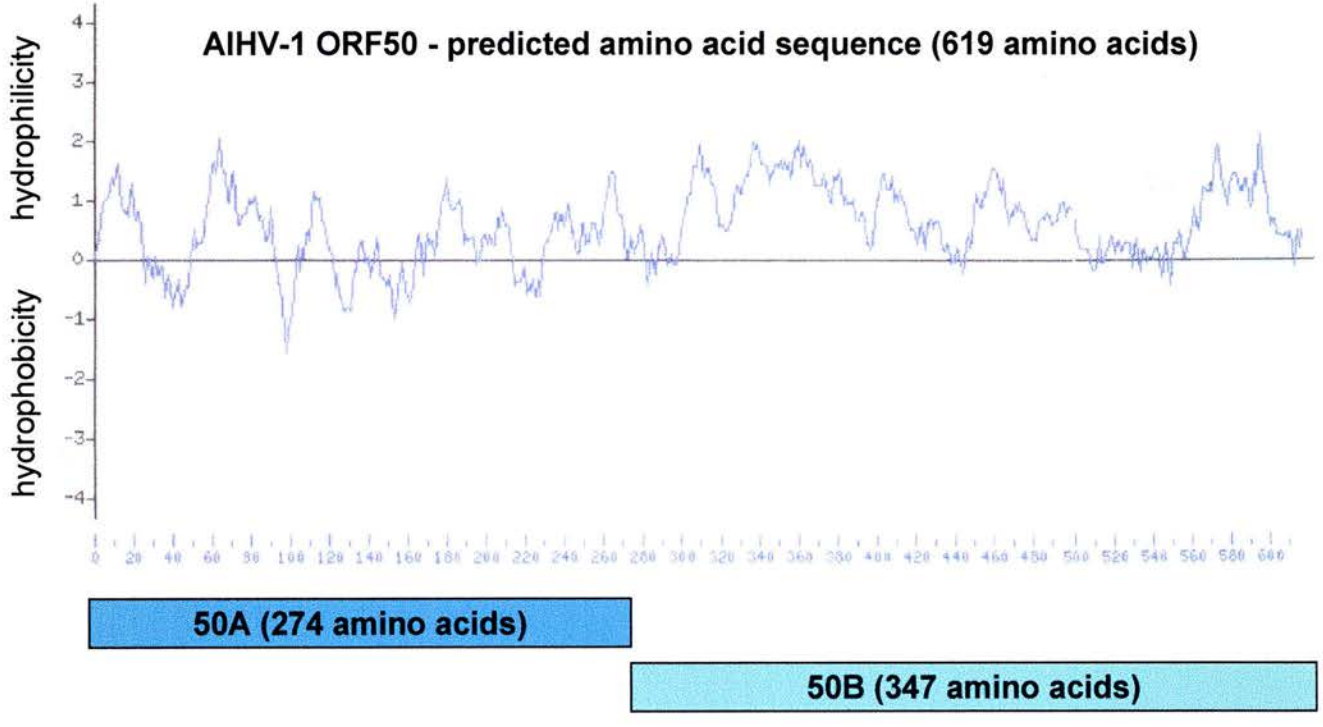

Figure 3.31: Hydrophilicity plot of the AlHV-1/Rta amino acid sequence.

The Kyte-Doolittle method of calculating hydrophilicity was used to generate a hydrophilicity plot of the AlHV-1/Rta amino acid sequence from Ensser *et al.* (1997).
Also shown are the relative positions of the products encoded by constructs pcDNA50A and pcDNA50B (see Figure 3.32).

sequence is largely hydrophilic with a small area of hydrophobic residues. Two constructs were generated containing truncated versions of the ORF50 sequence, an N-terminal and C-terminal region. These regions were generated by PCR amplification using the AlHV-1 genome as the template.

The N-terminal region of the ORF50 sequence was amplified using primers 1) 5' - AAG AAT TC**A TG**A GTG CCA ACA ACC CC (Nt 72825-72842) and 2) 5'- AAG GAT CCC ACA TAC CTC TGC CTG G (Nt 73868-73852) containing *Eco*RI and *Bam*HI restriction enzyme sites, respectively (underlined). The C-terminal region of the ORF50 sequence was amplified using primers 3) 5' - AAG AAT TC**A TG**A GGT ATG TGT TAC CAG (Nt 73859-73875) and 4) 5' - AAG GAT CCT ATG GTC TGG TCA CGG G (Nt 74902-74886) containing *Eco*RI and *Bam*HI restriction enzyme sites, respectively (underlined). Primer 3) also had a start codon (in bold) engineered into the primer. The PCR products were inserted into the pGEM-T Easy vector and then subcloned using the *Eco*RI and *Bam*HI sites into the pcDNA3.1*myc*/His vector to derive pcDNA50A and pcDNA50B. The full-length ORF50 was amplified by PCR using primers 1) and 4) above and inserted initially into pGEM-T Easy vector and then subcloned into pcDNA3.1*myc*/His to derive pcDNA50 (Figure 3.32). Primer 4) did not contain the ORF50 stop codon because there is a stop codon situated in-frame and downstream of the *myc*/His tag of the vector, which is at the 3' end of the cloned insert. The pcDNA3.1*myc*/His vector has the advantage that proteins can be detected via the C-terminal *myc* tag and/or purified via the His tag.

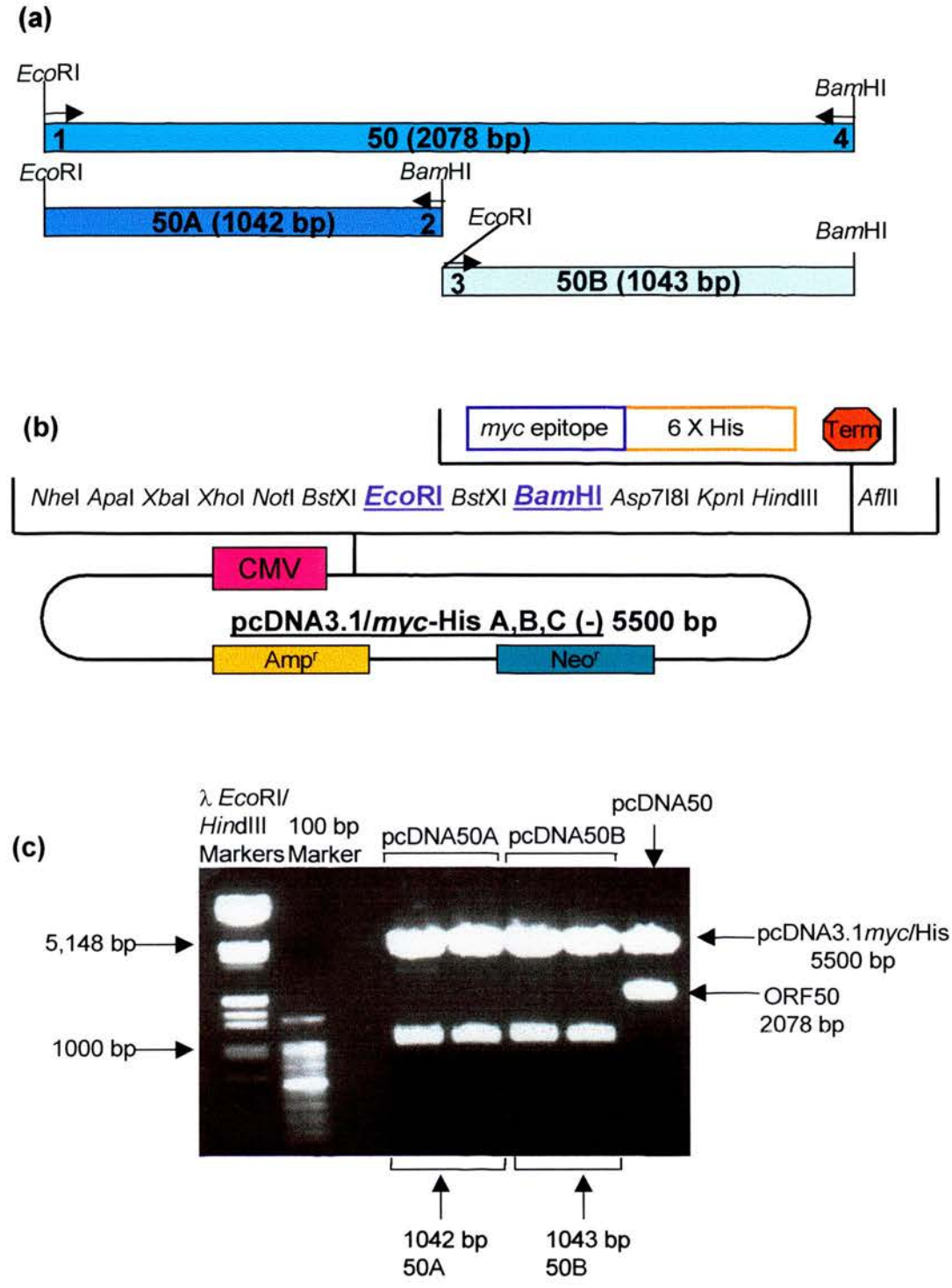

Figure 3.32: Construction of truncated versions of ORF50

(a) Diagram of full-length ORF50 and truncated sequences 50A and 50B, showing the location of PCR primers 1-4 used to amplify them, along with the restriction enzymes attached.
(b) Diagram of the pcDNA3.1*myc*/His vector, which has a C-terminal *myc* epitope and His tag. The multiple cloning site is illustrated.
(c) *Eco*RI and *Bam*HI digests of pcDNA50, pcDNA50A and pcDNA50B. The observed insert sizes are ~1 kb for 50A and 50B and ~2 kb for ORF50.

The three plasmids were used in an initial experiment to assess if the full-length ORF50 construct could transactivate 57prom similarly to pCMVORF50 (Figure 3.14 and 3.15) and also if pcDNA50A or pcDNA50B could activate the ORF57 promoter (see Figure 3.33(a) and Appendix 11). The pGL3-Basic and 57prom constructs were each transfected with or without pcDNA50, pcDNA50A or pcDNA50B.

The results shown in Figure 3.33(a) suggest that pcDNA50 activated the 57prom luciferase reporter similarly to pCMVORF50, as expected. However, neither of the domains of AlHV-1/Rta encoded by pcDNA50A and pcDNA50B had any effect on 57prom.

These constructs were then used in a further experiment to address if co-transfection of any of these constructs could interfere with the activity of the AlHV-1/Rta, encoded by pcDNA50, on 57prom. pcDNA50 was transfected with 57prom alone or together with pcDNA50A, pcDNA50B or pEGFP-N1. pEGFP-N1 expresses EGFP under the control of the CMV promoter and this was included to demonstrate that any effect of pcDNA50A or pcDNA50B on pcDNA50-mediated transactivation was due to the truncated protein interfering with the activity of the full-length AlHV-1/Rta and not due to dilution of transcription factors by the CMV promoter (Figure 3.33(b) and Appendix 12).

As seen in Figure 3.33(b), addition of pcDNA50B or pEGFP-N1 had no effect on the transactivation of 57prom by the AlHV-1/Rta gene product, since the fold induction in this sample was similar to that observed with 57prom and pcDNA50 alone. In

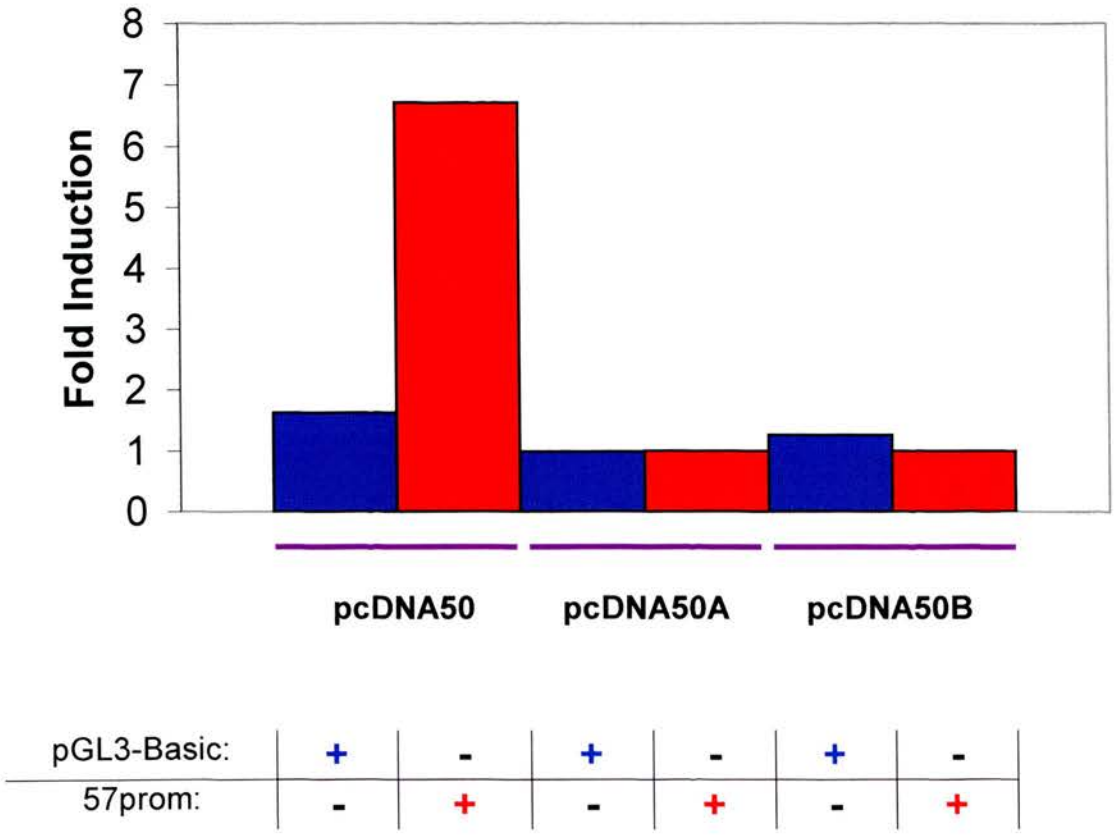

Figure 3.33 (a): Activity of 57prom when co-transfected with full-length or truncated ORF50 expression constructs

BHK cells were co-transfected with either 2 μg of pGL3-Basic or 57prom with or without 2 μg of pcDNA50, pcDNA50A or pcDNA50B. pRLSV40 (0.2 μg) was used as an internal control in each transfection. The fold induction of activity in the presence or absence of an ORF50 expression construct is shown.

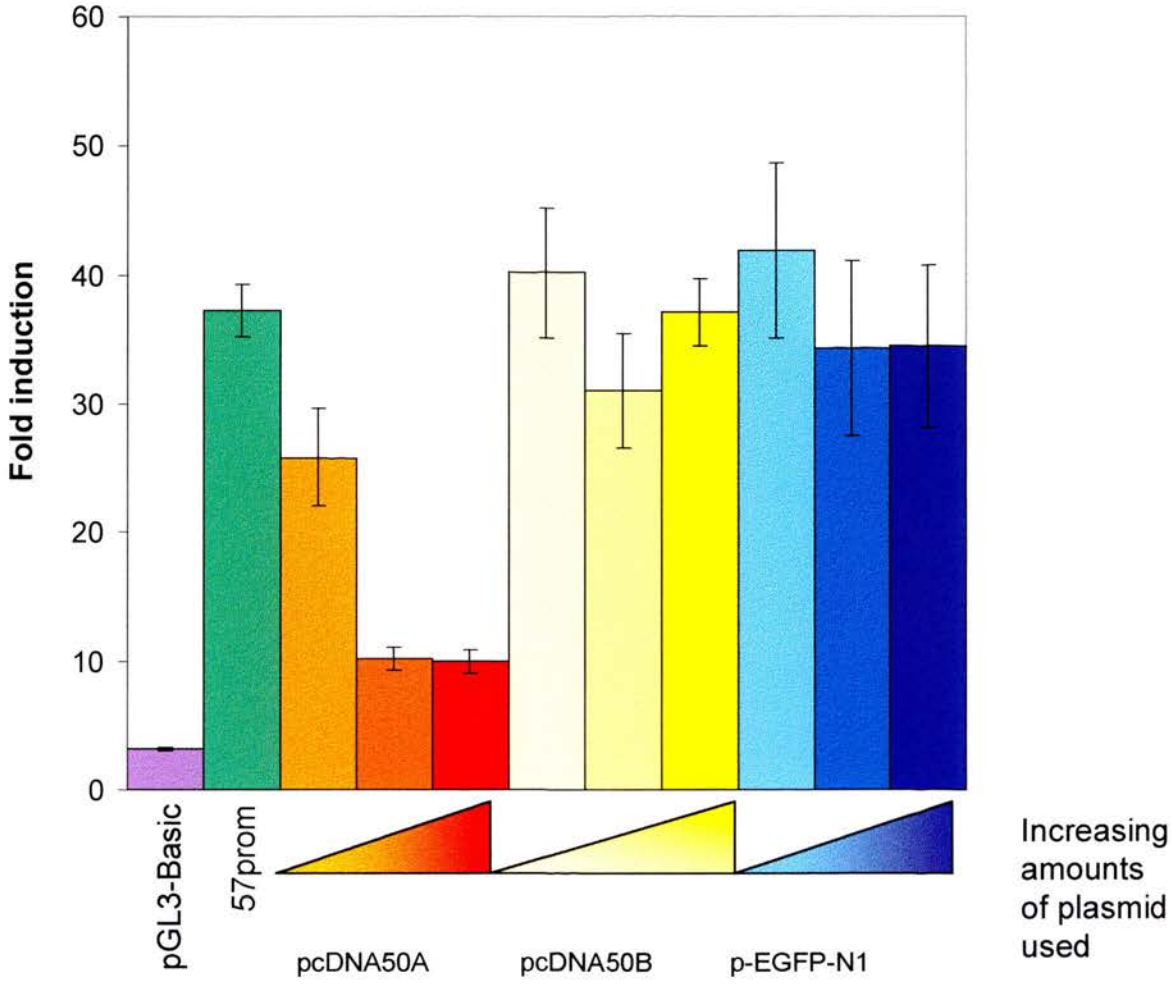

Figure 3.33 (b): Effect of ORF50 truncations on the ability of AlHV-1/Rta to transactivate the ORF57 promoter

BHK cells were transfected with the combinations of plasmids shown on the graph. BHK cells were transfected with pGL3-Basic or 57prom in the presence or absence of pCMVORF50 as a negative and positive control, respectively. In all other samples BHK cells were transfected with 57prom in the presence or absence of pCMVORF50 to permit fold induction to be calculated. These samples containing pCMVORF50 also contained one of pcDNA50A, pcDNA50B or pEGFP-N1 in three different concentrations (2 μg, 10 μg and 20 μg).

The results show the fold induction of activity in the presence and absence of ORF50 expression constructs. All samples were transfected with 0.2 μg of pRLSV40 as an internal transfection efficiency control. The experiment was performed in triplicate and error bars show the standard deviation.

contrast, addition of pcDNA50A did have an effect on AlHV-1/Rta-mediated transactivation of 57prom. Addition of increasing amounts of pcDNA50A diminished the activity of 57prom in a dose-dependent manner. Addition of 2 μg of pcDNA50A decreased the fold-induction observed with pcDNA50 alone by around 30% and of 10 μg by around 70%. Addition of 20 μg pcDNA50A did not lead to a further decrease in activity.

These results are consistent with the N-terminal region of AlHV-1/Rta (encoded by pcDNA50A) containing a DNA-binding domain. Thus, expression of the DNA-binding domain of AlHV-1/Rta alone could compete with AlHV-1/Rta for binding to DNA thereby decreasing transactivation of the ORF57 promoter. In the time available detection of expression from these constructs was not achieved and therefore it is not known if protein was expressed from pcDNA50B.

3.7 Analysis of AlHV-1 ORFA6

3.7.1 Construction of an ORFA6 expression construct – pCMVORFA6

Preliminary studies were initiated to investigate the possibility that ORFA6 encodes a transactivator. It was also of interest to determine if the ORFA6 gene product could act in synergy with AlHV-1/Rta. This hypothesis is based on the situation in EBV, where Rta (the ORF50 homologue) and Zta (a possible ORFA6 homologue) can act in synergy (Holley-Guthrie *et al.,* 1990).

The coding sequence for ORFA6 was amplified by PCR with primers 5' - AAG GAT CCT CAT GCA TAA GCA CTC TGC T (Nt 75224-75243) and 5' - AAG

CTA GCG TGT TAG CTT CAT GCA ACC T (Nt 75896-75877) containing *Bam*HI and *Nhe*I restriction enzyme sites, respectively (underlined). The PCR product was inserted into the pGEM-T Easy cloning vector. The ORFA6 sequence was then subcloned into the pEGFP-N1 plasmid by ligation of the *Bam*HI (blunt-ended), *Not*I restriction fragment with vector digested with *Not*I and *Nhe*I (blunt-ended) to derive pCMVORFA6. Again, as with pCMVORF50, the EGFP sequence was removed in this process and replaced with the ORFA6 sequence (Figure 3.34(a)).

3.7.2 Expression of pCMVORFA6 using RT-PCR

Transcription of ORFA6 from pCMVORFA6 was assessed by RT-PCR analysis. BHK cells were transfected with pCMVORFA6 (2 μg) or untransfected. Total cellular RNA was extracted (section 2.5.1), DNAse treated, reverse transcribed and amplified by PCR (section 2.2.2). The primers used to amplify the ORFA6 sequence for subcloning (section 3.7.1) were used for the RT-PCR analysis. Figure 3.34(b) clearly shows a band of the correct size, which is only present in the pCMVA6-transfected cells but not in the negative controls. Thus, ORFA6 is transcribed from this plasmid.

3.7.3 Analysis of the effect of pCMVORFA6 alone or in combination with pCMVORF50 on putative AlHV-1 promoters

pCMVORFA6 was used in transfection experiments in BHK cells alone or in combination with pCMVORF50 to assess its ability to transactivate 57prom, 6prom or TKprom. pGL3-Basic was again used as a background control. pCMVORFA6 had no effect on any of the promoters in this experiment (Figure 3.34(c) and Appendix 13). This is the result of a single experiment and therefore it is not possible to make

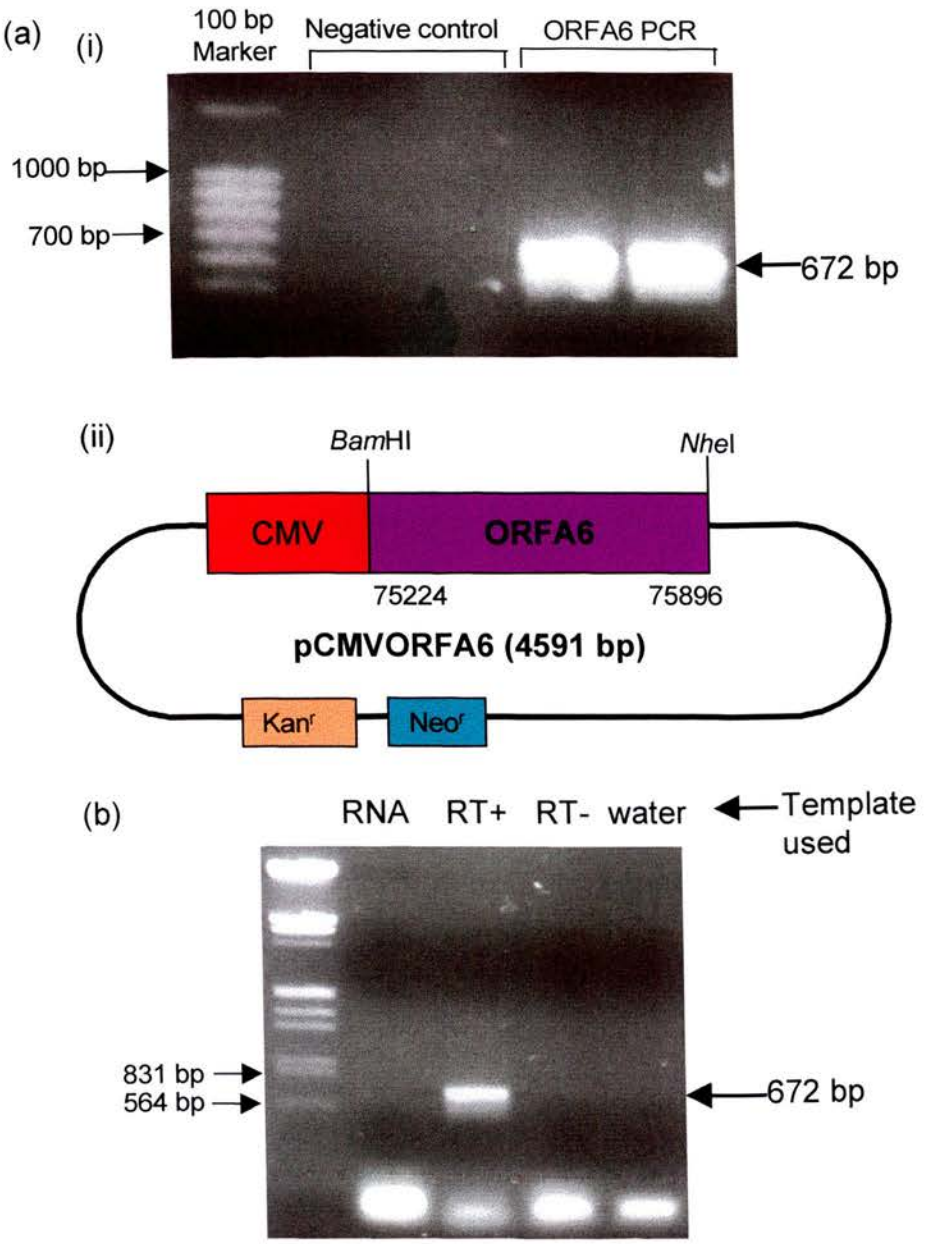

Figure 3.34:

(a) Construction of pCMVA6

(i) The ORFA6 sequence was amplified by PCR to yield a product of 672 bp. The negative control using water instead of AlHV-1 DNA is also shown.

(ii) Schematic representation of pCMVORFA6. The ORFA6 sequence was inserted into the *Bam*HI and *Nhe*I sites, replacing the EGFP sequence of pEGFP-N1.

(b) RT-PCR of pCMVA6

RT-PCR analysis was carried out on total RNA extracted from BHK cells, which had been transfected with 2 μg of pCMVORFA6 (RT+).Total RNA extracted from BHK cells transfected with pCMVORFA6 that had not been reverse transcribed (RT-), RNA from mock-transfected BHK cells (RNA) and water were all used as negative controls.

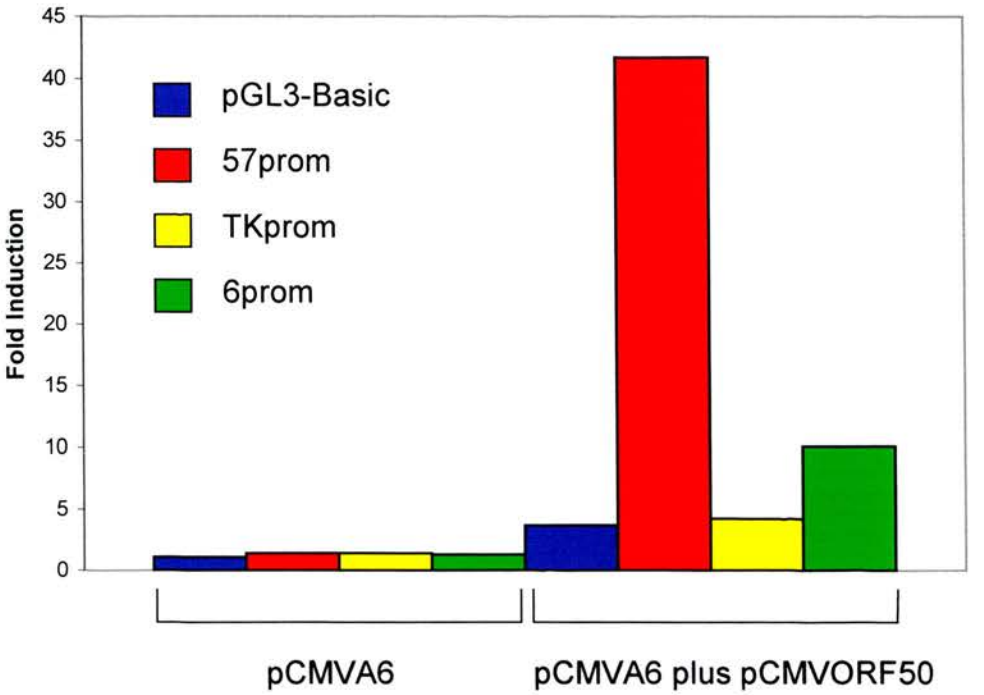

Figure 3.34 (c): Activity of pCMVA6 on AlHV-1 promoter constructs

BHK cells were transfected with 2 μg of pGL3-Basic, 57prom, TKprom or 6 prom with either 2 μg of pCMVA6 or 2 μg of pCMVA6 plus pCMVORF50 as indicated. The fold induction of activity in the presence and absence of expression constructs is shown. The results represent a single experiment.

conclusions regarding the ability of the ORFA6 gene product to behave as a transactivator.

3.8 Summary of Results

3.8.1 Expression of ORF50 and ORFA6

Examination of the slot blot experiment (Figure 3.4) suggests that ORF50 and ORFA6 are expressed as IE genes. RT-PCR experiments carried out on RNA extracted from virus-infected BT cells suggests that ORF50 is expressed at all times in the virulent virus but not the attenuated virus and that ORFA6 is expressed at all times in both the virulent and attenuated virus. However, results from the necessary controls were not satisfactory and therefore the expression pattern of ORF50 and ORFA6 within the virus has not been demonstrated unequivocally. Further work addressing the temporal control of ORF50 and ORFA6 in the virus life cycle would include a successful Northern blot. To address if ORF50 and ORFA6 are co-transcribed, and if the predicted SD and SA sites of ORF50 are used 5'-RACE could be performed.

3.8.2 The function of the AlHV-1/Rta

AlHV-1/Rta was shown to encode a transactivator protein. In transient transfection assays it can strongly activate the AlHV-1 ORF57 promoter and moderately activate the ORF6 promoter but not the TK promoter. TKprom and 6prom were shown to be functional using virus superinfection. 57prom was not shown to be functional by virus superinfection but was clearly shown to be functional in the subsequent transient transfection assays.

3.8.3 Analysis of the AlHV-1 ORF57 promoter

Transcription of the 57prom luciferase reporter construct was examined and the transcriptional start site was determined to lie within 409 bp upstream of the predicted translational start site. 5'-RACE was then carried out on total RNA from virus-infected cells to determine a more precise location for the transcriptional start site. These experiments revealed that the transcriptional start site was 24 bp upstream of the predicted start codon and 30 bp downstream from the predicted TATA box. SD and SA sites were also identified.

The ORF57 promoter was analysed further in transient transfection assays to determine the minimal length required for activation by AlHV-1/Rta and also to determine the location of potential AlHV-1/Rta-responsive elements.

Through the use of deleted and truncated constructs of 57prom, a potentially important sequence for the activation by AlHV-1/Rta was identified. The 57p(579) construct was activated by AlHV-1/Rta, whereas the 57p(466) construct was not. Thus, the sequence between 409-522 bp upstream from the translational start codon was identified as being important for activation by AlHV-1/Rta. As it was possible that a consensus sequence or motif responsible for conferring the AlHV-1/Rta-responsiveness was contained in this sequence and could be straddling the border between 57p(579) and 57p(466), a 155 bp fragment spanning this sequence was investigated further.

Prom57p(155) was used in transient transfection assays to test if this sequence alone could act as an AlHV-1/Rta-responsive enhancer. The results suggested that this sequence alone was not sufficient to confer AlHV-1/Rta-responsiveness.

57p(399) was generated to investigate if there was another element important for activation by AlHV-1/Rta. This construct showed around 50% activation compared to 57p(579) from which it was derived, indicating that the section 'excised' from the centre of 57p(579) to create 57p(399), although not essential, was important for activation by AlHV-1/Rta. It was concluded that this could either be because it contained an important sequence or because it is important in separating the other two fragments by a fixed distance.

3.8.4 EMSAs

To investigate whether AlHV-1/Rta interacted directly with ORF57 promoter sequences, EMSAs were carried out. Whole cell extracts were prepared from cells transfected with or without pCMVORF50. Double-stranded oligonucleotides E1-E7 were designed, which spanned the area of interest and which potentially contain an AlHV-1/Rta-responsive region. Several incidences of potentially specific binding were observed with double-stranded oligonucleotides E1, E2, E6 and E7. However, it was not clear if these involved AlHV-1/Rta, cellular proteins or a combination of the two. E7 was investigated further to test if the proteins bound to E7 also interacted with Oct-1 or E-box consensus sequences. Double-stranded oligonucleotides corresponding to these consensus sequences did not compete for binding to E7. A similar binding pattern was observed using extracts containing pCMVORF50 or the

control plasmid, suggesting that cellular protein(s) rather than AlHV-1/Rta was involved in the binding to oligonucleotide E7.

3.8.5 ORF50 truncations

To examine the domains of AlHV-1/Rta, two truncated versions of AlHV-1/Rta were constructed, consisting of the N-terminal and C-terminal regions of AlHV-1/Rta. These constructs were used to determine whether they were capable of competing with full-length AlHV-1/Rta activation of 57prom, in transient transfection assays. The N-terminal domain was capable of competing with AlHV-1/Rta-mediated transactivation. This is in agreement with the hypothesis that the N-terminal domain may be the DNA-binding domain.

3.8.6 Analysis of ORFA6

An expression plasmid of AlHV-1 ORFA6 was constructed to test if it could act as a transactivator. The ORFA6 gene product did not activate any of the tested promoters in this experiment.

Chapter 4 – RESULTS
Construction of a Recombinant AlHV-1

4.1 Introduction

A variety of methods have been employed to mutate genes in herpesviruses to determine their function. Initially this was carried out using mutagenic chemicals with a view to identifying the genotype change responsible for an altered phenotype. This approach was used decades ago to produce HSV-1 temperature-sensitive (ts) mutants (Schaffer *et al.,* 1970). This was a random process and could result in the occurrence of several mutations within a single genome, making assignment of a phenotypic change to one particular mutation difficult. The sequencing of herpesvirus genomes led to the development of a more targeted approach to create specific mutations. This involved recombination within eukaryotic cells between the virus DNA and a plasmid containing a marker gene and homologous sequences flanking the region of the virus genome to be replaced (Mocarski *et al.*, 1980; Post and Roizman, 1981; Spaete and Mocarski, 1987).

The experiments in Chapter 3 examined AlHV-1 ORF50 in isolation. An alternative approach was chosen to study the virus phenotype in the absence of ORF50. Initially this was attempted using homologous recombination to partially or completely remove the ORF50 sequences from the virus DNA, as described in section 4.2. If this had been achieved the intention would have been to purify the recombinant virus and test its ability to grow in tissue culture, and in the animal model, the rabbit, to allow changes in pathology to be observed. Changes in the phenotype of a virus lacking ORF50, compared to wild-type virus, would give an indication of possible roles for ORF50. Finally a revertant would have been made to confirm that the changes were due to the engineered mutation. Section 4.3 discusses an alternative approach that

was attempted where the intention was to generate a bacterial artificial chromosome (BAC) containing the AlHV-1 genome.

4.2 Attempts to make AlHV-1 lacking ORF50 using homologous recombination

The main aim of this part of the study was to make AlHV-1 lacking ORF50. Two approaches were attempted, which if successful would result in partial or complete removal of ORF50. Thus, no viable protein product would be expressed. Both strategies involved homologous recombination between the virus genome and a plasmid containing two sequences homologous to the virus DNA bisected with a marker gene.

4.2.1 Transfection of AlHV-1 DNA leads to virus production

It was not known whether or not transfection of AlHV-1 DNA resulted in productive virus replication and so this was tested. Figure 4.1 shows BT cells transfected with 0.1 μg, 1 μg, 5 μg and 10 μg of AlHV-1 DNA exhibiting characteristic CPE 24 days after transfection. Transfected cells were transferred onto fresh cells and CPE was again observed.

Thus transfection of AlHV-1 DNA can lead to virus production in BT cells. This meant that the virus DNA could be provided either by transfecting virus DNA or by virus infection of cells.

Figure 4.1: Images of bovine turbinate cells.

1 - mock-transfected BT cells.
2 - mock-transfected BT cells.
3 - BT cells transfected with 0.1μg of C500 AlHV-1 DNA.
4 - BT cells transfected with 1μg of C500 AlHV-1 DNA.
5 - BT cells transfected with 5μg of C500 AlHV-1 DNA.
6 - BT cells transfected with 10μg of C500 AlHV-1 DNA.

All photographs except 1 were taken 24 days after transfection.
Photograph 1 was taken a few days after transfection.

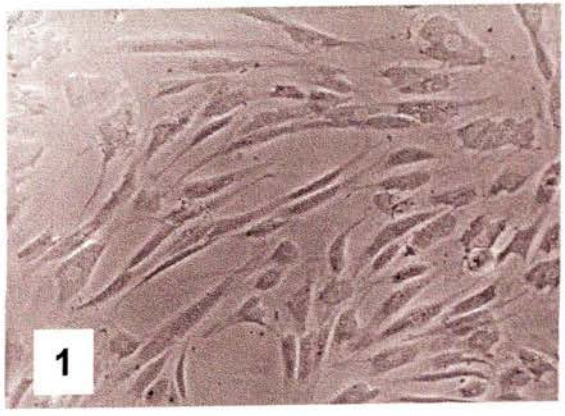
1

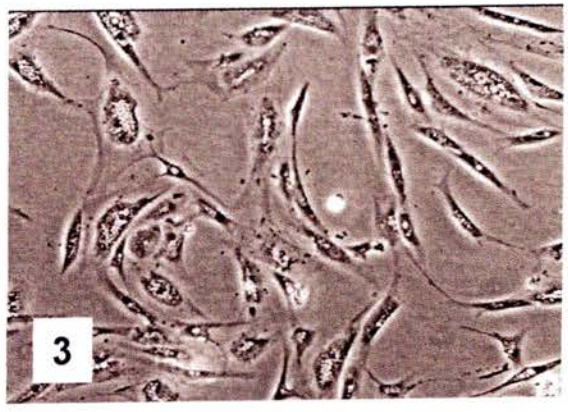
3

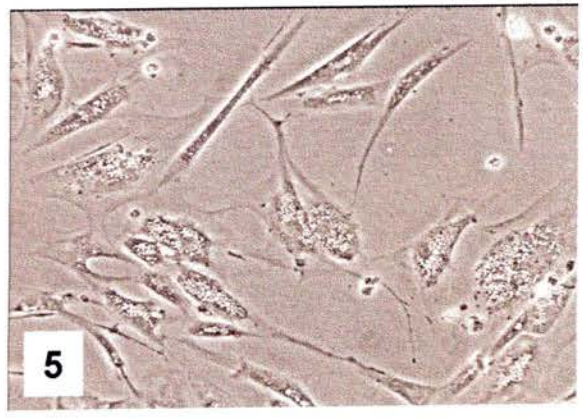
5

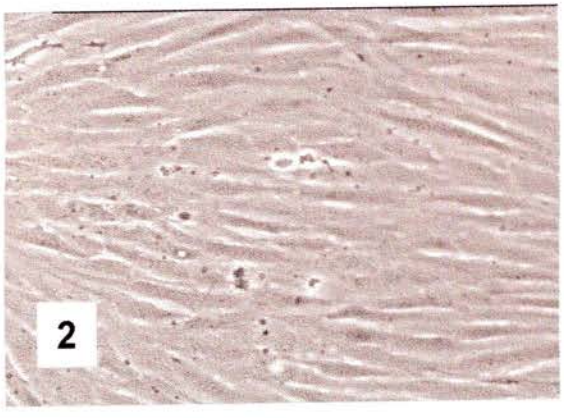
2

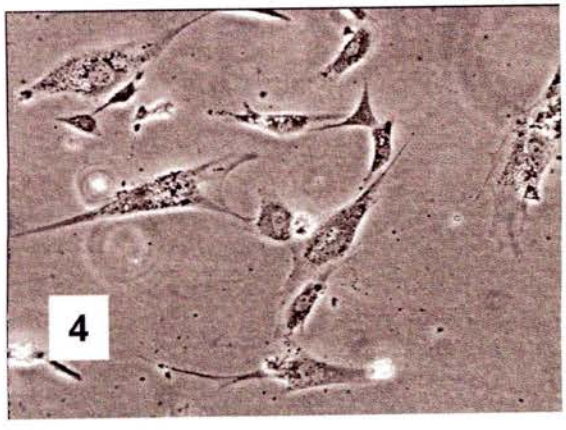
4

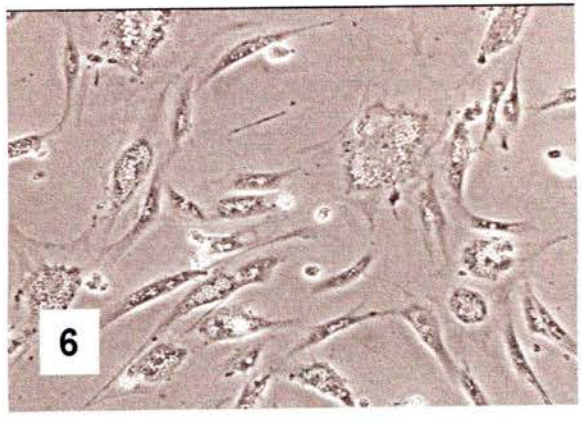
6

4.2.2 Strategy A – recombinant virus containing no ORF50 coding sequence.

Strategy A - construction of a plasmid containing only sequences flanking ORF50 but lacking any ORF50 coding sequences.

A plasmid was designed to have a marker gene encoding the green fluorescent protein flanked by virus sequences that lie upstream and downstream of ORF50 in the AlHV-1 genome. No ORF50 coding sequence was present in this construct. The sequences flanking ORF50 were amplified by PCR (see Table 4.1).

Table 4.1: Primers
The table shows the primers used to amplify the sequences flanking ORF50 sequence by PCR to construct a plasmid for use in strategy A. Regions underlined show the restriction endonuclease sites added to the primer sequences.

Name	Primer Sequence	Position in the AlHV-1 genome
50F1	TCCAACAGCAGAGCTAACC	72318-72336
50F2	GAATTCTTAATTAAGGATCCGGGTAGTCAAATTTGTGTGC *Eco*RI *Pac*I *Bam*HI	72822-72802
50F2a	GGGTAGTCAAATTTGTGTGC	72822-72802
50F3	GGATCCTTAATTAAGAATTCTGGGAGTGTAAACAGTAACC *Bam*HI *Pac*I *Eco*RI	74911-74930
50F3a	TGGGAGTGTAAACAGTAACC	74911-74930
50F4	CTCCATATCTTATCCATCGC	75443-75424
EGFP5'	GGTTAATTAAGTTCATAGCCCATATATGGAG *Pac*I	NA
EGFP 3'	GGTTAATTAACGCGTTAAGATACATTGATGAG *Pac*I	NA

In principle, this strategy would have resulted in flanking sequences of 504 bp and 540 bp. The restriction enzyme sequences on the end of primers 50F2 and 50F3 were designed to be used in overlap extension PCR creating a *Pac*I site between the two homologous ORF50 flanking regions. This would have allowed insertion of the CMV-EGFP cassette between the flanking sequences, since it was amplified using primers with *Pac*I restriction sites (see Figure 4.2). The overlap extension PCR was not successful and construction of this plasmid was not completed.

4.2.3 Strategy B - recombinant virus containing partial ORF50 coding sequences

Strategy B - construction of a plasmid containing only ORF50 coding sequences and no flanking sequences.

This strategy used the previously subcloned ORF50 sequence in the pGEM-T Easy vector (see Figure 3.1(a)). A 923 bp central portion of the ORF50 sequence was excised using *Hin*dIII and *Msc*I restriction enzymes and the CMV-EGFP expression cassette was excised from pEGFP-C1 using *Ase*I and *Mlu*I. Blunt-end ligations were carried out (section 2.2.6-2.2.8) to insert the CMV-EGFP cassette into the pGEM-T Easy-ORF50 plasmid. This resulted in homologous sequences of 739 bp and 416 bp of the ORF50 sequence flanking the CMV-EGFP cassette, deriving p50/EGFP (Figure 4.3(a) and (b)). This plasmid was sequenced to confirm the insertion of the CMV-EGFP cassette.

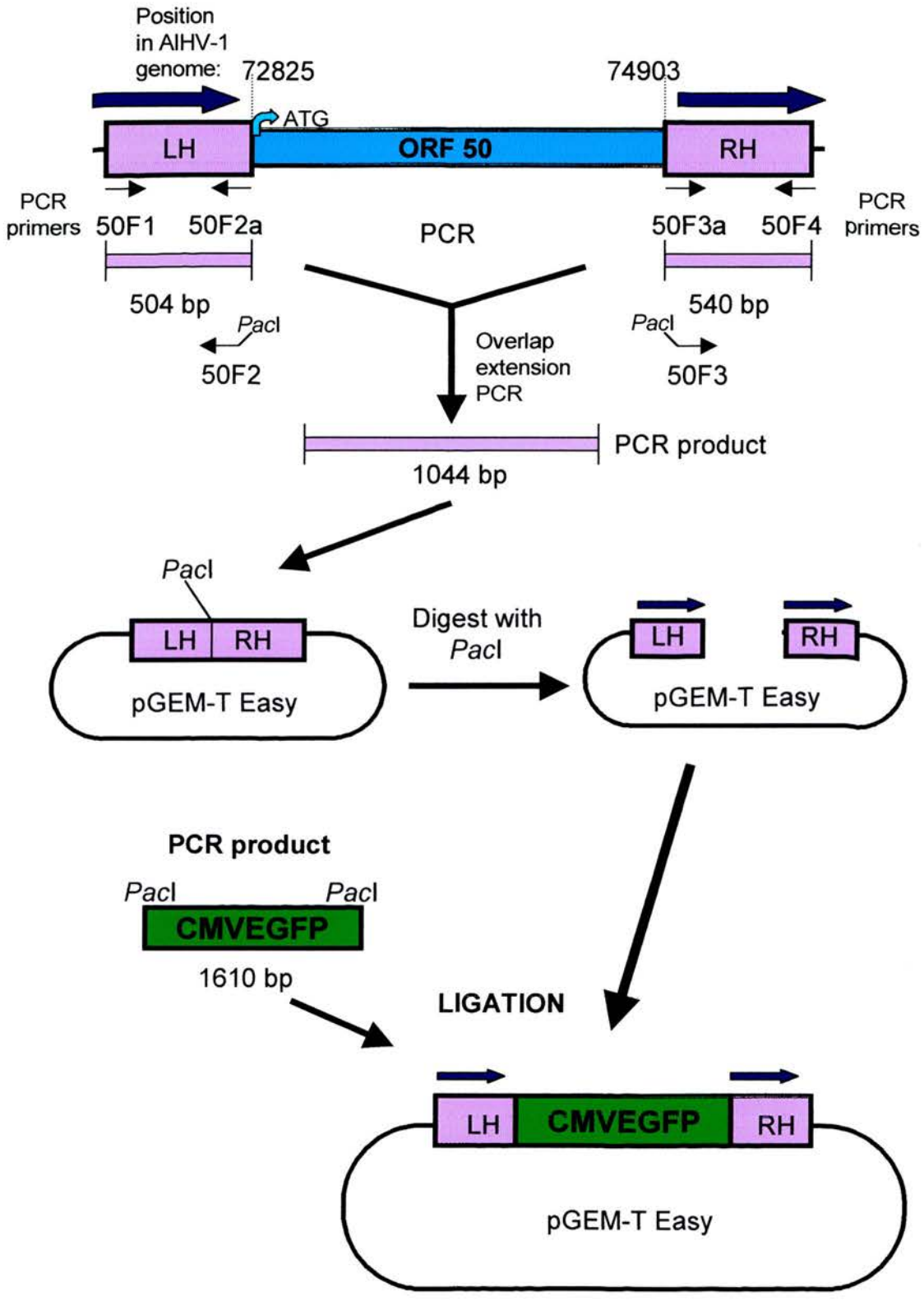

Figure 4.2: Construction of plasmid for strategy A

Schematic diagram showing the location of primers and construction of the plasmid designed in strategy A.
Blue arrows indicate the orientation of the cloned fragments.

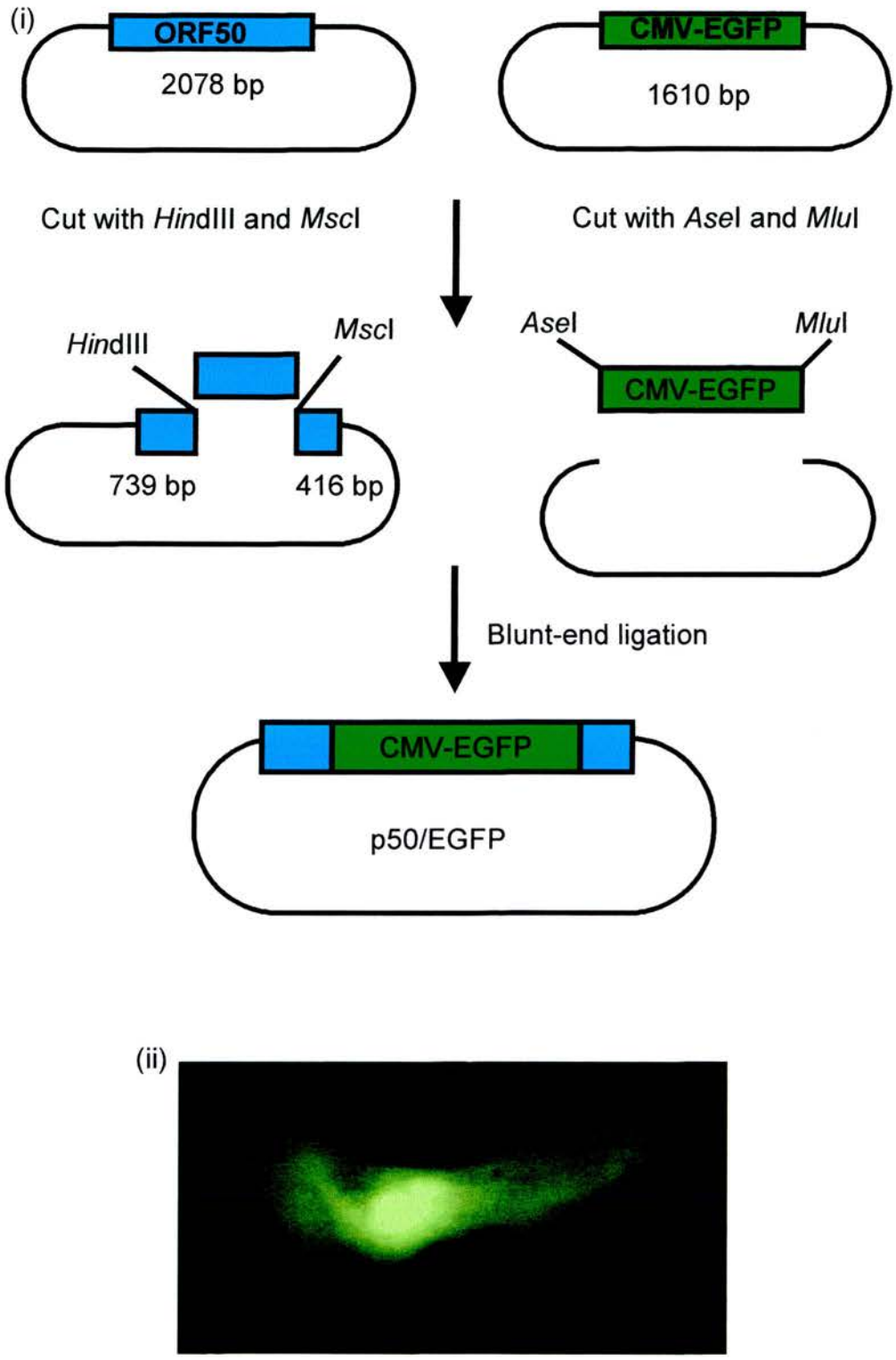

Figure 4.3 (a): Construction of p50/EGFP

(i) Construction of p50/EGFP, which contains a CMV-EGFP expression cassette flanked by ORF50 sequences.
(ii) Image of a BT cell fluorescing after transfection with p50/EGFP.

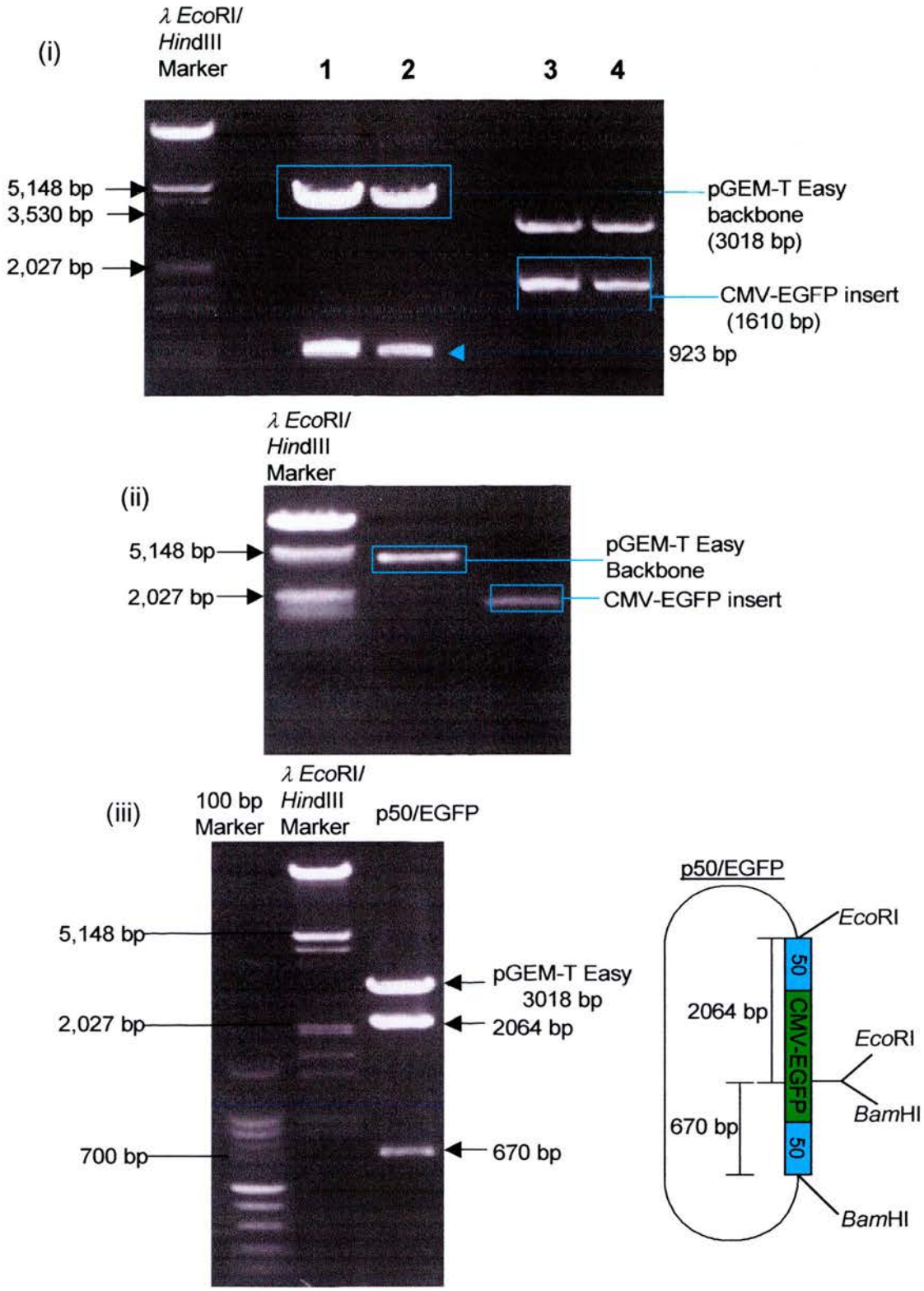

Figure 4.3 (b): Construction of p50/EGFP

(i) *Hin*dIII/*Msc*I digests of pGEM-T Easy-ORF50 (Lanes 1 and 2) and *Ase*I/*Mlu*I digests of pEGFP-C1 (Lanes 3 and 4).

(ii) Fragments highlighted in (i) were extracted from the gel and these gel-purified products are shown in this gel.

(iii) Successful insertion of the CMV-EGFP cassette into pGEM-T Easy-ORF50 to derive p50/EGFP. Digest with *Eco*RI and *Bam*HI. The CMV-EGFP cassette contains *Eco*RI and *Bam*HI restriction sites as shown on the right of the figure.

4.2.4 Transfections of plasmid and virus DNA to "knock out" ORF50

BT cells were transfected with 2 μg of p50/EGFP and after 48 h examined for fluorescence. Approximately 10% of the cells fluoresced green indicating that they expressed the CMV-EGFP cassette, and that this would therefore serve as a useful marker. (Figure 4.3(a)(ii)).

In an attempt to generate recombinant viruses, BT cells were co-transfected with between 0.1-10 μg of virus DNA along with 2 μg of p50/EGFP. BT cells were also transfected with 2 μg of p50/EGFP and infected with AlHV-1 24 h later (see Table 4.2).

Table 4.2: Experimental design.

Experiment 1: co-transfection of BT cells with p50/EGFP and different amounts of virus DNA.
Experiment 2: transfection of BT cells with p50/EGFP alone followed by infection 24 h later with different amounts of virus.
Mock-transfected cells acted as a negative control for both experiments.
100μl of AlHV-1 represents 2 x 10^5 infected cells exhibiting 70-80 % CPE.

Experiment 1	Cell treatment:
A	p50/EGFP (2 μg) and 10.0 μg of AlHV-1 DNA
B	p50/EGFP (2 μg) and 5.0 μg of AlHV-1 DNA
C	p50/EGFP (2 μg) and 1.0 μg of AlHV-1 DNA
D	p50/EGFP (2 μg) and 0.1 μg of AlHV-1 DNA
Experiment 2	Cell treatment:
A	p50/EGFP (2 μg) and infection with 20 μl AlHV-1
B	p50/EGFP (2 μg) and infection with 30 μl AlHV-1
C	p50/EGFP (2 μg) and infection with 40 μl AlHV-1
D	p50/EGFP (2 μg) and infection with 60 μl AlHV-1
Negative control	Mock transfection with sterile distilled water

After 24 h, all cells were assayed for successful transfection as determined by the appearance of green fluorescing cells. The presence of green fluorescing cells within areas of virus-induced CPE would suggest the presence of virus recombinants.

Experiment 1:

BT cells that had been transfected with virus DNA initially did not show evidence of CPE, although 10% of cells were fluorescing green. Five days after transfection, green fluorescence was still detected in the transfected cells although clear CPE was still not observed. Fourteen days after transfection, the cells were harvested, freeze-thawed and transferred to fresh BT cells in 75 cm^3 (T75) flasks. After further passaging, CPE was finally observed. However, green fluorescence was no longer observed.

Experiment 2:

After 48 h some CPE was observed in the plates with virus-infected cells and there were several green fluorescing cells within the areas of CPE (Figure 4.4). Five days after infection, the virus-infected cells were harvested and an aliquot was transferred onto fresh BT cells in 96-well plates and observed for green fluorescence. Three days later, from wells containing green fluorescence, cells were harvested and plated onto fresh cells in 60 mm plates. They were again observed for green fluorescence and passaged one further time onto fresh BT cells after they reached confluency.

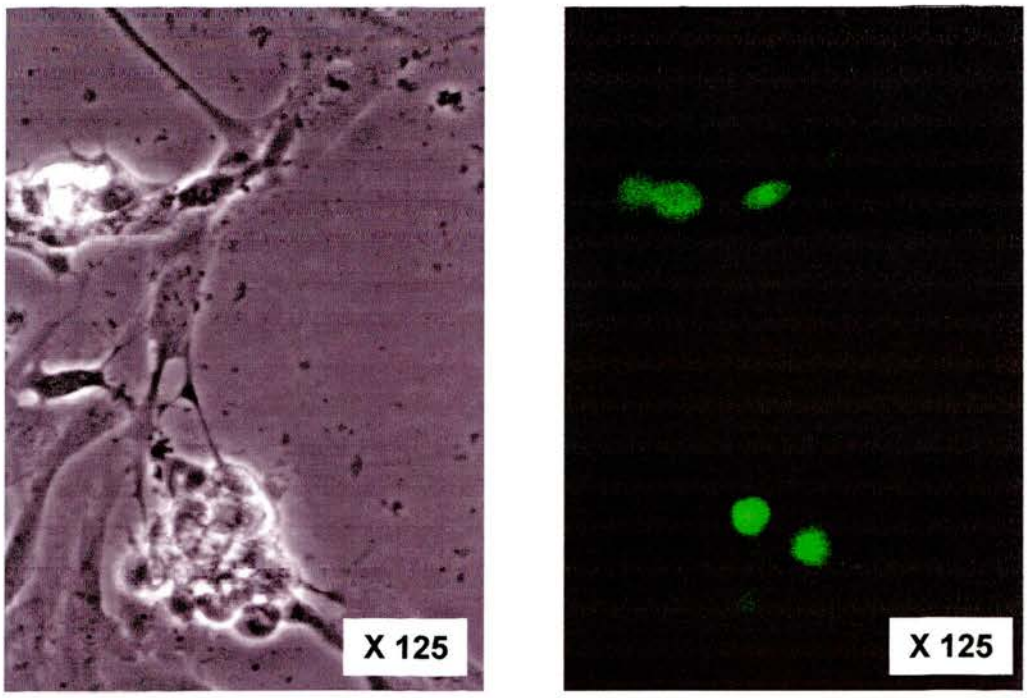

(a) (b)

Figure 4.4: Bovine turbinate cells transfected with p50/EGFP and infected with C500 AlHV-1.

(a) Light microscopy indicating rounding up of cells, which is characteristic of the CPE observed following AlHV-1 infection.
(b) Fluorescent microscopy of the same field as (a) indicating fluorescent green cells within the area of CPE.

In both experiments, although CPE continued to be observed in some samples, green fluorescence was not. The procedure was repeated using virus DNA once the optimum electroporation conditions for BT cells had been determined (Figure 3.9), but this was also without success.

At this point, this method of obtaining an ORF50 knockout virus was abandoned, as it was felt that in order to obtain sufficient amounts of virus DNA, the virus would have to be repeatedly passaged, thereby increasing the risk of additional, unwanted mutations. Another challenge with this method included the purification of recombinant virus. As AlHV-1 does not cause defined plaques in the cell monolayer, purification involved selecting areas of CPE that were fluorescent. The intention was to use limiting dilution to select recombinant virus. During the procedure, after several rounds of selection, the green fluorescence was eventually lost, and recombinant virus was not purified. It was hoped that as green fluorescent areas of CPE were selected the amount of green fluorescence would be amplified due to the amplification of the recombinant virus. It was not possible to establish if recombinant virus was present in these areas, if the marker gene had been rejected or down regulated, or if the recombination had been unsuccessful. For these reasons, a different approach with more potential applications was pursued.

4.3 Strategy to make a bacterial artificial chromosome containing the AlHV-1 genome

Several new approaches have been developed to allow the manipulation of herpesvirus genomes. One of the first developments was to clone virus genomes into several cosmids. Cosmids, which can hold 35-45 kb of DNA, allow packaging of

DNA into phage particles. This development enabled researchers to exploit bacterial systems to mutate a particular area of one of the cosmids. Following transfection into mammalian cells the cosmids undergo homologous recombination resulting in a productive virus replication. This method has been used successfully for HSV-1 (Cunningham and Davison, 1993; Kong *et al.,* 1999), MCMV (Ehsani *et al.,* 2000) and pseudorabies virus (PRV) (van Zijl *et al.,* 1988). The main advantage of this method is that selection for the mutated cosmid occurs in the bacterial system, therefore no selection against wild type virus is necessary. Two disadvantages are that there is a risk of unwanted mutations when the cosmids are undergoing recombination in mammalian cells, and cosmids can be unstable (Brune *et al.,* 2000).

Recently there has been much interest and activity in the area of artificial chromosomes. These were developed to provide a solution to the limitations of the size of DNA insert that can be contained in plasmids and cosmids.

Yeast artificial chromosomes (YACs) are linear vectors containing the insert of interest flanked by telomeres and containing an origin of replication and centrosome. They hold between 100-2000 kb of DNA. YACs have been crucial in the mapping of large genomes of higher organisms (Burke *et al.,* 1987; Anand *et al.,* 1989; Schlessinger, 1990; Monaco and Larin, 1994) as they can hold large genes along with all of their control elements. They have been used to make transgenic mice. A human adenovirus genome has been produced as a YAC clone allowing it to be manipulated and it has proved to be infectious (Ketner *et al.,* 1994).

YACs have several disadvantages. They are prone to chimaerism, they can be unstable which results in some regions being deleted and the YAC cannot be separated from the yeast chromosomes very easily (Monaco and Larin, 1994). The possibility of cloning the AlHV-1 genome into a YAC was considered, but it was thought that the repeat regions at the ends of the genome would be unstable in the YAC system.

Other methods based on bacterial systems have also been developed. At the start of this work, less information was available on these methods. However, there has since been an increase in their utilisation. They have advantages over YACs with respect to their lack of chimaerism and ease of purification, but they accommodate less DNA than YACs. The P1 cloning system uses the loxP recombination sites and packaging site from bacteriophage P1 and can hold 70-100 kb of DNA. P1-derived artificial chromosomes (PACs) can hold 100-300 kb of DNA and, as well as containing elements from the P1 system, are based on the F-factor plasmid which is the bacterial sex or fertility plasmid. BACs can hold up to 300 kb and are also based on the F-factor plasmid for which the replication is strictly controlled. BACs do not require separate packaging systems like the P1 system, and are more stable than YACs (Monaco and Larin, 1994; Brune *et al.,* 2000). PACs and BACs can be purified using standard bacterial selection procedures and methods of plasmid preparation with only a few modifications, and they can also be directly sequenced (Yang *et al.,* 1997).

BACs had previously only been used for the purposes of mapping and sequencing; methods of modifying them were not available. There have since been significant

developments in this area. In 1997, the first modification of a BAC and generation of transgenic mice using pronuclear injection of a BAC were reported (Yang *et al.,* 1997).

The stability of BACs and their ability to hold up to 300 kb of DNA are attractive features for the study of herpesvirus genomes. The first herpesvirus cloned into a BAC was MCMV (Messerle *et al.,* 1997). Transfection of a BAC containing the virus genome resulted in a productive virus infection. A targeted mutation in one of the IE genes was carried out and a mutant virus was produced. Subsequently, BACs have been constructed that contain the genomes of HSV-1 (Horsburgh *et al.,* 1999), EBV (Delecluse *et al.,* 1998), PRV (Smith and Enquist, 1999), HCMV (Borst *et al.,* 1999) and MHV-68 (Adler *et al.,* 2000).

It was decided to attempt to insert the entire AlHV-1 genome into a BAC. As has been outlined in Chapter 1, when the C500 virulent strain of AlHV-1 is passaged through tissue culture it eventually becomes attenuated through genome alterations. For this reason it is difficult to obtain large amounts of virulent AlHV-1 C500 DNA. If an AlHV-1-BAC was available it could be grown in bacteria and large amounts of virus DNA would be able to be produced with less risk of mutation. The use of the BAC system also has the advantage that it avoids the selection procedure involving limiting dilution, which had previously proved to be a challenge with AlHV-1, partly owing to the lack of defined plaques. Once a recombinant was made using the AlHV-1-BAC, pure stocks of a virus mutant could be obtained through the bacterial selection system.

At the time of initiating this strategy, only two instances of herpesviruses being cloned into BACs were known, MCMV (Messerle *et al.,* 1997) and HSV-1 (B. Horsburgh, pers. comm.). The BAC vector was inserted into an area at the right hand end of the MCMV genome that had been shown to be nonessential for *in vitro* replication. Successful insertion was determined by inclusion of a marker gene in the BAC. In HSV-1, the BAC was inserted into the TK locus, disrupting it, thereby allowing selection against wild-type virus TK activity.

The method used for HSV-1 was adopted as a means for making an AlHV-1-BAC since no nonessential regions of AlHV-1 have been identified. As part of the strategy, a selection method to select for TK- recombinant viruses was required. The principle of the method is to add a drug which inhibits replication of wild type virus but which has no effect on recombinant TK- virus. Two possibilities were to use 4'-S-Etdu (2' deoxy-5-ethyl-beta 4'-thiou`ridine), also called "C9" (Glaxo SmithKline) (Barnes *et al.*, 1999), or 9-[(2-hydroxyethoxy) methyl] guanine, called acyclovir. C9 and acyclovir have been shown to inhibit virus replication of other herpesviruses. Before construction of an AIHV-1-BAC was initiated, both of these drugs were tested to determine if they inhibited the growth of wild-type AlHV-1.

4.3.1 Testing C9 as an agent to select against wild type AlHV-1 replication

C9 has previously been shown to inhibit replication of MHV-68 and to delay the onset of viral latency (Barnes *et al.*, 1999). To test the sensitivity of AlHV-1 to C9, a range of concentrations encompassing the dose known to be effective against MHV-

68 replication, 2 μg/ml, was used. Subconfluent BHK cells and BT cells were plated on to 60 mm plates, then infected with AlHV-1 in the presence or absence of different concentrations of C9 (outlined in Table 4.3). Uninfected cells treated with C9, infected cells without C9, and uninfected, untreated cells were included as controls. The amount of virus added was equivalent to 2 x 10^5 cells with 70-80% CPE. After observation for 7 days, the cells with virus alone and those with virus plus C9 showed equivalent amounts of CPE. It was concluded that AlHV-1 replication was not inhibited by C9 at the concentrations used.

Table 4.3 Testing C9 as a selection agent.
Additions to each sample are indicated (+, added; -, not added). Also indicated is whether or not CPE was observed (Y – yes, N – no).

Samples	1	2	3	4	5	6	7	8
Virus	-	+	-	-	-	+	+	+
C9 (μg/ml	0	0	1	2	10	1	2	10
CPE	N	Y	N	N	N	Y	Y	Y

4.3.2 Testing acyclovir as an agent to select against AlHV-1

Acyclovir is a guanosine analogue and is an effective inhibitor of HSV-1, HSV-2 and VZV replication, but not of EBV and CMV. It is phosphorylated by the virus-encoded TK and is then further phosphorylated by cellular kinases to produce acyclovir triphosphate. This is incorporated into DNA by the viral DNA polymerase, causing chain termination (Fields *et al.*, 1996).

For MHV-68, 0.2 μg/ml of acyclovir reduces the ability of the virus to grow by 50% and 2 μg/ml completely inhibits virus replication. A 96-well plate was set up with serial dilutions of AlHV-1 virus, in the presence of either of these concentrations of acyclovir. Controls included cells with virus in the absence of acyclovir, uninfected cells treated with acyclovir, and untreated, uninfected cells.

Acyclovir did not inhibit the replication of AlHV-1. This has also been observed by H. Reid (pers. comm.).

4.3.3 Bromodeoxyuridine (BUdR) as a selection agent.

Since C9 and acyclovir were shown to be ineffective against AlHV-1, bromodeoxyuridine (5-bromo-2'-deoxyuridine, BUdR) was considered. BUdR is a chain terminating thymidine analogue that is selectively incorporated into DNA during S-phase and inhibits growth (Boccadoro *et al.,* 1986). As BUdR is phosphorylated by cellular and viral TK, TK- cells were required. AlHV-1 can cause disease in hamsters (Jacoby *et al.,* 1988a and b) and infects BHK cells (Figure 3.11). Also, BHK cells gave much higher transfection efficiency than BT cells (section 3.3.8). Therefore, the cell line chosen was tk^- ts13 (ATCC CRL-1632), a temperature sensitive, TK- derivative of the BHK-21 cell line from a Syrian golden hamster (a kind gift from Dr. H. Marsden, University of Glasgow) (Talavera and Basilico, 1977).

4.3.4 Construction of pBeloBAC11 containing AlHV-1 TK sequences.

A vector containing sequences homologous to the AlHV-1 TK region was

constructed. Primers were designed to amplify regions spanning and incorporating parts of the TK locus in AlHV-1 (Table 4.4). Initially, PCR amplification did not work using virus DNA as the template, and so cosmids (c339P and c454B) were obtained from Dr. Armin Ensser. These cosmids had been used in the sequencing of the virus genome and contained the TK locus (Ensser *et al.,* 1997) making them useful templates for PCR. The primers TK1, TK2, TK3 and TK4 used in the PCR reactions are shown in Table 4.4 and Figure 4.5. Primers TK1 and TK4 contained the *Pac*I restriction endonuclease sequence. Primers TK1 and TK2 were used to amplify the left-hand section of the TK locus, TKA. Primers TK3 and TK4 were used to amplify the right-hand region of the TK locus, TKB. The PCR products were cloned into the pGEM-T Easy vector.

Table 4.4: Primers used to amplify AlHV-1 TK regions. *Pac*I restriction enzyme sites are underlined.

Name	Sequence	Position in genome (Nt)
TK1	AATTAATTAATGGTATAGGAGCTGC	37781-37795
TK2	TCGTCATCTGATAGCGTCTGGC	39141-39120
TK3	AGCACTCATGTCTGTGAATGTGGA	39505-39526
TK4	AATTAATTAAGCTTTGGTAGGATGC	41085-41071

Both clones were digested with *Pac*I to ensure a functional *Pac*I site had been formed and they were also sequenced to determine the orientation. Fragment TKB1 was excised via the *Pac*I and *Sac*II sites and inserted adjacent to fragment TKA1 in the pGEM-T Easy vector (Figures 4.6 and 4.7). The combined fragments are referred to as TKAB.

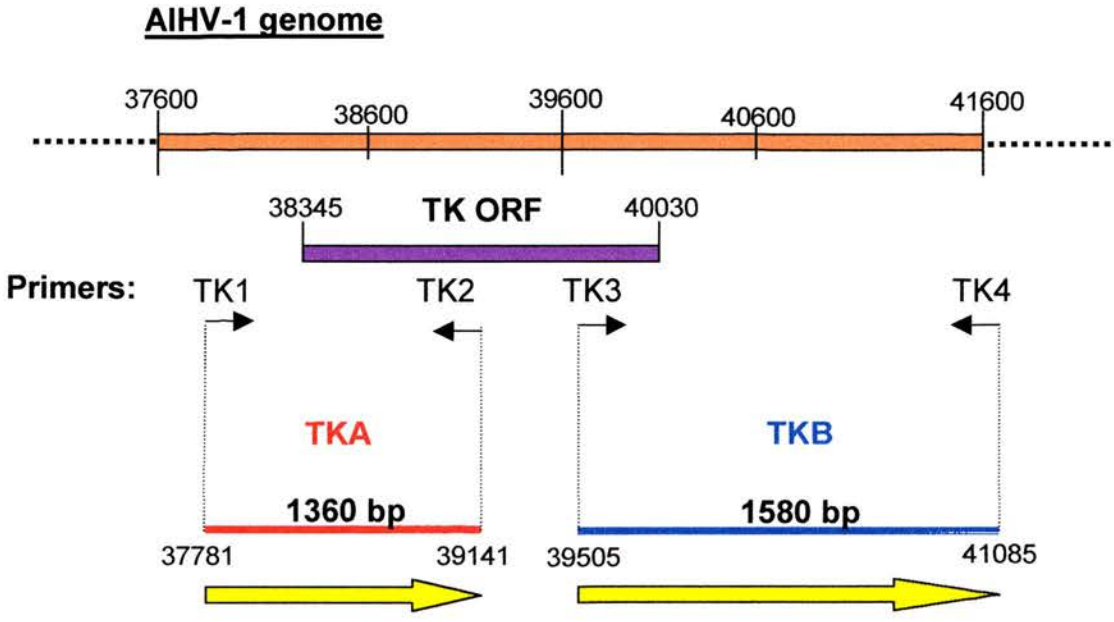

Figure 4.5: Position of primers in TK region

Diagram showing the location of the TK ORF in the AlHV-1 genome, the positions of primers used to amplify the TK regions for insertion into pBeloBAC11 (see Table 4.4) and the PCR products obtained. Arrows indicate the orientation of each sequence.

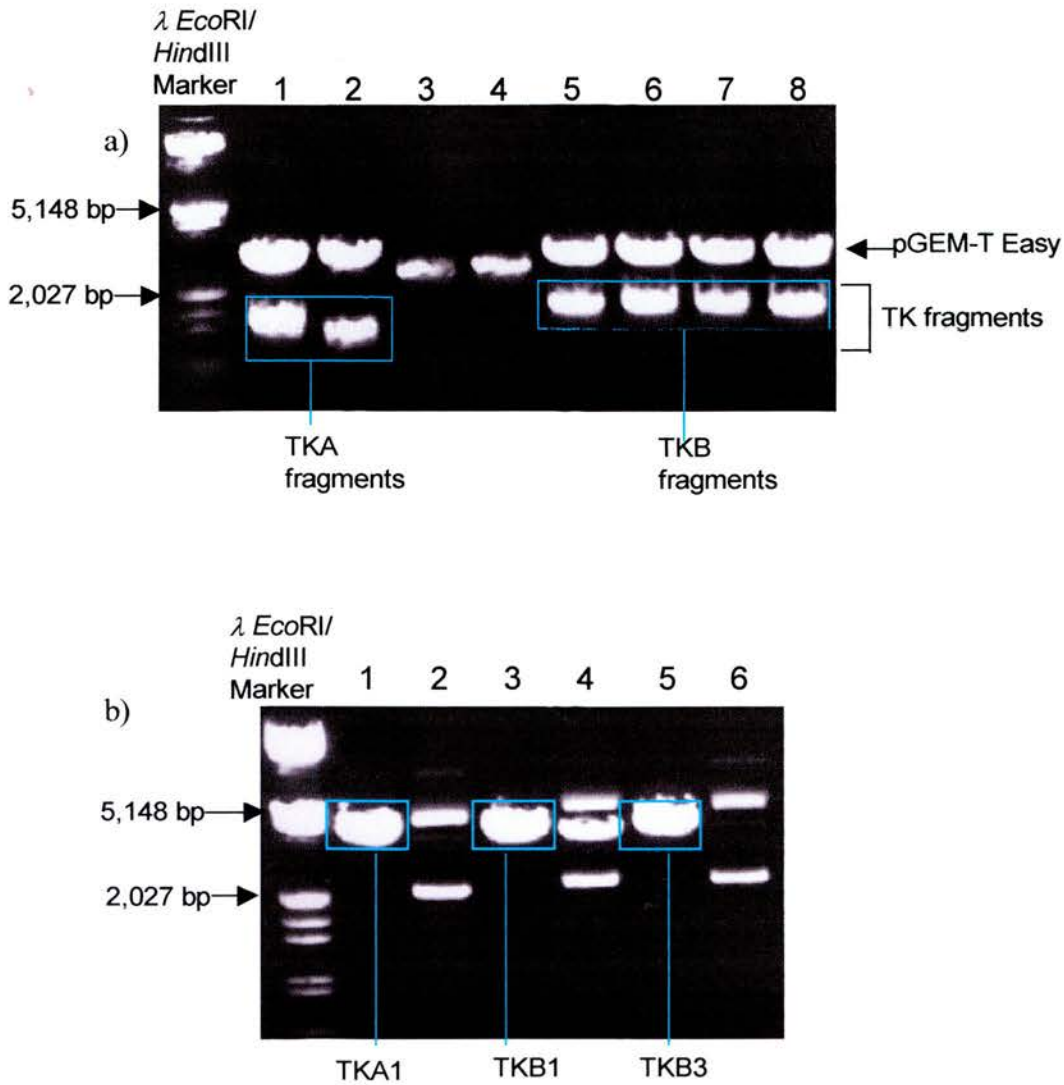

Figure 4.6: Subcloning of the AlHV-1 TK fragments

a) Lanes 1 and 2 contain clones with TKA inserts. Lanes 5-8 contain clones with TKB inserts. All clones were digested with *Not*I.
b) Lanes 1 and 2 contain TKA clones and lanes 3-6 contain TKB clones. Only clones in lanes 1, 3 and 5 show the expected pattern following digestion with *Pac*I.

Figure 4.7: Construction of TKAB

(a) Flow diagram showing how TKAB was constructed.
(b) Linearisation of pGEM-T Easy containing TKA1 with *Sac*II and *Pac*I to allow insertion of the TKB1 insert, which has been released from the pGEM-T Easy vector via *Sac*II and *Pac*I.
(c) *Not*I and *Pac*I digests showing successful subcloning of TKB inserted adjacent to TKA producing TKAB. All lanes (1-4) contain TKAB.

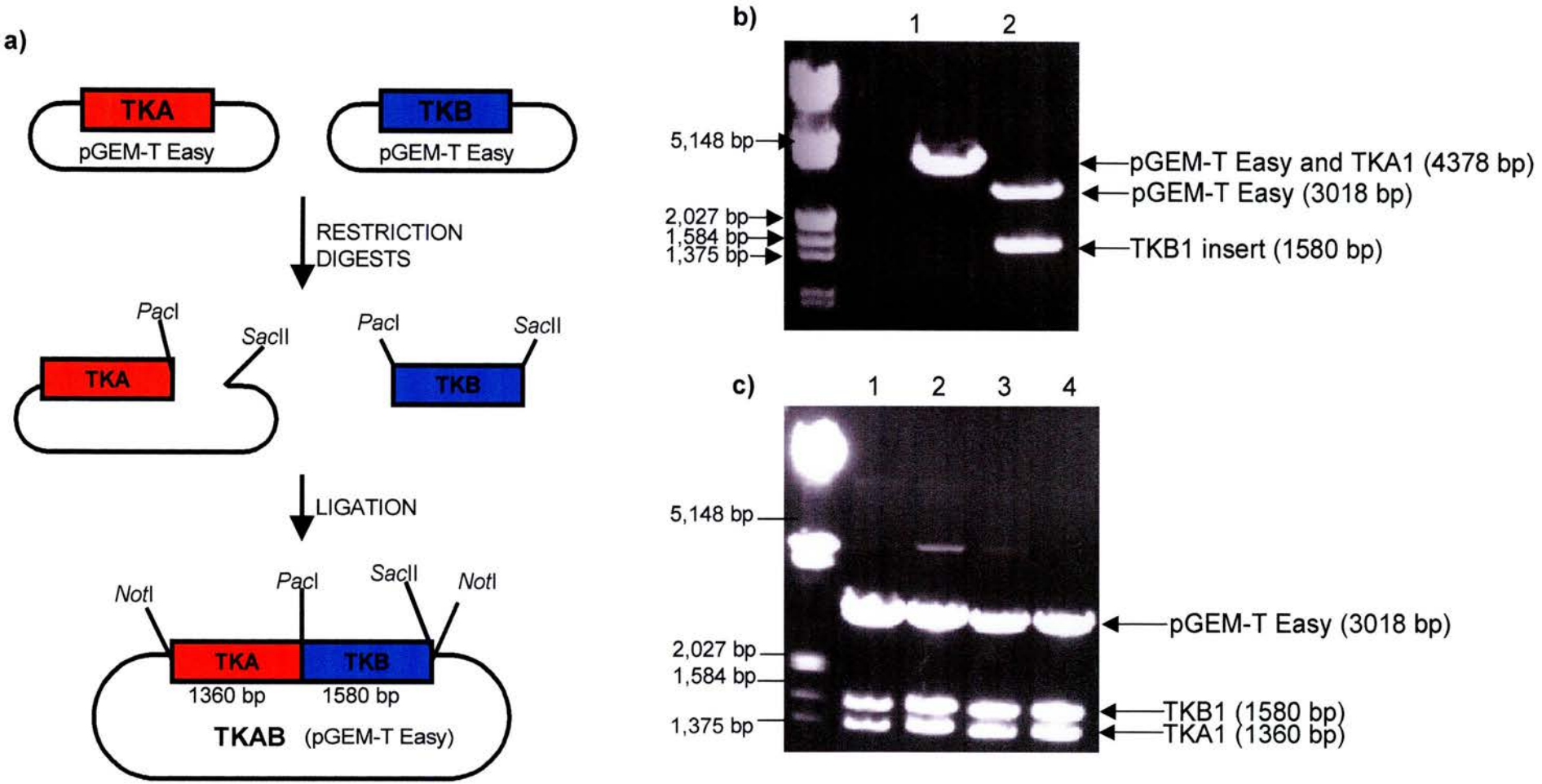
a)
TKA
pGEM-T Easy
TKB
pGEM-T Easy
RESTRICTION DIGESTS
PacI
SacII
TKA
PacI
SacII
TKB
LIGATION
NotI
PacI
SacII
NotI
TKA
TKB
1360 bp
1580 bp
TKAB (pGEM-T Easy)
b)
1
2
5,148 bp
2,027 bp
1,584 bp
1,375 bp
pGEM-T Easy and TKA1 (4378 bp)
pGEM-T Easy (3018 bp)
TKB1 insert (1580 bp)
c)
1
2
3
4
5,148 bp
2,027 bp
1,584 bp
1,375 bp
pGEM-T Easy (3018 bp)
TKB1 (1580 bp)
TKA1 (1360 bp)

The pGEM-T Easy vector is 3018 bp and the TKAB fragment is 2940 bp, and so the two fragments cannot be distinguished on a gel. Therefore, for subcloning of the TKAB fragment, *Sca*I was used in a double digest with *Not*I since *Not*I excises the TKAB fragment and *Sca*I does not cut the TKAB fragment but cuts the pGEM-T Easy plasmid backbone into two pieces. The whole TKAB region was excised from the pGEM-T Easy plasmid with *Not*I and inserted into the pBeloBAC11 vector (accession number - U51113; obtained from Dr Linda Mullins) (see Figures 4.8, 4.9(a) and 4.9(b)).

4.3.5 Transfection of TK- BHK cells with BAC-TK and virus DNA

TK- BHK cells were co-transfected with BAC-TK and virus DNA with or without the pCMVORF50 expression construct. The rationale for including the latter construct was that Rta homologues in EBV, HVS, MHV-68 and KSHV can reactivate virus from latency (Zalani *et al.*, 1996; Ragoczy *et al.*, 1998; Gradoville *et al.*, 2000; Wu *et al.*, 2000; Goodwin et al., 2001). If AlHV-1/Rta behaves similarly it could potentially facilitate the initiation of virus transcription from the virus DNA and thus make replication more efficient. Problems with genomic contamination of the BAC-TK preparation were rectified prior to the experiment by using the QIAGEN maxiprep kit with modifications for large plasmids (section 2.3.4 and 2.3.5). The experimental design is shown in Table 4.5.

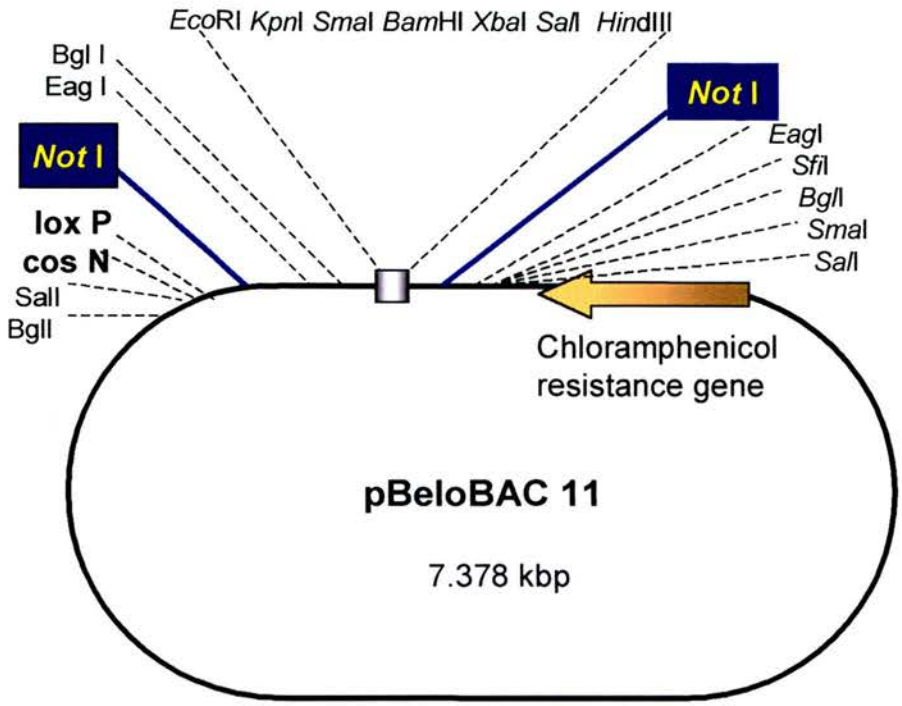

Figure 4.8: Diagram of pBeloBAC11

The *Not*I sites which were used for the insertion of TK sequences are boxed in blue. The deletion of the sequence between these sites reduced the size of the vector to 6749 bp.

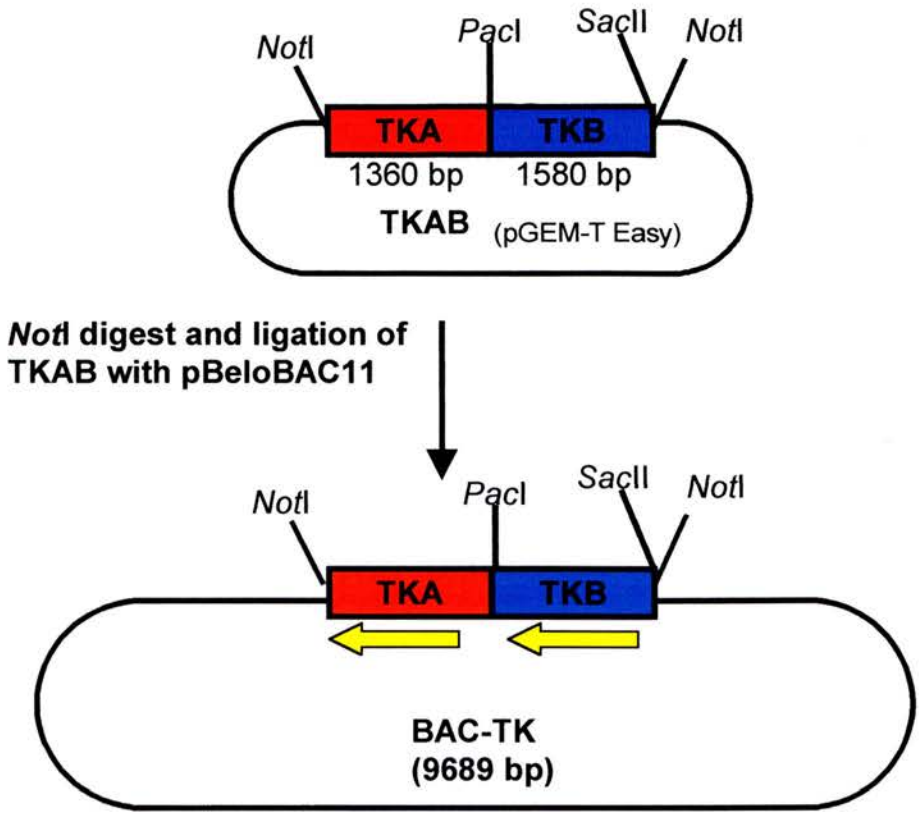

Figure 4.9 (a) Construction of BAC-TK

Diagram showing how the TKAB fragments, amplified from the AlHV-1 cosmids, were subcloned into pBeloBAC11. The TKAB fragment was excised from the pGEM-T Easy vector using the *Not*I sites in the multiple cloning site and inserted into the *Not*I sites in pBeloBAC11. The yellow arrows show the orientation of the TKA and TKB sequences. The orientation can be compared to the arrows in Figure 4.5.

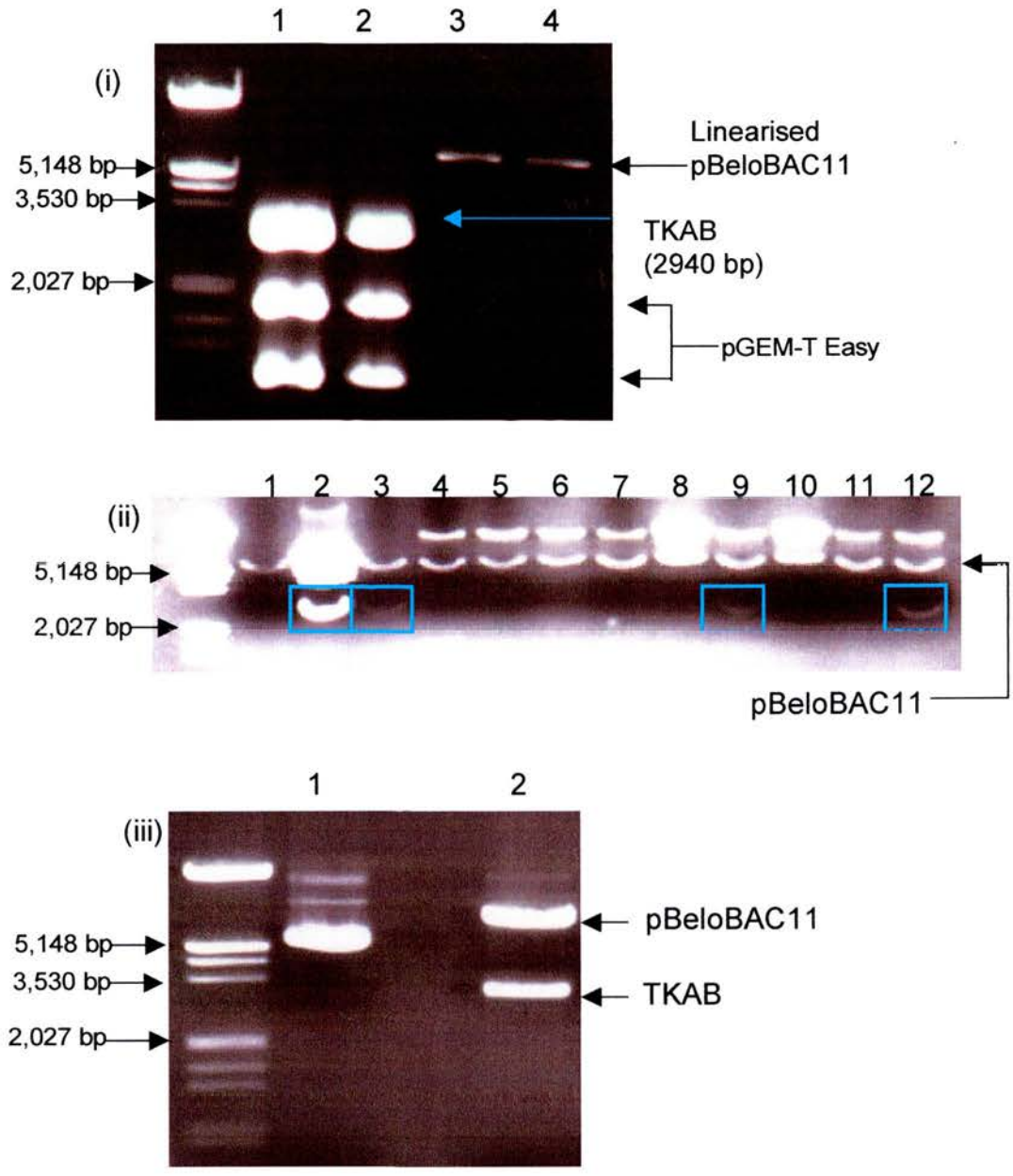

Figure 4.9 (b): Construction of BAC-TK

(i) *Not*I digests of pBeloBAC11 (lanes 3 + 4) and *Sca* I/*Not*I digests of pGEM-T Easy-TKAB (lanes 1 + 2).

(ii) Digests of BAC-TK showing successful subcloning of TKAB into pBeloBAC11. Clones containing TKAB are in lanes 2,3,9,12. Boxed bands are TKAB fragments excised from the pBeloBAC11 backbone.
The top band is *E. coli* genomic DNA contamination.

(iii) Large preparation of BAC-TK. Lane 1 shows uncut BAC-TK. Lane 2 shows TKAB excised from pBeloBAC11 by *Not*I. Note the lack of genomic DNA contamination in this preparation.

Table 4.5: Experimental design and results
TK- cells were transfected with different constructs in the presence and absence of BUdR, as indicated in the table, to allow insertion of BAC-TK into the AlHV-1 genome. Also indicated is whether or not CPE was observed (Y – yes, N – no).

Additions	Samples							
	1	2	3	4	5	6	7	8
BUdR (25 μg/ml)	+	-	+	-	+	-	+	-
Virus DNA (1 μg)	+	+	+	+	+	+	-	-
BAC-TK (0.2 μg)	-	-	+	+	+	+	-	-
pCMVORF50 (2 μg)	-	-	-	-	+	+	-	-
CPE	N	Y	Y	Y	Y	Y	N	N

Only samples 3 and 5 contained potential recombinants because they contained virus DNA and BAC-TK and were under BUdR selection. The other samples were included as controls for the following reasons:

1 - cells with BUdR and virus DNA to ensure the BUdR selection was effective.

2 - cells with virus DNA only to ensure virus was being produced.

4 - cells with virus DNA and BAC-TK to ensure that CPE occurred using these components without BUdR selection.

6 - cells with virus DNA, BAC-TK and pCMVORF50 to ensure that CPE occurred using these components without BUdR selection.

7 - cells with BUdR only to ensure BUdR did not affect the cells.

8 - cells alone to allow for comparison with other samples.

The areas of CPE observed in the samples suggested that the BUdR drug selection was acting as predicted and that virus was being produced (Table 4.5). The addition of pCMVORF50 did not result in increased areas of CPE. When CPE was observed

(Figure 4.10), cells from samples 3 and 5 were harvested and plated onto fresh subconfluent TK- BHK cells in media containing 25 μg/ml BUdR. Areas of CPE that developed were again harvested and plated onto fresh cells. Cells were harvested and aliquots were tested by slot blot analysis using pBeloBAC11 DNA as a probe (section 2.5.7). Separate aliquots were tested by PCR amplification using primers that straddled the pBeloBAC11 and AlHV-1 sequences to determine whether the BAC had inserted in the correct place. For both the slot blots and PCR, crude preparations of cell extract were used as described in section 2.4.10. The results obtained were all negative. The next step for this strategy would be to clean up these preparations to try to obtain signals or products. In addition, the CPE was not well defined and so it would be beneficial to be able to identify areas of CPE with more certainty.

4.3.6 Progression of Strategy

Owing to the lack of defined areas of CPE, it was reasoned that an additional selection was required. To achieve this a CMV-EGFP expression cassette, amplified from the p-EGFP-C1 vector (Genbank accession number U55763) was inserted into a *Sac*II site, in BAC-TK, deriving BAC-TK-EGFP. Cells could then be screened for areas of green fluorescing CPE in the presence of BUdR (see Table 4.6).

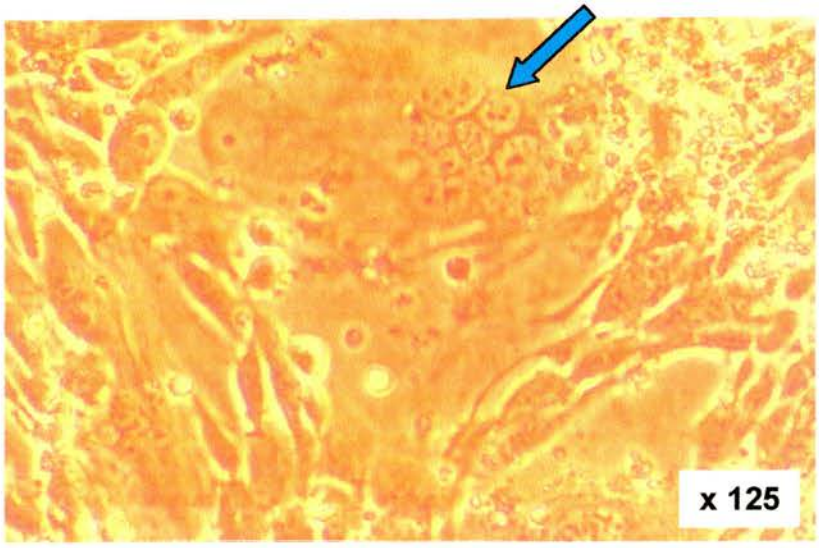

Figure 4.10: TK- BHK cells transfected with C500 AlHV-1 virus DNA and BAC-TK

An area of CPE, which resembles the syncytia caused by C500 AlHV-1 infection, is indicated by an arrow.

Table 4.6: Primers used to amplify the CMV-EGFP expression cassette.

*Sac*II restriction sites were engineered onto each primer (underlined).

Primer	Sequence	Position
5'	TACCGCGGGTTCATAGCCCATATATGGAG	35
3'	TACCGCGGCGCGTTAAGATACATTGATGAG	1645

The GFP cassette was successfully cloned into BAC-TK (Figure 4.11(a) and (b)).

4.3.7 Transfection of virus DNA and BAC-TK-EGFP

A similar experimental procedure was carried out to that described in Table 4.5, using 5 μg of BAC-TK-EGFP, 2 μg of virus DNA and 25 μg/ml BUdR. Fluorescence was observed in an initial experiment, but the transfection efficiency was low. The SuperFect method of transfection (section 2.4.7) was optimised for BHK cells and gave much improved transfection efficiency compared with electroporation. The optimal conditions involved adding 5μg of BAC-TK-EGFP to 2 x 10^5 cells on a 60 mm plate in transfection reagent for 2 h. Two days after transfection the cells were passaged onto 90 mm plates. The samples with potential recombinants, determined by the presence of green cells, were passaged onto further plates. This experiment was repeated in triplicate (see Table 4.5 for experimental design) varying the amount of virus DNA and the amount of BAC-TK-EGFP DNA (see Table 4.7). From 42 90 mm plates, 28 areas of CPE were harvested and plated onto 60 mm plates. Although fluorescence was detected up to 12 days after transfection (see Figure 4.12), no amplification of 'green areas' occurred and no

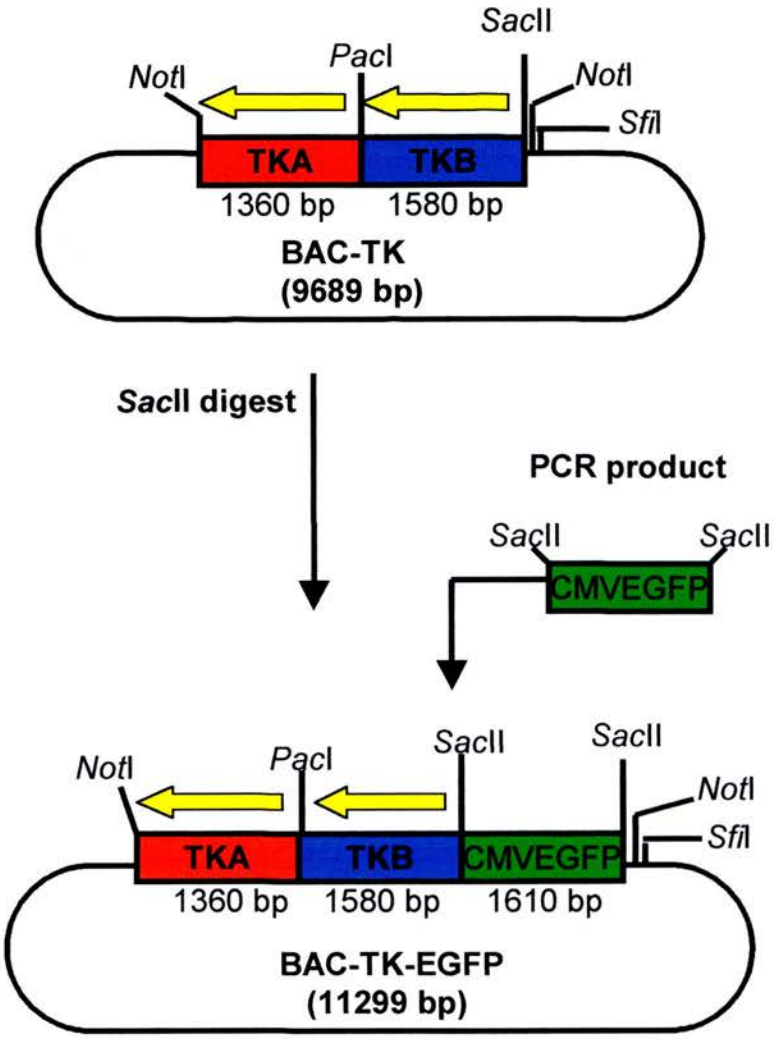

Figure 4.11 (a): Construction of BAC-TK-EGFP

Schematic diagrams showing construction of BAC-TK-EGFP. BAC-TK-EGFP was generated by inserting the CMVEGFP cassette into the *Sac*II site in BAC-TK (Figure 4.9 (a)). The *Sfi*I and *Pac*I sites were used to determine the orientation of the TKAB fragment and the CMVEGFP cassette relative to the pBeloBAC11 sequence (Figure 4.11 (b)).

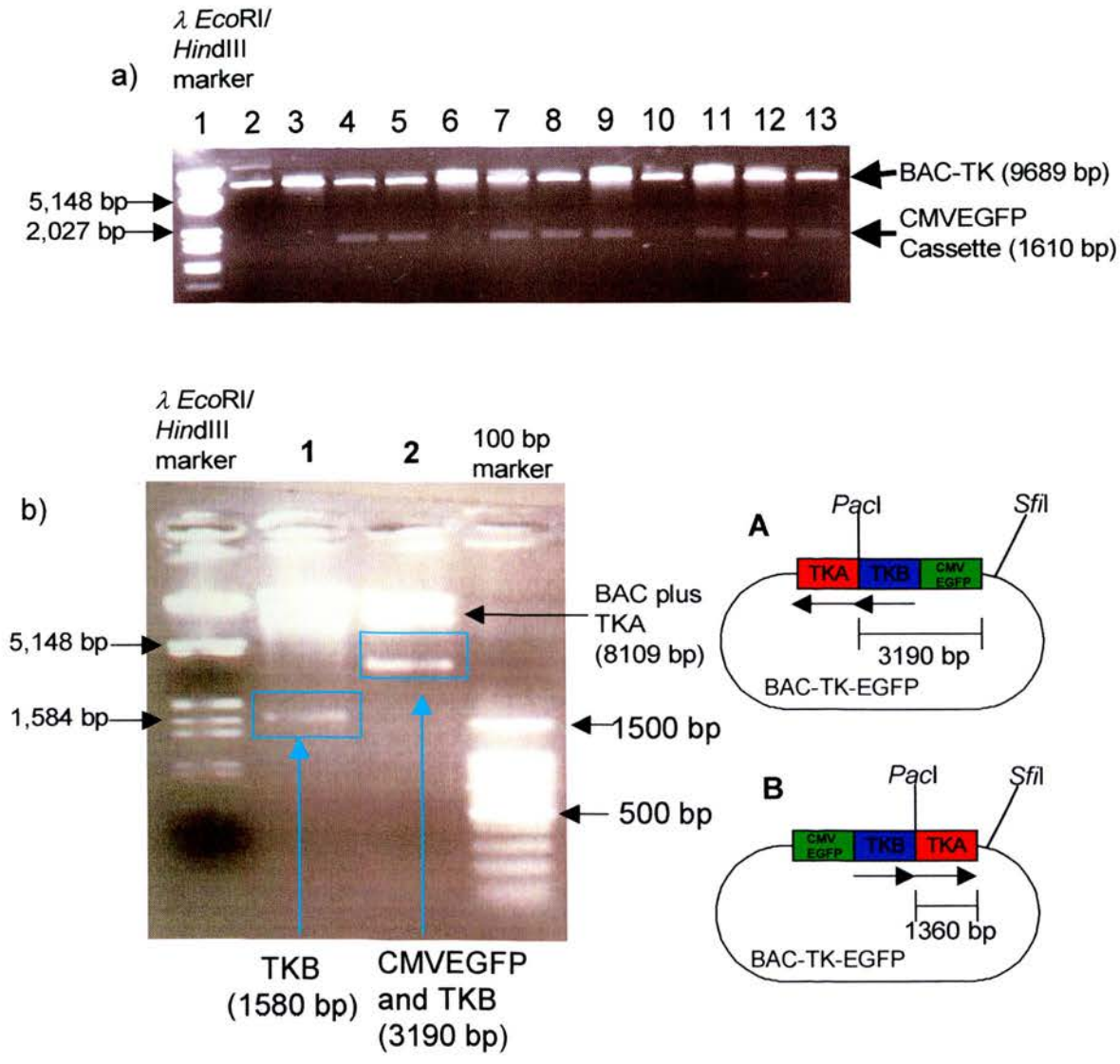

Figure 4.11 (b): Construction of BAC-TK-EGFP

a) *Sac*II digest showing successful cloning of the CMVEGFP expression cassette into BAC-TK. Clones containing CMVEGFP are in lanes 4,5,7,8, 9,11,12 and 13.

b) To establish the orientation of the TKAB fragment and also the CMVEGFP cassette relative to it, *Pac* I and *Sfi*I digests were carried out on BAC-TK (lane 1) and BAC-TK-EGFP (lane 2). This digest excised TKB from BAC-TK. The two possible orientations are shown for BAC-TK-EGFP (A and B). Diagram A shows the actual orientation.

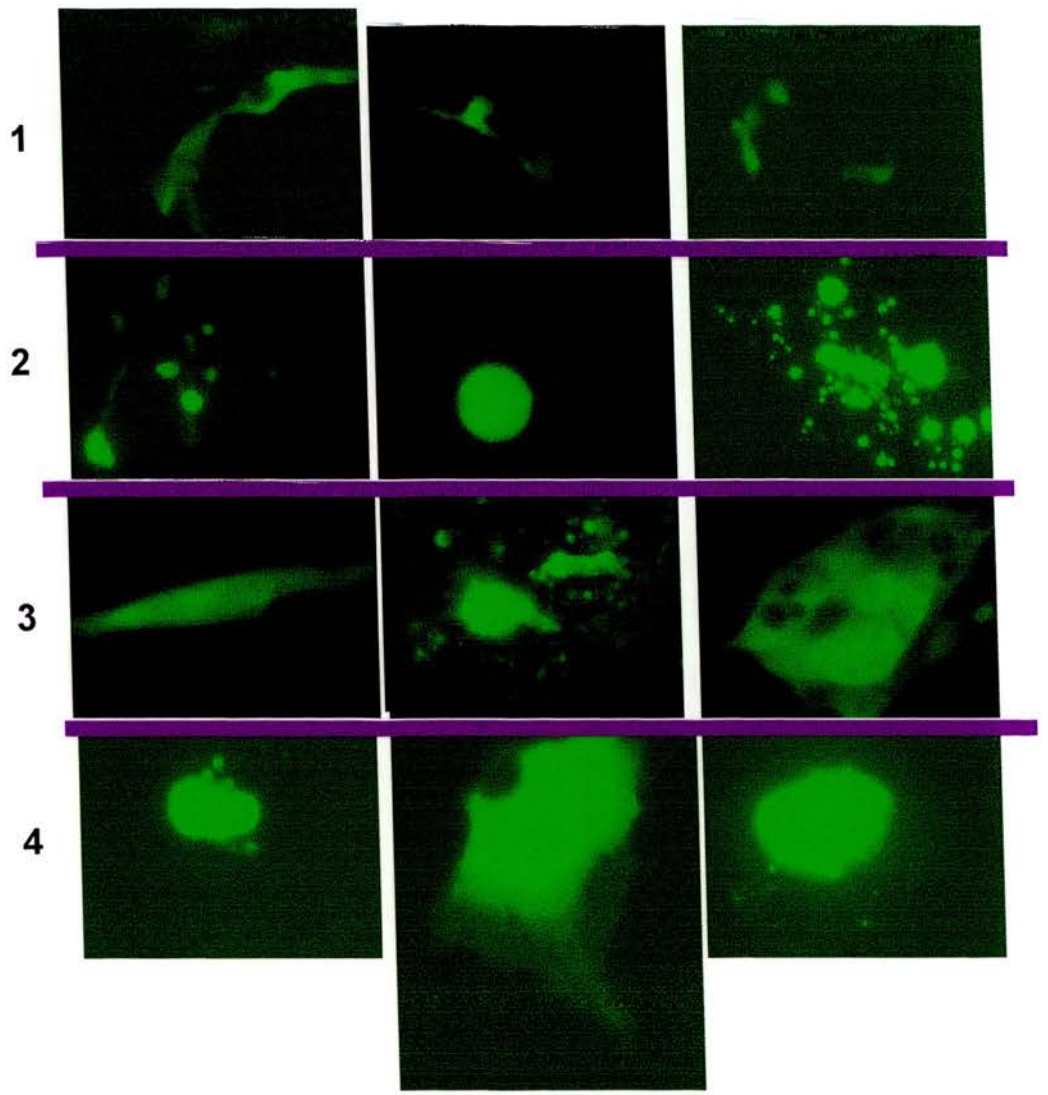

Figure 4.12 : TK- BHK cells transfected with virus DNA and BAC-TK-GFP. Examples of green fluorescing cells are shown. The images are arranged in 4 numbered rows, each row showing examples of cells from a different timepoint. Row 1 - 1 day after transfection, Row 2 - 2 days after transfection, Row 3 - 3 days after transfection, Row 4 - 9 days after transfection.

clear CPE was observed. It was at this point that the attempts to make an AlHV-1-BAC and ORF50 mutant were halted due to time constraints.

Table 4.7: Experimental Design

Varying amounts of BAC-TK-EGFP DNA and virus DNA used in transfections to insert the BAC into AlHV-1.

Experiment	A	B	C
Virus DNA (μg)	2	5	5
BAC-TK-EGFP (μg)	5	5	7.5

4.4 Future Work

During the period when these attempts were being made, substantially more literature was published on the process of making a BAC containing an entire herpesvirus genome. New considerations have been unearthed and ingenious strategies have been developed to cope with these.

The key difference between traditional methods and this method of creating mutant viruses is that the recombinant virus can be made using recombination in a prokaryotic system rather than a eukaryotic system. This means the process is more precise and faster: in theory, it can take 7 days to make a mutant virus (Horsburgh *et al.,* 1999). However, this can only occur once the virus DNA has already been cloned into the BAC vector. Construction of a BAC containing a virus genome can be a laborious procedure and is the most difficult part of the method largely owing to dependence upon recombination in a eukaryotic system. Direct cloning of virus DNA into the BAC vector is possible, but is not very efficient, although it can be done if

very large numbers of colonies are screened. However, the more common method involves homologous recombination of the virus genome into the BAC vector in eukaryotic cells. This approach can be problematic as success depends on how tolerant the virus is to having extra DNA inserted into its genome. The first MCMV BAC construct replicated similarly to wild–type virus *in vitro* but was attenuated *in vivo* (Messerle *et al.,* 1997). These workers overcame this issue by developing a method whereby the BAC sequences, after the MCMV BAC had been manipulated, were excised from the recombinant viral DNA and the deleted region of MCMV sequence was replaced, thereby eliminating the possibility that the insertion of BAC sequences disrupts the virus life cycle.

A method has recently been developed involving the use of the Cre-lox system. A cassette consisting of a marker gene flanked by loxP sites is inserted by homologous recombination into the herpesvirus genome. Recombinants that have excised the marker gene by recombination, leaving a single loxP site, are then selected. A BAC vector containing one loxP site can then be recombined into the genome in eukaryotic cells. Manipulations can then be carried out in a prokaryotic system, and mutants obtained by transfecting into mammalian cells. The Cre recombinase excises the BAC from the virus genome leaving no BAC DNA in the virus. The system was developed such that the Cre-lox system is not functional in the prokaryotic host because a synthetic intron was engineered into the Cre recombinase gene, which is present on the BAC, and therefore it is only transcribed and translated in mammalian cells (Smith and Enquist, 2000).

Cloning of herpesvirus genomes into BACs is a growth area. There are a variety of new developments emerging that achieve the same aim, but all have merits and pitfalls. This work has explored various strategies with the aim of constructing a recombinant AlHV-1 virus and has illustrated some of the challenges when working with AlHV-1. It is not known if AlHV-1 would accept insertion of the BAC vector as outlined. However, with the new methods now available, there is potential for a successful strategy to be found.

Chapter 5 – DISCUSSION

5.1 Project Aim

The aim of this project was to characterise AlHV-1 ORF50. Two approaches were taken:

1) To analyse the function of AlHV-1/Rta, the ORF50 gene product, in isolation.

2) To attempt to create a virus lacking ORF50.

5.2 Characterisation of AlHV-1 ORF50

5.2.1 Analysis of the function of AlHV-1/Rta

Examination of the functions of Rta homologues in other γHVs led to the hypothesis that AlHV-1/Rta may encode a transactivator. Transient transfection assays showed that AlHV-1/Rta transactivates the AlHV-1 ORF57 and ORF6 promoters but does not transactivate the TK promoter (Figure 3.14 and 3.15). This is similar to findings in other γHVs. The Rta homologues of HVS (Whitehouse *et al.,* 1997b), KSHV (Lukac *et al.,* 1999), EBV (Ragoczy *et al.,* 1999) and MHV-68 (Liu *et al.,* 2000) all activate the cognate ORF57 promoter. In addition, the Rta homologues of KSHV (Lukac *et al.,* 1998), HVS (Whitehouse *et al.,* 1998a) and BHV-4 (van Santen 1993) transactivate the cognate ORF6 promoter. However, in contrast to the results obtained with AlHV-1/Rta, KSHV/Rta activates the KSHV TK promoter (Lukac *et al.,* 1998).

5.2.2 Transcription of ORF57

ORF57 was subjected to 5'-RACE analysis (Figure 3.18). The results indicate that the ORF57 transcriptional start site is at nucleotide position 84438 of the genome, which is 30 bp downstream of the TATA box and 24 bp upstream of the translational

initiation codon predicted by Ensser *et al.,* (1997). SD and SA sites are located at positions 84513 and 84605, respectively. Cavener and Ray (1991) published a comprehensive analysis of sequences surrounding start codons for a variety of organisms, including vertebrate viruses. AlHV-1 ORF57 has the most common arrangement of nucleotides in key positions (-1), (-2) and (-3) from the predicted initiation codon, i.e. AACATG.

Comparison of AlHV-1 ORF57 with ORF57 from other γHVs showed notable similarities in the length of their exons and introns as well as the positions of their splice sites. ORF57 in AlHV-1 and in KSHV both have an SD site 50 bp downstream from the initiation codon while HVS ORF57 has an SD site 18 bp downstream from the initiation codon. The introns of ORF57 in AlHV-1, KSHV and HVS are 92 bp, 105 bp and 87 bp, respectively. The predicted lengths of the AlHV-1 and HVS ORF57 proteins are 435 aa and 410 aa, respectively, which is similar to the observed length of 435 aa for the KSHV ORF57 protein (Russo *et al*., 1996; Whitehouse *et al.,* 1998b; Bello *et al.,* 1999; Kirshner *et al*., 2000).

Ensser *et al.* (1997) also performed 5'-RACE on ORF57 of AlHV-1, and their results are in agreement with the results presented here with regard to the positions of the SD and SA sites. However, these workers identified the transcriptional start site of ORF57 as being located only 7 bp upstream of the start codon rather than 24 bp upstream. Both studies relied on data from one clone and there were experimental differences between them. The RNA used in this project was harvested from virus-infected BT cells treated with cycloheximide, and so only IE transcripts would have

been present. Ensser *et al.* (1997) used virus-infected bovine epithelial kidney cells in the absence of cycloheximide, and thus the RNA harvested would be expected to contain IE, E and L transcripts. It is possible that alternate initiation sites are used at different times throughout the virus life cycle, but this remains to be tested.

5.2.3 Control of gene expression by AlHV-1/Rta

From studies with EBV and HVS it could be inferred that AlHV-1/Rta might bind directly to DNA (Quinlivan *et al.,* 1990; Gruffat and Sergeant, 1994; Hall *et al.,* 1999). Specific response elements (REs) have been identified for EBV (Figure 5.1(a)) (Kenney *et al.,* 1989b; Chevalier-Greco *et al.,* 1989; Manet *et al.,* 1991; Gruffat *et al.*, 1992; Gruffat and Sergeant, 1994) and HVS Rta homologues (Whitehouse *et al.,* 1997b). The consensus RE for HVS Rta is CCN_9GG. Various workers reported four binding sites for EBV Rta (see Figure 5.1(a)). Gruffat and Sergeant (1994) analysed a pool of random DNA sequences to determine conserved sites within these REs. Initially the consensus sequence was defined as $GNCCN_9GGNG$ but subsequently a simplified form of the prototype Rta-binding site was proposed as CCN_9GG, which is identical to the consensus sequence determined independently for HVS Rta.

Two distinct REs have been found in two different sets of lytic genes activated by KSHV/Rta (Figure 5.1(a)). RE1 is found in the ORF57 and K-bZIP promoters, which encode virus regulatory proteins, and are highly responsive to KSHV/Rta. RE2 is found in DE promoters for PAN-RNA and kaposin, which are less responsive to KSHV/Rta. (Lukac *et al.,* 2000). Support for the latter of these findings comes from

Virus	Response Element (RE)	Gene promoter containing RE	Reference
HVS	**CC**NNNNNNNNN**GG**	ORF6	Whitehouse *et al.*, 1997b
EBV	GN**CC**NNNNNNNNN**GG**NG	random sequences	Gruffat and Sergeant 1994
EBV	TTGTC**CC**GTGGACAAT**G**TCC	DR promoter	Chevalier-Greco *et al.*, 1989
EBV	**CC**GTGGAGAAT**G**TC	BMLF1	Kenney *et al.*, 1989b
EBV	TGTG**CC**TTGTCCCGTG**G**ACAATGTCC	DR/DL promoter	Manet *et al.*, 1991
EBV	catGTC**CC**CtctatcatG**G**CGCagac	BMLF1	Gruffat *et al.*, 1992
EBV Consensus	**CC**NNNNNNNNN**GG**		
KSHV	GTATAAAA**CC**TGTCCAATC**GG**TGGGTAAA	PAN-RNA	Song *et al.*, 2001
KSHV	GTATAAAACCTGT**CC**AATCGGTGG**G**TAAA	PAN-RNA	Song *et al.*, 2001
KSHV	**CC**CAATCGGTG**GG**TAAAAACC	PAN-RNA, kaposin	Lukac *et al.*, 2000 (RE2)
KSHV	**CC**AAAAATGGGT**G**GCTAACCC	PAN-RNA, kaposin	Lukac *et al.*, 2000 (RE2)
KSHV	GTGTAACAATAATGTTCCCAC	K-bZIP, ORF57	Lukac *et al.*, 2000 (RE1)
KSHV	CACCCTTGTAATAACAATGTG	K-bZIP, ORF57	Lukac *et al.*, 2000 (RE1)

Figure 5.1(a): Table of Rta response elements of gammaherpesviruses.
Table of response elements from EBV, HVS and KSHV. Nucleotides represented in bold are conserved between all response elements. KSHV RE2 sequences are shown in inverse orientation.

work by Song *et al.* (2001) in which a specific sequence in the PAN-RNA promoter, corresponding to RE2, was shown to bind KSHV/Rta directly. KSHV/Rta recombinant protein has also been shown to bind to RE1 (Lukac *et al.*, 2001).

To assess the regions important for transcriptional control by AlHV-1/Rta, truncations of the ORF57 promoter were made. The results obtained with these deletion constructs suggested that a 113 bp region, 409-522 bp upstream of the ORF57 start codon, was critical for transactivation since a construct lacking this part of the promoter was not activated by AlHV-1/Rta (Figure 3.19(b)). This suggests that the transcription of AlHV-1 ORF57 by AlHV-1/Rta relies on a sequence situated at a considerable distance upstream from the translational start codon. The RE in the HVS ORF57 promoter also lies at a considerable distance from the transcriptional start site, between 751 bp and 764 bp (Whitehouse *et al.,* 1998a), whereas in the HVS ORF6 promoter the RE is only 127-259 bp upstream of the transcriptional start site (Whitehouse *et al.*, 1997b). Thus, the distance of the REs from the transcriptional start site does not appear to be conserved in HVS promoters that are transactivated by Rta, or indeed between ORF57 promoters of different viruses. A 565 bp MHV-68 ORF57 putative promoter sequence was activated by MHV-68/Rta suggesting that although the REs have not yet been identified, they are contained within this 565 bp region (Liu *et al.,* 2000).

Comparisons between the AlHV-1 ORF57 promoter sequence and the various REs discussed above highlighted two sequences within the promoter that contain the HVS and EBV CCN_9GG consensus motif (Figure 5.1(b)). One of these motifs is located

(i)

Virus	Response elements
HVS EBV	CCNNNNNNNNNGG CCNNNNNNNNNGG
	Sequence similarities
AIHV-1 (84038-84050) AIHV-1 (84381-84393)	CCAAGTGTTTTGG CCACCCCTTTAGG

(ii)

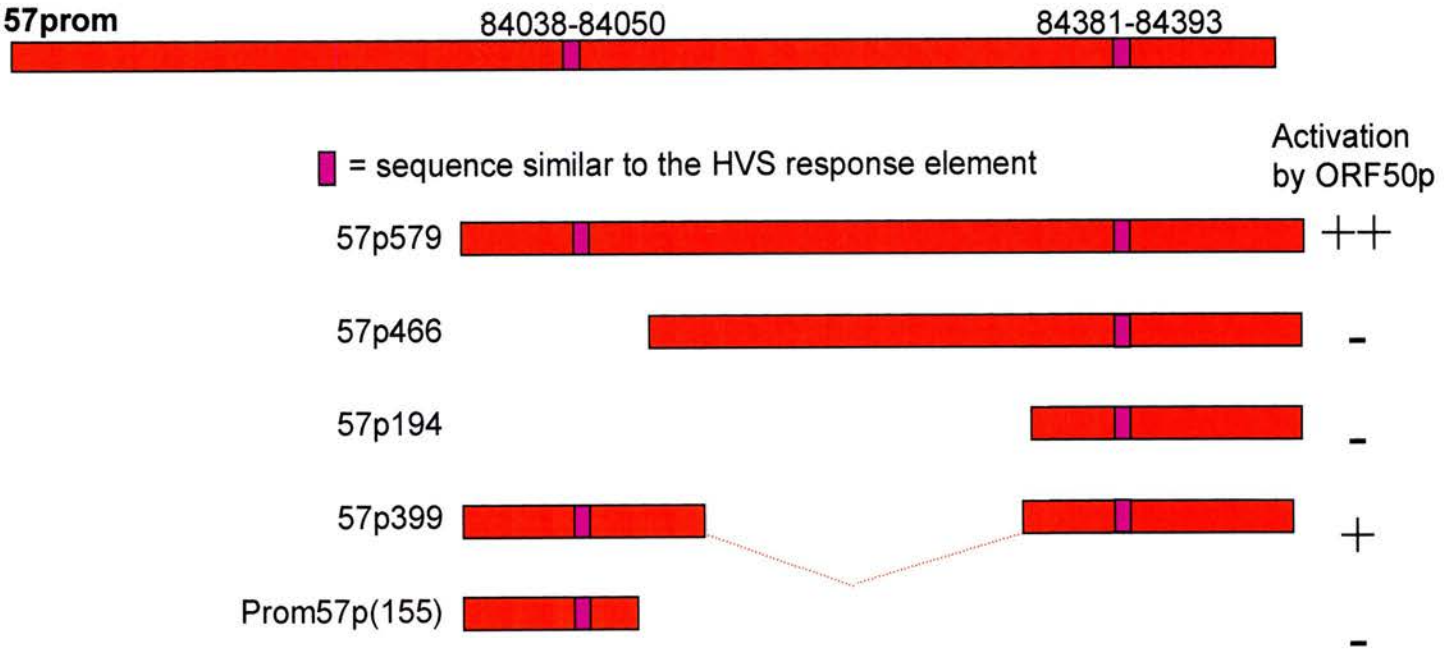

Figure 5.1 (b): Comparison of AlHV-1 ORF57 promoter sequence and Rta response elements of other gammaherpesviruses.

(i) Table showing consensus sequences for the response elements for the HVS Rta and EBV Rta compared with two areas in the AlHV-1 ORF57 promoter sequence.

(ii) Positions of the sequences similar to response elements in AlHV-1 ORF57 promoter and diagrammatic representation of some of the ORF57 truncations along with their activation by AlHV-1 Rta.

in the 113 bp sequence and this study showed that removal of this sequence abolished activation by AlHV-1/Rta (Figure 3.19(b) and (c)). The other motif is located close to the start codon and this study showed that 194 bp of promoter sequence containing this motif was not activated by AlHV-1/Rta (Figure 3.19(b) and (c)). The positions of these sequences are shown in Figure 5.1(b). The similarity of sequences in the AIHV-1 ORF57 promoter to known REs in other γHVs is noteworthy but the functional significance is yet to be fully tested.

To test if the 113 bp sequence was responsive to AlHV-1/Rta, a construct was generated that encompassed this region and extended 42 bp 3' downstream, termed Prom57p(155). However, it did not act as an AlHV-1/Rta-responsive sequence (Figure 3.20). It may be that this region of the promoter is required in addition to downstream sequences in order to respond to AlHV-1/Rta. The position of this sequence relative to the transcriptional start may also be important. The two possibilities were tested by constructing 57p(399), which contained both of the putative REs as determined by similarity to the HVS and EBV REs. 57p(399) included 205 bp at the 5' end of 57p(579) and 194 bp at the 3' end but lacked the middle 180 bp. The activity of 57p(399) was around half that of 57p(579), indicating that the central 180 bp, although not essential, was important for AlHV-1/Rta activation (Figure 3.21(a) and (b)). This may be because of elements in its sequence or because it spatially distances the other two sections containing the putative REs. To test which of these two scenarios is correct, Gavin Borthwick (Honours student) is in the process of making a construct containing a 180 bp fragment from the AlHV-1 glycoprotein B gene, which will be flanked by the 205 bp and 194 bp sequences.

This should help to determine whether it is the precise spacing or the sequence that is important for AlHV-1/Rta-mediated transactivation of the ORF57 promoter.

To examine this further, nucleotides in the conserved CCN_9GG motif could be mutated by site-directed mutagenesis. Alternatively, the sequences forming the putative REs could be multimerised and placed upstream of a reporter gene. In both cases, the ability of AlHV-1/Rta to activate or bind to these sequences could be tested.

5.2.4 EMSAs

EMSAs were used to investigate whether AlHV-1/Rta bound to part of the 113 bp sequence. In some cases no evidence for specific binding of AlHV-1/Rta to this sequence was found, as the extracts containing or lacking AlHV-1/Rta gave similar results. It was concluded that cellular factors were responsible for binding. In other cases the pattern of bands using the extracts containing or lacking AlHV-1/Rta differed, and therefore it could be inferred that AlHV-1/Rta might be involved in some binding (Figures 3.23-3.29).

To clarify whether or not AlHV-1/Rta directly binds DNA, a next step would be to use purified AlHV-1/Rta. Towards the end of this project, a plasmid was constructed which encodes AlHV-1/Rta with the *myc* epitope and His tag at the C-terminus. The protein could be purified via the His tag, and utilised in EMSAs.

5.2.5 AlHV-1/Rta truncations

The amino acid sequence of AlHV-1/Rta was compared with the Rta homologues of other γHVs (Table 5.1 and Figure 5.2). Although there is well documented functional homology of the Rta homologues of γHVs, the amino acid sequence is weakly conserved between them. The sequence alignment in Figure 5.2 shows that there is slightly more similarity in the N-terminal region than the C-terminal region. The N-terminal regions of EBV and KSHV Rtas contain DNA binding domains that bind to specific response elements (Manet *et al.*, 1991; Lukac *et al.*, 2001). The higher sequence identity of these regions between viruses is in accord with the conservation of the response elements (Figure 5.1).

Table 5.1: Percent identity of γHV Rta homologues

The percent identity of amino acid sequences of Rta homologues from the γHVs indicated. Percentages were obtained from Albrecht *et al.* (1992), Russo *et al.* (1996), Ensser *et al.* (1997) and Virgin *et al.* (1997).

Virus	AlHV-1	HVS	MHV-68	KSHV	EBV
AlHV-1	100	17.2	–	19.2	20.2
HVS	17.2	100	26.6	24.9	22.7
MHV-68	–	26.6	100	16.4	13.1
KSHV	19.2	24.9	16.4	100	19.0
EBV	20.2	22.7	13.1	19.0	100

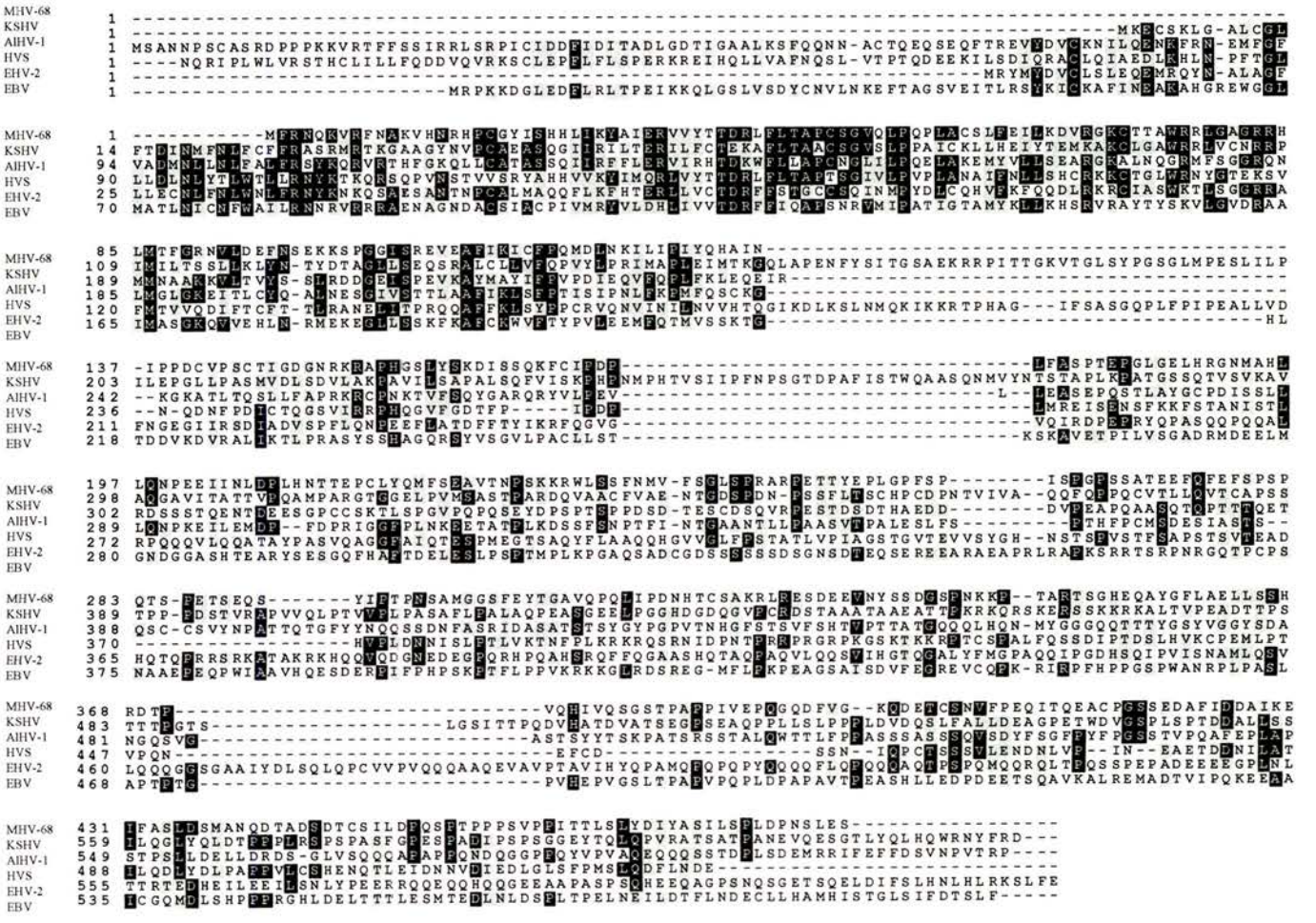
MHV-68
KSHV
AlHV-1
HVS
EHV-2
EBV

To investigate the functional domains of AlHV-1/Rta, two truncated versions were constructed. In co-transfection experiments it was found that only the N-terminal portion of AlHV-1/Rta inhibited full-length AlHV-1/Rta-mediated transactivation of the ORF57 promoter (Figure 3.33(b)). It may be inferred from this that the N-terminal region contains a DNA-binding domain and therefore may prevent binding of full-length AlHV-1/Rta. Alternatively, it might contain the activation domain, in which case it may sequester transcription factors required for activation. The C-terminal regions of EBV Rta, HVS Rta and KSHV Rta have potent activation domains. The EBV Rta contains important hydrophobic residues that are conserved in the HSV-1 VP16 transactivator (Hardwick *et al.,* 1992). It is likely that the overall low sequence identity is due to the adaptation of this regulatory gene to different host and cell environments. Regarding the activation domain, it is more likely that there are a few crucial residues involved, as is the case with EBV Rta (Hardwick *et al.*, 1992), which would require experimental verification.

To confirm whether or not the N-terminal region of AlHV-1/Rta contains a DNA-binding domain, the N-terminal product expressed from pcDNA50A could be purified by using the His tag and tested in EMSAs. The putative activation domain could be investigated by joining it to a known DNA-binding domain and assessing its activity in transient transfection assays.

5.2.6 Expression pattern of AlHV-1 ORF50 within the AlHV-1 virus life cycle

Northern blots and RT-PCR were used to determine when ORF50 was expressed in the virus life cycle. Clear results were not obtained even though the RNA was of

good quality and the RT control reactions worked. This may have been because the mRNA of ORF50 is unstable or present in very small amounts.

5.2.7 Transcription patterns of ORF50 homologues

HVS ORF50 is transcribed from two distinct promoters in two temporal phases of gene expression; ORF50a is an E spliced transcript and ORF50b is a DE unspliced transcript which is produced from a promoter within the second exon of the ORF50a DNA sequence (Whitehouse *et al.,* 1997a). The transcription of MHV-68 ORF50, an IE gene, is initiated from several sites within a 34 bp region, and is transcribed in spliced and unspliced forms (Liu *et al.,* 2000). There are two main transcripts encoding ORF50 in KSHV, one of which also encodes K8 (Seaman *et al.,* 1999). KSHV ORF50 and K8 are IE and E genes, respectively. BRLF1 of EBV is translated from a bicistronic mRNA, which also encodes BZLF1; both are IE genes (Hardwick *et al.*, 1988). In light of these findings, it is possible that AlHV-1 ORF50 may also encode multiple transcripts.

5.2.8 Possible functions of AlHV-1/Rta

Studies carried out by other members of the laboratory indicate that AlHV-1/Rta activates the ORFA9 promoter (K. Knudson, pers. comm.). ORFA9 encodes a potential Bcl-2 homologue (Ensser *et al.,* 1997; Coulter *et al.,* 2001), which in mammalian cells is an anti-apoptotic protein. It has also been shown that the AlHV-1 ORF57 protein, whose promoter is activated by AlHV-1/Rta, can activate the ORF50 promoter (L. Devi, pers. comm.) suggesting a potential feedback regulation system.

Several of the Rta homologues have been shown to play a critical role in the latent to lytic transition, acting as a 'molecular switch' (Goodwin *et al.*, 2001; Sun *et al.,* 1998; Wu *et al.,* 2000; Lukac *et al.,* 1999; Gradoville *et al.,* 2000). Future studies should therefore assess the role of AlHV-1/Rta in reactivation of the virus from latency. This could be examined by introducing an AlHV-1/Rta expression plasmid into cell lines that contained latent virus genomes e.g. LGLs harbouring latent AlHV-1. Reactivation could then be assessed by detecting early and late gene transcripts, which are not transcribed during latency as well as virus replication and release of virus, as described in previous studies (Wu *et al.,* 2000; Sato *et al.,* 1990).

5.3 Recombinant Virus

The attempts to make a recombinant AlHV-1 lacking ORF50 are described in Chapter 4. The premise behind creating a virus lacking ORF50 stemmed from the discovery of an attenuated version of the virus, which resulted from repeated passage in tissue culture (Handley *et al.,* 1995). The precise alterations that occurred in the attenuated virus are not known and so the creation of a virus lacking only ORF50 would allow the role of this gene to be assessed. It would be envisaged that a revertant would be made, thus enabling accurate assignment of the function of ORF50.

5.3.1 Attempts to make AlHV-1 lacking ORF50 by homologous recombination

The first attempt in this project involved replacing part of ORF50 with a marker gene. This method was chosen because it was less likely to disrupt adjacent regulatory sequences. The lack of success of this procedure may have been due to

recombinants not being generated, rejection of the inserted GFP cassette by the virus or the possibility that the recombinant virus was less productive than wild-type virus.

In other studies, complete purification or recombinant virus has been reported to be unsuccessful owing to the disadvantageous nature of the mutation. To overcome this problem, a complementary cell line has been used (DeLuca *et al.*, 1985).

During homologous recombination, insertion of the whole plasmid can sometimes occur due to a single recombination event (Lee *et al.*, 1992). The use of greater lengths of homologous sequences increases the chances of two recombination events occurring either side of the marker gene. In the case of AlHV-1, greater lengths of homologous sequences could be used to enhance homologous recombination.

5.3.2 Attempts to make an AlHV-1 BAC

The insertion of the whole AlHV-1 genome into a BAC was attempted since its construction could have been a useful tool to generate viruses lacking one or more genes. Mutant virus genomes could be constructed irrespective of their viability in a eukaryotic host since the recombinant is purified after manipulation and selection in bacteria. This approach has an advantage over homologous recombination in eukaryotic cells, since the lack of recombinants from eukaryotes could be due to either failure of the recombination event or lack of viability of the mutant virus. However, the initial generation of the BAC still involves homologous recombination in eukaryotic cells.

If the method outlined had been successful, it would be important to restore the TK gene before generating further mutations so that they could be compared with the wild-type phenotype.

5.3.3 Future Strategies

To improve the chances of generating an AlHV-1-BAC the following approaches could be used:

1) Introduce more selection methods to overcome the poorly defined areas of CPE and improve the chances of recovering a recombinant virus.
2) Improve the introduction of virus DNA into cells by enhancing transfection efficiency.
3) Increase the lengths of sequences flanking the marker gene for use in homologous recombination.
4) Develop a screening method to enable large numbers of areas of CPE to be analysed for recombinant virus.
5) Overcome potential problems due to extra DNA in the virus genome, which may affect the packaging of the virus and its growth efficiency, by pursuing strategies that utilise the BAC system but result in mutant viruses lacking BAC sequences.

5.4 Concluding Remarks

This project partially characterised the function of AlHV-1/Rta and initiated investigations into its mechanism of action. Some aspects of the results obtained are similar to those observed with other γHV homologues. Several avenues for future

investigations have been proposed, including how to develop the methodology that will enable construction of an AlHV-1 BAC and eventually an AlHV-1 virus lacking ORF50.

References

Abbas, A.K., A.H. Lichtman and J.S. Pober. 1994. Cellular and Molecular Immunology, 2nd ed. W.B. Saunders Company, London.

Adler, H., M. Messerle, M. Wagner and U.H. Koszinowski. 2000. Cloning and mutagenesis of the murine gammaherpesvirus 68 genome as an infectious bacterial artificial chromosome. J. Virol. **74:**6964-6974.

Albrecht, J.C. 2000. Primary structure of the Herpesvirus ateles genome. J. Virol. **74:**1033-1037.

Albrecht, J.C., J. Nicholas, D. Biller, K.R. Cameron, B. Biesinger, C. Newman, S. Wittmann, M.A. Craxton, H. Coleman and B. Fleckenstein. 1992. Primary structure of the herpesvirus saimiri genome. J. Virol. **66:**5047-5058.

Anand, R., A. Villasante and C. Tyler-Smith. 1989. Construction of yeast artificial chromosome libraries with large inserts using fractionation by pulsed-field gel electrophoresis. Nucleic Acids Res. **17:**3425-3433.

Anonymous. 1976. Malignant catarrhal fever in deer. Surveillance **3:**22.

Baer, R., A.T. Bankier, M.D. Biggin, P.L. Deininger, P.J. Farrell, T.J. Gibson, G. Hatfull, G.S. Hudson, S.C. Satchwell and C. Seguin. 1984. DNA sequence and expression of the B95-8 Epstein-Barr virus genome. Nature **310:**207-211.

Barnard, B.J., R.G. Bengis and S.F. Voges. 1990. Epidemiology of wildebeest-derived malignant catarrhal fever in South Africa: inability to transfer the disease with an African face fly *Musca xanthomelas* (Diptera: Muscidae). Onderstepoort J. Vet. Res. **57:**89-93.

Barnard, B.J. and H.E. Van de Pypekamp. 1988. Wildebeest-derived malignant catarrhal fever: unusual epidemiology in South Africa. Onderstepoort J. Vet. Res. **55:**69-71.

Barnes, A., H. Dyson, N.P. Suril-Chandra, P. Collins and A.A. Nash. 1999. 2' deoxy-5-ethyl-beta 4'-thiouridine inhibits replication of murine gammaherpesvirus and delays onset of viral latency. Antiviral Chemistry and Chemotherapy **10**:321-326.

Baum, C., P. Forster, S. Hegewisch-Becker and K. Harbers. 1994. An optimized electroporation protocol applicable to a wide range of cell lines. Biotechniques **17:**1058-1062.

Baxter, S.I., I. Pow, A. Bridgen and H.W. Reid. 1993. PCR detection of the sheep-associated agent of malignant catarrhal fever. Arch. Virol. **132:**145-159.

Baxter, S.I., A. Wiyono, I. Pow and H.W. Reid. 1997. Identification of ovine herpesvirus-2 infection in sheep. Arch. Virol. **142:**823-831.

Bello, L.J., A.J. Davison, M.A. Glenn, A.Whitehouse, N. Rethmeier, T.F. Schulz and J.B. Clements. 1999. The human herpesvirus-8 ORF 57 gene and its properties. J. Gen. Virol. **80:**3207-3215.

Biggin, M., M. Bodescot, M. Perricaudet and P. Farrell. 1987. Epstein-Barr virus gene expression in P3HR1-superinfected Raji cells. J. Virol. **61:**3120-3132.

Blake, J.E., N.O. Nielsen and W.P. Heuschele. 1990. Lymphoproliferation in captive wild ruminants affected with malignant catarrhal fever: 25 cases (1977-1985). J. Am. Vet. Med. Assoc. **196:**1141-1143.

Boccadoro, M., V. Redoglio, P. Gavarotti and A. Pileri. 1986. Multiple myeloma plasma cell kinetics: rapid and reliable evaluation using 5-bromo-2-deoxyuridine (BrdUrd) DNA incorporation detected by an anti-BrdUrd monoclonal antibody. Tumor **72:**135-137.

Borst, E.M., G. Hahn, U.H. Koszinowski and M. Messerle. 1999. Cloning of the human cytomegalovirus (HCMV) genome as an infectious bacterial artificial chromosome in Escherichia coli: a new approach for construction of HCMV mutants. J. Virol. **73:**8320-8329.

Bridgen, A. 1991. The derivation of a restriction endonuclease map for alcelaphine herpesvirus 1 DNA. Arch. Virol. **117:**183-192.

Bridgen, A., A.J. Herring, N.F. Inglis and H.W. Reid. 1989. Preliminary characterization of the alcelaphine herpesvirus 1 genome. J. Gen. Virol. **70:**1141-1150.

Bridgen, A., R. Munro and H.W. Reid. 1992. The detection of alcelaphine herpesvirus-1 DNA by in situ hybridization of tissues from rabbits affected with malignant catarrhal fever. J. Comp. Pathol. **106:**351-359.

Bridgen, A. and H.W. Reid. 1991. Derivation of a DNA clone corresponding to the viral agent of sheep-associated malignant catarrhal fever. Res. Vet. Sci. **50:**38-44.

Brune, W., M. Messerle and U.H. Koszinowski. 2000. Forward with BACs: new tools for herpesvirus genomics. Trends Genet. **16:**254-259.

Burke, D.T., G.F. Carle and M.V. Olson. 1987. Cloning of large segments of exogenous DNA into yeast by means of artificial chromosome vectors. Science **236:**806-812.

Burrells, C. and H.W. Reid. 1991. Phenotypic analysis of lymphoblastoid cell lines derived from cattle and deer affected with "sheep-associated" malignant catarrhal fever. Vet. Immunol. Immunopathol. **29:**151-161.

Buxton, D. and H.W. Reid. 1980. Transmission of malignant catarrhal fever to rabbits. Vet. Rec. **106:**243-245.

Buxton, D., H.W. Reid, J. Finlayson and I. Pow. 1984. Pathogenesis of 'sheep-associated' malignant catarrhal fever in rabbits. Res. Vet. Sci. **36:**205-211.

Castro, A.E., G.G. Daley, M.A. Zimmer, D.L. Whitenack and J. Jensen. 1982. Malignant catarrhal fever in an Indian gaur and greater kudu: experimental transmission, isolation, and identification of a herpesvirus. Am. J. Vet. Res. **43:**5-11.

Castro, A.E., W.P. Heuschele, M.L. Schramke and J.F. Dotson. 1985. Ultrastructure of cellular changes in the replication of the alcelaphine herpesvirus-1 of malignant catarrhal fever. Am. J. Vet. Res. **46:**1231-1237.

Cavener, D.R. and S.C. Ray. 1991. Eukaryotic start and stop translation sites. Nucleic Acids Res. **19:**3185-3192.

Chang, Y., F. Cesarman, M.S. Pessin, F. Lee, J. Culpepper, D.M. Knowles and M.P.S. Moore. 1994. Identification of herpesvirus-like DNA sequences in AIDs-associated Kaposi's sarcoma. Science **266:**1865-1869.

Chang, Y.N., D.L. Dong, G.S. Hayward and S.D. Hayward. 1990. The Epstein-Barr virus Zta transactivator: a member of the bZIP family with unique DNA-binding specificity and a dimerization domain that lacks the characteristic heptad leucine zipper motif. J. Virol. **64:**3358-3369.

Chen, J., K. Ueda, S. Sakakibara, T. Okuno and K. Yamanishi. 2000. Transcriptional regulation of the Kaposi's sarcoma-associated herpesvirus viral interferon regulatory factor gene. J. Virol. **74:**8623-8634.

Chevallier-Greco, A., H. Gruffat, E. Manet, A. Calender and A. Sergeant. 1989. The Epstein-Barr virus (EBV) DR enhancer contains two functionally different domains: domain A is constitutive and cell specific, domain B is transactivated by the EBV early protein R. J. Virol. **63:**615-623.

Chevallier-Greco, A., E. Manet, P. Chavrier, C. Mosnier, J. Daillie and A. Sergeant. 1986. Both Epstein-Barr virus (EBV)-encoded trans-acting factors, EB1 and EB2, are required to activate transcription from an EBV early promoter. EMBO J. **5:**3243-3249.

Cohen, J.I., F. Wang, J. Mannick and E. Kieff. 1989. Epstein-Barr virus nuclear protein 2 is a key determinant of lymphocyte transformation. Proc. Natl. Acad. Sci. USA. **86:**9558-9562.

Cook, C.G. and G.A. Splitter. 1988. Lytic function of bovine lymphokine-activated killer cells from a normal and a malignant catarrhal fever virus-infected animal. Vet. Immunol. Immunopathol. **19:**105-118.

Cooper, M., D.J. Goodwin, K.T. Hall, A.J. Stevenson, D.M. Meredith, A.F. Markham and A. Whitehouse. 1999. The gene product encoded by ORF 57 of herpesvirus saimiri regulates the redistribution of the splicing factor SC-35. J. Gen. Virol. **80:**1311-1316.

Coulter, L.J., H. Wright and H.W. Reid. 2001. Molecular genomic characterization of the viruses of malignant catarrhal fever. J. Comp. Path. **124:**2-19.

Countryman, J. and G. Miller. 1985. Activation of expression of latent Epstein-Barr herpesvirus after gene transfer with a small cloned subfragment of heterogeneous viral DNA. Proc. Natl. Acad. Sci. USA. **82:**4085-4089.

Cox, M.A., J. Leahy and J.M. Hardwick. 1990. An enhancer within the divergent promoter of Epstein-Barr virus responds synergistically to the R and Z transactivators. J. Virol. **64:**313-321.

Cunningham, C. and A.J. Davison. 1993. A cosmid-based system for constructing mutants of herpes simplex virus type 1. Virology **197:**116-124.

Damania, B., J.K. Choi and J.U. Jung. 2000. Signaling activities of gammaherpesvirus membrane proteins. J. Virol. **74:**1593-1601.

Daniels, P., W. Sudarisman and P. Ronohgardijo. 1988. Malignant Catarrhal Fever in Asian Livestock, Australian Centre for International Research, Canberra, pp. 20-31. ACIAR publications.

Daubney, R. and J.R. Hudson. 1936. Transmission experiments with bovine malignant catarrh. J. Comp. Path. Therap. **XLIX:**63-89.

Davison, A.J. 1991. Varicella-zoster virus. The Fourteenth Fleming lecture. J. Gen. Virol. **72**:475-486.

Deiss, L.P., J. Chou and N. Frenkel. 1986. Functional domains within the *a* sequence involved in the cleavage-packaging of herpes simplex virus DNA. J. Virol. **59:**605-618.

Delecluse, H.J., T. Hilsendegen, D. Pich, R. Zeidler and W. Hammerschmidt. 1998. Propagation and recovery of intact, infectious Epstein-Barr virus from prokaryotic to human cells. Proc. Natl. Acad. Sci. USA. **95:**8245-8250.

DeLuca, N.A., A.M. McCarthy and P.A. Schaffer. 1985. Isolation and characterisation of the deletion mutants of HSV-1 in the gene encoding IE regulatory protein ICP4. J. Virol. **56:**558-570.

Deng, H., A. Young and R. Sun. 2000. Auto-activation of the rta gene of human herpesvirus-8/Kaposi's sarcoma-associated herpesvirus. J. Gen. Virol. **81:**3043-3048.

Denholm, L.J. and H.A. Westbury. 1982. Malignant catarrhal fever in farmed rusa deer (*Cervus timorensis*) 1. Clinico-Pathological Observations. Aust. Vet. J. **58:**81-87.

Dinter, Z. and B. Morein. 1990. Virus Infections of Vertebrates - Virus Infections of Ruminants. Elsevier Science Publishers B.V., Oxford.

Edington, N. and J. Patel. 1981. The location of primary replication of the virus of bovine malignant catarrhal fever in rabbits. Vet. Microbiol. **6:**107-112.

Edington, N. and W. Plowright. 1980. The protection of rabbits against the herpesvirus of malignant catarrhal fever by inactivated vaccines. Res. Vet. Sci. **28:**384-386.

Efstathiou, S., Y.M. Ho, S. Hall, C.J. Styles, S.D. Scott and U.A. Gompels. 1990. Murine herpesvirus 68 is genetically related to the gammaherpesviruses Epstein-Barr virus and herpesvirus saimiri. J. Gen. Virol. **71:**1365-1372.

Ehsani, M.E., T.W. Abraha, C. Netherland-Snell, N. Mueller, M.M. Taylor and B. Holwerda. 2000. Generation of mutant murine cytomegalovirus strains from overlapping cosmid and plasmid clones. J. Virol. **74:**8972-8979.

Ensser, A., R. Pflanz and B. Fleckenstein. 1997. Primary structure of the alcelaphine herpesvirus 1 genome. J. Virol. **71:**6517-6525.

Epstein, M.A., B.G. Achong, and Y.M. Barr. 1964. Virus particles in cultured lymphoblasts from Burkitt's lymphoma. Lancet. **1:**702-703.

Epstein, M. A. and D. H. Crawford. 1998. Gammaherpesvirus: Epstein-Barr virus, pp. 351-366. *In* L. Collier and B.W.J. Mahy (eds), Topley and Wilson's Microbiology & Microbial Infection, 9th ed., Arnold, London.

Farrell, P.J. 1989. Epstein-Barr Virus Genome, pp. 103-132. *In* G. Klein (ed.), Advances in Viral Oncology, Vol. 8. Raven Press Ltd., New York.

Fenner, F.J., E.P.J. Gibbs, F.A. Murphy, R. Rott, M.J. Studdert and D.O. White. 1993. Herpesviridae, Chapter **19:**366-367, Veterinary Virology, Academic Press, London.

Fields, B.N., D.M. Knipe and P.M. Howley. 1996. Fundamental Virology, 3rd edn Lippincott-Raven, Philadelphia.

Flemington, E.K., A.E. Goldfeld and S.H. Speck. 1991. Efficient transcription of the Epstein-Barr virus immediate-early BZLF1 and BRLF1 genes requires protein synthesis. J. Virol. **65:**7073-7077.

Florzinek, M.C. 1990. Virus Infections of Vertebrates. Elsevier Science Publishers B.V., Oxford.

Frohman, M.A., M.K. Dush and G.R. Martin. 1988. Rapid production of full-length cDNAs from rare transcripts: amplification using a single gene-specific oligonucleotide primer. Proc. Natl. Acad. Sci. USA. **85:**8998-9002.

Gilmour, B.P., G.R. Fanger, C. Newton, S.M. Evans and P.D. Gardner. 1991. Multiple binding sites for myogenic regulatory factors are required for expression of the acetylcholine receptor gamma-subunit gene. J. Biol. Chem. **266**:19871-19874.

Goetze, R. and J. Liesse. 1930. Untersuchungen uber das bosartige Katarrhalfieber des Rindes II Schafe als Ubertrager. Deutsch Tierarztlieche Wochenschrift. **37:**433-437.

Gong, M. and E. Kieff. 1990. Intracellular trafficking of two major Epstein-Barr virus glycoproteins, gp350/220 and gp110. J. Virol. **64:**1507-1516.

Goodwin, D.J., K.T. Hall, M.S. Giles, M.A. Calderwood, A.F. Markham and A. Whitehouse. 2000. The carboxy terminus of the herpesvirus saimiri ORF 57 gene contains domains that are required for transactivation and transrepression. J. Gen. Virol. **81:**2253-2265.

Goodwin, D.J., M.S. Walters, P.G. Smith, M. Thurau, H. Fickenscher and A. Whitehouse. 2001. Herpesvirus saimiri open reading frame 50 (Rta) protein reactivates the lytic replication cycle in a persistently infected A549 cell line. J. Virol. **75:**4008-4013.

Gradoville, L., J. Gerlach, E. Grogan, D. Shedd, S. Nikiforow, C. Metroka and G. Miller. 2000. Kaposi's sarcoma-associated herpesvirus open reading frame 50/Rta protein activates the entire viral lytic cycle in the HH-B2 primary effusion lymphoma cell line. J. Virol. **74:**6207-6212.

Gruffat, H., N. Duran, M. Buisson, F. Wild, R. Buckland and A. Sergeant. 1992. Characterization of an R-binding site mediating the R-induced activation of the Epstein-Barr virus BMLF1 promoter. J. Virol. **66:**46-52.

Gruffat, H., S. Portes-Sentis, A. Sergeant and E. Manet. 1999. Kaposi's sarcoma-associated herpesvirus (human herpesvirus-8) encodes a homologue of the Epstein-Barr virus bZip protein EB1. J. Gen. Virol. **80:**557-561.

Gruffat, H. and A. Sergeant. 1994. Characterization of the DNA-binding site repertoire for the Epstein-Barr virus transcription factor R. Nucleic Acids Res. **22:**1172-1178.

Gulland, F.M., H.W. Reid, D. Buxton, J.C. Lewis, R.A. Kock and J.K. Kirkwood. 1989. Malignant catarrhal fever in a roan antelope (*Hippotragus equinus*) at Regent's Park. Vet. Rec. **124:**42-43.

Gutsch, D.E., K.B. Marcu and S.C. Kenney. 1994. The Epstein-Barr virus BRLF1 gene product transactivates the murine and human c-myc promoters. Cell. Mol. Biol. **40:**747-760.

Hall, K.T., A.J. Stevenson, D.J. Goodwin, P.C. Gibson, A.F. Markham and A. Whitehouse. 1999. The activation domain of herpesvirus saimiri R protein interacts with the TATA-binding protein. J. Virol. **73:**9756-9763.

Hamilton, A.F. 1990. Account of three outbreaks of malignant catarrhal fever in cattle in the Republic of Ireland [published erratum appears in Vet. Rec. 1990 Oct 27;127(17):420]. Vet. Rec. **127:**231-232.

Handley, J.A., D.R. Sargan, A.J. Herring and H.W. Reid. 1995. Identification of a region of the alcelaphine herpesvirus-1 genome associated with virulence for rabbits. Vet. Microbiol. **47:**167-181.

Hardwick, J.M., P.M. Lieberman and S.D. Hayward. 1988. A new Epstein-Barr virus transactivator, R, induces expression of a cytoplasmic early antigen. J. Virol. **62:**2274-2284.

Hardwick, J.M., L. Tse, N. Applegren, J. Nicholas and M.A. Veliuona. 1992. The Epstein-Barr virus R transactivator (Rta) contains a complex, potent activation domain with properties different from those of VP16. J. Virol. **66:**5500-5508.

Hill, F.I., D.G. Arthur and J. Thompson. 1993. Malignant catarrhal fever in a swamp buffalo (*Bubalus bubalis*). NZ Vet. J. **41**:35-38.

Hoffman, D., S. Sobironingsih, B.C. Clarke, P.J. Young and I. Sendow. 1984. Transmission and virological studies of a malignant catarrhal fever syndrome in the Indonesian swamp buffalo (*Bubalus bubalis*) Aust. Vet. J. **61:**113-116.

Hoffman, D. and M.P. Young. 1989. Malignant catarrhal fever. Aust. Vet J. **66:**405-406.

Holley-Guthrie, E.A., E.B. Quinlivan, E.C. Mar and S. Kenney. 1990. The Epstein-Barr virus (EBV) BMRF1 promoter for early antigen (EA-D) is regulated by the EBV transactivators, BRLF1 and BZLF1, in a cell-specific manner. J. Virol. **64:**3753-3759.

Horsburgh, B.C., M.M. Hubinette, D. Qiang, M.L.E. MacDonald and F. Tufaro. 1999. Allele replacement an application that permits rapid manipulation of herpes simplex virus type 1 genomes. Gene Therapy **6:**922-930.

Howard, J. L. 1993. Sections 7, 10 and 15., Current Veterinary Therapy 3: Food Animal Practice. W.B. Saunders Company, London.

Huck, R. A., A. Shand, P.J. Allsop and A.B. Paterson. 1961. Malignant catarrh of deer. Vet. Rec. **73:**457-465.

Jacoby, R.O., D. Buxton and H.W. Reid. 1988a. The pathology of wildebeest-associated malignant catarrhal fever in hamsters, rats and guinea-pigs. J. Comp. Pathol. **98:**99-109.

Jacoby, R.O., H.W. Reid, D. Buxton and I. Pow. 1988b. Transmission of wildebeest-associated and sheep-associated malignant catarrhal fever to hamsters, rats and guinea-pigs. J. Comp. Pathol. **98:**91-98.

Javier, R.T., J.G. Stevens, V.B. Dissette and E.K. Wagner. 1988. A herpes simplex virus transcript abundant in latently infected neurons is dispensable for establishment of the latent state. Virology **166:**254-257.

Jones, T.C., R.D. Hunt and N.W. King. 1997. Chapters 10, 21 and 27, Veterinary Pathology, 6th edn, Williams and Wilkins, London.

Kasamatsu, H. and A. Nakanishi. 1998. How do animal DNA viruses get to the nucleus? Ann. Rev. Microbiol. **52:**627-686.

Kenney, S., E. Holley-Guthrie, E.C. Mar and M. Smith. 1989b. The Epstein-Barr virus BMLF1 promoter contains an enhancer element that is responsive to the BZLF1 and BRLF1 transactivators. J. Virol. **63:**3878-3883.

Kenney, S., J. Kamine, E. Holley-Guthrie, J.C. Lin, E.C. Mar and J. Pagano. 1989a. The Epstein-Barr virus (EBV) BZLF1 immediate-early gene product differentially affects latent versus productive EBV promoters. J. Virol. **63:**1729-1736.

Ketner, G., F. Spencer, S. Tugendreich, C. Connelly and P. Hieter. 1994. Efficient manipulation of the human adenovirus genome as an infectious yeast artificial chromosome clone. Proc. Natl. Acad. Sci. USA. **91:**6186-6190.

Kirshner, J.R., D.M. Lukac, J. Chang and D. Ganem. 2000. Kaposi's sarcoma-associated herpesvirus open reading frame 57 encodes a post transcriptional regulator with multiple distinct activities. J. Virol. **74:**3586-3597.

Kong, Y., T. Yang and A.I. Geller. 1999. An efficient in vivo recombination cloning procedure for modifying and combining HSV-1 cosmids. J. Virol. Methods. **80:**129-136.

Krajcsi, P. and W.S. Wold. 1998. Viral proteins that regulate cellular signalling. J. Gen. Virol. **79:**1323-1335.

Laquerre, S., R. Argnani, D.B. Anderson, S. Zucchini, R. Manservigi and J. C. Glorioso. 1998. Heparan sulfate proteoglycan binding by herpes simplex virus type 1 glycoproteins B and C, which differ in their contributions to virus attachment, penetration, and cell-to-cell spread. J. Virol. **72:**6119-6130.

Lee, M.A., O.J. Kim and J.L. Yates. 1992. Targeted gene disruption in Epstein-Barr virus. Virology **189:**253-265.

Lehman, I.R. and P.E. Boehmer. 1999. Replication of herpes simplex virus DNA. J Biol. Chem. **274:**28059-28062.

Li, H., N. Dyer, J. Keller and T.B. Crawford. 2000a. Newly recognized herpesvirus causing malignant catarrhal fever in white-tailed deer (*Odocoileus virginianus*). J. Clin. Microbiol. **38:**1313-1318.

Li, H., J. Keller, D.P. Knowles and T.B. Crawford. 2001. Recognition of another member of the malignant catarrhal fever virus group: an endemic gammaherpesvirus in domestic goats. J. Gen. Virol. **82:**227-232.

Li, H., G. Snowder and T.B. Crawford. 1999. Production of malignant catarrhal fever virus-free sheep. Vet. Microbiol. **65:**167-172.

Li, H., G. Snowder, D. O'Toole and T.B. Crawford. 1998. Transmission of ovine herpesvirus 2 in lambs. J. Clin. Microbiol. **36:**223-226.

Li, H., G. Snowder, D. O'Toole and T.B. Crawford. 2000b. Transmission of ovine herpesvirus 2 among adult sheep. Vet. Microbiol. **71:**27-35.

Lieberman, P.M. and A.J. Berk. 1990. In vitro transcriptional activation, dimerization, and DNA-binding specificity of the Epstein-Barr virus Zta protein. J. Virol. **64:**2560-2568.

Lieberman, P.M. and A.J. Berk. 1991. The Zta trans-activator protein stabilizes TFIID association with promoter DNA by direct protein-protein interaction. Genes Dev. **5:**2441-2454.

Liggitt, H.D. and J.C. DeMartini. 1980a. The pathomorphology of malignant catarrhal fever. I. Generalized lymphoid vasculitis. Vet. Pathol. **17:**58-72.

Liggitt, H.D. and J.C. DeMartini. 1980b. The pathomorphology of malignant catarrhal fever. II. Multisystemic epithelial lesions. Vet. Pathol. **17:**73-83.

Liggitt, H.D., J.C. DeMartini, A.E. McChesney, R.E. Pierson and J. Storz. 1978. Experimental transmission of malignant catarrhal fever in cattle: gross and histopathologic changes. Am. J. Vet. Res. **39:**1249-1257.

Liggitt, H.D., J.C. DeMartini, J. Storz and G.R. Coulter. 1980. Synovitis and bovine syncytial virus isolation in experimentally induced malignant catarrhal fever. J. Comp. Pathol. **90:**519-533.

Lin, S.F., D.R. Robinson, G. Miller and H.J. Kung. 1999. Kaposi's sarcoma-associated herpesvirus encodes a bZIP protein with homology to BZLF1 of Epstein-Barr virus. J. Virol. **73:**1909-1917.

Liu, S., I.V. Pavlova, H.W. Virgin and S.H. Speck. 2000. Characterization of gammaherpesvirus 68 gene 50 transcription. J. Virol. **74:**2029-2037.

Liu, C., N.D. Sista and J.S. Pagano. 1996. Activation of the Epstein-Barr virus DNA polymerase promoter by the BRLF1 immediate-early protein is mediated through USF and E2F. J. Virol. **70:**2545-2555.

Løken, T., M. Aleksandersen, H. Reid and I. Pow. 1998. Malignant catarrhal fever caused by ovine herpesvirus-2 in pigs in Norway. Vet. Rec. **143:**464-467.

Lukac, D.M., J. Chang and D. Gamen. 2000. The KSHV lytic switch protein ORF50 activates viral promoters using at least two mechanisms: Identification of unique direct DNA binding sites and response elements. 25th International Herpesvirus Workshop, Portland, Oregon. (cited with permission).

Lukac, D.M., J.R. Kirshner and D. Ganem. 1999. Transcriptional activation by the product of open reading frame 50 of Kaposi's sarcoma-associated herpesvirus is required for lytic viral reactivation in B cells. J. Virol. **73:**9348-9361.

Lukac, D.M., L. Garibyan, J.R. Kirshner, D. Palmeri and D. Ganem. 2001 (In Press). DNA binding by Kaposi's sarcoma-associated herpesvirus lytic switch protein is necessary for transcriptional activation of two viral delayed early promoters. J. Virol. **75**.

Lukac, D.M., R. Renne, J.R. Kirshner and D. Ganem. 1998. Reactivation of Kaposi's sarcoma-associated herpesvirus infection from latency by expression of the ORF 50 transactivator, a homolog of the EBV R protein. Virology **252:**304-312.

Manet, E., A. Rigolet, H. Gruffat, J. F. Giot, and A. Sergeant. 1991. Domains of the Epstein-Barr virus (EBV) transcription factor R required for dimerization, DNA binding and activation. Nucleic Acids Res. **19:**2661-2667.

Maruyama, I.N., T.L. Rakow and H.I. Maruyama. 1995. cRACE: a simple method for identification of the 5' end of mRNAs. Nucleic Acids Res. **23:**3796-3797.

Mellerick, D.M. and N.W. Fraser. 1987. Physical state of the latent herpes simplex virus genome in a mouse model system: evidence suggesting an episomal state. Virology **158:**265-275.

Messerle, M., I. Crnkovic, W. Hammerschmidt, H. Ziegler, and U.H. Koszinowski. 1997. Cloning and mutagenesis of a herpesvirus genome as an infectious bacterial artificial chromosome. Proc. Natl. Acad. Sci. USA. **94:**14759-14763.

Mettam, R.W.M. 1923. Snotsiekte in Cattle. Dir. Vet. Educ. Res. Union, S. Africa, Report Nos. 9 and 10, pp. 395-432.

Metzler, A.E. 1991. The malignant catarrhal fever complex. Comp. Immunol. Microbiol. Inf. Dis. **14:**107-124.

Millhouse, S. and B. Wigdahl. 2000. Molecular circuitry regulating herpes simplex virus type 1 latency in neurons. J. Neurovirol. **6:**6-24.

Milne, E.M. and H.W. Reid. 1990. Recovery of a cow from malignant catarrhal fever. Vet. Rec. **126:**640-641.

Minson, A.C., A. Davison, R. Eberle, R.C. Desrosiers, B. Fleckenstein, D.J. McGeoch, B. Roizman and D.M.J. Studdert. 2000. Family *Herpesviridae*, pp. 203-225. *In* M.H.V. van Regenmortel, C.M. Fauquet, D.H.L. Bishop, E. B. Carstens, M.K. Estes, S.M. Lemon, J. Maniloff, M.A. Mayo, D.J. McGeoch, C.R. Pringle and W.R.B. (eds), Virus Taxonomy. Seventh Report of the International Committee on Taxonomy of Viruses. Academic Press, San Diego.

Mirangi, P.K. 1991a. Attempts to immunize cattle against virulent African malignant catarrhal fever virus (alcelaphine herpesvirus-1) with a herpesvirus isolated from American cattle. Vet. Microbiol. **28:**129-139.

Mirangi, P.K. 1991b. Failure of sheep to respond to repeated inoculations with an alcelaphine herpesvirus-1-like virus, isolated from a case of malignant catarrhal fever in American cattle. Vet. Rec. **129:**360-361.

Monaco, A.P. and Z. Larin. 1994. YACs, BACs, PACs and MACs: artificial chromosomes as research tools. Trends in Biotechnology **12:**280-286.

Mocarski, E.S., L.E. Post and B. Roizman. 1980. Molecular engineering of the herpes simplex virus genome: insertion of a second L-S junction into the genome causes additional genome inversions. Cell **22:** 243-255.

Murphy, F.A., E.P.J. Gibbs, M.C. Horzinek and M.J. Studdert (eds). 1999. Veterinary Virology. Academic Press, London.

Mushi, E.Z., L. Karstad and D.M. Jessett. 1980. Isolation of bovine malignant catarrhal fever virus from ocular and nasal secretions of wildebeest calves. Res. Vet. Sci. **29:**168-171.

Mushi, E.Z. and F.R. Rurangirwa. 1981a. Epidemiology of bovine malignant catarrhal fevers, a review. Vet. Res. Commun. **5:**127-142.

Mushi, E.Z. and F.R. Rurangirwa. 1981b. Malignant catarrhal fever virus infectivity in rabbit macrophages and monocytes. Vet. Res. Commun. **5:**51-56.

Mushi, E.Z., F.R. Rurangirwa and L. Karstad. 1980. Effect of Levamisole on the course of malignant catarrhal fever virus infection in rabbits. Trop. Anim. Health Prod. **13:**112.

Nakajima, Y., E. Momotani, Y. Ishikawa, T. Murakami, N. Shimura and M. Onuma. 1992. Phenotyping of lymphocyte subsets in the vascular and epithelial lesions of a cow with malignant catarrhal fever. Vet. Immunol. Immunopathol. **33:**279-284.

Nash, A.A., B.M. Dutia, J.P. Stewart and A.J. Davison. 2001. Natural history of murine γ-herpesvirus infection. Phil. Trans. Roy. Soc. **356:**569-579.

Neipel, F., J.C. Albrecht and B. Fleckenstein. 1997. Cell-homologous genes in the Kaposi's sarcoma-associated rhadinovirus human herpesvirus 8: determinants of its pathogenicity? J. Virol. **71:**4187-4192.

Nicholas, J. 2000. Evolutionary aspects of oncogenic herpesviruses. Molecular Pathology. **53:**222-237.

Nicholas, J., L.S. Coles, C. Newman and R.W. Honess. 1991. Regulation of the herpesvirus saimiri (HVS) delayed-early 110-kilodalton promoter by HVS immediate-early gene products and a homolog of the Epstein-Barr virus R trans activator. J. Virol. **65:**2457-2466.

Orr, M.B. 1986. Diagnoses of malignant catarrhal fever in deer at Invermay. Surveillance. **1394:**22-23.

O'Toole, D., H. Li, D. Miller, W.R. Williams and T.B. Crawford. 1997. Chronic and recovered cases of sheep-associated malignant catarrhal fever in cattle. Vet. Rec. **140:**519-524.

Patel, J. R. and N. Edington. 1981. The detection and behaviour of the herpesvirus of malignant catarrhal fever in bovine lymphocytes. Arch. Virol. **68:**321-326.

Pierson, R.E., F.M. Hamdy, A.H. Dardiri, D.H. Ferris and G.M. Schloer. 1979. Comparison of African and American forms of malignant catarrhal fever: transmission and clinical signs. Am. J. Vet. Res. **40:**1091-1095.

Pierson, R.E., H.D. Liggitt, J.C. DeMartini, A. McChesney and J. Storz. 1978. Clinical and clinicopathologic observations in induced malignant catarrhal fever of cattle. J. Am. Vet. Med. Assoc. **173:**833-837.

Pierson, R.E., D. Thake, A.E. McChesney and J. Storz. 1973. An epizootic of malignant catarrhal fever in feedlot cattle. J. Am. Vet. Med. Assoc. **163:**349-350.

Plowright, W. 1964. (Thesis) Studies on bovine malignant catarrhal fever of cattle, University of Pretoria, Pretoria. 336 pp.

Plowright, W. 1968. Malignant catarrhal fever. J. Am. Vet. Med. Assoc. **152:**795-804.

Plowright, W., R.D. Ferris and G.R. Scott. 1960. Blue wildebeest and the aetiological agent of bovine malignant catarrhal fever. Nature **188:**1167-1169.

Plowright, W., K.A. Herniman, D.M. Jessett, M. Kalunda and C.S. Rampton. 1975. Immunisation of cattle against the herpesvirus of malignant catarrhal fever: failure of inactivated culture vaccines with adjuvant. Res. Vet. Sci. **19:**159-166.

Plowright, W., R.F. Macadam and J.A. Armstrong. 1963. Growth and characterization of the virus of bovine malignant catarrhal fever in East Africa. J. Gen. Microbiol. **39:**253-266.

Pomp, D. and J.F. Medrano. 1991. Organic solvents as facilitators of polymerase chain reaction. Biotechniques **10:**58-59.

Post, L.E. and B. Roizman. 1981. A generalized technique for deletion of specific genes in large genomes: αgene 22 of herpes simplex virus is not essential for growth. Cell **25:**227-232.

Preston, C. M. 2000. Repression of viral transcription during herpes simplex virus latency. J. Gen. Virol. **81:**1-19.

Quinlivan, E.B., E. Holley-Guthrie, E.C. Mar, M.S. Smith and S. Kenney. 1990. The Epstein-Barr virus BRLF1 immediate-early gene product transactivates the human immunodeficiency virus type 1 long terminal repeat by a mechanism which is enhancer independent. J. Virol. **64:**1817-1820.

Ragoczy, T., L. Heston and G. Miller. 1998. The Epstein-Barr virus Rta protein activates lytic cycle genes and can disrupt latency in B lymphocytes. J. Virol. **72:**7978-7984.

Ragoczy, T. and G. Miller. 1999. Role of the Epstein-Barr virus Rta protein in activation of distinct classes of viral lytic cycle genes. J. Virol. **73:**9858-9866.

Reid, H. W. 2000. Malignant catarrhal fever. Inf. Dis. Rev. **2:**20-22.

Reid, H.W., D. Buxton, E. Berrie, I. Pow and J. Finlayson. 1984. Malignant Catarrhal Fever. Vet. Rec. **114:**581-583.

Reid, H.W., D. Buxton, W. Corrigall, A.R. Hunter, D.A. McMartin and R. Rushton. 1979. An outbreak of malignant catarrhal fever in red deer (*Cervus Elephus*). Vet. Rec. **104:**120-123.

Reid, H.W., D. Buxton, W.A. McKelvey, J. A. Milne and W.T. Appleyard. 1987. Malignant catarrhal fever in Père David's deer. Vet. Rec. **121:**276-277.

Reid, H.W., D. Buxton, I. Pow and J. Finlayson. 1986. Malignant catarrhal fever: experimental transmission of the 'sheep-associated' form of the disease from cattle and deer to cattle, deer, rabbits and hamsters. Res. Vet. Sci. **41:**76-81.

Reid, H.W., D. Buxton, I. Pow and J. Finlayson. 1989. Isolation and characterisation of lymphoblastoid cells from cattle and deer affected with 'sheep-associated' malignant catarrhal fever. Res. Vet. Sci. **47:**90-96.

Rodriguez, A., M. Armstrong, D. Dwyer and E. Flemington. 1999. Genetic dissection of cell growth arrest functions mediated by the Epstein-Barr virus lytic gene product, Zta. J. Virol. **73:**9029-9038.

Roizman, B. and J. Baines. 1991. The diversity and unity of Herpesviridae. Comp. Immunol. Microbiol. Infect. Dis. **14:**63-79.

Roizman, B., R.C. Desrosiers, B. Fleckenstein, C. Lopez, A.C. Minson and M.J. Studdert. 1992. The family Herpesviridae: an update. The Herpesvirus Study Group of the International Committee on Taxonomy of Viruses. Arch. Virol. **123:**425-449.

Rossiter, P.B. 1981. Antibodies to malignant catarrhal fever virus in sheep sera. J. Comp. Pathol. **91:**303-311.

Rossiter, P.B. 1982. Attempts to protect rabbits against challenge with virulent, cell-associated, malignant catarrhal fever virus. Vet. Microbiol. **7:**419-425.

Rossiter, P.B. 1983. Antibodies to malignant catarrhal fever virus in cattle with non-wildebeest-associated malignant catarrhal fever. J. Comp. Pathol. **93:**93-97.

Rossiter, P.B., D.M. Jessett and L. Karstad. 1983. Role of wildebeest fetal membranes and fluids in the transmission of malignant catarrhal fever virus. Vet. Rec. **113:**150-152.

Rurangirwa, F.R. and E.Z. Mushi. 1982. Target cells for malignant catarrhal fever virus in rabbits. Vet. Res. Commun. **5:**285-288.

Rurangirwa, F.R. and E.A. Mushi. 1984. Course of malignant catarrhal fever in immunosuppressed and immunostimulated rabbits. Vet. Res. Commun. **8:**47-54.

Russell, P.H. 1980. Malignant catarrhal fever virus in rabbits - reproduction of clinical disease by cell-free virus and partial protection against such disease by vaccination with inactivated virus. Vet. Microbiol. **5:**161-163.

Russo, J.J., R.A. Bohenzky, M.C. Chien, J. Chen, M. Yan, D. Maddalena, J.P. Parry, D. Peruzzi, I.S. Edelman, Y. Chang and P.S. Moore. 1996. Nucleotide sequence of the Kaposi sarcoma-associated herpesvirus (HHV8). Proc. Natl. Acad. Sci. USA. **93:**14862-14867.

Sambrook, J., E.F. Fritsch and T. Maniatis. 1989. Molecular Cloning : a laboratory manual, 2nd edn, Cold Spring Harbour Laboratory Press, Cold Spring Harbour, New York.

Sato, H., T. Takimoto, S. Tanaka, J. Tanaka and N. Raab-Traub. 1990. Concatameric replication of Epstein-Barr virus: structure of the termini in virus-producer and newly transformed cell lines. J. Virol. **64:**5295-5300.

Schaffer, P., V. Vonka, R. Lewis and M. Benyesh-Melnick. 1970. Temperature-sensitive mutants of herpes simplex virus. Virology **42:**1144-1146.

Schlessinger, D. 1990. Yeast artificial chromosomes: tools for mapping and analysis of complex genomes. Trends Genet. **6:**248, 255-258.

Schock, A. and H.W. Reid. 1996. Characterisation of the lymphoproliferation in rabbits experimentally affected with malignant catarrhal fever. Vet. Microbiol. **53:**111-119.

Schuller, W., S. Cerny-Reiterer and R. Silber. 1990. Evidence that the sheep associated form of malignant catarrhal fever is caused by a herpes virus. Zentralbl Veterinarmed [B]. **37:**442-447.

Schultheiss, P.C., J.K. Collins, T.R. Spraker and J.C. DeMartini. 2000. Epizootic malignant catarrhal fever in three bison herds: differences from cattle and association with ovine herpesvirus-2. J. Vet. Diagn. Invest. **12:**497-502.

Schulz, T.F. 1998. Kaposi's sarcoma-associated herpesvirus (human herpesvirus-8). J. Gen. Virol. **79:**1573-1591.

Seal, B.S., W.P. Heuschele, R.B. Klieforth. 1989. Prevalence of antibodies to alcelaphine herpesvirus-1 and nucleic acid hybridization analysis of viruses isolated from captive exotic ruminants. Am. J. Vet. Res. **50:**1447-1453.

Seaman, W.T., D. Ye, R.X. Wang, E.E. Hale, M. Weisse and E.B. Quinlivan. 1999. Gene expression from the ORF50/K8 region of Kaposi's sarcoma-associated herpesvirus. Virology **263:**436-449.

Searles, R.P., E.P. Bergquam, M.K. Axthelm and S.W. Wong. 1999. Sequence and genomic analysis of a Rhesus macaque rhadinovirus with similarity to Kaposi's sarcoma-associated herpesvirus/human herpesvirus 8. J. Virol. **73:**3040-3053.

Selman, I.E., A. Wiseman, M. Murray and N.G. Wright. 1974. A clinico-pathological study of bovine malignant catarrhal fever in Great Britain. Vet. Rec. **94:**483-490.

Selman, I.E., A. Wiseman, N.G. Wright and M. Murray. 1978. Transmission studies with bovine malignant catarrhal fever. Vet. Rec. **102:**252-257.

Shih, L.M., Y.C. Zee and A.E. Castro. 1989. Comparison of genomes of malignant catarrhal fever-associated herpesviruses by restriction endonuclease analysis. Arch. Virol. **109:**145-151.

Sinclair, A.J., M. Brimmell, F. Shanahan and P.J. Farrell. 1991. Pathways of activation of the Epstein-Barr virus productive cycle. J. Virol. **65:**2237-2244.

Smith, G.A. and L.W. Enquist. 1999. Construction and transposon mutagenesis in Escherichia coli of a full-length infectious clone of pseudorabies virus, an alphaherpesvirus. J. Virol. **73:**6405-6414.

Smith, G.A. and L.W. Enquist. 2000. A self-recombining bacterial artificial chromosome and its application for analysis of herpesvirus pathogenesis. Proc. Natl. Acad. Sci. USA. **97:**4873-4878.

Song, M.J., H.J. Brown, T.T. Wu and R. Sun. 2001. Transcription activation of polyadenylated nuclear RNA by rta in human herpesvirus 8/Kaposi's sarcoma-associated herpesvirus. J. Virol. **75:**3129-3140.

Spaete, R.R. and E.S. Mocarski. 1987. Insertion and deletion mutagenesis of the human cytomegalovirus genome. Proc. Natl. Acad. Sci. USA. **84:**7213-7217.

Steiner, I. 1996. Human herpes viruses latent infection in the nervous system. Immunol. Rev. **152:**157-173.

Stevens, J.G. 1989. Human herpesviruses: a consideration of the latent state. Microbiol. Rev. **53:**318-332.

Stoker, M. and I. Macpherson. 1961. Studies on transformation of hamster cells by polyoma virus *in vitro*. Virology **14:**359-370.

Sturm, R., T. Baumruker, B.R. Franza and W. Herr. 1987. A 100-kD HeLa cell octamer binding protein (OBP100) interacts differently with two separate octamer-related sequences within the SV40 enhancer. Genes Dev. **1:**1147-1160.

Suggs, S.V., T. Hirose, E.H. Myake, M.J. Kawashima, K.I. Johnson and R.B. Wallace. 1981. Using purified genes, ICN-UCLA Symp. Mol. Cell. Biol. **23:**683-693.

Sun, R., S.F. Lin, L. Gradoville, Y. Yuan, F. Zhu and G. Miller. 1998. A viral gene that activates lytic cycle expression of Kaposi's sarcoma-associated herpesvirus. Proc. Natl. Acad. Sci. USA. **95:**10866-10871.

Sun, R., S.F. Lin, K. Staskus, L. Gradoville, E. Grogan, A. Haase and G. Miller. 1999. Kinetics of Kaposi's sarcoma-associated herpesvirus gene expression. J. Virol. **73:**2232-2242.

Swenson, J.J., A.E. Mauser, W.K. Kaufmann and S.C. Kenney. 1999. The Epstein-Barr virus protein BRLF1 activates S phase entry through E2F1 induction. J. Virol. **73:**6540-6550.

Takada, K., N. Shimuzu, S. Sakuma and Y. Ono. 1986. Transactivation of the latent Epstein-Barr virus (EBV) genome after transfection of the EBV *Bam* HI Z DNA fragment. J. Virol. **57:**1016-1022.

Talavera, A. and C. Basilico. 1977. Temperature sensitive mutants of BHK cells affected in cell cycle progression. J. Cell Physiol. **92:**425-436.

Taneichi, A., H. Niizeki, Y. Murakami and Y. Nakajima. 1986. Sheep-associated malignant catarrhal fever of beef cattle in Japan. Vet. Rec. **118:**612-613.

Telford, E.A., M.S. Watson, H.C. Aird, J. Perry and A.J. Davison. 1995. The DNA sequence of equine herpesvirus 2. J. Mol. Biol. **249:**520-528.

Thompson, J.D., D.G. Higgins and T.J. Gibson. 1994. CLUSTAL W: improving the sensitivity of progressive multiple sequence alignment through sequence weighting, position specific gap penalties and weight matrix choice. Nucleic Acids Res. **22**:4673-4680.

Tomkinson, B., E. Robertson, R. Yalamanchili, R. Longnecker and E. Kieff. 1993. Epstein-Barr virus recombinants from overlapping cosmid fragments. J. Virol. **67:**7298-7306.

van Santen, V. L. 1993. Characterization of a bovine herpesvirus 4 immediate-early RNA encoding a homolog of the Epstein-Barr virus R transactivator. J. Virol. **67:**773-784.

van Zijl, M., W. Quint, J. Briaire, T. de Rover, A. Gielkens and A. Berns. 1988. Regeneration of herpesviruses from molecularly cloned subgenomic fragments. J. Virol. **62:**2191-2195.

Virgin, H.W., P. Latreille, P. Wamsley, K. Hallsworth, K.E. Weck, A.J. Dal Canto and S.H. Speck. 1997. Complete sequence and genomic analysis of murine gammaherpesvirus 68. J. Virol. **71:**5894-5904.

Vlazny, D.A., A. Kwong and N. Frenkel. 1982. Site-specific cleavage/packaging of herpes simplex virus DNA and the selective maturation of nucleocapsids containing full-length viral DNA. Proc. Natl. Acad. Sci. USA. **79:**1423-1427.

Wheatley, S.C., C.L. Dent, J.N. Wood and D.S. Latchman. 1991. A cellular factor binding to the TAATGARAT DNA sequence prevents the expression of the HSV immediate-early genes following infection of nonpermissive cell lines derived from dorsal root ganglion neurons. Exp. Cell Res. **194:**78-82.

Whitehouse, A., I.M. Carr, J.C. Griffiths and D.M. Meredith. 1997a. The herpesvirus saimiri ORF50 gene, encoding a transcriptional activator homologous to the Epstein-Barr virus R protein, is transcribed from two distinct promoters of different temporal phases. J. Virol. **71:**2550-2554.

Whitehouse, A., M. Cooper, K.T. Hall and D.M. Meredith. 1998a. The open reading frame (ORF) 50a gene product regulates ORF 57 gene expression in herpesvirus saimiri. J. Virol. **72:**1967-1973.

Whitehouse, A., M. Cooper and D.M. Meredith. 1998b. The immediate-early gene product encoded by open reading frame 57 of herpesvirus saimiri modulates gene expression at a posttranscriptional level. J. Virol. **72:**857-861.

Whitehouse, A., A.J. Stevenson, M. Cooper and D.M. Meredith. 1997b. Identification of a cis-acting element within the herpesvirus saimiri ORF 6 promoter that is responsive to the HVS.R transactivator. J. Gen. Virol. **78:**1411-1415.

Whiteley, A., B. Bruun, T. Minson and H. Browne. 1999. Effects of targeting herpes simplex virus type 1 gD to the endoplasmic reticulum and trans-Golgi network. J. Virol. **73:**9515-9520.

Wu, T.T., E.J. Usherwood, J.P. Stewart, A.A. Nash and R. Sun. 2000. Rta of murine gammaherpesvirus 68 reactivates the complete lytic cycle from latency. J. Virol. **74:**3659-3667.

Yang, X.W., P. Model and N. Heintz. 1997. Homologous recombination based modification in Escherichia coli and germline transmission in transgenic mice of a bacterial artificial chromosome. Nat. Biotechnol. **15:**859-865.

Young, L.S., C.W. Dawson and A.G. Eliopoulos. 2000. The expression and function of Epstein-Barr virus encoded latent genes. Mol. Pathol. **53:**238-247.

Zacny, V.L., J. Wilson and J.S. Pagano. 1998. The Epstein-Barr virus immediate-early gene product, BRLF1, interacts with the retinoblastoma protein during the viral lytic cycle. J. Virol. **72:**8043-8051.

Zalani, S., E.A. Holley-Guthrie, D.E. Gutsch, and S.C. Kenney. 1992. The Epstein-Barr virus immediate-early promoter BRLF1 can be activated by the cellular Sp1 transcription factor. J. Virol. **66:**7282-7289.

Zalani, S., E. Holley-Guthrie and S. Kenney. 1996. Epstein-Barr viral latency is disrupted by the immediate-early BRLF1 protein through a cell-specific mechanism. Proc. Natl. Acad. Sci. USA. **93:**9194-9199.

Zhang, Q., D. Gutsch, and S. Kenney. 1994. Functional and physical interaction between p53 and BZLF1: implications for Epstein-Barr virus latency. Mol. Cell Biol. **14:**1929-1938.

Zhu, F.X., T. Cusano and Y. Yuan. 1999. Identification of the immediate-early transcripts of Kaposi's sarcoma-associated herpesvirus. J. Virol. **73:**5556-5567.

Appendices

The following appendices contain the 'raw' luciferase values and fold induction values for all the luciferase assay results shown in Chapter 3.

In experiments utilising pRLSV40, the *Renilla* luciferase value was divided by either 10 or 100. This did not alter the fold induction values.

Appendix 1

Raw luciferase values for Figure 3.8

Construct	Luciferase Values		
	No additions	Plus Virus	Plus pLXSN-ORF50
pGL3-Basic	0.037	0.224	0.039
57 prom	0.063	0.277	0.248
TKprom	0.080	0.990	0.061
6prom	0.073	1.366	0.057

Construct	Fold Induction	
	Plus Virus	Plus pLXSN-ORF50
pGL3-Basic	6.05	1.05
57prom	3.60	3.94
TKprom	12.375	0.76
6prom	18.71	0.78

Appendix 2

Raw luciferase values for Figure 3.9

Voltage	Luciferase Value
220	240.3
240	162.8
260	223.2
280	242.4
300	428.4

Appendix 3

Raw luciferase values for Figure 3.12

Single Pulse	Luciferase Value	Double Pulse	Lucerifase Value
220	1297	650	401.5
240	1733	700	365.7
260	1877	750	367.6
280	1777	800	415.1
300	2468	850	391.1

Appendix 4

Raw luciferase values for Figure 3.13

Construct	Luciferase Values		
	No Additions	Plus pCMVORF50	Fold Induction
1 pGL3-Basic	70.550	293.600	4.20
57prom	9.198	1648.000	179.20
TKprom	90.200	517.400	5.70
6prom	27.440	601.900	21.90
2 pGL3-Basic	0.097	0.397	4.10
57prom	0.059	23.330	395.00
TKprom	0.152	1.251	8.23
6prom	0.115	1.786	15.53
3 pGL3-Basic	0.438	0.843	1.90
57prom	0.027	6.737	249.00
TKprom	0.106	0.259	2.40
6prom	0.067	0.862	12.86

Appendix 5

Raw luciferase values for Figure 3.14

1	Firefly luceriferase Value	Renilla luciferase value	Firefly value / Renilla value
pGL3-Basic	0.781	0.916	0.85
57prom	0.440	0.976	0.45
TKprom	2.526	0.880	2.86
6prom	1.455	0.931	1.56
Plus pCMVORF50			
pGL3-Basic	4.055	0.942	4.30
57prom	24.760	0.835	29.60
TKprom	5.482	0.923	5.90
6prom	16.440	0.882	18.60

2	Firefly luciferase Value	Renilla luciferase value	Firefly value / Renilla value
pGL3-Basic	0.168	0.5880	0.286
57prom	0.089	0.4614	0.193
TKprom	0.467	0.6157	0.758
6prom	0.241	0.5481	0.440
Plus pCMVORF50			
pGL3-Basic	1.829	0.6097	2.999
57prom	4.171	0.4429	9.417
TKprom	1.986	0.6280	3.162
6prom	4.211	0.4884	8.622

3.	Firefly luciferase Value	Renilla luciferase value	Firefly value / Renilla value
pGL3-Basic	2.485	1.603	1.55
57prom	0.925	1.533	0.60
TKprom	6.153	1.178	5.20
6prom	5.983	1.485	4.03
Plus pCMVORF50			
pGL3-Basic	11.76	1.638	7.12
57prom	64.55	1.606	40.19
TKprom	16.91	1.680	10.00
6prom	78.05	1.561	50.00

Constructs	Fold Induction
pGL3Basic	5.06 10.49 4.59
57prom	65.78 48.79 66.98
TKprom	2.05 4.17 1.93
6prom	11.92 19.59 12.41

Appendix 6

Raw luciferase values for Figure 3.15

	Firefly luciferase value	Renilla luciferase Value	Firefly value / Renilla value
pGL3-Basic	0.832	0.263	3.17
	0.932	0.277	3.36
	0.624	0.161	3.87
pGL3-Basic Plus pCMVORF50	3.228	0.508	6.35
	3.259	0.520	6.26
	2.687	0.402	6.69
57prom	0.226	0.282	0.80
	0.475	0.269	1.76
	0.443	0.288	1.54
57prom Plus pCMVORF50	12.640	0.438	28.87
	11.700	0.437	26.75
	10.330	0.409	25.28
TKprom	3.138	0.307	10.22
	3.478	0.309	11.27
	3.592	0.361	9.96
TKprom Plus pCMVORF50	7.056	0.447	15.77
	8.529	0.451	18.90
	9.450	0.454	20.83
6prom	3.360	0.272	12.17
	3.321	0.312	10.66
	4.515	0.234	19.27
6prom Plus pCMVORF50	38.91	0.484	80.46
	36.42	0.426	85.49
	29.66	0.372	79.71

Construct	Fold Induction
pGL3Basic	2.00
	1.86
	1.73
57prom	36.09
	15.19
	16.42
TKprom	1.54
	1.68
	2.09
6prom	6.61
	8.01
	4.12

Appendix 7

Raw luciferase values for Figure 3.16

Constructs	No additions	Plus pCMVORF50	Fold induction
pGL3-Basic	1.55	5.04	3.25
pGL3-Basic	1.78	5.42	3.04
pGL3-Basic	1.32	4.27	3.23
pHSV-TKluc	974.6	816.9	0.84
pHSV-TKluc	631.5	824.6	1.30
pHSV-TKluc	597.1	1008.0	1.69
pRLSV40	415.1	780.1	1.88
pRLSV40	440.0	937.0	2.13
pRLSV40	380.5	775.7	2.03
pCMVluc	838.1	885.3	1.06
pCMVluc	825.0	798.1	0.97
pCMVluc	767.5	931.9	1.21

Appendix 8

Raw luciferase values for Figure 3.19 (b) and (c)

Figure 3.19(b) shows a summary of several experiments, the results of which are shown in graphs in Figure 3.19 (c).

Raw luciferase values for Figure 3.19 (c) (i)

1	Firefly luciferase value	Renilla luciferase value	Firefly value / Renilla value
pGL3Basic	0.781	0.916	0.85
57prom	0.440	0.976	0.45
57p(768)	0.501	0.970	0.52
57p(579)	0.571	1.026	0.56
57p(466)	0.654	0.955	0.68
plus pCMVORF50			
pGL3Basic	4.055	0.942	4.3
57prom	24.76	0.835	29.6
57p(768)	41.08	0.723	56.8
57p(579)	26.10	0.986	26.5
57p(466)	3.780	0.923	4.19

2	Firefly luciferase value	Renilla luciferase value	Firefly value / Renilla value
pGL3Basic	0.168	0.5880	0.286
57prom	0.089	0.4614	0.193
57p(768)	0.106	0.5786	0.183
57p(579)	0.123	0.5529	0.222
57p(466)	0.189	0.5543	0.341
plus pCMVORF50			
pGL3Basic	1.829	0.6097	2.999
57prom	4.171	0.4429	9.417
57p(768)	10.47	0.5328	19.651
57p(579)	6.557	0.5407	12.127
57p(466)	0.936	0.6029	1.552

3	Firefly luciferase Value	Renilla luciferase value	Firefly value / Renilla value
pGL3Basic	2.485	1.603	1.55
57prom	0.925	1.533	0.6
57p(768)	1.166	1.818	0.6
57p(579)	1.157	1.516	0.763
57p(466)	1.095	1.075	1.01
plus pCMVORF50			
pGL3Basic	11.76	1.638	7.12
57prom	64.55	1.606	40.19
57p(768)	72.85	1.585	45.96
57p(579)	38.16	1.550	24.6
57p(466)	20.62	1.796	11.48

Constructs	Fold Induction
pGL3Basic	5.06
	10.49
	4.59
57prom	65.78
	48.79
	66.98
57p(768)	109.23
	107.38
	76.6
57p(579)	47.32
	54.63
	32.42
57p(466)	6.16
	4.55
	11.37

Raw luciferase values for Figure 3.19 (c) (ii).

Constructs	Firefly luciferase value	Renilla luciferase value	Firefly value / Renilla value
pGL3Basic	0.970	0.1809	5.36
	1.029	1.7150	6.00
	1.053	1.7560	5.99
pGL3Basic plus pCMVORF50	3.234	0.2377	13.60
	1.855	0.1656	11.20
	2.268	0.1930	11.75
57prom	0.286	0.1964	1.46
	0.307	0.1611	1.90
	0.217	0.1938	1.12
57prom plus pCMVORF50	7.947	0.2117	37.54
	5.633	0.1482	38.01
	5.955	0.1488	40.02
57p(466)	0.433	0.1756	2.46
	0.396	0.1590	2.49
	0.496	0.1879	2.64
57p(466) plus pCMVORF50	1.442	0.2022	7.13
	1.828	0.2163	8.45
	1.689	0.2029	8.32
57p(686)	0.310	0.1630	1.90
	0.368	0.1746	2.11
	0.410	0.2095	1.96
57p(686) plus pCMVORF50	10.00	0.1652	60.53
	9.272	0.1831	50.64
	7.193	0.1293	55.63
57p(180)	2.298	0.1429	16.08
	2.350	0.1701	13.82
	1.763	0.1299	13.57
57p(180) plus pCMVORF50	6.281	0.1992	31.53
	6.847	0.2552	26.83
	6.235	0.1815	34.35

Constructs	Fold Induction
pGL3Basic	2.54
	1.89
	1.96
57prom	25.71
	20.00
	35.73
57p(466)	2.90
	3.39
	3.15
57p(686)	31.86
	24.00
	28.38
57p(180)	1.96
	1.94
	2.53

Raw luciferase values for Figure 3.19 (c) (iii)

Constructs	Firefly luciferase value	Renilla luciferase value	Firefly value / Renilla value
pGL3Basic	7.135	5.587	1.30
	5.656	2.961	10.90
	6.405	3.638	1.80
pGL3Basic plus pCMVORF50	19.990	4.203	4.76
	27.870	1.808	15.40
	41.130	5.026	8.2
57prom	2.204	6.109	0.36
	1.449	2.062	0.70
	1.902	4.084	0.50
57prom plus pCMVORF50	149.900	7.101	21.10
	47.790	1.109	43.10
	134.000	6.808	19.70
57p(466)	4.234	6.743	0.63
	2.299	2.198	1.04
	3.490	4.124	0.85
57p(466) plus pCMVORF50	15.560	4.157	3.70
	30.710	3.752	8.20
	13.450	3.670	3.66
57p(194)	0.723	6.096	0.12
	0.487	4.138	0.12
	0.428	2.243	0.19
57p(194) plus pCMVORF50	2.081	4.933	0.42
	2.081	5.308	0.40
	1.093	2.140	0.50

Constructs	Fold Induction
pGL3Basic	3.66
	8.10
	4.5
57prom	58.61
	61.57
	39.4
57p(466)	5.87
	7.88
	4.3
57p(194)	3.5
	3.3
	2.63

Raw luciferase values for 3.19 (c) (iv).

Constructs	Firefly luciferase value	Renilla luciferase value	Firefly value / Renilla value
pGL3Basic	0.217	0.3001	0.72
	0.489	0.3383	1.40
	0.425	0.3151	1.35
pGL3Basic plus pCMVORF50	1.227	0.5803	2.10
	1.436	0.6473	2.20
	1.476	0.6848	2.10
57prom	0.196	0.3052	0.64
	0.198	0.3323	0.59
	0.135	0.3562	0.38
57prom plus pCMVORF50	4.997	0.7560	6.60
	5.866	0.6646	8.83
	4.965	0.5308	9.30
57p(466)B	0.180	0.3359	0.53
	0.116	0.3564	0.32
	0.201	0.4074	0.49
57p(466)B plus pCMVORF50	1.079	0.6905	1.56
	0.727	0.5708	1.27
	0.639	0.5566	1.10
57p(133)	0.131	0.3236	0.40
	0.303	0.3301	0.92
	0.269	0.4006	0.67
57p(133) plus pCMVORF50	0.718	0.6676	1.07
	0.584	0.6261	0.93
	0.497	0.4900	1.00

Constructs	Fold Induction
pGL3Basic	2.92
	1.57
	1.55
57prom	10.31
	14.97
	24.47
57p(466)B	2.94
	3.97
	2.24
57p(133)	2.675
	1.01
	1.49

Appendix 9

Raw luciferase values for Figure 3.20

Constructs	Firefly luciferase value	Renilla luciferase value	Firefly value / Renilla Value
pGL3promoter	42.40	0.224	189.03
	51.46	0.271	190.09
	55.93	0.302	185.38
pGL3-promoter plus pCMVORF50	78.28	0.378	206.70
	16.88	0.114	148.20
	64.95	0.390	166.62
Prom57p(155)	102.80	0.457	224.89
	125.20	0.496	252.16
	113.40	0.416	272.33
Prom57p(155) plus pCMVORF50	304.00	0.829	366.50
	321.20	0.999	321.65
	264.40	0.775	341.07

Constructs	Fold Induction
pGL3-promoter	1.09
	0.78
	0.90
Prom57p(155)	1.63
	1.27
	1.25

Appendix 10

Raw values for Figure 3.21 (b).

Constructs	Firefly luciferase value	Renilla luciferase value	Firefly value / Renilla value
pGL3Basic	6.064	2.135	2.84
	6.969	1.220	5.7
	6.201	1.464	4.24
pGL3Basic plus pCMVORF50	29.81	1.673	17.82
	33.34	1.775	18.8
	29.12	1.725	16.9
57prom	2.274	1.256	1.81
	2.173	1.449	1.5
	2.478	1.426	1.74
57prom plus pCMVORF50	73.75	1.773	41.6
	75.04	1.624	46.21
	62.74	1.623	38.66
57p(579)	2.341	1.822	1.285
	2.975	1.495	1.99
	2.925	1.658	1.76
57p(579) plus pCMVORF50	69.76	1.982	35.2
	52.52	1.593	32.97
	59.31	1.734	34.2
57p(399)	2.682	1.181	2.27
	2.427	1.222	1.99
	2.491	1.072	2.32
57p(399) plus pCMVORF502.478	38.04	1.570	24.23
	34.86	1.476	23.62
	37.94	1.490	25.46

Constructs	Fold Induction
pGL3Basic	6.27
	3.30
	3.98
57prom	22.98
	30.81
	22.22
57p(579)	27.39
	16.57
	19.43
57p(399)	10.67
	11.87
	10.97

Appendix 11

Raw luciferase values for the Figure 3.33 (a)

Promoter Construct	Expression Construct	Firefly luciferase value	Renilla luciferase value	Firefly value / Renilla value
PGL3-Basic	None	0.770	0.1661	4.6
57prom	None	0.541	0.1910	2.8
PGL3-Basic	pcDNA50	1.909	0.2556	7.5
57prom	pcDNA50	6.350	0.3378	18.8
PGL3-Basic	pcDNA50A	1.009	0.3687	4.5
57prom	pcDNA50A	0.705	0.4395	2.8
PGL3-Basic	PcDNA50B	1.234	0.2248	5.8
57prom	PcDNA50B	0.647	0.2501	2.8

Constructs	Fold Induction
pGL3-Basic plus pcDNA50	1.60
57prom plus pcDNA50	6.70
pGL3-Basic plus pcDNA50A	0.97
57prom plus pcDNA50A	1.00
pGL3-Basic plus pcDNA50B	1.26
57prom plus pcDNA 50B	1.00

Appendix 12

Raw luciferase values for Figure 3.33 (b)

	Firefly luciferase value	Renilla luciferase Value	Firefly value / Renilla value
pGL3-Basic	1.892	1.209	1.56
	2.356	1.332	1.78
	1.428	1.085	1.32
pGL3-Basic	8.239	1.634	5.04
plus pcDNA3.1-50	9.267	1.709	5.42
	5.745	1.346	4.27
57prom	1.117	1.169	0.95
	1.015	1.259	0.81
	1.040	1.297	0.80
57prom	59.61	1.725	34.5
plus pcDNA3.1-50	58.12	1.814	32.04
	44.54	1.552	28.7
57prom	38.30	1.693	22.6
plus pcDNA3.1-50	29.63	1.555	19.05
plus pcDNA3.1-50A (2 µg)	32.87	1.361	24.15
57prom	16.31	1.780	9.16
plus pcDNA3.1-50	16.90	1.859	9.09
plus pcDNA3.1-50A (10 µg)	13.26	1.718	7.72
57prom	18.03	2.125	8.5
plus pcDNA3.1-50	14.46	1.771	8.16
plus pcDNA3.1-50A (20 µg)	13.85	1.594	8.69
57prom	55.88	1.712	32.6
plus pcDNA3.1-50	68.42	1.985	34.5
Plus pcDNA3.1-50B (2 µg)	63.42	1.821	34.83
57prom	57.55	2.224	25.9
plus pcDNA3.1-50	43.72	1.801	24.27
plus pcDNA3.1-50B (10 µg)	50.57	1.764	28.67
57prom	84.61	2.607	32.4
plus pcDNA3.1-50	66.97	2.163	30.96
plus pcDNA3.1-50B (20 µg)	71.62	2.300	31.14
57prom	55.26	1.653	33.4
plus pcDNA3.1-50	60.08	1.777	33.81
plus pEGFP-N1 (2 µg)	55.16	1.415	38.98
57prom	48.48	1.827	26.5
plus pcDNA3.1-50	58.15	2.143	27.13
plus pEGFP-N1 (10 µg)	57.78	1.741	33.19
57prom	64.38	2.485	25.91
plus pcDNA3.1-50	70.65	2.280	30.99
plus pEGFP-N1 (20 µg)	65.22	2.146	30.39

Constructs	Fold Induction
pGL3-Basic plus pcDNA50	3.23 3.04 3.23
57prom plus pcDNA50	36.31 39.55 35.87
57prom plus pcDNA50 plus pcDNA50A (2 μg)	23.79 23.52 30.19
57prom plus pcDNA50 plus pcDNA50A (10 μg)	9.64 11.22 9.65
57prom plus pcDNA50 plus pcDNA50A (20 μg)	8.95 10.07 10.86
57prom plus pcDNA50 plus pcDNA50B (2 μg)	34.31 42.59 43.54
57prom plus pcDNA50 plus pcDNA50B (10 μg)	27.26 29.96 35.84
57prom plus pcDNA50 plus pcDNA50B (20 μg)	34.10 38.22 38.92
57prom plus pcDNA50 plus pEGFP-N1 (2 μg)	35.16 41.74 48.50
57prom plus pcDNA50 plus pEGFP-N1 (10 μg)	27.89 33.49 41.49
57prom plus pcDNA50 plus pEGFP-N1 (20 μg)	27.27 38.26 37.99

Appendix 13

Raw luciferase values for Figure 3.34(c)

Promoter Construct	Expression Construct	Firefly luciferase value	Renilla luciferase value	Firefly value Renilla value
pGL3-Basic	None	0.235	0.075	3.13
57prom		0.078	0.092	0.85
TKprom		0.521	0.086	6.06
6prom		0.466	0.087	5.36
pGL3-Basic	pCMVORFA6	0.303	0.088	3.54
57prom		0.097	0.083	1.20
TKprom		0.7888	0.089	8.80
6prom		0.606	0.089	6.80
pGL3-Basic	pCMVORFA6 plus pCMVORF50	0.884	0.076	11.60
57prom		2.768	0.078	35.50
TKprom		1.417	0.055	25.76
6prom		9.203	0.170	54.13

Constructs	Fold Induction
pGL3-Basic plus pCMVORFA6	1.1
57prom plus pCMVORFA6	1.4
TKprom plus pCMVORFA6	1.4
6prom plus pCMVORFA6	1.3
pGL3-Basic plus pCMVA6 plus pCMVORF50	3.7
57prom plus pCMVA6 plus pCMVORF50	41.7
TKprom plus pCMVA6 plus pCMVORF50	4.2
6prom plus pCMVA6 plus pCMVORF50	10.1

Appendix 14

Fold Induction of pGL3-Basic with pCMVORF50
5.06
4.59
2.00
1.86
1.73
3.25
3.04
3.23
2.54
1.89
1.96
3.66
8.10
4.5
2.92
1.57
1.55
6.27
3.30
3.98

Average = 3.69 +/- 2.28